CANADIAN THESES ON MICROFICHE

THÈSES CANADIENNES SUR MICROFICHE

NOTICE

The quality of this microfiche is heavily dependent upon the quality of the original thesis submitted for microfilming. Every effort has been made to ensure the highest quality of reproduction possible.

If pages are missing, contact the university which granted the degree.

Some pages may have indistinct print especially if the original pages were typed with a poor typewriter ribbon or if the university sent us an inferior photocopy.

Previously copyrighted materials (journal articles, published tests, etc.) are not filmed.

Reproduction in full or in part of this film is governed by the Canadian Copyright Act, R.S.C. 1970, c. C-30. Please read the authorization forms which accompany this thesis.

AVIS

La qualité de cette microfiche dépend grandement de la qualité de la thèse soumise au microfilmage. Nous avons tout fait pour assurer une qualité supérieure de reproduction.

S'il manque des pages, veuillez communiquer avec l'université qui a conféré le grade.

La qualité d'impression de certaines pages peut laisser à désirer, surtout si les pages originales ont été dactylographiées à l'aide d'un ruban usé ou si l'université nous a fait parvenir une photocopie de qualité inférieure.

Les documents qui font déjà l'objet d'un droit d'auteur (articles de revue, examens publiés, etc.) ne sont pas microfilmés.

La reproduction, même partielle, de ce microfilm est soumise à la Loi canadienne sur le droit d'auteur, SRC 1970, c. C-30. Veuillez prendre connaissance des formules d'autorisation qui accompagnent cette thèse.

THIS DISSERTATION HAS BEEN MICROFILMED EXACTLY AS RECEIVED

LA THÈSE A ÉTÉ MICROFILMÉE TELLE QUE NOUS L'AVONS REÇUE

Canada

0-315-19655-5

67541

PERMISSION TO MICROFILM — AUTORISATION DE MICROFILMER

• Please print or type — Écrire en lettres moulées ou dactylographier

Full Name of Author — Nom complet de l'auteur

Brian Curtis Flintoff

Date of Birth — Date de naissance

September 15, 1948

Country of Birth — Lieu de naissance

Canada

Permanent Address — Résidence fixe

5 Menlo Crescent
Sherwood Park, Alberta
T8A 0R8

Title of Thesis — Titre de la thèse

An On-Stream Coal Ash Analyser for Fine Particle Slurries

University — Université

University of Alberta

Degree for which thesis was presented — Grade pour lequel cette thèse fut présentée

Doctor of Philosophy

Year this degree conferred — Année d'obtention de ce grade

1983

Name of Supervisor — Nom du directeur de thèse

L. R. Plitt

Date

October 5, 1983

Signature

Brian C Flintoff

THE UNIVERSITY OF ALBERTA

An On-Stream Coal Ash Analyser for Fine Particle Slurries

by

B.C. Flintoff

A THESIS

SUBMITTED TO THE FACULTY OF GRADUATE STUDIES AND RESEARCH

IN PARTIAL FULFILMENT OF THE REQUIREMENTS FOR THE DEGREE

OF Doctor of Philosophy

IN

Mineral Engineering

Department of Mineral Engineering

EDMONTON, ALBERTA

Fall 1983

THE UNIVERSITY OF ALBERTA

RELEASE FORM

NAME OF AUTHOR   B.C. Flintoff

TITLE OF THESIS   An On-Stream Coal Ash Analyser for Fine

Particle Slurries

DEGREE FOR WHICH THESIS WAS PRESENTED   Doctor of Philosophy

YEAR THIS DEGREE GRANTED   Fall 1983

       Permission is hereby granted to THE UNIVERSITY OF

ALBERTA LIBRARY to reproduce single copies of this

thesis and to lend or sell such copies for private,

scholarly or scientific research purposes only.

       The author reserves other publication rights, and

neither the thesis nor extensive extracts from it may

be printed or otherwise reproduced without the author's

written permission.

(SIGNED) .Brian..C.Flintoff...

PERMANENT ADDRESS:

....5..Menlo..Crescent......

....Sherwood..Park..........

....Alberta....T8A 0R8......

DATED ....October 5....1983

THE UNIVERSITY OF ALBERTA

FACULTY OF GRADUATE STUDIES AND RESEARCH

The undersigned certify that they have read, and
recommend to the Faculty of Graduate Studies and Research,
for acceptance, a thesis entitled An On-Stream Coal Ash
Analyser for Fine Particle Slurries submitted by B.C.
Flintoff in partial fulfilment of the requirements for the
degree of Doctor of Philosophy in Mineral Process
Engineering.

....

Supervisor

....

....

....

....

External Examiner

Date.. September. 30., 1983....

DEDICATION

I would like to dedicate this thesis to my family. To my parents for their constant support and to my wife, Marilyn, and daughters, Erin and Kerry, who have made many personal sacrifices to permit me to complete this work, I am truly grateful!

ABSTRACT

This project involved the design and evaluation of a radioisotope on-stream coal ash analyser for use in fine coal preparation circuits. The instrument was designed to predict the solids concentration and ash content of a slurry flowstream while accommodating changes in the mineral matter composition, without recalibration.

The work included the development of a methodology for establishing the economic merit and technical feasibility of regulatory control systems, under the umbrella of process optimization. Some plant experimental work was conducted to justify the project and to provide the parameters necessary for both the equipment and the experimental designs.

A review of the literature revealed that a limited amount of instrumentation development had occurred in this area, mostly in monitoring the ash content of coarse dry coal. A number of candidate designs were considered and the one studied by Kawatra on a bench scale was adopted for further investigation on the prototype scale. The theory of instrument operation was developed in some detail to provide both design information as well as semi-empirical calibration models.

A prototype instrument was constructed and calibration studies performed in the laboratory. The experimental results on simulated froth flotation product flowstreams met the evalutaion criteria, with one exception. The latter was the direct result of a design problem and should be easily

corrected in the next generation of instrument development.

The laboratory results were sufficiently encouraging to warrant a plant trial of the prototype. Although experimental problems partially masked the true potential of the device, it was still possible to obtain a successful instrument calibration. This exercise served to demonstrate that an on-stream ash analyser of the type studied could be used in process monitoring and in the process control of fine coal preparation circuits.

ACKNOWLEDGEMENTS

The author would like to acknowledge the contributions of several individuals and organizations in helping to bring this project to a successful conclusion:

-Professor L.R. Plitt who recognized the need for an on-stream coal ash analyser in the western Canadian coal preparation plants and arranged the funding for such a project, initiated it and provided assistance throughout all stages of the work. He was also an invaluable "sounding board" for ideas expressed by the author.

-Mr. R.A. Konzuk who helped in the mechanical design of the OSCAA components and was singularly responsible for their fabrication. In addition, he helped in the installation, at various stages of the laboratory work and in setting up for the plant trial. The author spent a considerable amount of time discussing various aspects of the project with Mr. Konzuk and is most appreciative of his input.

-Mr. B. Mohammedbhai who participated in the early stages of the work in helping the author to develop and debug both the analytical procedures and certain facets of the equipment design. Mr. Mohammedbhai made many suggestions regarding the project, the majority of which were implemented.

Special thanks are due to other members of the technical staff of the Department of Mineral Engineering, B. Snider, T. Forman, C. Barker and R. Smith for their

Table of Contents

x

List of Tables

List of Figures

List of Plates

1. INTRODUCTION

1.1 INDUSTRY OVERVIEW

Coal preparation (coal washing, coal cleaning, coal beneficiation) is the art and science of removing inert inorganic material from the run-of-mine raw coal. The principal reasons for undertaking this step in the mining sequence are:

a) to comply with market specifications on product quality,

b) to minimize the cost of transporting the coal to distant markets.

According to statistics compiled in January, 1981(1), Canadian coal production was estimated at 36.5 million tonnes per year. Of this, 19.5 million tonnes (53%) were prepared to some extent prior to shipment. This coal is destined primarily for international and distant domestic metallurgical and thermal coal markets. Recent forecasts(2,3,4) predict a substantial increase in coal production over the next two decades. Although the current economic downturn has slowed growth in both areas of utilization, significant growth is still expected to occur, even in the short term(4). In view of these figures and the expected trends, coal production and specifically coal preparation plays an important role in the Country's economy, particularly in the international trade balance.

Most of the Canadian coal preparation plants are relatively new having been commissioned in the period since

1

1970. However, since this represents a re-emergence of coal after an extended period of stagnation, the industry lags the other process industries in terms of design and operating practice, as well as in research and development. While much of the newer design and operating philosophy has been borrowed from overseas experience (eg. UK- National Coal Board) this is not a panacea. Canadian coals possess some unique preparation problems, in particular the requirement to treat large amounts of fine coal, for which borrowed technology is largely inapplicable.

In the process industries, understanding process mechanism (through modelling) and installing regulatory control systems are pre-requisites to optimal plant operation. The coal producers recognize this as an important area and are concerned with improving upon existing methods, especially in the treatment of fine coal.

1.2 AN INTRODUCTION TO COAL PREPARATION

It is assumed that the reader may not be familiar with coal preparation. In order that he may more easily understand some of the material which follows, a cursory treatment of the subject is provided.

The overall objective of coal preparation is to treat the material from the mine in such a manner that the organic material is effectively separated from the extraneous mineral matter producing a maximum amount 'of clean coal'

'It is implicit that maximum production ensures maximum profit.

which complies with the sales contract specifications.

It is necessary to define some of the jargon:

COAL: A naturally occurring, rocklike derivative of forest type vegetation which contains ≥50% by weight of organic material.

MINERAL MATTER: The inorganic (usually solid) portion of the coal which consists primarily of silaceous material. Material which is colloidally dispersed in the coal organics matrix, as a result of the depositional environment, and which cannot be separated by physical means, is called **Inherent Mineral Matter.** Material which is loosely bound to the organic material arising from dilution during mining or interbedded seams, and which can effectively be removed by physical means, is called **Extraneous Mineral Matter.**

ASH: The residue which remains after complete combustion of the organic portion of the coal. Since there is some volatile matter associated with the mineral matter (eg. water of hydration), the ash fraction of the coal is always less than the mineral matter fraction. However, for a particular deposit the **Mineral Matter to Ash Ratio** is approximately constant (≈ 1.1).

YIELD: The ratio of clean coal produced to the feed on a weight basis for a particular separation (eg. unit, circuit, plant).

CLEAN COAL: The organic rich product of a separation.

REFUSE(REJECT): The mineral matter rich product of a separation.

Historically, coal cleaning was based on exploiting the difference between the specific gravity of the organic fraction (typically $1.25 \leq sg \leq 1.45$) and the mineral matter fraction (typically $2.3 \leq sg \leq 2.8$). (It must be recognized that as a result of the incomplete liberation of the extraneous mineral matter there is a continuous distribution of solid material with specific gravity.) Unit operations such as the jig, table and, more recently, dense medium vessels and dense medium cyclones were used to effect separation. In general, separation efficiency decreases with decreasing particle size. The inability of these devices to effectively treat fine coal coupled with increased need to do so has necessitated the development or application of new process technology. This includes devices which will separate on the basis of specific gravity (eg. automedium cyclone) or on the basis of surface properties (eg. froth flotation)

To obtain maximum separation efficiency in a plant, the feed material is usually classified on the basis of size, into two or three streams. Typically a coarse cut is made at 12.5mm and a fine cut at 0.6mm, resulting in three separate feed streams. This design allows optimal equipment selection with respect to maximizing separation efficiency, assuming that economic justification exists. A general flowsheet of a standard western Canadian coal preparation plant is included in figure 1.1 to illustrate these design concepts.
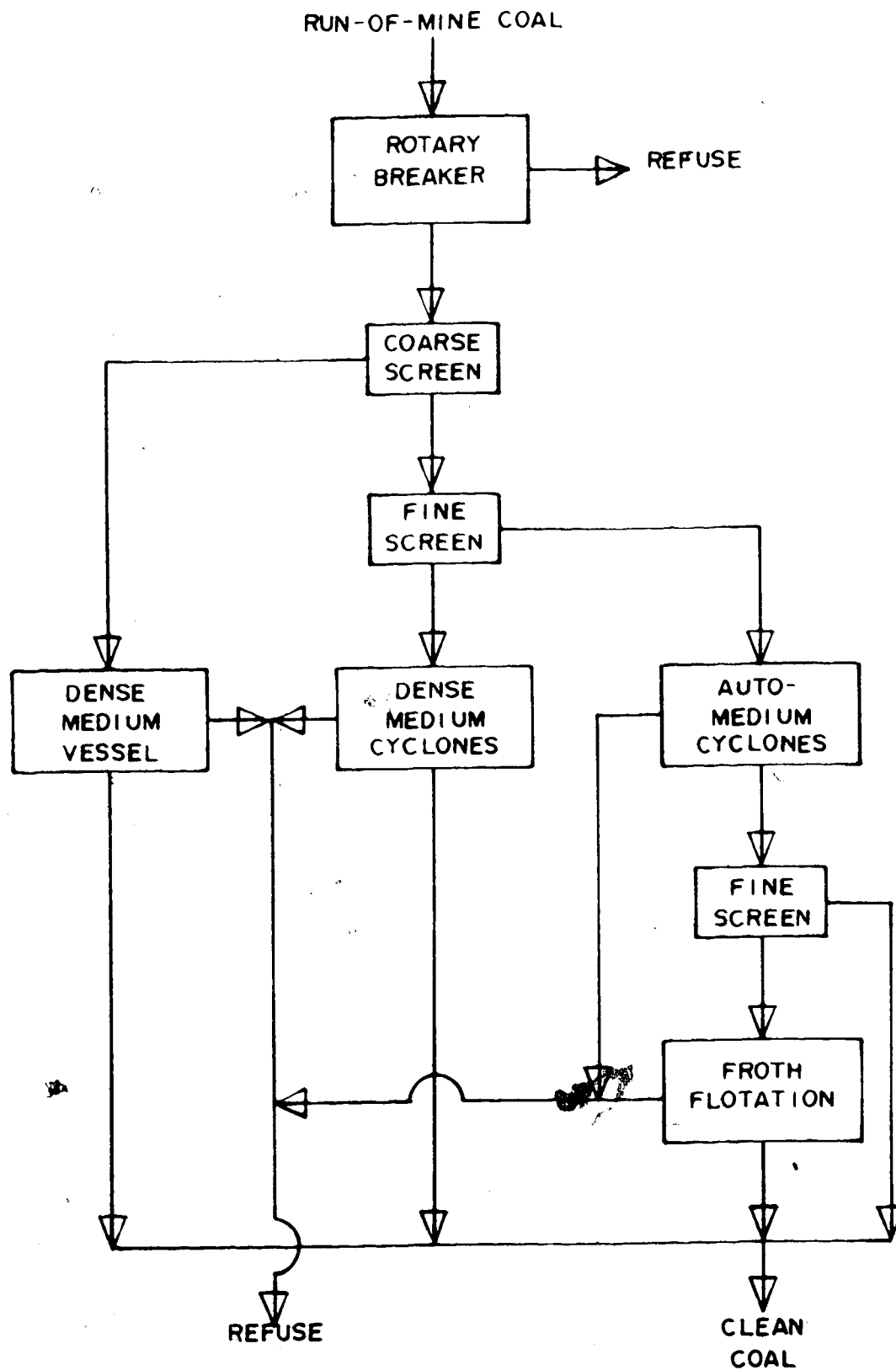
Figure 1.1 A Typical Western Canadian Coal Preparation Plant Flowsheet.

1.3 PROJECT HISTORY

Western Canadian coals are very friable, particularly the metallurgical coals in the Rocky Mountain region. This results in a very high percentage (typically ≥25%) of fine material, nominally ≤0.6mm, in the preparation plant feed. In this respect these plants are unique for they must wash very substantial tonnages of this fine coal in an efficient manner, using processes which are relatively new to the field. Unlike coarse coal washing, this task is quite difficult because of the general lack of process understanding and the absence of the necessary process control equipment, in particular, on-stream analytical devices.

The beneficiation of fine coal is an area which requires a considerable amount of research and development work. Some of this work has been undertaken at the plant level but this is usually in response to an operating crisis such as very poor separation efficiency. This leaves the majority of the more fundamental research to be performed by publicly funded research organizations and the universities. In recognition of this need for research in fine coal preparation, L.R. Plitt[2] conceived a "Coal Beneficiation Project." In response to his proposal the Department of Energy and Natural Resources of the Province of Alberta provided a capital grant of $250,000 in support of this work. It was envisaged that the work would proceed on two

----

[2] Chairman, Department of Mineral Engineering, University of Alberta.

fronts, namely:

(1)   laboratory and plant analysis of the process unit

operations (eg. froth flotation, automedium

cyclones, classifying cyclones, screens, etc...)

(2)   instrumentation and control of fine coal separation

processes.

Within the objectives of the project it was deemed that the

development of an On-Stream Coal Ash Analyser (OSCAA) should

be given the highest priority. The reasoning was that the

successful development of such a device would provide the

basic tool for process control. Furthermore, it would

facilitate process studies in the plant by eliminating what

would otherwise be a horrendous sampling and analytical

overhead.

The OSCAA project was the subject of this thesis

investigation. It officially began in September, 1978.

Funding for the operating expenses was obtained from the

Alberta/Canada Energy Resources Research Fund (A/CERRF) at

the following levels:

YEAR 1 $33,000

YEAR 2 $40,000

The goals of the OSCAA project were: (1) to develop a

prototype instrument in the form of a laboratory pilot plant

system, (2) to calibrate (or otherwise study) the equipment

performance in the laboratory, and, (3) to test the

prototype in the operating plant environment.

Under the conditions defined by the Alberta/Canada
Energy Resources Research Fund (A/CERRF), an Alberta based
producing company was to be chosen to participate in this
project. McIntyre Mines Ltd., Grande Cache, Alberta, was
selected because of their expressed interest in the work as
well as the strong personal contacts between this group and
the university personnel involved.

2. OPTIMIZATION IN COAL PREPARATION

2.1 INTRODUCTION

Before proceeding with the experimental portion of the thesis it was necessary to justify the work. While the project was intuitively justified, experimental evidence was required to allow for an independent and unbiased assessment to be made. The problem was that there existed a void in the technology, namely a methodology for evaluating the impact of process optimization. In short, a description of what measurements had to be made and how they were to be analysed.

Process optimization requires that the various circuits within a plant be manipulated in some organized pattern such that the optimization objective is ultimately met. Implicit in this manipulation is process stability. Since stability is rarely inherent some form of process control is frequently required. In such cases process sensors are necessary to allow control strategy development and implementation as well as in the subsequent process manipulation. In this context, optimization includes two broad areas; the short term - process stabilization, and the long term - process manipulation.

The material which follows represents an effort to develop a methodology to assist in process analysis as well as in the *a-priori* justification of process instrumentation. With respect to the longer term activity the steady state

optimization criteria are defined and their practicality discussed. For the shorter term activity, methods of assessing the economic merit and technical feasibility of process control systems are presented. This provides the theory which the operator requires to make an independent, and not intuitive, evaluation of the plant performance.

The author recognizes that this material is not strictly a part of the development of the OSCAA prototype instrument. However, it is his opinion that such a treatise was absolutely essential as the foundation for project justification. Moreover, this chapter by itself represents a scientific contribution to the industry and, as a consequence, should be included in the thesis.

2.2 OPTIMIZATION: OBJECTIVES AND OBSTACLES

Once a washery has been commissioned and most of the initial mechanical bottlenecks have been removed, it remains to optimize the preparation plant system. Optimization in coal preparation is simply making the maximum economic use of the available coal reserves. This translates to maximizing clean coal production from the reserves subject to the constraints (quality and quantity) of the sales contract(s) and the external regulatory processes. It would be desirable to have the flexibility of rapid tuning of the plant to take advantage of spot markets as they present themselves.

The ideal situation for the coal preparation plant engineer is to have a totally homogeneous plant feed (composition, size, and density distributions) and a well, controlled plant. Under these conditions the individual cleaning circuits within the plant may be tuned (e.g. EVOP(5), SSDEVOP(6)) to provide for maximum profitability over the lifetime of the sales contract. However, because of the varying nature of the coal deposit quality, the reliability characteristics of the mining system, and the lack of process control equipment in the plant, this is very seldom possible. More typically the engineer is faced with defining optimum operating policy on a daily basis given:

a) the upstream feed disturbances caused by variations in seam quality and mine production,

b) poor mining methods,

c) the downstream constraints of the product specifications,

d) recent production history,

e) his knowledge of process behaviour.

Considering the stochastic nature of (a), the problems associated with obtaining a reliable material balance in (d) and the general lack of process understanding in the industry, this is a difficult task. Another serious problem arises in (b). Since coal preparation unit costs are often significantly lower than the mining unit costs, it is not uncommon for the mine to off-load much of its "selection" reponsibilities to the plant. The problem is that coal which

is expensive to mine usually requires a high washery

efficiency. This serves to further complicate the quality

control function.

2.3 THE THEORETICAL STEADY STATE OPTIMIZATION STRATEGY

In principle, it is easy to define the steady state

optimization objective for a coal preparation plant.

"Maximize the yield of clean coal from the available

reserves while maintaining the the specified product

quality."

Mathematically,

Maximize:

$$Y = \sum_j \sum_i M_{ij} Y_{ij} \qquad \text{...(2.1)}$$

Subject to:

$$\frac{\sum_j \sum_i M_{ij} Y_{ij} A_{ij} \leq A_0}{\sum_j \sum_i M_{ij} Y_{ij}} \qquad \text{...(2.2)}$$

where: Y = objective function (plant yield).
M_{ij} = the fraction of raw coal from block j (which has homogeneous properties) in the deposit which reports to cleaning circuit i in the plant with $\Sigma\Sigma M_{ij} = 1$.
Y_{ij} = the fractional yield of M_{ij} to the clean coal product.
A_{ij} = the value of some cumulative attribute in the clean coal product (e.g. ash, sulfur, calorific value).
A_0 = the quality specification for the attribute.

The attribute of greatest interest in Canadian operations is

the ash content. Sulfur is of lesser importance because of

its relatively low concentration. Furthermore, for most

deposits, calorific value can be inferred from a functional

(usually linear) relationship with the ash content.

Therefore, ash content is generally the attribute with which the operator's characterize the various solids flowstreams. For this reason equations (2.1) and (2.2) will be solved for the ash constraint. However, any number of constraints could be included one of which would determine the extent to which plant yield may be maximized.

For any attribute, such as cumulative ash, which increases monotonically with increasing yield, maximum yield will be obtained when the constraint of equation (2.2) is a strict equality. By nature, the physical and physiochemical separation operations employed in beneficiation exhibit operating yield-ash curves which are monotonically increasing in the region of interest. In a properly operated plant the overall yield-ash curve will also be monotonically increasing in the region of interest. An example of a yield-ash curve for a simulated three circuit thermal coal preparation plant is presented in Figure 2.1 to illustrate this monotonicity. It is possible that some particular combination of these units will produce an overall plant product curve which does not meet this condition (e.g. see (7)-Figure 18-18). This is the result of unusual operation and should be infrequently encountered in practice. Therefore, in normal operation, the plant yield-ash curve is such that the strict equality of equation (2.2) will ensure maximum yield.

The system of equations (2.1) and (2.2) can be solved analytically using the method of Lagrangian Multipliers(8).
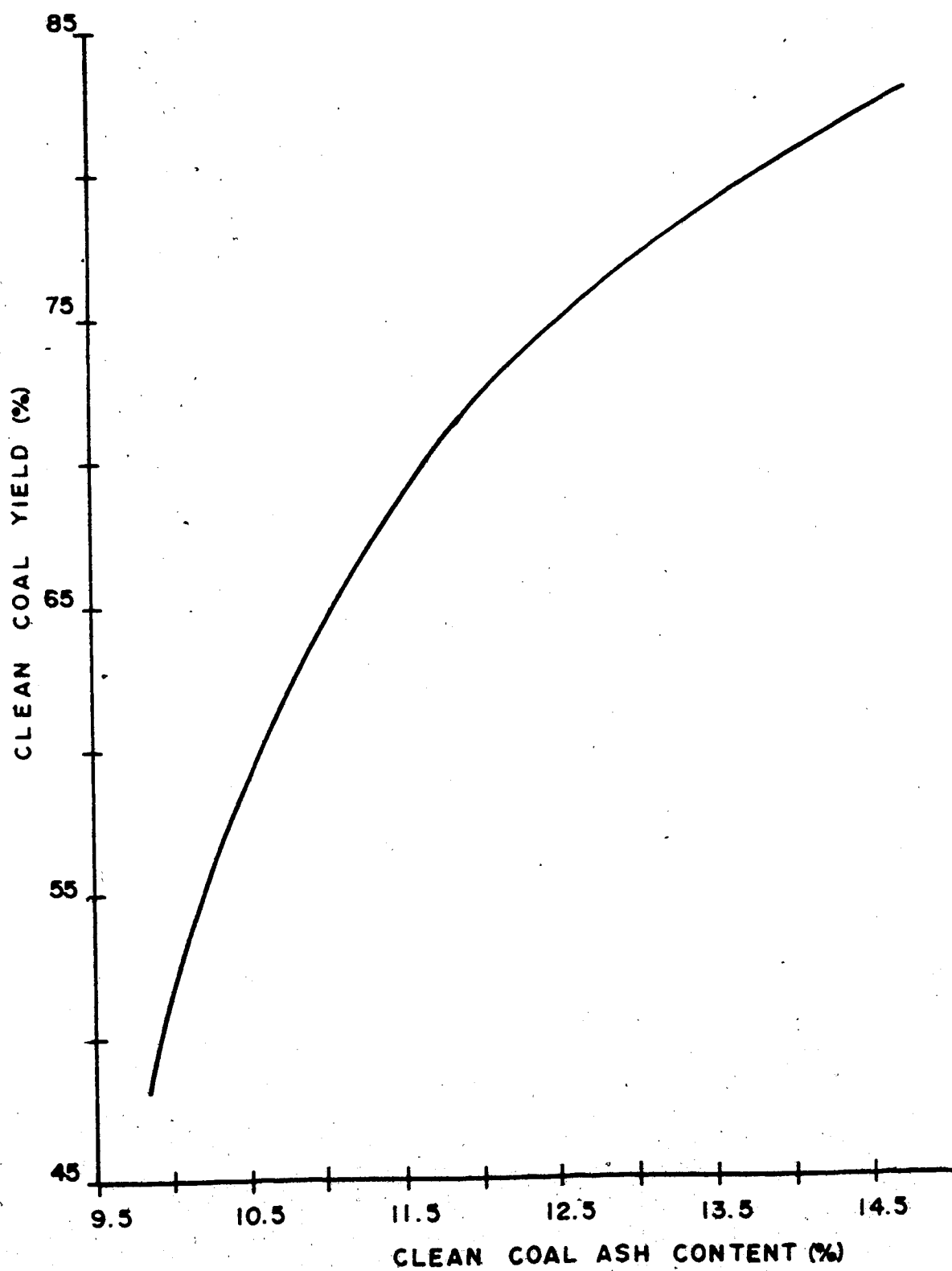
Figure 2.1 The Yield-Ash Curve for a Simulated Thermal Coal Preparation Plant.

Incorporating the constraint into the objective function gives the Lagrangian:

Maximize:

$$L(Y,\lambda) = \sum_j \sum_i M_{ij}Y_{ij} - \lambda \left(\sum_j \sum_i M_{ij}Y_{ij}A_{ij} - A_0 \sum_j \sum_i M_{ij}Y_{ij} \right) \quad ...(2.3)$$

where: λ = the Lagrangian Multiplier.

Every circuit has some control variable(s) which can be altered to produce a change in Y_{ij} (A_{ij}). Equation (2.3) can be maximized with respect to the Y_{ij} which then defines the control variable settings and A_{ij}. Taking the general partial derivative, setting the result equal to zero and rearranging gives:

$$\frac{\delta(Y_{ij}A_{ij})}{\delta Y_{ij}} = \frac{(1+\lambda A_0)}{\lambda} \quad ...(2.4)$$

The interesting result is that the right hand side of equation (2.4) is a constant, regardless of the coal block or cleaning circuit being considered. Now the ash content, a'_i of an incremental yield element ΔY of coal is defined as:

$$a^i = \frac{YA \big|_{Y+\Delta Y} - YA \big|_Y}{\Delta Y} \quad ...(2.5)$$

where: Y = yield.
A = ash.
a' = the ash content of the incremental yield element, hereinafter referred to as <u>incremental ash.</u>

In the limit as $\Delta Y \rightarrow 0^\cdot$, equation (2.5) reduces to the differential equation:

$$a^i = \frac{\delta(YA)}{\delta Y} \qquad \qquad ...(2.6)$$

From equations (2.4) and (2.6) the following important

conclusion can be drawn:

> To maximize production the coal must be washed to a
> constant incremental ash level regardless of the
> source or separation method. The actual value of
> this incremental ash is defined by A_0 and by the
> circuit yield-ash curves.

This argument, albeit restricted to perfect separators', was

advanced by Bird and Marshall in 1931(9). The result is

intuitive if, for example, one considers the specific case

of a two circuit plant. If these circuits are not operating

at the same incremental ash level then it is theoretically

possible to increase the plant yield while maintaining the

oduct ash quality. If circuit 1 has the lower

ntal ash then suppose an increment in production is

ed from this circuit with an equivalent decrement in

uit 2. The result is that the overall yield will remain

hanged but the product ash will decrease as a result of

quality differences in the production elements. When

ere is no difference in the incremental ash levels there

s no further driving force for change. This difference is

ploited until the yield is maximized at the product ash

specification.

'In perfect separators the incremental ash is equivalent to
the "elementary ash", a term which is frequently encountered
in washability studies.

To provide an appreciation of the importance of abiding by the steady state optimization criteria, Figure 2.2 is presented. This figure shows yield isopleths at a constant plant product ash quality for the simulated thermal coal plant mentioned in connection with Figure 2.1. (The axes represent the control variables for the two dense medium circuits employed in the simulation, i.e. the specific gravity of separation.) As expected, the optimal (maximum) yield corresponds to the solution of equation (2.4) for the particular value of A_0 chosen (11.5%). While the response surface is relatively flat in the neighbourhood of the optimum it is apparent that yield decrements on the order of $\approx 1\%$ could be easily incurred with slightly off-optimum operation. Even with thermal coal, losses of this nature represent a significant economic penalty.

2.4 CONSTRAINTS ON STEADY STATE OPTIMIZATION

Having defined the optimum operating scenario it is important to look at the technical practicality of implementation. It would be very difficult to measure incremental ash on-line. Probably the easiest method of implementing this strategy would involve model inference. This requires an accurate knowledge of the washability characteristics of the coal as well as the separation characteristics (partition curves) of the various unit operations in the flowsheet. (A further requirement is stable operation through close regulation of the process
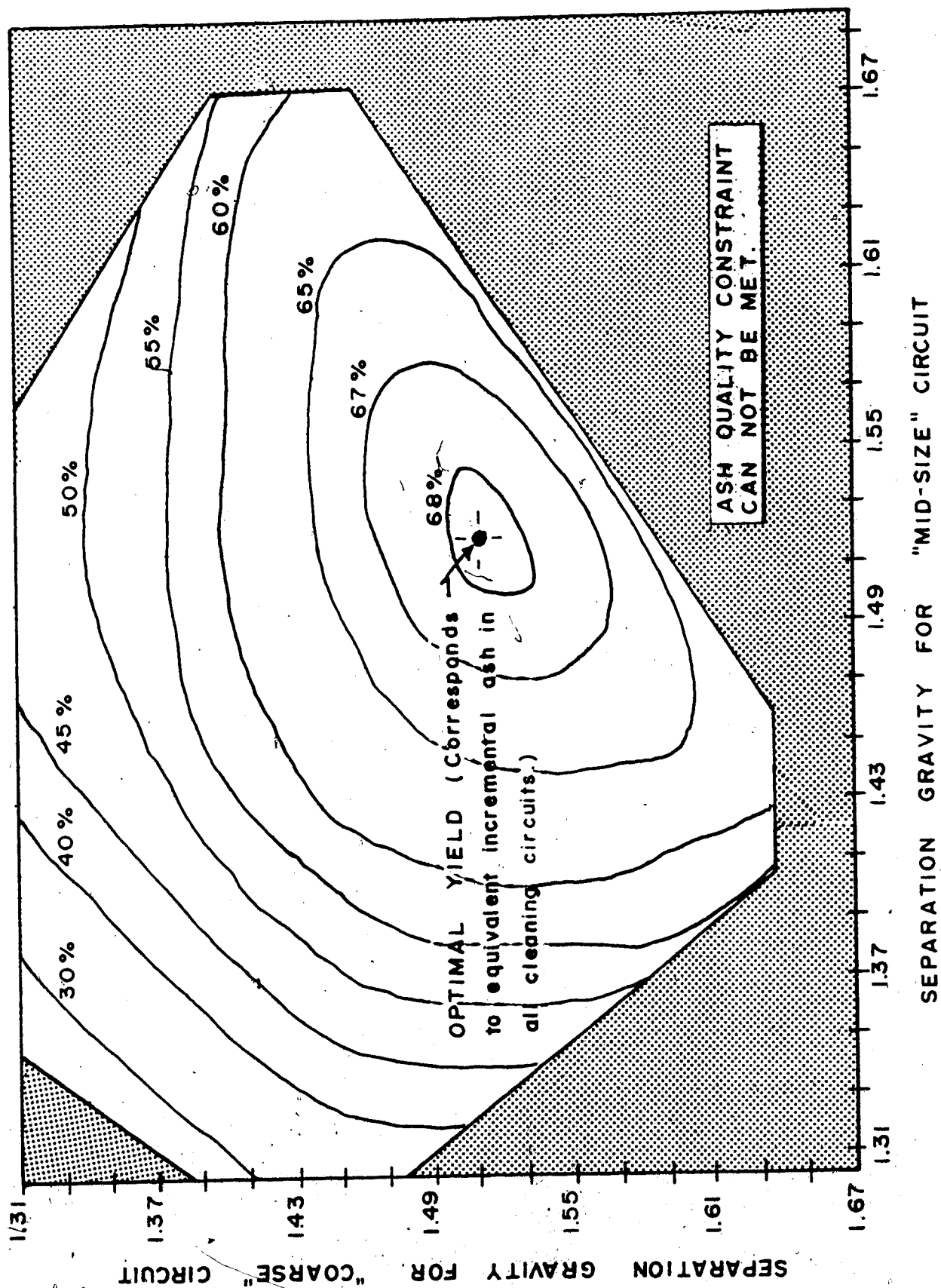
Figure 2.2 Yield Isopleths for a Given Product Ash in the Simulated Thermal Coal Plant.

control variables.) Implementing such a technique would require a very extensive investigative effort.

It has been argued that for density separators, which have near ideal partition curves, the incremental ash is strongly correlated with specific gravity. Therefore, fixing the specific gravity of separation will fix the incremental ash. Unfortunately, the ash-gravity correlation is often not that good, and the partition curves may deviate from near ideality depending upon changes in the operating conditions. Specifically, rigorous control of the separation density cannot be guaranteed under manual control. In summary, although the plant steady state optimization criteria are known, it is seldom possible to conform to them unless both the plant feed and plant operation remain stable over fairly long periods of time.

This raises another practical constraint on the theoretical steady state optimization strategy. That is, while the overall ash specification will be met in the long term, in the short term plant product quality may deviate considerably from A_0. This depends upon the washability characteristics of the particular coal block being treated at the time. This kind of deviation may not be tolerable and therefore it would be impractical to optimize production over the entire deposit. There is a time constraint (period) over which this methodology should be implemented, which is considerably shorter than the lifetime of the sales contract. The reason is that the buyer is expecting a

consistent product for coke blending or steam raising purposes. That is, each shipload of coal must meet contract specifications or be subject to penalty. For a typical cargo ship with a payload of 100,000 tonnes and a "typical" coal plant producing 2.5 million tonnes of clean coal per year, this time period is about 15 days. Furthermore, there exists an additional time constraint because of both unexpected upstream variations in the plant feed* as well as the methods used for storing coal at the terminal. In the latter case, stacking will result in additional product blending which may be deleterious to the anticipated quality of the shipment. The result is that the true optimization period is the time required to fill one unit train (capacity $\approx$10,000 tonnes) or approximately 1.5 days. In view of this time scale, and while longer term optimization remains important, the emphasis shifts to the shorter term optimization activity.

Considering this time constraint and the practical difficulty of implementing the constant incremental ash control philosophy, the operators attempt to maintain a constant plant clean coal product ash, A_t. (This target value is frequently slightly below the specification, A_0, to leave room for error. This is costly in terms of lost production.) For multi-circuit plants*, the operators set

----
* If, for some reason, the mining plan is altered, then the optimization exercise will be invalid if the coal to be cleaned has different washability properties from that which was expected.
* Most of the newer Canadian coal preparation plants feature multi-circuit flowsheets.

<u>individual circuit ash control targets which, based on their</u>

<u>knowledge of the plant feed characteristics, will provide</u>

<u>the desired quality of clean coal at a maximum yield for the</u>

<u>daily production</u>.

2.5 EXTERNAL OPTIMIZATION ASSISTANCE

There are a variety of means by which the coal
preparation quality control function can be made easier,
both from within and outside of the plant. Considering the
latter case, there are three principal methods of reducing
the "disturbance load" on quality control in the washery.

a) Blending and Feed Forward Control Through Mine

Production Scheduling.

Provided that a reasonable model (preferrably from

geostatistical analysis) of the deposit exists, the mine

is capable of providing quality information to the

preparation plant in advance of raw coal delivery. This

information may be used to set the plant for optimal

cleaning of a particular blend*.

b) Pre-Process Homogenization'

The use of large raw coal feed homogenization operations

(e.g. stacker and reclaimer) prior to the preparation

----

*Some interesting work has been done in France where the the
parameter set which describes the washability of the coal
has been modelled using a geostatistical approach. In this
case the mine could supply the plant with the washability
curves for the coal they will be receiving which would
simplify the control problem. (see J. Int. Ass. Math. Geol.,
Vol. 13, No. 4, 1981, pg. 321)
'These methods are much more rigorous in their attempt to
blend the coal than the standard product surge stockpiles
common to all coal preparation plants.

stage will yield a more consistent plant feed. A more

consistent feed reduces the demand for process control

action and will improve yield.

c) Post-Process Homogenization

This method involves the homogenization of plant

product, as described by Butcher and Beninger(10). In

essence, the implications on preparation pant operation

are identical to those in (b), however, the total solids

to be handled is significantly reduced in comparison.

Of the three methods, only (a) is practiced to any

extent in North America. Method (b) is popular in Europe and

method (c) has been investigated by various operating

concerns but has never been implemented on a large scale.

2.6 PROBLEMS WITH CURRENT PROCESS CONTROL PRACTICE

It was stated above that the typical operator process

control strategy was to establish target clean coal product

ash values for the various cleaning circuits. Using "grab

samples" with turn-around times of from 2 h to 24 h,

depending upon the plant, the control variables are modified

in an effort to maintain the product ash close to set point.

In many instances this feedback control loop is ineffective

for the following reasons:

a) sample frequency is too low,

b) sample is not representative,

c) the human controller does not have a quantitative

understanding of the process, i.e. the relationship

between control variables and process behaviour.
In these cases only long term (i.e. daily or weekly) control
action is specified depending upon trends in the the
cumulative plant product quality.

The task of maintaining clean coal product quality
while maximizing yield from a preparation plant is not easy
under present conditions. There is strong motivation to
improve upon current methods.

2.7 OPTIMIZATION THROUGH PROCESS CONTROL: ECONOMIC IMPLICATIONS

Choosing a target ash value in each cleaning circuit to
achieve optimum yield is, in essence, the operators's
physical solution to equations (2.1) and (2.2), under the
constraints previously discussed. However, even though
control set points are established, it can be easily
demonstrated in most plants that there is a significant
variation in product ash. Furthermore, the mean values may
not correspond to the targets. These variations are the
combined effects of process disturbances and ineffective
process control. The disturbances may be classified as:

(1)   **Intrinsic Disturbances**
        Those disturbances resulting from changes in the
        physical and/or physiochemical properties of the
        coal (e.g. washability characteristics, size
        consist, floatability, etc...).

(2)   **Extrinsic Disturbances**

Those disturbances resulting from changes in the normal process equipment operation, the control variable settings and the "gross" character of the feed stream (e.g. mass flowrate, slurry solids content, media density, etc...).

Changes which arise from intrinsic disturbances require that the target value for the circuit be re-assessed. This requires detailed knowledge of both the new properties as well as of process behaviour. It is important that the operator identify and react to changes of this type, however, this is not an easy task. In fact, solutions to control problems of this type can only be evaluated when successful strategies and systems have been developed for extrinsic disturbances.

Extrinsic disturbances are important since, in these cases, deviations from set point are undesirable. In general, each washing circuit within a coal preparation plant is operated independently, reflecting their physical independence. (e.g. see Figure 1.1) Each circuit should be controlled to maintain target for the sake of operational simplicity. The discussion which follows relates to the economic implications of extrinsic disturbances under this set of circumstances.

In the discussion, it is implicity assumed that the target ash set points for the individual circuits are set to provide equivalent incremental ash in the clean coal products. Clearly, any deviation from this condition will

result in a production loss. Because of the complexity of the control problem it is expected that this production loss is beyond the limits of the control systems currently envisaged for coal preparation plants. For this reason this type of production loss is excluded from further consideration.

One can consider two contributions to production loss which result from variation in product ash due to extrinsic disturbances. The first arises simply because of the variation itself (direct production loss) and the second arises from conservative set point specification (indirect production loss) as a result of the variation. They are treated separately below.

2.7.1 Direct Production Loss

There are a number of mathematical means of demonstrating that production from a process, operating on a given yield-ash curve, is maximized if the process is maintained at the set point. To minimize the number of restrictive assumptions which are required for analytical solution and to demonstrate the interrelationship of the variables, a simple technique is presented.

Rather than operate exclusively at set point, coal cleaning units, or circuits, or plants, show a distribution of operating regimes about the overall mean. This can be seen by sampling a product stream over time and analysing for the solids ash content. The distribution can be thought

of as balanced periods of undercleaning and overcleaning such that the overall mean ash content is maintained. This is the approach used by Cammack and Balint(11). Although arriving at the correct conclusion their algebraic proof was unsatisfactory, in the opinion of the author. An alternate solution is offered here.

The ash balance for the off-average operating periods is written as:

$$\bar{A} = \frac{FY_x A_x t_x + FY_z A_z t_z}{FY_x t_x + FY_z t_z} \qquad \ldots (2.7)$$

where: $(\bar{A},\bar{Y})$ =mean operating point on the yield-ash curve.
(A_x,Y_x) =overcleaning (i.e. $A_x<\bar{A}$) operating point.
(A_z,Y_z) =undercleaning (i.e. $A_z>\bar{A}$) operating point.
t_z,t_x =time of undercleaning and overcleaning respectively.
F =solids mass flowrate to the cleaning process.

Assuming that in the neighbourhood of $(\bar{A},\bar{Y})$, the yield-ash curve can be approximated by a linear function of the form:

$$Y=\bar{Y}+m(A-\bar{A}) \qquad \ldots (2.8)$$

where:

$$m=\frac{dY}{dA}\bigg|_{(\bar{A},\bar{Y})} \qquad \ldots (2.9)$$

the tonnage loss, L, over the combined period (t_z+t_x) is calculated as:

$$L=F\{\bar{Y}(t_x+t_z)-Y_x t_x-Y_z t_z\} \qquad \ldots (2.10)$$

Substitution of the appropriate form of equation (2.8) into equations (2.7) and (2.10) with rearrangement allows

equation (2.10) to be written in the form:

$$L = Fm(\bar{A} - A_x) t_x \left[1 - \frac{\bar{Y} - m(\bar{A} - A_x)}{\bar{Y} + m(A_z - \bar{A})} \right]$$

...(2.11)

This equation constrains L to be non-negative. The production loss is observed to increase with';

a) an increase in the slope, m, of the yield-ash curve at the mean operating point,

b) the magnitude of the differences between the off-average ash values and the mean,

c) the duration of the off-average operation.

On the basis of this analysis the process control or optimization objective is to minimize the effects of (b) and (c) on process system performance.

To translate these observations into the production environment and to illustrate the effects of (b) in particular, consider the curves shown in Figures 2.3(A) and 2.3(B). This simplified example indicates the impact of variance reduction on direct production loss. Case 1 on Figure 2.3(A) shows a separation with a highly varying instantaneous product ash. Combining this instantaneous ash curve with the yield ash curve of Figure 2.3(B) allows the cumulative production statistics to be calculated, $(\bar{A}, \bar{Y})$. Observe that the cumulative product ash (as $t \to \infty$) has a value of $\bar{A}_1 = 9.21\%$ which is greater than the mean value of the instantaneous ash, $\bar{a}_1 = 9.0\%$. This is expected since the slope

_____

'These findings have been verified using numerical methods.
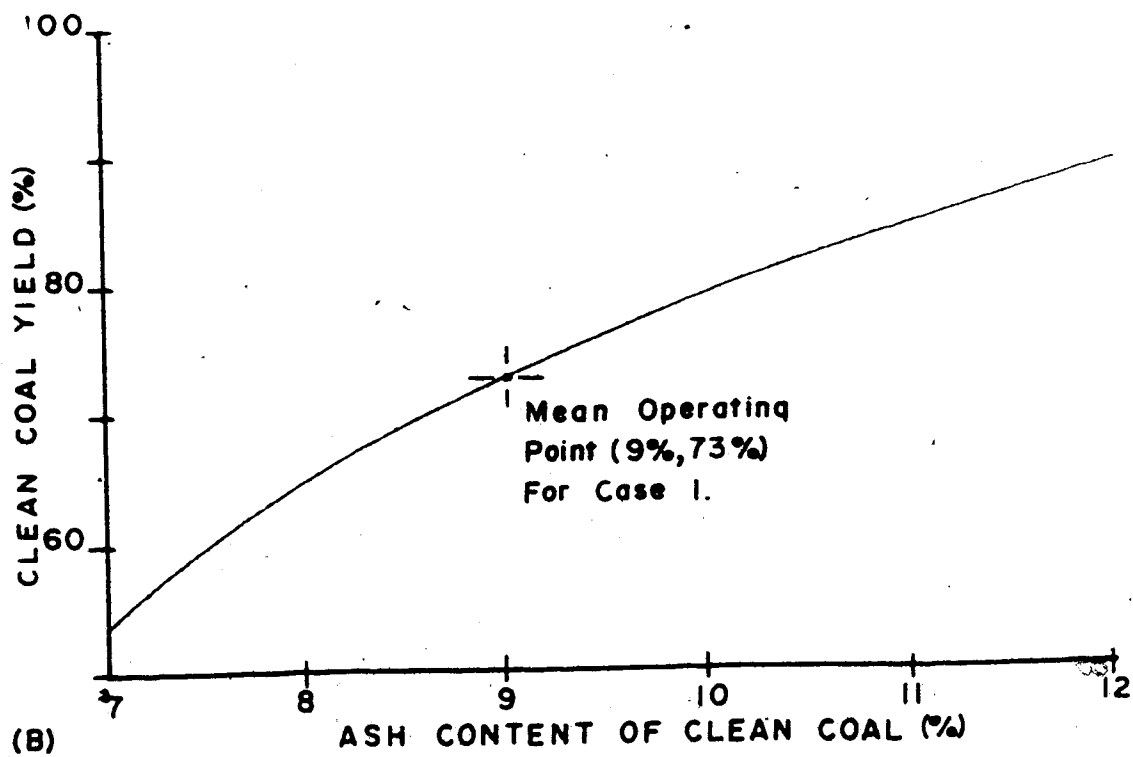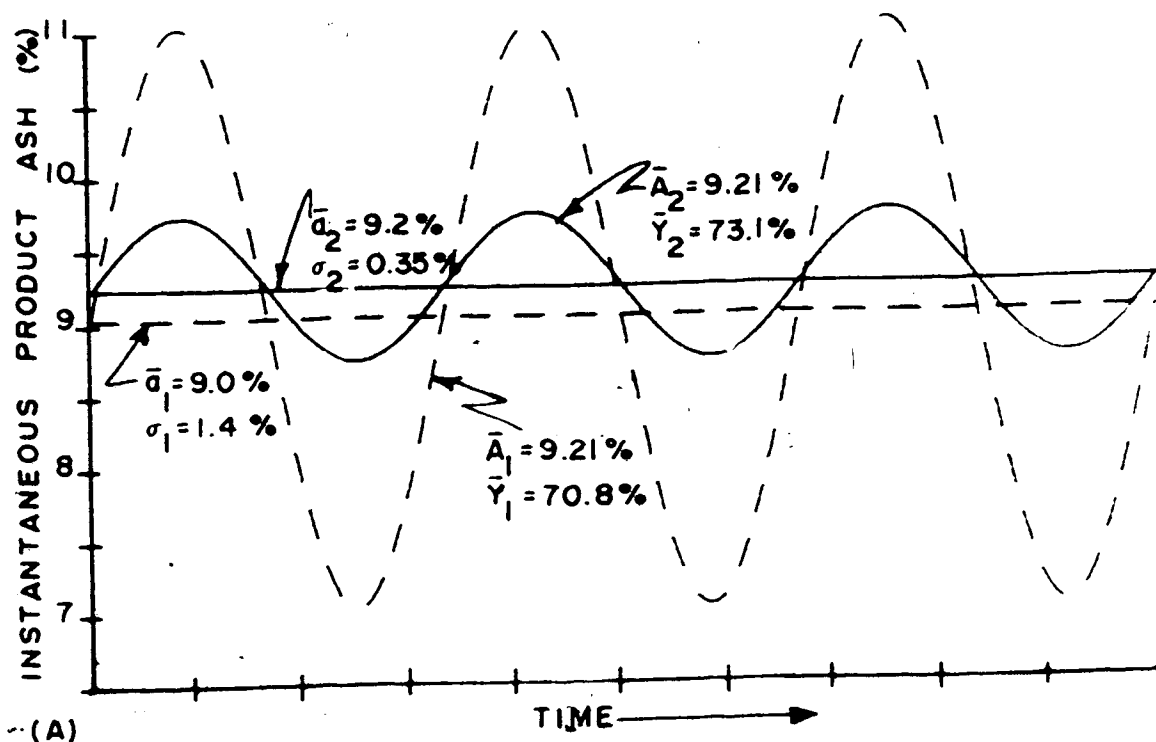
Figure 2.3 An Illustration of Direct Production Loss Through Quality Variation.

of the yield-ash curve at the mean operating point is non-zero. Now, assuming that the variance in the instantaneous product ash can be reduced by $\approx 94\%$ gives the results shown for case 2. Here, the mean instantanteous product ash value, $\bar{a}_2$, has been adjusted to make the cumulative ash values equal, $\bar{A}_1 = \bar{A}_2$. The important observation is that the yield increase obtained by reducing the variance is significant (2.3% for the example). Moreover, as the variance is reduced and, as a consequence, $\bar{A} \to \bar{a}^\cdot$, the potential for improving the yield decreases very rapidly. However, experience has shown that many western Canadian coal processing circuits have a rather substantial variance in the instantaneous product ash and there is considerable economic incentive to pursue variance reduction through improved process control. An example of this will be given in sub-section 2.7.3.2.

2.7.2 Indirect Production Loss

Producers generally specify the plant product ash value, $A_\cdot$, to be somewhat lower than the sales contract value A_0. The magnitude of the difference, $A_0 - A_\cdot$, is governed by the variance of $A_\cdot$ in the shipments. The objective is to reduce the probability of delivering coal with an ash value greater than A_0. Methods of reducing this variance such as those described above will allow $A_\cdot$ to be increased while maintaining the low probability of over specification shipments. This is illustrated in Figure 2.4

where, for the sake of simplicity, the ash quality of the

clea▮▮▮ shipments has been assumed to be normally

dist▮▮▮▮ (Wells (see (12) Chap. 3) has used this in

anal▮ economic payback of control systems.)

▮cre▮▮ will result in an increase in plant yield, $Y.$,

▮d h▮▮ reduce the indirect production losses.

2.▮ ▮ethods of Assessing the Economic Impact of Improved
Process Control

Before committing the required capital and operating

fu▮ to a process control project, management has to be

con▮▮ced that;

a)   ▮▮e technology to do the job either exists or can be
developed with the resources at hand,

b)   t▮ project makes good economic sense (e.g. acceptable
▮▮unted cash flow rate of return).

This sub-section deals with some facets of (b).

In order to perform the economic analysis it is

necessary to estimate the direct and indirect production

changes which are expected from the reduction in product ash

variance. This knowledge also allows the operator to

establish priorities within the plant. There are two methods

which may be used to quantify the production change.

2.7.3.1 Direct Estimation of Yield Increase

Based on the experience of other plants which have

undertaken similar projects, or, on good engineering

judgement, one estimates the yield increase expected
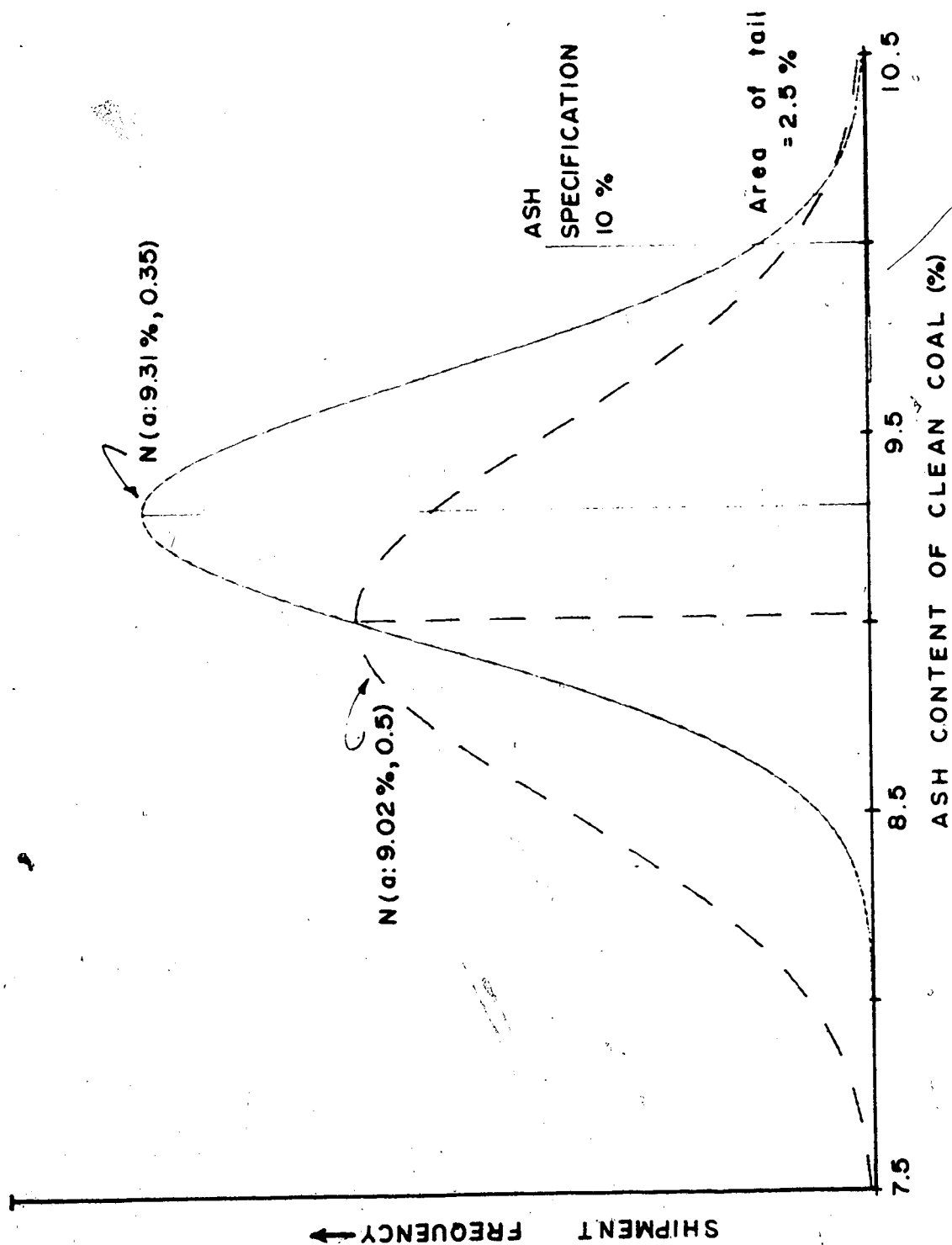
Figure 2.4 An Illustration of Indirect Production Loss.

from improved process control. The additional production can be calculated from the feed rate to the process system, and, after correction for the increased operating and capital costs, the before tax cash flow is estimated. In the absence of any other information Wells(12) suggests that a yield increase of ≈1% is a good conservative estimate.

2.7.3.2 Estimation of Yield Increase Through Variance Reduction

This method represents a more realistic means of estimating the yield increase discussed above. It is a generalization of the concepts introduced in the example presented in Figure 2.3. (The "best" technique for quantifying the reduction is treated in detail in the next section.) It was been observed in connection with equation (2.11), point (b), that variance reduction has the overall effect of reducing direct production loss and allowing for the reduction of indirect production losses. The former is generally much easier to calculate than the latter. The reason is that the contribution of the product ash variation of a circuit to the overall plant product ash variation is a function of the period required to produce a shipment. That is, it is required that the variation in ash quality per shipment period from the circuit be known. This depends upon the frequency of the disturbances which enter the circuit and their effects on product quality. This kind of

information is only available through extensive
sampling. <u>It is suggested that economic calculations be
based on direct losses, recognizing that there will be
some further benefit which may accrue from indirect loss
reduction.</u>

To estimate direct production change from variance
reduction requires the following:

a) A knowledge of the typical distribution of product
ash quality in time. This is usually obtained by
high frequency sampling (i.e. >3 samples per h)over
an extended period (>100 samples).

b) A knowledge of the yield ash curve over the region
of interest. This can be obtained through
experimentation, by mathematical models and digital
simulation, or by good engineering judgement.

There are a number of theoretical sampling distributions
which may be used, in preference to the experimental
histogram, to model the data from (a), although the
normal approximation is commonly employed'. The fact
that the ash data are not independent is not of concern
since it will not affect the calculations. The
distribution is simply a convenient way of summarizing
the observed data. If f(a) is the probability density
function describing the distribution of the measured
product ash content such that:

'The validity of this assumption should be be checked using
a χ^2 test.

$$\int_{-\infty}^{+\infty} f(a)\,da = 1 \qquad\qquad \ldots(2.12)$$

and;

$$N\{f(a); \bar{a}, \sigma(a)\}$$

where: a = "instantaneous" product ash.

$\bar{a}$ = arithmetic mean product ash derived from the sampling campaign.

$\sigma(a)$ = the standard deviation of a, also derived from the sample data.

$N\{f(a); a, \sigma(a)\}$ = a normally distributed variate, $f(a)$, with mean, $\bar{a}$, and standard deviation, $\sigma(a)$.

the cumulative product ash from the system is calculated

as:

$$\bar{A} = \frac{\displaystyle\int_{-\infty}^{+\infty} Y(a)\,a\,f(a)\,da}{\displaystyle\int_{-\infty}^{+\infty} Y(a)\,f(a)\,da} \qquad\qquad \ldots(2.13)$$

where: $\bar{A}$ = cumulative product ash.

$Y(a)$ = the functional relationship between yield and ash.

Now, if one speculates on the fractional variance

reduction, r, then a new distribution function $f'(a)$ is

defined where:

$$N\{f'(a); \bar{a}', \sqrt{r}\sigma(a)\}$$

with: $0 \leq r \leq 1$

Re-solving equation (2.13) under the conditions $\bar{a}' = \bar{a}$

provides a new value for the overall product ash, $\bar{A}'$,

which will be less than $\bar{A}$. To satisfy the condition that

$\bar{A}' = \bar{A}$ requires an iterative solution for $\bar{a}'$, and, since

this $\bar{a}'$ will be greater than $\bar{a}$, the average yield

(denominator in eqn. (2.13)) will increase. The yield difference is the estimate required in the previous sub-section. A word of caution is necessary. It is <u>very</u> <u>important</u> that the relationship Y(a) be as accurate as possible since the yield difference is very sensitive to this function.

To illustrate, a local metallurgical coal plant treats 2.8 million tonnes of raw coal per year. There are two circuits in the plant, one for the coarse coal (>0.6mm)' and one for the fine coal. The fine material is prepared entirely by froth flotation and represents, on average, 35% of the plant feed. A sampling campaign on the froth product from the fines circuit gave the following results $\bar{a}$=8.75%, and σ(a)=1.5%. Composite sampling over a bank of flotation cells provided the estimate of the functional form of Y(a) as:

$$Y(a) = \begin{cases} 70.1+7.56(a-8.625)-1.24(a-8.625)^2 \; ; \; a \leq 9.75 \\ 80.0+0.1(a-9.75) \; ; \; a>9.75 \end{cases} \quad \ldots (2.14)$$

Assuming that f(a) is normally distributed and solving equation (2.13) by numerical methods yields; $\bar{A}$=8.99% and $\bar{Y}$=68.3%. If a variance reduction of 25% (i.e. r=0.75) can be reasonably expected, the iterative solution of equation (2.13) for the case $\bar{A}'=\bar{A}$=8.99% yields; $\bar{a}'$=8.82% and $\bar{Y}'$=69.6%. The expected yield increase is 1.3%. At the production levels specified and using a coal price

of $50/tonne f.o.b the mine gate, the increase in yearly
cash flow before tax is $637,000. This neglects any
additional operating and capital costs which may be
incurred, although these are expected to be small. The
economics suggest that there is good reason to improve
upon process control in the fine coal preparation
circuit.

2.8 AN IMPROVED METHOD OF ESTIMATING THE POTENTIAL REDUCTION IN ASH QUALITY VARIANCE

In the previous sub-section a method of estimating the
economic impact of reducing the product ash variance was
discussed. It required that a <u>reasonable</u> estimate of
variance reduction be made. However, in the absence of
detailed knowledge of the time trajectory of the ash content
the resulting estimates can provide grossly misleading
results. For example, if the ash "signal" contains primarily
very high frequency "noise" then little, if any, variance
reduction can be effected by conventional feedback control
systems. (In this case the investigator must establish what
the "generator" is for this noise and attempt to deal with
it first.) This section provides a method of making
reasonable estimates of the potential variance reduction
from extrinsic disturbances using automatic control systems.
In addition, the information extracted can be used to
speculate on the technical feasibilty of such control
systems. It is discussed in a "recipe" format to keep the

treatment as brief as possible.

The technique to be described is part of the general subject of "Spectral Analysis." There are a multitude of books on the subject but the one by Rayner(13) is particularly readable, even for the neophyte. In essence, the method involves fitting a Fourier series to suitably transformed data and then estimating the variance components according to frequency. Low frequency contributions of less than one cycle per hour are expected to be virtually eliminated by automatic feedback control systems. Thus variance reduction can be be more accurately estimated and, in addition, the amenability of the process to control can be evaluated. Another feature of the variance versus frequency spectrum is the identification of "noise" generators, conspicuous by peaks in the spectrum. This may provide the operator with important "clues" in the search for physical causes of process upset.

The method is taken almost directly from Rayner's book. Since this represents a condensation of the underlying theory and because additional comments are required relative to this application, the method is given in detail rather than simply by reference. To illustrate the results of calculating a variance spectrum and to provide a test case for the reader an example is included.

Step (1):Gathering the Raw Data

For the purposes of this analysis the operator is required to sample the process stream of interest at regular intervals for an extended period of time. For statistical integrity of the data at least 100 samples (see Wells-Chap. 3) must be collected. Ideally the entire exercise would be repeated several times although the variance spectrum is often observed to be more stable than the Fourier coefficient spectrum. For coal preparation units, or circuits, or plants, sampling frequencies of greater than 1 sample per h, typically 3 samples per h, are recommended. In addition, it is desirable to make some high frequency cuts (say >6 samples per h) prior to finalizing the sampling schedule. This allows an estimate of the contribution from the very high frequency component and is useful in defining the sampling interval. High frequency contributions which are present but not accounted for will manifest themselves through the phenomenon of aliasing (superimposed on lower frequencies) and provide an incorrect spectrum. In coal preparation this component is often observed to be negligible.

The data must be contiguous in time and obtained at regular intervals. If the latter can not be strictly adhered to in all samples, interpolation may be used. If mechanical interruptions are experienced, both the control as well as the process variables must be set to the previous levels after start-up and sufficient run-in time allowed before restarting the sampling. If the ash level varies

significantly over the interruption the analysis can not be applied. If there are too many mechanical interruptions then perhaps the biggest problem in plant operation is not process stabilization.

Symbolically, the data points are referred to as the set of (j, a_j); $j = 0, 1, \ldots, d-1$, where a total of d samples were taken.

Step (2) Remove the Mean and Long Term Trends

The mean and long term linear trend are removed from the ash data to reduce them to a perturbation measure. This is required to suppress their influences from appearing in the zero frequency component which can also blur the higher frequencies. This step is accomplished by first regressing a_j on j using the simple linear model:

$$\hat{a}_j = b_0 + b_1 j \qquad \ldots (2.15)$$

where: b_0, b_1 = the unweighted least squares estimate of the intercept and slope respectively.
$\hat{a}_j$ = the predicted value of ash at "time" j.

If the regression is significant, i.e. if an "F-test" shows that the true slope is different from zero, then the raw ash data is transformed as:

$$a_j' = a_j - \hat{a}_j \qquad \ldots (2.16)$$

otherwise the raw data is transformed by subtracting the mean ash value, $\bar{a}$:

$$a_j' = a_j - \bar{a} \qquad \ldots (2.17)$$

where: a_j' =perturbation quantity.

Step (3) Applying the Window Function (Tapering)

The perturbation quantity from step (2) must be multiplied by a window function to render the theoretical development of the variance equations valid. The one suggested by Rayner is Tukey's cosine bell. Here, the first 10% (an arbitrary value in the range 5%-25%) of the data are multiplied by a rising cosine bell and the final 10% by a falling cosine bell. Let g=d/10, then this function will have the form:

$$h_j = \begin{cases} 0.5\{1-\cos(\pi j/g)\}; & 0 \leq j < g \\ 1 ; & g \leq j \leq d-g \\ 0.5\{1-\cos(\pi[d-j]/g)\}; & d-g < j \leq d-1 \end{cases} \qquad ...(2.18)$$

where: h_j =window (filter) function at time j.

and the new variable to be used in the subsequent calculations is aa_j, where:

$$aa_j = a_j' h_j \qquad ...(2.19)$$

This second transformation has the effect of reducing the overall variance somewhat but should not alter the variance spectrum appreciably. The result of this operation is that the estimate of variance at a particular frequency is not a discrete estimate, rather it is the estimate for a band

centred at that frequency.

Step (4) Adding Zeroes

Zeroes may be added to the end of the data record of aa_j. This is done to adjust the frequency bands in the variance histogram to the desired widths and central frequencies (see Step (6)). This "cosmetic" alteration reduces the overall variance by a predictable amount but leaves the spectrum unaffected.

The number of zeroes to be added is made equal to n-d such that a total of n entries are in the aa_j data record.

Step (5) Compute the Fourier Coefficients

The data record from step (4) can be fitted with a Fourier series of the form:

$$aa_j = \frac{c_0}{2} + \sum_{k=1}^{k_{max}} \{c_k \cos(2\pi kj/n) + s_k \sin(2\pi kj/n)\} \quad ...(2.20)$$

where the Fourier coefficients are calculated from the expressions'[*]:

$$c_k = \frac{2}{n} \sum_{j=0}^{n} aa_j \cos(2\pi kj/n) \quad ; \quad 0 \le k \le k_{max} \quad ...(2.21)$$

and,

$$s_k = \frac{2}{n} \sum_{j=0}^{n} aa_j \sin(2\pi kj/n) \quad ; \quad 0 \le k \le k_{max} \quad ...(2.22)$$

where:

'[*]Other, faster methods may be employed to expedite these calculations.

$$k_{max} = \begin{cases} n/2 & \text{; if } n \text{ even} \\ (n-1)/2 & \text{; if } n \text{ odd} \end{cases} \qquad \ldots (2.23)$$

since there must be only as many coefficients as there are data points.

Step (6) Calculation of the Variance Spectrum

For periodic or non-periodic data[']['] the variance contributions from the various frequencies ($k=0,1,\ldots,$kmax cycles per sampling period) are calculated as:

$$V_0 = \left[\frac{c_0}{2}\right]^2 ; \qquad k=0$$

$$V_k = \left[\frac{c_k^2 + s_k^2}{2}\right] ; \quad 1 \le k \le k_{max} - 1 \qquad \ldots (2.24)$$

$$V_{kmax} = \left[\frac{c_{kmax}}{2}\right]^2 ; \quad k = k_{max}$$

where: V_k =variance contribution from frequency k. These values are collected according to the standard rules of histogram generation and displayed in this form as the variance spectrum.

Table 2.1 and Figure 2.5(A) contain some hypothetical plant data for the previously discussed flotation circuit (sub-section 2.7.3.2). It is hypothetical in the sense that it represents two contiguous records obtained on consecutive days and "pieced" together for this example. Samples of the flotation concentrate were taken every 20 minutes and the solids analysed for ash. In step (2), the regression was

----
[']['] In the theoretical development of this method the data is assumed to be non-periodic. There are few truly periodic functions in nature.

Table 2.1 Hypothetical Data for Spectral Analysis

TIME(j)	ASH(%)	TIME(j)	ASH(%)	TIME(j)	ASH(%)
1	7.24	31	9.80	61	9.38
2	6.81	32	9.10	62	9.08
3	7.08	33	8.40	63	9.34
4	6.37	34	8.30	64	9.68
5	7.68	35	8.20	65	9.45
6	7.42	36	8.70	66	8.98
7	8.46	37	8.40	67	8.98
8	10.77	38	7.90	68	9.72
9	11.58	39	7.40	69	10.66
10	11.56	40	7.13	70	9.91
11	11.69	41	6.98	71	9.86
12	10.71	42	6.70	72	9.66
13	10.66	43	10.12	73	9.87
14	10.16	44	10.38	74	10.01
15	11.32	45	9.81	75	10.04
16	11.70	46	9.64	76	10.15
17	13.25	47	10.83	77	10.31
18	11.88	48	11.33	78	10.44
19	11.90	49	10.82	79	10.12
20	10.90	50	8.64	80	10.13
21	9.73	51	7.51		
22	9.18	52	8.14		
23	9.24	53	6.69		
24	11.74	54	7.00		
25	10.90	55	6.98		
26	9.50	56	6.90		
27	10.50	57	9.29		
28	10.94	58	9.26		
29	9.70	59	9.57		
30	10.00	60	9.20		

insignificant and the raw data were transformed using equation (2.17). In step (4), twenty zeroes were added to the record for a total of n=100 points. This was done to have the class boundaries in the spectrum histogram integer valued. The variance spectrum is shown in Figure 2.5(B) and given in Table 2.2.

Table 2.2 The Variance Spectrum for the Hypothetical Data

CENTRAL FREQUENCY K	VARIANCE COMPONENT	PERCENT CONTRIBUTION
0	0.5209	34.93
4	0.4888	32.77
8	0.2239	15.01
12	0.0846	5.67
16	0.0536	3.59
20	0.0512	3.43
24	0.0183	1.22
32	0.0213	1.43
36	0.0182	1.22
40	0.0042	0.28

The estimate of variance reduction, assuming that components with a frequency lower than about one per one and one-half hours can be eliminated, is 92%. If this were real data, then, since the sampling period was quite short, i.e. <27 h, it would probably be fair to say that the observed trajectory is predominantly the effect of extrinsic disturbances. Thus, at least on the basis of this analysis, process control would have a very significant effect in stabilizing the operation and reducing direct production losses.
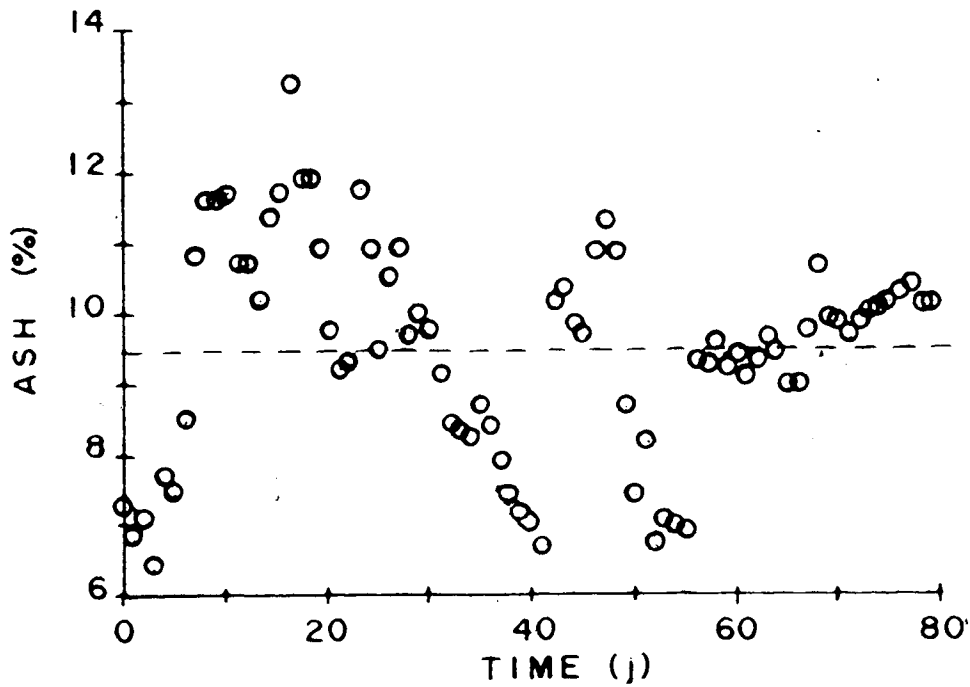
(A)
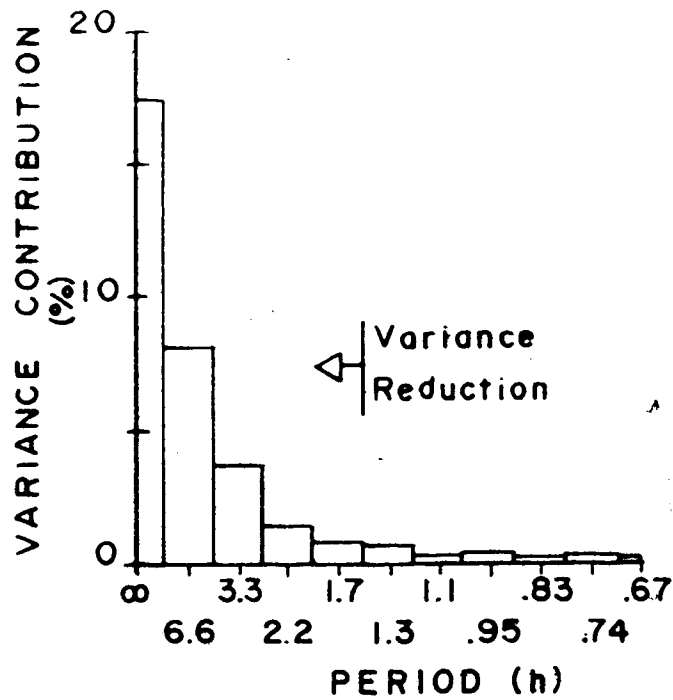
(B)

Figure 2.5 The Hypothetical Data and the Resulting Variance Spectrum.

2.9 SUMMARY

It has been shown that, in theory, it is desirable to have each circuit within a coal preparation plant operating at steady state with a constant incremental ash in the clean coal products, subject to an overall product ash constraint. In practice this is extremely difficult to do and it is observed that the operator specifies control set points on product ash, as an indirect measure of incremental ash, in his attempt to optimize plant performance. However, the lack of effective plant control systems results in significant variations in product quality and hence both direct and indirect production losses are experienced. While some of this variation is "genuine", in the sense that it is caused by intrinsic disturbances, the balance is a result of extrinsic disturbances and must be eliminated. Methods have been presented for quantitatively assessing the technical feasibility and economic impact of control systems. There is considerable potential for improving process performance through optimization. This should lend some impetus to improving process control systems, principally through the development of sensors (instrumentation) and through increased process understanding.

3. PRELIMINARY IN-PLANT TESTING

3.1 THE DATA ACQUISITION PROGRAM

Before designing the laboratory experimental program to evaluate the OSCAA prototype it was necessary to define some of the relevant operating parameters. Since McIntyre Mines Ltd. had been chosen to take part in the plant trial phase of the project it was decided that these values should be determined in this plant. A plant data acquisition campaign was conducted at the mine site in August, 1979. The detailed results of this work are reported elsewhere(14) and a summary of the relevant information is given below. For background information and because it will discussed again in Chapter 8, a brief description of the McIntyre operation is given.

The McIntyre Mines Ltd. coal preparation plant is designed to produce approximately 2 million tonnes of clean coal per year. The product is shipped primarily to Japan for use in steel manufacture. The plant consists of two washing circuits. A heavy medium cyclone circuit is used to prepare the coarse coal (>0.6mm) and a froth flotation circuit treats the fine fraction. The fine material in the plant feed averages 35% by weight and excursions to 40% are not uncommon. A schematic of the flotation circuit is presented in Figure 3.1. It consists of four parallel and identical banks of four WEMCO #120 flotation cells. Process control is practiced on two levels. For short term modifications to the
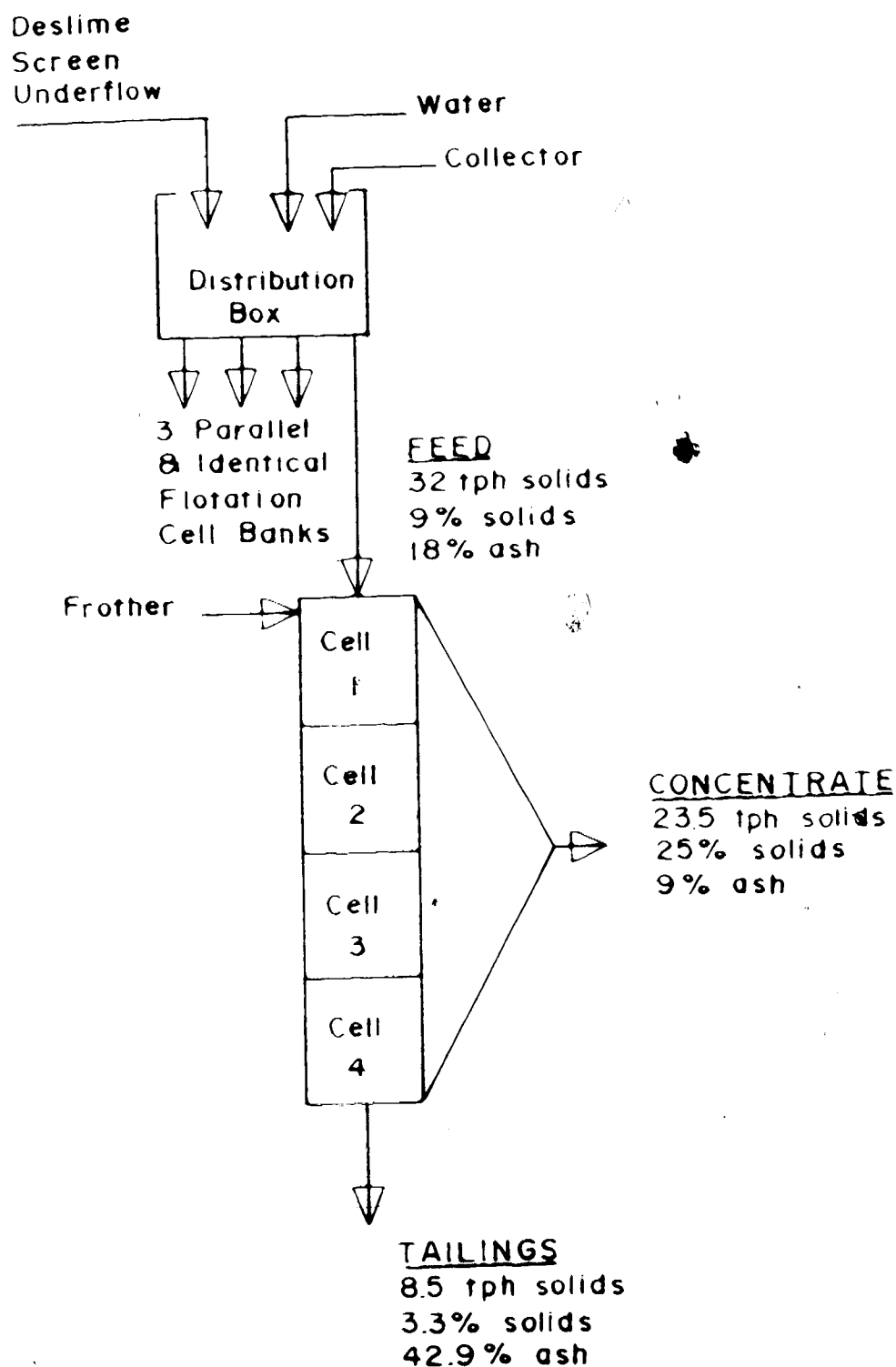
Figure 3.1 The Flotation Section at McIntyre Mines (after McIntyre(15)).

control variables the operators use a visual interpretation of process behaviour. In this regard, pulp level seems to be the principal manipulated variable. Reagent addition rates are modified on orders from the quality control laboratory personnel. Decisions on these rates are made on the basis of daily composite sample ash values for the clean coal product in conjunction with historical trends in product quality. The target ash value for the flotation circuit is 8.5%. It appears that, as a result of the ill-defined nature of the flotation process, fine tuning on plant product quality is done principally by adjustments in the coarse coal circuit.

When compared to other metallurgical coal plants treating coal in the same general geological setting, McIntyre's fine coal circuit is uniquely simple. This single unit operation approach is possible because the "oily" nature of their coal gives it a high inherent floatability. However, blocks of oxidized coal which are encountered from time to time are essentially lost to tailings under this processing scheme. In other plants, the coarser fraction of the fine material (typically -.6mm $\leq$ X $\leq$ .15mm) is treated using the automedium cyclone which effectively separates on the basis of particle specific gravity (see Figure 1.1).

3.1.1 Fine Coal Preparation Circuit Behaviour

The purpose of this portion of the data acquisition campaign was to observe the flotation circuit ash quality both on a long term (daily composite) and a short term ($\approx$20

minute intervals) basis. The results were used to define the need for improved process control as well as to establish calibration ranges for the laboratory investigation of OSCAA. The "long term" data were obtained from the Quality Control Lab. at McIntyre while for the latter, a particular bank of flotation cells was sampled.

Figure 3.2 illustrates the variation in the fine coal product ash over a 30 day production period in the summer of 1979. The quality control target of 8.5% is shown as the dashed line. The samples from which the data were derived represent a 24 hour composite with a total of 3 cuts, one per shift. It is evident by inspection that there is a significant fluctuation in quality around the target value. The two moments of interest calculated from the data are; mean ash=8.9%, and the variance=0.55%^{2}. Not only are there fluctuations in quality, but the long term observed mean does not correspond to the set point. It is impossible to determine whether these deviations are due to intrinsic or extrinsic disturbances. However, the fact that a target value is defined and very seldom met is a comment on the control problem using existing methods. For example, there are several consecutive-day periods where a substantially constant offset was experienced with no apparent success in modifying circuit performance. These results demonstrate a need for improved process control methods in the McIntyre fine coal preparation circuit.
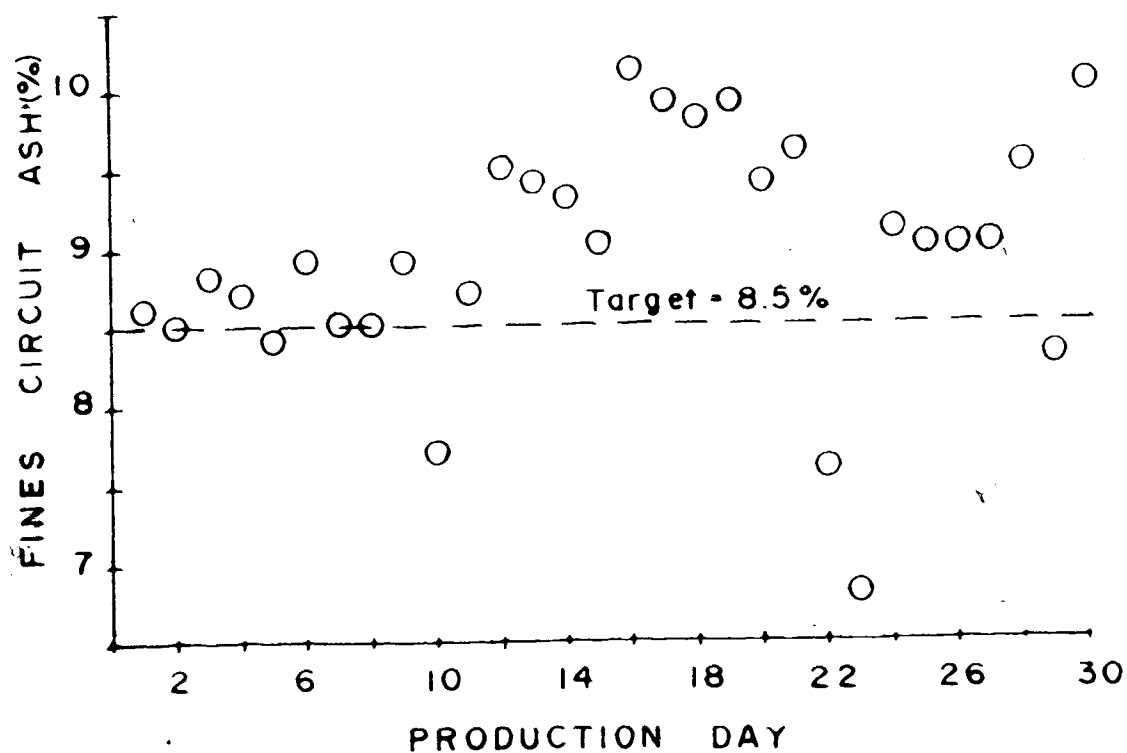
Figure 3.2 The Daily Variation in The Fine Circuit Product Quality.

High frequency sampling was carried out on the number four flotation cell bank for an 8 hour period on consecutive days. (The lack of man-power precluded a sampling exercise which would have provided the data record required for the analysis method described in section 2.8) The objective was to establish the frequency and amplitude of the fluctuations of selected stream attributes (%solids, %ash) around the cell bank. Initially, samples were obtained for the feed, concentrate and tailings streams, however, the extreme difficulty in filtering the latter required that it be excluded from the high frequency testwork. The results are presented in Figures 3.3 through 3.6. For approximately two hours on August 9, the sampling interval was reduced from 20 minutes to 10 minutes. The purpose was to identify the very high frequency components. (The error bars represent the 95% confidence limits assuming a normally distributed variate. The variance was a pooled estimate from duplicate cuts.) The plant throughput was essentially constant on both days with the exception of a mechanical interruption at noon on August 9.

It is readily apparent from the figures illustrating the attribute variation for the feed stream that any trend is effectively masked by the sampling and analysis error. This relatively large error arises because of the method used to sample the feed stream. (A dipping bucket is submerged in the distribution box (Figure 3.1) to obtain the sample.) Despite any apparent trend in the measured
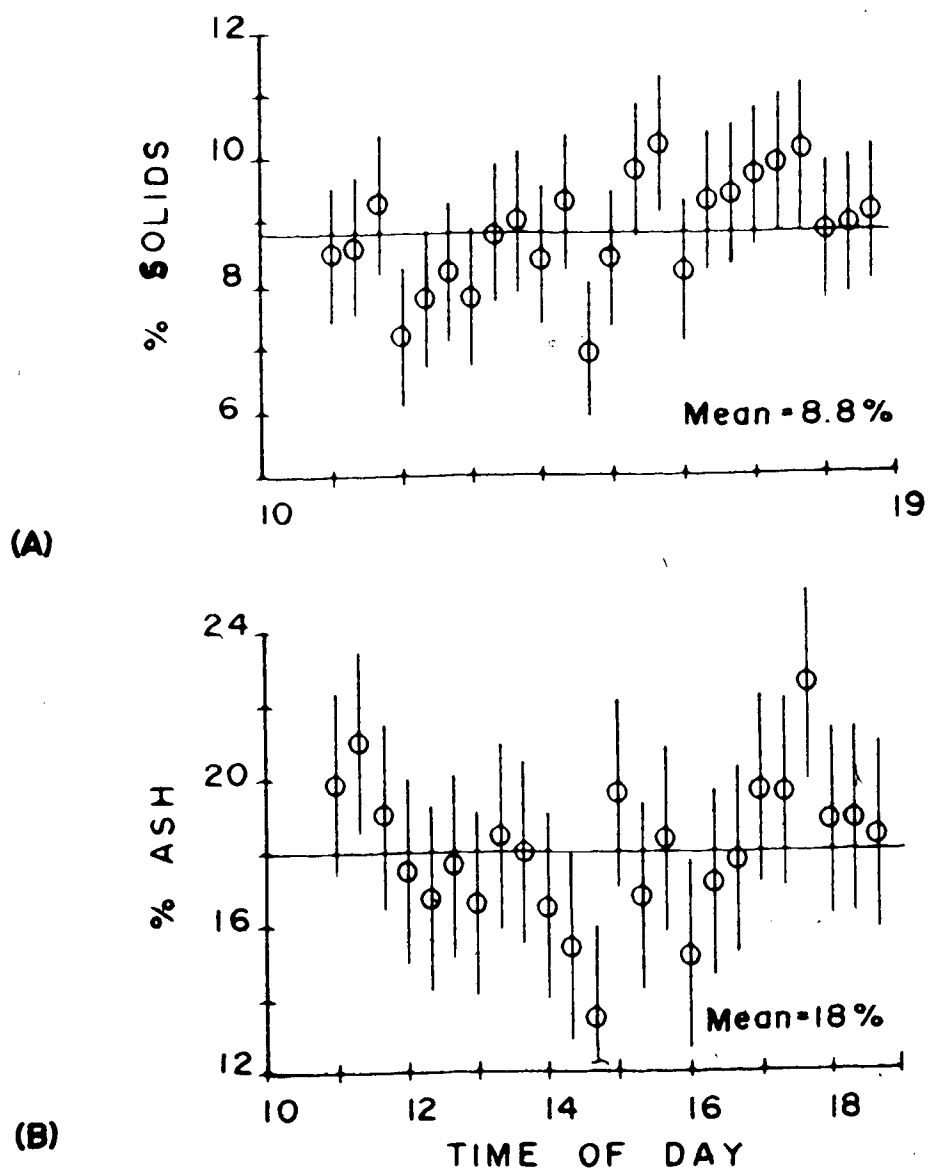
Figure 3.3 High Frequency Sampling Results for the Flotation
Feed-August 8, 1979.

(A)

(B)
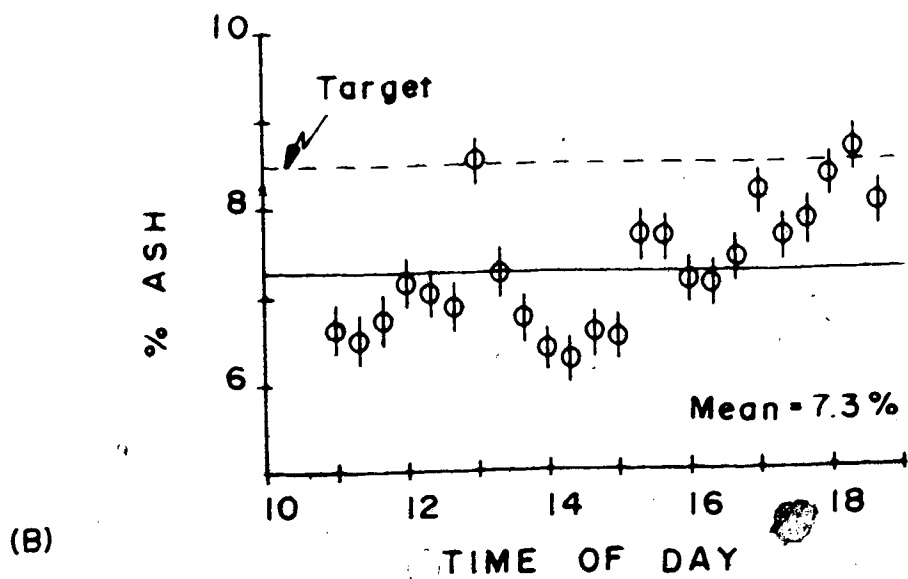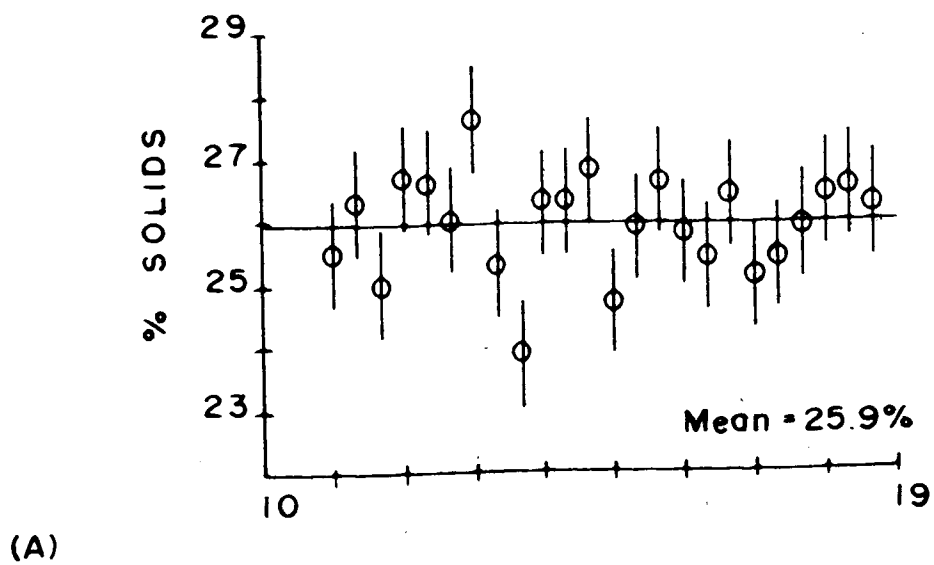
Figure 3.4 High Frequency Sampling Results for the Flotation Concentrate-August 8, 1979.

(A)

(B)
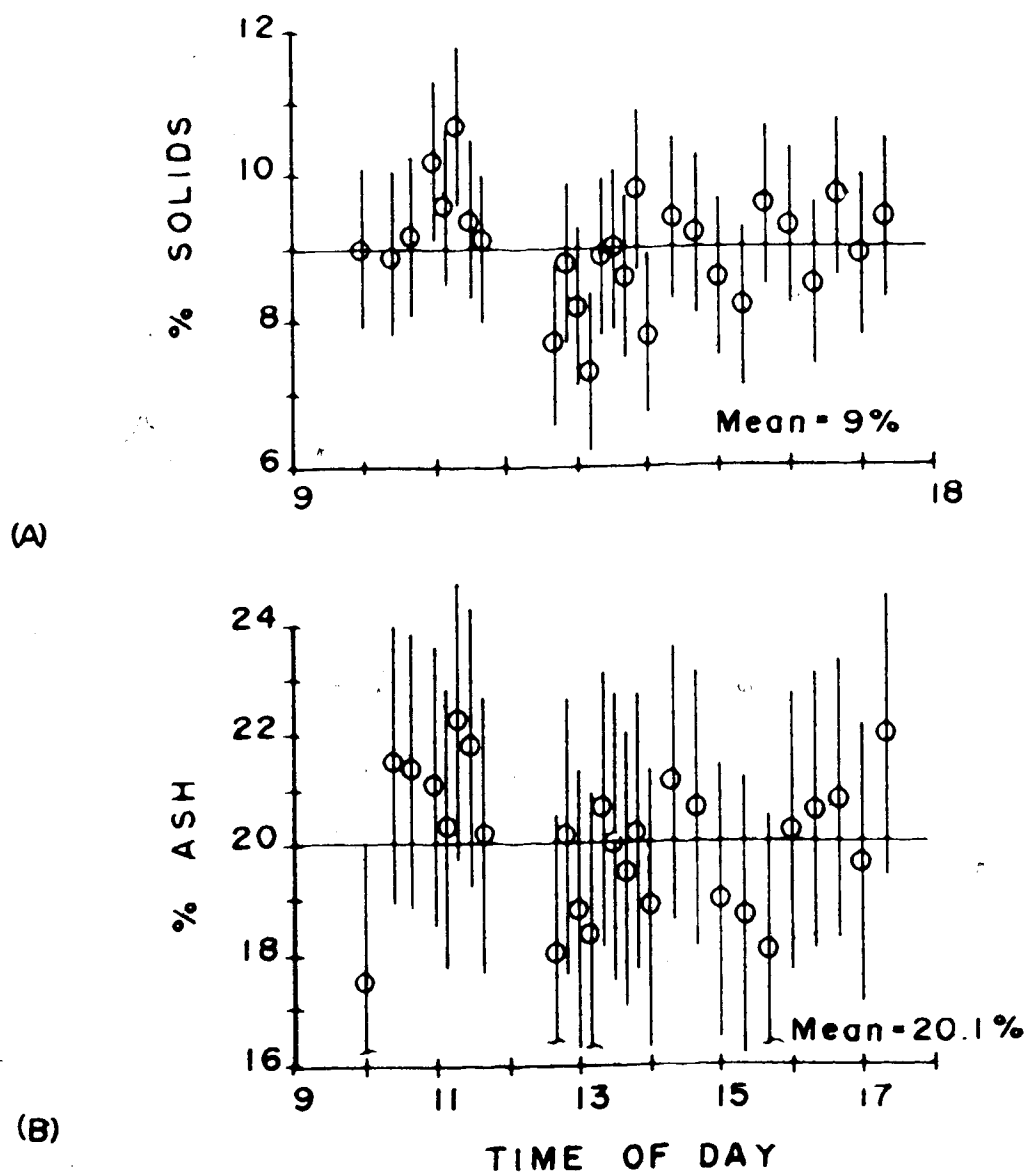
Figure 3.5 High Frequency Sampling Results for the Flotation
Feed-August 9, 1979.

(A)

(B)
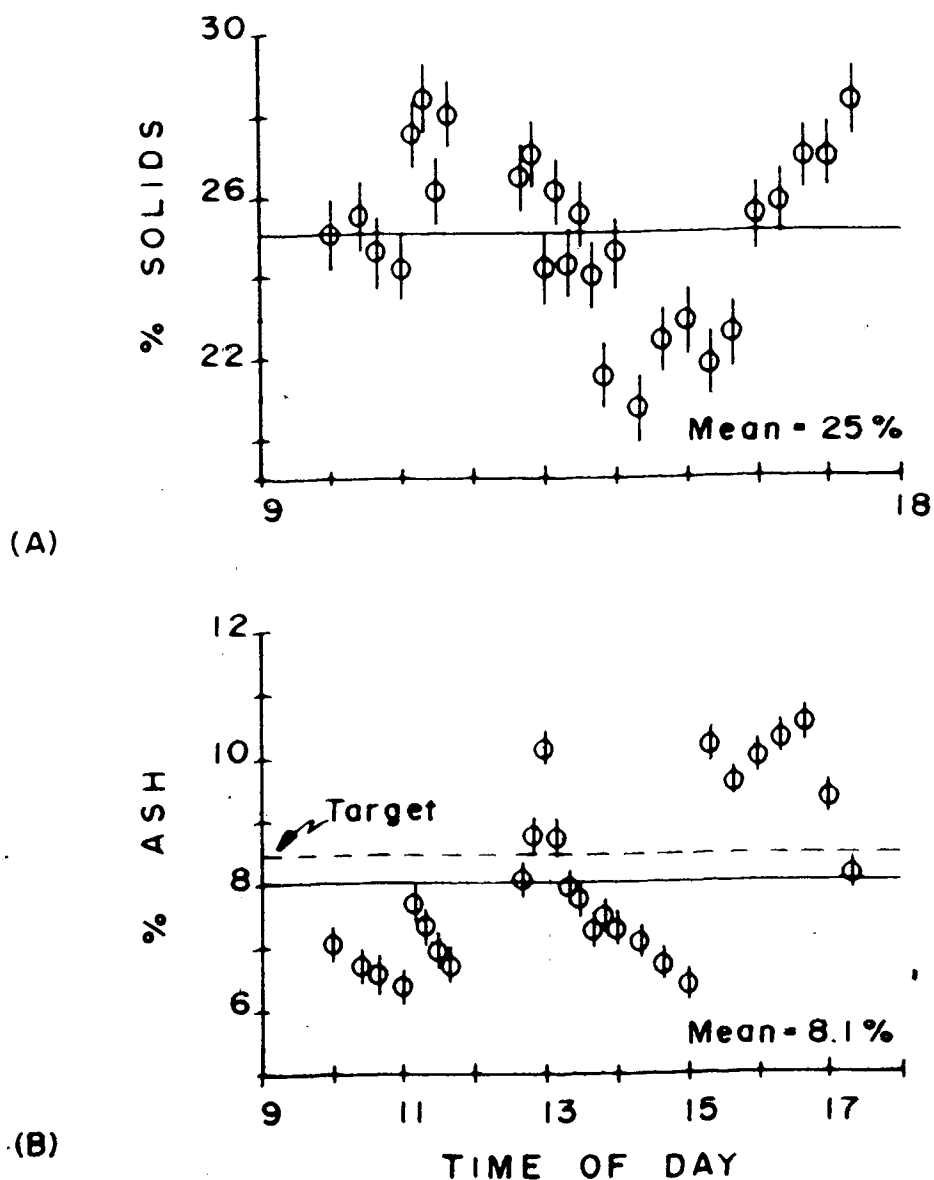
Figure 3.6 High Frequency Sampling Results for the Flotation
Concentrate-August 9, 1979.

variables it was suspected that the deviations were primarily the result of sampling error.

To test this suspicion the following calculations were done. Each attribute on each day was assumed to be a normally distributed variate. Using Chauvenet's Criterion, outliers were rejected. Only in one of the two data sets were observations excluded and in this instance only two points were rejected. Using the data subset from outlier rejection the normality assumption was verified using a x^2test. Subsequently, the measured variable variance was tested for homogeneity against the sampling and analysis variance obtained from the duplicate cuts. In all cases the calculated "F" statistic was significantly lower than the tabulated value at the 95% confidence level. Thus, it was concluded that, for the feed stream, the % solids and % ash values were substantially constant over the high frequency sampling periods.

The measured attributes in the concentrate stream do exhibit a considerable variation in time with minimal contribution from the high frequency components. Since product quality is the principal control variable, the discussion will be restricted to the % ash data of Figures 3.4(B) and 3.6(B). Again, as in the previous data, the mean operating level did not correspond to the control target. The quality trend is one which makes the process potentially amenable to process control. Furthermore, since these test periods were relatively short, there is a high probability

that the deviations are due primarily to extrinsic disturbances.

From the figures the following typical operating conditions were defined. These were used together with other available information in setting the factor levels for the laboratory experimental program(see Chap. 6).

Table 3.1 The High Frequency Statistics for %Ash and %Solids.

STREAM	% SOLIDS	% ASH
FEED	8.9%±3.4%	19.1%±4.9%
CONC.	25.5%±5%	7.7%±3.3%

The intervals quoted represent the 99% confidence limits for a normally distributed variate. It is recognized that the mean values are probably not good overall estimates of the true mean (see Figure 3.2). However, the variances are probably reasonable estimates since this statistic is generally more homogeneous.

Even though this data was obtained from McIntyre Mines Ltd., based upon discussions with other operators the process behaviour illustrated above is typical and is by no means an extreme case.

3.1.2 The Yield-Ash Curve in Coal Flotation

A knowledge of the yield-ash relationship is important in estimating the economic impact of improved process control in coal preparation. To gain an appreciation of the

nature of this curve in coal flotation a "kinetic" study was done. (It is implicit that other independent variables are expected to have an effect on the relationship somewhat similar to that of flotation time.) Composite samples were taken from the number four flotation cell bank on August 9 from 4:30 pm to 5:30 pm. In addition to the cell bank feed, concentrate and tailings streams, samples of the concentrate and tailings streams from each cell were obtained. Each sample was analysed for %solids and %ash. Using a general least squares solution to the overdetermined material balance problem (MATBAL 2), the measured data was adjusted to provide a consistent material balance(16). Using the adjusted data the cumulative yield-cumulative ash curve was constructed and is shown in Figure 3.7(A).

The data points on the curve correspond to the different sequential groupings of the flotation cells. For comparative purposes the target ash and expected yield values are included. It is apparent that under the operating conditions which prevailed during sampling, the final two flotation cells were serving to contaminate the concentrate product, relative to the target. This suggests that air flow may be a useful control variable in a process control scheme.

Using a quadratic approximation to the curve in Figure 3.7(A) and the appropriate numerical methods, it was possible to construct the incremental ash versus cumulative ash curve. This is shown in Figure 3.7(B). It is quite clear
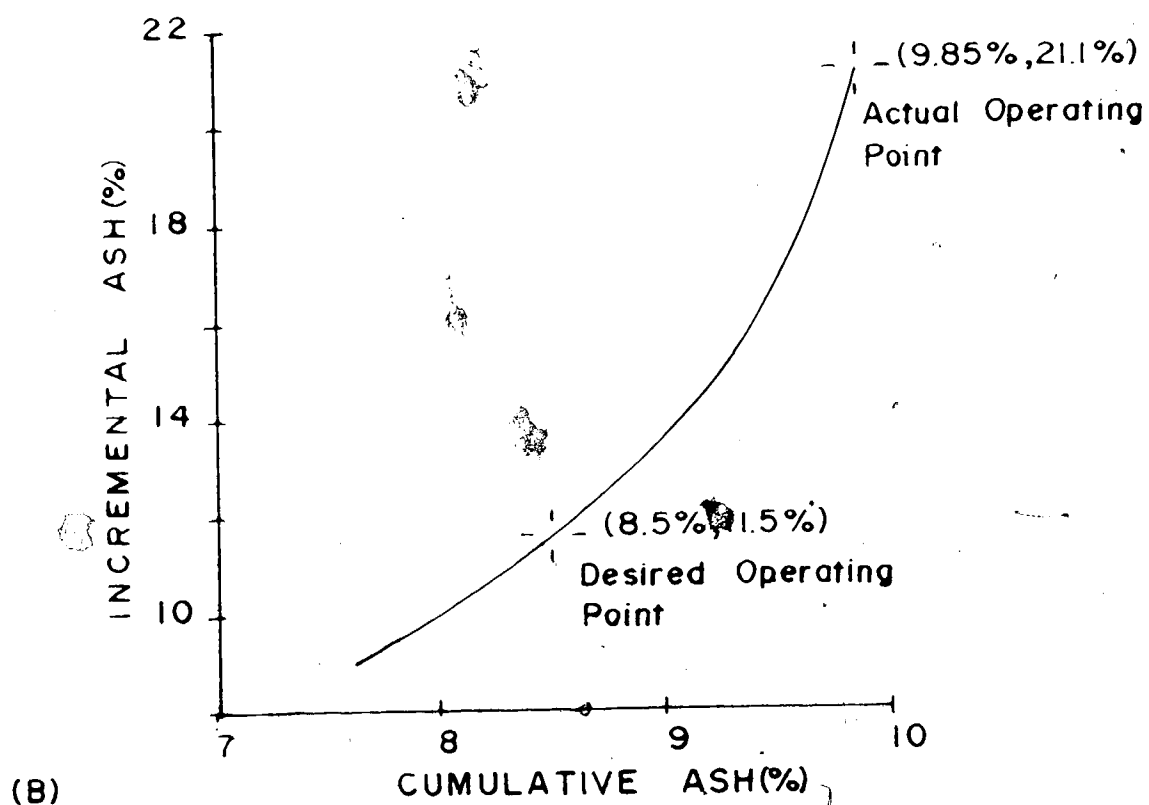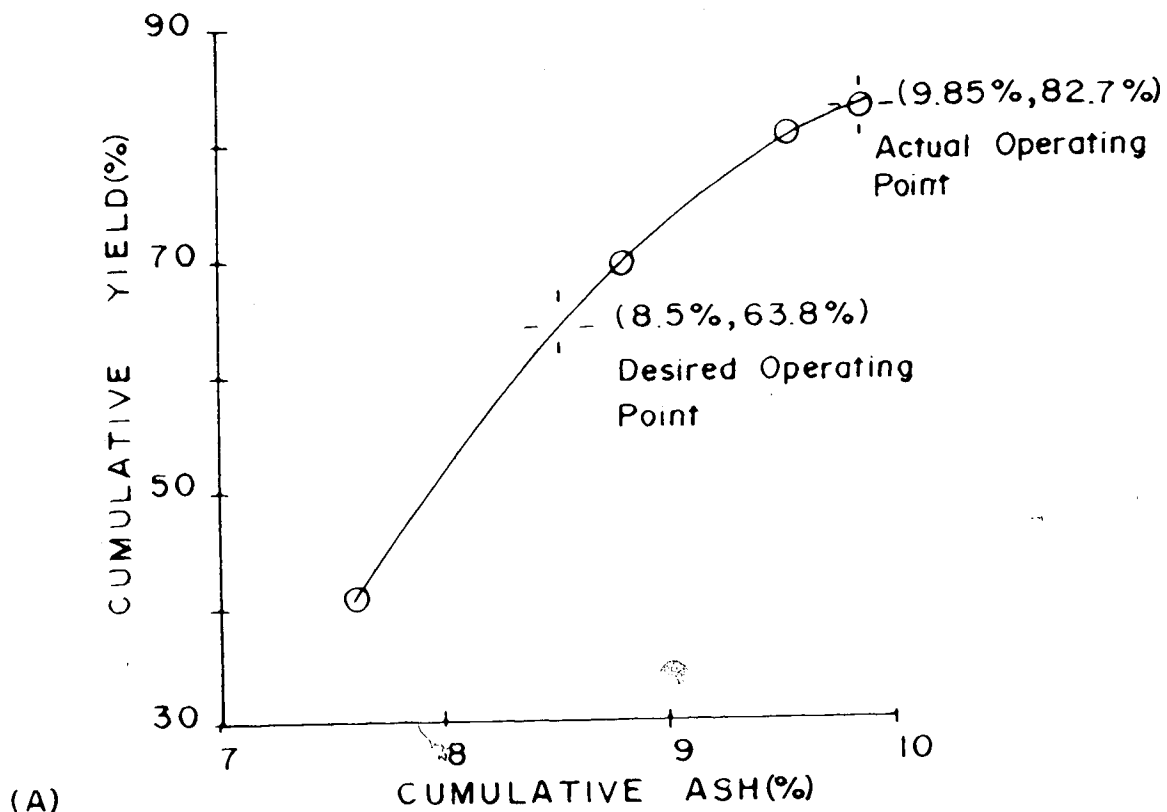
Figure 3.7 The Yield-Ash Curve and Incremental Ash in Coal Flotation.

that if the target of 8.5% ash represents the optimal operation relative to incremental ash, the actual operating point is grossly in error.

3.1.3 Nominal Residence Time of the Flotation Circuit

To assist in defining the "turn around" time for an OSCAA system set of attribute analyses, it was necessary to determine the nominal (or mean) residence time of a flotation cell bank. This parameter is a measure of the time scale of the process and is frequently used in process control loop tuning.

For the purposes of this experiment the following assumptions were made:

   a) The residence time distribution (RTD) of the solid particles and the water are identical in the cell bank. This allows the overall nominal residence time to be inferred from experimental data obtained on water.

   b) The flotation cell bank functions as a single input-single output (SISO) system. This allows sampling on the flotation tailings stream only, neglecting water losses to the concentrate stream.

The standard impulse tracer test was performed on the number four flotation cell bank at McIntyre Mines Ltd. NaCl (specifically Na^+) was used as the tracer. The experimental RTD profile is shown in Figure 3.8 where Na^+ concentration is plotted as function of the time

after the impulse addition to the feedstream.

The estimation of the nominal residence time, τ, from the experimental profile is straightforward and is only briefly documented in the discussion below. For more background the reader is referred to any basic chemical engineering textbook dealing with process analysis.

If a quantity of tracer, M, is added as an impulse to the feed end of a constant holdup SISO system operating at steady state with a constant volumetric throughput, q, then if c(t) is the concentration of tracer in the vessel discharge stream at time t, the fraction of material having spent a time, t, in the vessel is given by:

$$E(t)dt = \frac{c(t)qdt}{M} \qquad \ldots(3.1)$$

where: E(t)dt = fraction of feed stream material spending a time t in the vessel.
c(t) = tracer concentration in the vessel discharge stream.
q = volumetric flow rate through the vessel.
dt = infinitesimal time increment.
M = quantity of the traced species added in the impulse.

The function E(t) is referred to as the **exit age distribution function** and has the character of a probability density function with;

$$\int_0^{+\infty} E(t)dt = 1 \qquad \ldots(3.2)$$

The nominal residence time is computed by the standard methods of statistics as:
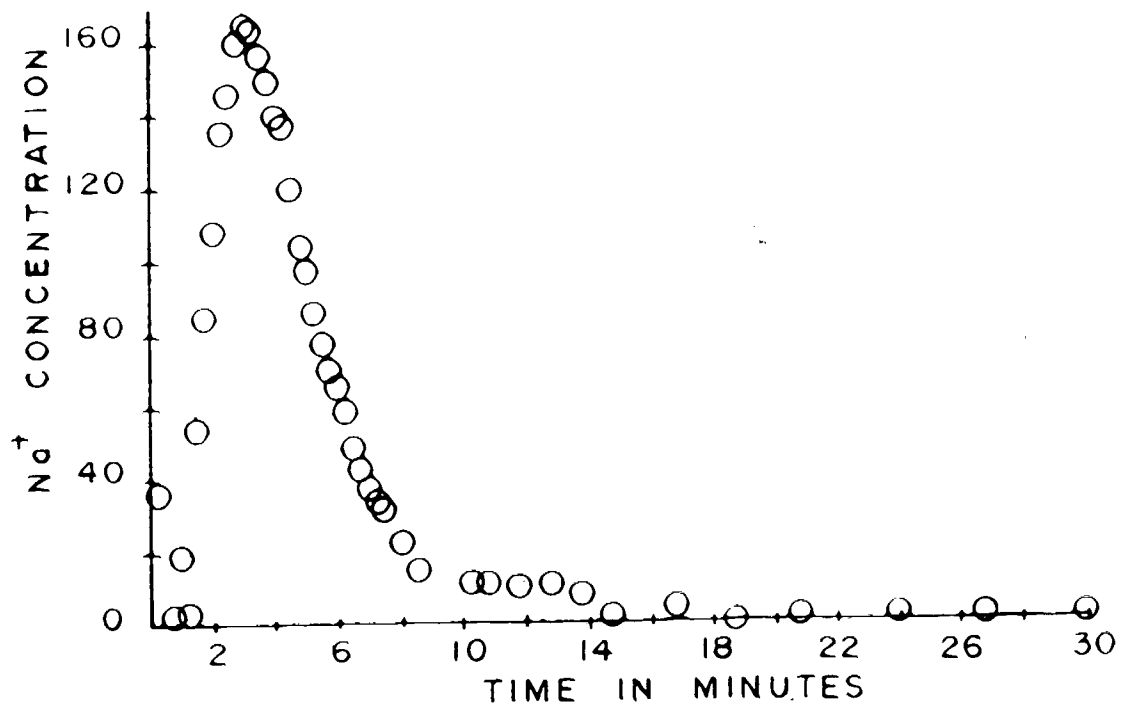
Figure 3.8 The RTD for Water in the Number Four Flotation
Cell Bank.

$$\tau = \int_{0}^{+\infty} tE(t)\,dt \qquad \ldots (3.3)$$

where: τ = nominal (mean) residence time.

Applying the appropriate numerical methods to the data of Figure 3.8 the solution of equation (3.3) gives an estimate of $\tau = 4.8$ minutes, under the experimental flow conditions. These conditions, specifically the volumetric flow rate, were observed by the operators to be typical of plant operation.

Control system designers would prefer to have process measurements available with a sampling interval of roughly one-tenth of the nominal residence time. However, in this case, given the practical constraints of the sampling and measurement system, the nominal residence time and the product quality variations of Figures 3.4(B) and 3.6(B), it is evident that an interval of up to 20 minutes could be tolerated without seriously impairing the control system performance. Thus an OSCAA system should be capable of providing a set of analyses on an interval of from 5 to 20 minutes to be useful in the process control of the McIntyre flotation circuit.

3.2 SUMMARY

There is a substantial day-to-day variation in the product ash for the McIntyre fine coal preparation circuit. These daily variations arise from relatively low frequency

variations in the flotation concentrate product quality. In

principle it should be possible to practice effective

process control around this circuit, provided that an OSCAA

type sensor is available. The response time of this

analytical device should be in the range of from five to

twenty minutes.

4. A REVIEW OF ON-STREAM ASH ANALYSIS TECHNIQUES

4.1 THE FUNDAMENTALS OF ON-LINE ASH MEASUREMENT

The principal methods for the instrumental determination of ash which have been considered so far are based either on the measurement of specific gravity, on the effective atomic number of the coal measured by β^-, X, or γ radiation, or on neutron activation. These methods are non-destructive and rapid (relative to the more conventional off-line methods), but are indirect and hence assume a strong correlation between ash and mineral matter as well as between mineral matter and the parameters being measured.

With respect to the nuclear techniques, Clayton(17) has provided a good general overview of the applications in the coal industry which deals, in part, with the on-line determination of ash content.

4.2 PHYSICAL MODELS OF THE PROCESS FLOWSTREAM

In most of the analytical methods employed to estimate the solids ash content, some physical model of the process flow stream is either implicitly or explicitly adopted for the purposes of calibration. The model generally assumes that the process flow stream consists of from two to four phases, depending upon the exact nature of the measurement system and the application. Associated with each phase a set of physical and chemical properties which can employed in constructing the calibration model.

To illustrate, consider the simplest case of a dry solids flow stream. In a basic measurement system the solids would be assumed to consist of a coal organics phase and a mineral matter phase. Each phase would have its own mean chemical composition, density, etc... These phases and their properties would be the basis of a calibration model (as will be illustrated in the next section). Clearly, the models are a simplification of the real system, but a necessary one since there are usually only several (≤ 3) independent measurements made on the flow stream. Since, in all models, the mass fraction of the phases must sum to unity, one less equation (or independent measurement) than phases is required to exactly compute flow stream composition in terms of the model phases. Thus, for the example, a single measurement is required. Any change in the petrography or mineralogy of either of the phases will invalidate the physical model and require that the characteristic properties be re-determined.

Finally, consider the most complex case of a fine coal slurry flow stream where an iron correction is required to circumvent frequent re-calibration (i.e. estimation of the phase properties). Here the flow stream would be assumed to consist of four phases, water, coal organics, iron-free mineral matter, and some characteristic iron mineral.

4.3 DENSITY MEASUREMENT

There is a significant density difference between the organic portion of the coal (S.G.$\cong$1.35) and the mineral matter (S.G.$\cong$2.6). Assuming a two phase physical model of the coal solids, with the further assumption that the mineral matter to ash ratio is constant, permits the construction of a calibration model based on measured solids density:

$$a = \frac{100}{Rma} \left[\frac{\rho_s - \rho_0}{\rho_{mm} - \rho_0} \right] \left[\frac{\rho_{mm}}{\rho_s} \right] \qquad \qquad ...(4.1)$$

where: a = ash content of the coal solids.
Rma = mineral matter to ash ratio for the coal solids.
ρ_s = measured coal solids density.
ρ_0 = coal organics density.
ρ_{mm} = mineral matter density.

The model parameters (phase properties) can be estimated from calibration data by standard curve fitting techniques. In some cases, where the range of a is small, empirical approximations of the form $a=f(\rho_s)$, ($f(\rho_s)$ linear or quadratic), are used. In essence these are simply truncated Taylor Series expansions of the more general model given by equation (4.1). Of course, changes in petrography or mineralogy, which can and do occur quite frequently, invalidate the assumed physical model since the phase properties change.

Three types of coal-ash monitoring devices based on density measurement have been developed. The first is simply batch weighing using water or some organic liquid as the

displacement medium. This method, while not an on-stream
technique in the strictest sense, can be quickly performed
by the operator to provide an ash content for process
control purposes. The second method, which has been
described by Crosland(18), measures the bulk density of an
essentially dry coal stream. Assuming a constant void
fraction, the coal density is calculable. The third type of
monitor involves measurements made at the feed end of a coal
preparation plant, where the solids are slurried with water
prior to wet processing. This device has been described by
Mikhail(19) and, to date, has only been tested in a pilot
plant setting. This unit requires a mass flow measurement of
both solids and water flow to the plant. Subsequently a
slurry density measurement is made and the solids density
back-calculated.

These devices have the advantage of requiring minimal
sample preparation, however, they are very dependent upon a
stable ash-density correlation. In addition, they cannot be
applied in systems where the feed is already in the form of
a slurry.

4.4 NEUTRON ACTIVATION

This kind of method, because of its complexity and
expense, has seen only limited application. Those units
which are in operation deal exclusively with monitoring the
feed to thermal power plants. Rogers et. al.(20) have
described a particular unit known commercially as the CONAC.

In principle, a uniform bed of coal is irradiated with fast neutrons most of which experience deccelerating collisions with the nuclei of the elements in the coal solids. When the neutrons are reduced to a sufficiently low energy they are captured by a nucleus creating an unstable isotope. The instability of the nucleus results in the prompt emission of a γ-ray(s). These gamma rays have a characteristic energy and their intensity provides the means of estimating chemical composition.

A similar device has been proposed by Sowerby(21) which dispenses with the sample metering requirement and employs a separate γ-ray backscatter measurement to correct for the coal sample bulk density and thickness.

4.5 TRANSMISSION AND BACKSCATTER OF ELECTROMAGNETIC RADIATION

These methods employ atomic number inference to estimate the ash content of the coal solids. In fact, it is the mass absorption coefficient which is measured but which is related to the atomic number. There is a significant difference between the atomic number of the coal organics ($Z \approx 6$) and that of the mineral matter ($Z \approx 12$). Assuming a two phase physical model of the coal solids, changes in composition are reflected by changes in the measured effective atomic number of the coal. Since the derivation of the calibration model pre-supposes a knowledge of both the instrument design as well as the means by which

electromagnetic radiation interacts with matter, discussion on this topic is deferred to the next chapter. As with the density methods, the mineral matter to ash-ratio is assumed to be constant. Of course, changes in the chemical composition of these phases, particularly heavy elements in the mineral matter, will alter the effective atomic number of the component and thus invalidate the assumed physical model.

This general method of coal-ash analysis appears to have been the most widely investigated to date. Specifically, those methods which employ γ-ray and/or X-ray irradiation have received the greatest attention because they are superior to the β techniques. Calculation of the ash content of coal through correlation with the atomic number is more reliable and applicable than the density methods and much less expensive than neutron activation. The major difference in the implementation is the geometrical arrangement of the irradiation/detection equipment of the ash-analysis subsystem.

Figure 4.1 illustrates the differences between transmission and backscatter geometry. In transmission, the radiation source and detector are located on opposite sides of the sample. As a result, the majority of the radiation which reaches the detector are primary photons which have passed through the sample without interaction. In backscatter, the source and detector are located on the same side of the sample. As a result, all of the radiation which

reaches the detector is the result of an interaction of the primary photons with the sample. With regard to classifying the ash analyser, the device geometry is taken from that part of the instrument which is sensitive to atomic number (or mass absorption), i.e. the ash analysis sub-system.

These methods can be further subdivided on the basis of application. One class of instruments is applied to coarse, essentially dry solids while the other is applied to fine particle slurries. The existence of high concentrations of water, which has both a density and an effective atomic number similar to the coal organics, complicates the measurement task appreciably. A further complication which can arise in slurry applications is the presence of varying quantities of entrained air in the pulp. This will distort the pulp density measurement which is usually made with a sub-system in the transmission geometry. As a result, much of the development work has been done on the dry solids analysers and only recently have these ideas been transferred to the slurry measurement problem.

The underlying theory of operation of all of these on-stream analysis devices is presented in the next chapter where the physics of the OSCAA prototype are described in detail.

There is a relatively large number of off-line implementations of these techniques discussed in the published literature as well(for example:22-27).

RADIATION SOURCE

Primary Photons

SAMPLE

Transmitted Photons

DETECTOR

(A) TRANSMISSION GEOMETRY

RADIATION
SOURCE

DETECTOR

Primary
Photons

Backscatterred
Photons

SAMPLE
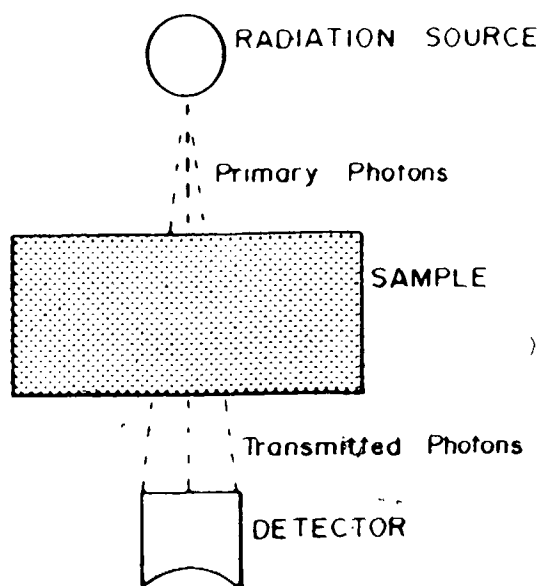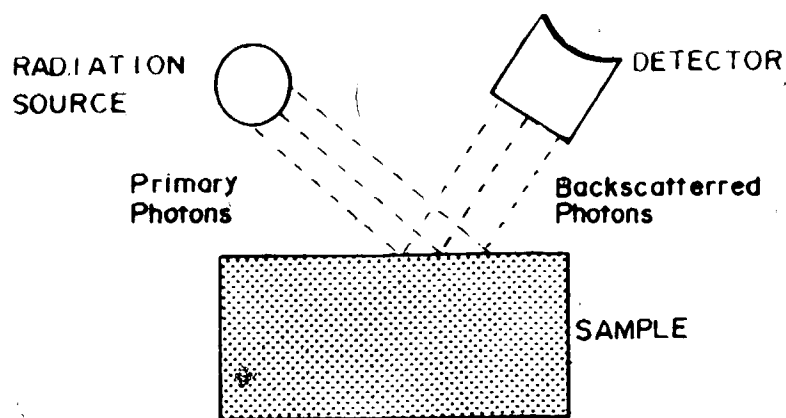
(B) BACKSCATTER GEOMETRY

Figure 4.1 Geometrical Variations in Analysers Using

Electromagnetic Radiation.

4.5.1 Transmission Methods

In general, transmission methods are well suited to this analysis problem because they are very sensitive to changes in atomic number. They are limited in flexibility, however, because additional radiation measurements, which may be necessary for compensation purposes, require duplication of the basic transmission measurement equipment.

4.5.1.1 Dry Solids Applications

Three classes of devices have been successfully applied to essentially dry solids, at least on the laboratory prototype scale. The first class involves a single transmission measurement. Starnes and Clark(28) and Nagy and Varga(29) describe systems which involve fairly elaborate sample handling (comminution) and sample metering equipment control to ensure sample homogeneity and constant mass per unit area respectively. The single, low energy photon, attenuation measurement provides an estimate of the mass absorption coefficient (atomic number) which is correlated to the ash content for calibration purposes. The second class involves a dual transmission system as decribed by Fushimi(30). In this case, a high energy photon attenuation measurement is also obtained to correct for the sample bulk density. This obviates the difficult task of controlling mass per unit area, however, size reduction is required to provide uniformity of field. (This device operates in a batch mode.) The third class,

described by Fookes et. al.(31), employs three transmission measurements. Their unit is virtually the same as Fushimi's but includes a second, low energy photon, attenuation measurement to partially compensate for possible mineralogical variation in the mineral matter.

4.5.1.2 Slurry Applications

Two devices have been proposed/applied to the ash monitoring problem for coal slurries. Starnes and Clarke altered the design of their dry solids unit to accommodate fine particle slurries. They included a slow speed agitator in the supply tank to facilitate deaeration. In addition, a pulp density gauge was added to the system and the flow cell modified to allow for both transmission and fluorescence radiation measurements, the latter for compensation purposes. The author knows of no industrial applications of their device in this form. Lyman(32), using Fushimi's system as a basis, included a high pressure pump to alleviate any problems which might arise from slurry aeration. Lyman's device, known as Automatic Slurry High Speed Coal Analyser (ASHSCAN), has been extensively field tested in Australia and is apparently ready for commercial distribution. Lyman has acknowledged the potential problem of compositional variance in the long term accuracy of ASHSCAN. He has suggested that a system similar to the one described by Fookes et. al. would

offer a solution to this problem. Since ASHSCAN is
typical of instruments based on transmission geometry,
and because it is intended for the same application as
OSCAA, a schematic representation is included in Figure
4.2.

Interestingly, while Starnes and Clarke and Lyman
make provision for slurry deaeration, work by Churchill
et. al.(33) on lead ore slurries did not mention serious
aeration problems.

4.5.2 Backscatter Methods

In general, while backscatter methods are less
sensitive to changes in atomic number than are transmission
methods, they appear to have been much more widely studied
and developed, specifically for monitoring dry solids. A
major reason for this is the relative ease of compensation
through fluorescence measurements as opposed to the
duplication of equipment. This inherent flexibility of the
backscatter geometry in slurry applications makes it a
logical candidate for further development.

4.5.2.1 Dry Solids Applications

The first commercial unit of this class was the
CENDREX developed by the Dutch State Mines(34). Since
this unit was designed for on-stream application using
low energy X-rays, a rather elaborate (ref. 28,29)
sample presentation system was required. CENDREX
utilizes a conventional tube/target assembly to produce
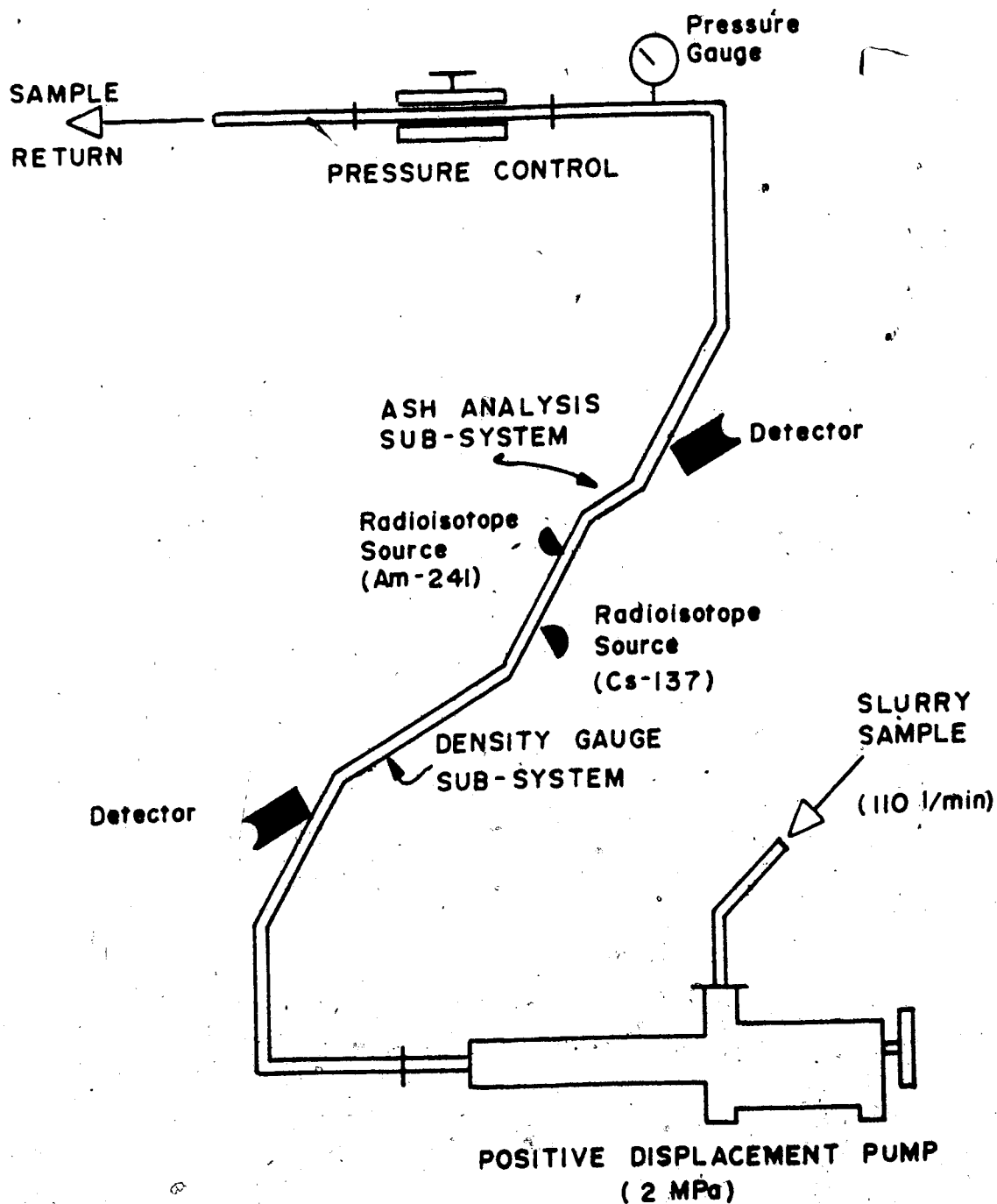
Figure 4.2 A Schematic of Lyman's ASHSCAN Device(32).

the radiation. Crosland et. al. describe the evolution of a similar device which utilizes a radioisotope source. This work led to the development of the SORTEX unit which has been described by Cammack and Balint(11). Very similar work by Hardt(35) led to the development of another coal-ash monitor which is also commercially available. In all three systems, the intensity of the backscattered radiation is the measure of the coal solids mass absorption coefficient. The major differences among these three devices lie in the sample presentation sub-system, the energy of the radiation employed and the method of (iron) compensation. In all cases they are claimed to have been successfully applied to dry coal streams yielding the required accuracy in acceptable measurement time.

Fookes et. al. have suggested that a dual source excitation system would provide good results in backscatter geometry as well. In this case the second measurement would have the same function as fluorescence in compensation. They do not provide any experimental support for this statement.

4.5.2.2 Slurry Applications

Thusfar, only one implementation of the backscatter geometry for monitoring coal-ash in fine particle slurries has been suggested. Kawatra and Dalton(36) describe the successful calibration of a laboratory bench scale unit. As in ASHSCAN, two measurement

sub-systems are incorporated. One to measure the pulp
density and the other to measure backscatter and
fluorescence radiation. This is the system upon which
the OSCAA design was based[1]. A schematic of the
laboratory scale test rig used by Kawatra and Dalton is
presented in Figure 4.3.

4.6 IMPORTANT DESIGN CRITERIA IN SLURRY MEASUREMENT SYSTEMS

In conducting this literature review in the light of
the goals of the OSCAA project, several important design
criteria for slurry application units were frequently
encountered. These are briefly discussed below with
reference to the analytical devices concerned. Special
emphasis is given to their impact on the design of an OSCAA
type system.

4.6.1 Air Sensitivity

In ASHSCAN, Lyman has eliminated the entrained air
problem by pressurizing the system to the extent that the
air bubbles collapse. On the other hand, Kawatra has not
made an explicit attempt to deaerate. Since OSCAA, like
ASHSCAN, requires an accurate pulp density measurement, the
current prototype may need design modification to handle the
air problem. This could include anything from using
mild/strong centrifugal forces to the pressurization

----

[1] It has come to the author's attention very recently that
Kawatra et al.(37) are essentially duplicating the OSCAA
study but their work is not sufficiently completed to allow
comparison of results.
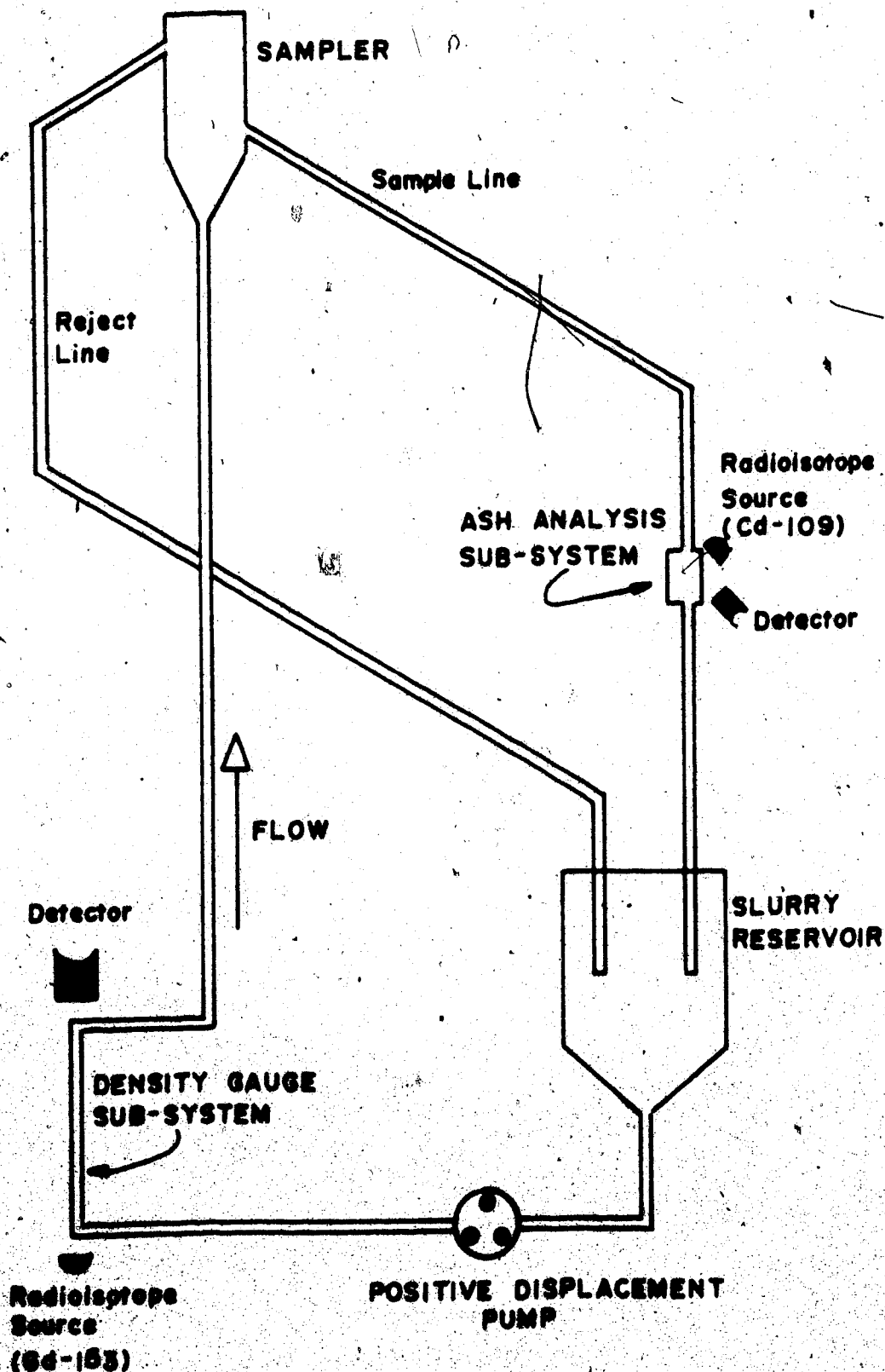
Figure 4.3 A Schematic of the OSCAA Laboratory Prototype of Kawatra and Dalton(36).

technique employed in ASHSCAN.

4.6.2 Sampling Characteristics

Lyman's device utilizes transmission measurements with turbulent flow in near vertical pipe runs. Under these conditions essentially all particles in the flow stream are "sampled" in the analysis. In the backscatter geometry, a flow cell equipped with a thin mylar viewing window is used. As a result only a "thin slice" of the pulp in the neighbourhood of this window is sampled. Proper design of the flow cell and the correct choice of the incident radiation energy will enhance the "sampling" capability of such a system. This is the approach employed in the on-stream X-Ray Fluorescence (XRF) analysers common in mineral processing plants.

4.6.3 Heavy Element Correction

Changes in the concentration of the heavy elements in the mineral matter can have a devastating effect on the performance of Lyman's analyser. Theoretically, for every element whose concentration changes significantly another transmission measurement would be required. However, in the backscatter geometry, fluorescence measurements can be used to compensate for such changes with little modification to the system hardware, apart from the detection/spectral resolution equipment.

4.6.4 Compatibility/Flexibility

In an operating plant, it is supposed that a multitude of streams will require monitoring. For a device like ASHSCAN this will necessitate a considerable duplication of equipment and extensive stream multiplexing. The OSCAA system is quite compatible with existing on-stream XRF hardware. In these devices both multiplexing and duplication are minimized. It is expected that the manufacturers of such equipment could quickly produce a commercial version of OSCAA with excellent product support.

4.7 SUMMARY

There has been a substantial amount of development work in the area of on-stream coal ash analysis, in particular with those methods utilizing electromagnetic radiation. Most of this work has concentrated on the analysis of coarse dry solids. Unfortunately, since most of the preparation plants employ wet separation methods, this class of device is not well suited to feedback control applications. Furthermore, the mechanical problems associated with the sampling and sample presentation sub-systems make them difficult to operate. Research into devices for use in fine particle slurries has begun only recently. Lyman has developed the ASHSCAN system to the point where it is apparently ready for commercial distribution. The other geometrical variant in this area, OSCAA, has only recently been proven. Given the important design criteria for such devices, the backscatter

geometry would be the preferred implementation. However, it
is possible that in some plants, the entrained air problem
may be severe, enough to warrant appropriate design
modifications to the prototype described in this thesis.

5. THE PHYSICS OF THE OSCAA MEASUREMENT SYSTEM

5.1 INTRODUCTION

This chapter describes the physical principles upon which the OSCAA system is based and from which certain design parameters were deduced. In addition, the possible calibration equations for OSCAA are presented.

In order that the material which follows be put into context, it is necessary to briefly discuss the OSCAA unit. (A more detailed description is given in Chapter 6.) OSCAA consists of three sub-systems, one for sample presentation, one for pulp density measurement and one for backscattered and fluorescent radiation measurements, together with their associated support equipment. The pulp density sub-system employs a Gd-153 radioisotope with a principal photon energy of ≈100 kev, in the transmission geometry. The ash analysis (backscatter/fluorescence) sub-system employs a Cd-109 radioisotope with a principal photon energy of ≈22 kev. In this case, the slurry sample is irradiated through a thin mylar window. The resultant detectable backscattered incident and fluorescent radiation return through the same window.

Since γ-ray and X-ray photons are physically indistinguishable, the same laws of physics apply to both[*].

---

[*] γ-rays and X-rays are distinguished on the basis of their origin. γ-rays result from nuclear transformations while X-rays result from electron rearrangement.

5.1.1 Practical Considerations in Measurement System Design and Operation

This chapter is intended to develop the theory underlying the OSCAA system and there has been no attempt to include any discussion on practical considerations which may influence system operation. While the performance of the detector and resolution equipment are critical factors in ensuring successful operation, these topics are sufficiently general that much has been written about them in the standard textbooks. For example, Bertin(52) provides a good description of detector structure and operation, including choking, shifts, escape peaks, etc...(Chap. 6), as well as of resolution equipment (Chap. 8) and counting statistics (Chap. 11). The philosophy adopted by the author is that before one can begin to design and operate a system such as OSCAA, the theory of operation must be understood. The practical considerations become important in the final design and operation stages. Since the latter have been treated by many authors, material of this is nature excluded from the thesis to avoid needless duplication.

5.2 THE INTERACTION OF PHOTONS WITH MATTER

The mathematical model of the physical principles upon which nuclear transmission measurements rest is given by Lambert's (Beer's) law:

$$I = I_0 \exp(-\rho\mu x) \qquad \qquad ...(5.1)$$

where: I_0 = intensity of radiation in a narrow colinear beam which is incident upon the absorbing medium.

I = the intensity of the incident colinear beam after transmission through the absorbing medium.

ρ = the density of the absorbing medium.

μ = the mass absorption coefficient of the absorbing medium.

x = the distance which the photon beam travels through the absorbing medium.

This law is observed to hold for a narrow, perfectly collimated beam of mono-energetic photons.

A parameter of particular interest in equation (5.1) is the mass absorption coefficient, μ. The magnitude of this parameter is dependent upon the incident photon energy (E) and the effective atomic number (Z) of the absorbing medium. This is illustrated in Figure 5.1 where μ is plotted against Z for three photon energies. The range of Z chosen represents the range of major elements found in coal solids; hydrogen to iron. The effective atomic numbers of the coal organics ($Z \approx 6$), and the mineral matter or ash ($Z \approx 12$), are also indicated on Figure 5.1.

In the photon energy range of interest in this work, i.e. $E \leq 700$ kev, the mass absorption coefficient is the sum of the coefficients for three mutually exclusive events, namely;.

(i) photoelectric absorption (τ)

(ii) Compton scattering (σ_m)

(iii) Rayleigh scattering (σ_{nm})

Mathematically
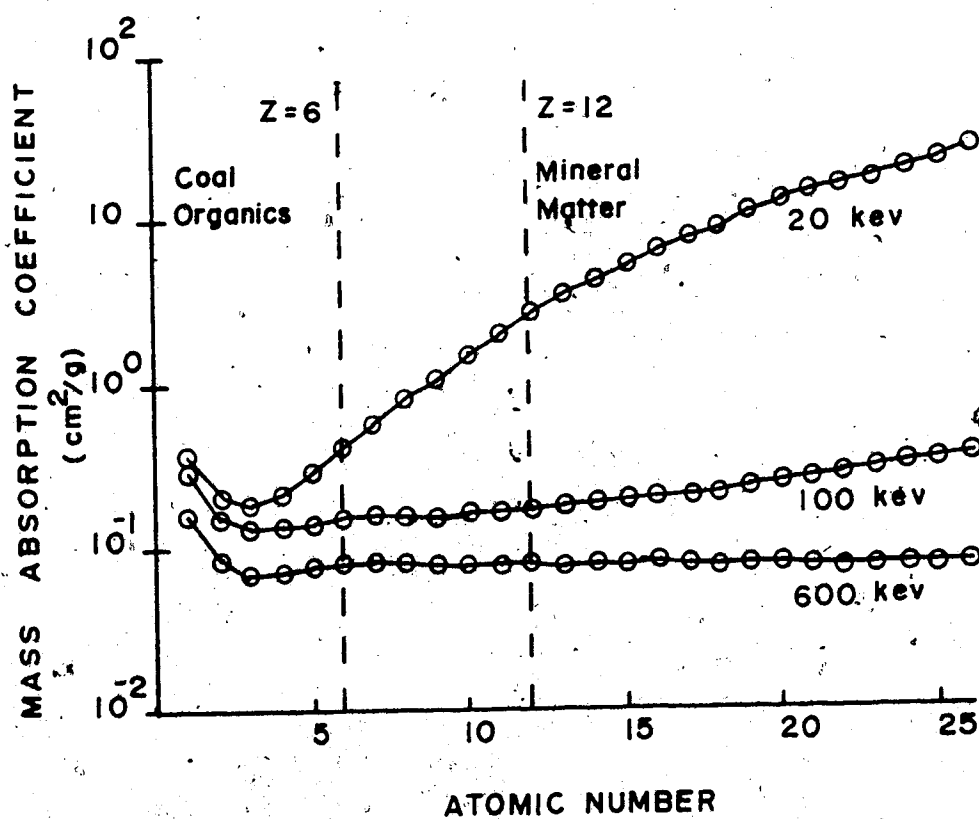
Figure 5.1 The Mass Absorption Coefficient as a Function of Photon Energy and Atomic Number.

$$\mu = \tau + \sigma_m + \sigma_{nm}$$ ...(5.2)

These processes are briefly described below and are schematically illustrated in Figure 5.2.

Photoelectric Effect

"An incident photon disappears and an atomic electron (usually from the proximity of the nucleus) leaves its atom at high speed, having absorbed the photon energy. This effect predominates for lower energy gamma rays, especially in high Z materials."(38) The electron rearrangement which follows this event gives rise to the phenomenon of X-ray fluorescence. When an electron in a higher energy orbital moves to fill the vacancy left by the photoelectron an X-ray of characteristic energy is emitted.

Compton (Inelastic) Scattering

"A photon is scattered inelastically and an atomic electron recoils out of an atom, much as though it had been initially free. The energy taken up by the electron depends primarily on its recoil momentum. This effect predominates for gamma rays of 1-5 Mev in high Z materials, and even more greatly and over a much wider energy range in low Z materials.

The recoil electron flies off predominantly in the direction of the incident photon, the more nearly so the higher the fraction of photon energy it carries away and the higher the photon energy. It never recoils backwards."(38)
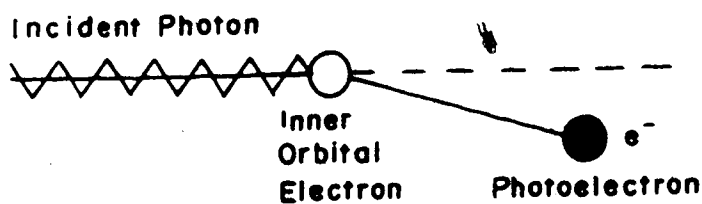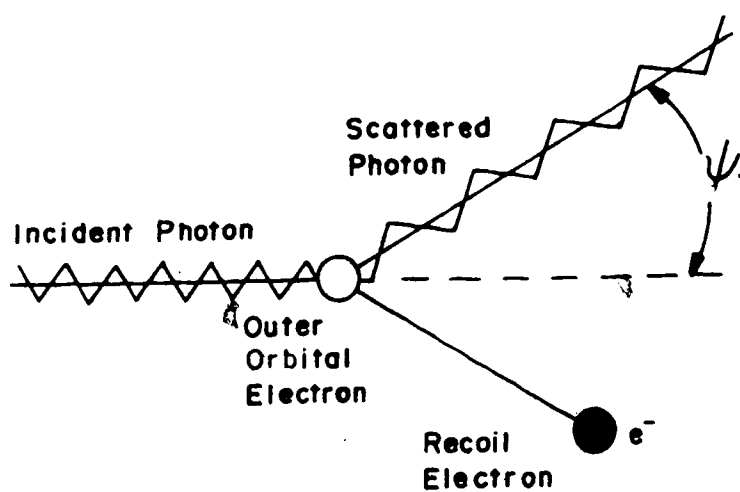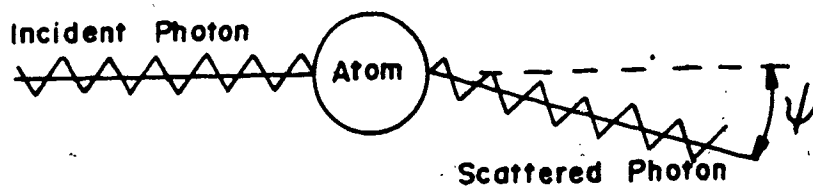
Figure 5.2 The Absorption Processes for Low Energy Photons (E<1 Mev).

Rayleigh (Elastic) Scattering

"Gamma rays scattered by small angles impart only a small recoil, especially when their energy is low. The recoil is then absorbed by the whole atom or molecule so that the scattering action of different atomic electrons combines coherently. Coherent combination enhances the probability of this effect so that it prevails greatly at low energies. This scattering is more likely for high Z than for low Z materials."(38)

Narrow beam measurements yield only μ, but the coefficients for the individual processes are usually provided by the theory or by special experiments. Numerical values for these coefficients are available in tabular form (for example: (39)).

5.3 THE PRINCIPLES OF PULP DENSITY SUB-SYSTEM OPERATION

Nuclear pulp density measurement has a relatively long history in both mineral processing and coal preparation applications. This type of pulp density gauge has a number of desirable features which include:

a) it is indirect,

b) it is mechanically reliable and geometrically flexible,

c) it "samples" a large portion of the pulp stream.

The installation of a nuclear pulp density gauge requires that the following factors be taken into

account:

a) avoid a buildup of one phase (e.g. solids) in the radiation pathway.

b) ensure that the slurry pipeline is running full.

c) minimize entrained air in the pulp.

d) minimize pipeline vibration to avoid associated intrumentation problems.

e) ensure adequate shielding to avoid radiation contamination.

The first two requirements are usually met by mounting the gauge on a vertical section of the slurry pipeline where the direction of flow is upward. Point (c) is often dictated by the nature of the operation. However, this can be become an important factor in high accuracy measurement systems. The final points are partly compensated for when off-the-shelf instrumentation is used. Vendor equipment is generally quite rugged and must pass strict safety inspection.

The two most common industrial gauge geometries are schematically illustrated in Figure 5.3. The reason for the different configurations arises from sensitivity considerations which are discussed later.

5.3.1 Applying Lambert's Law

In slurry applications the absorbing medium is a multicomponent mixture, by definition. Thus, while equation (5.1) remains valid, provided that the implicit geometrical
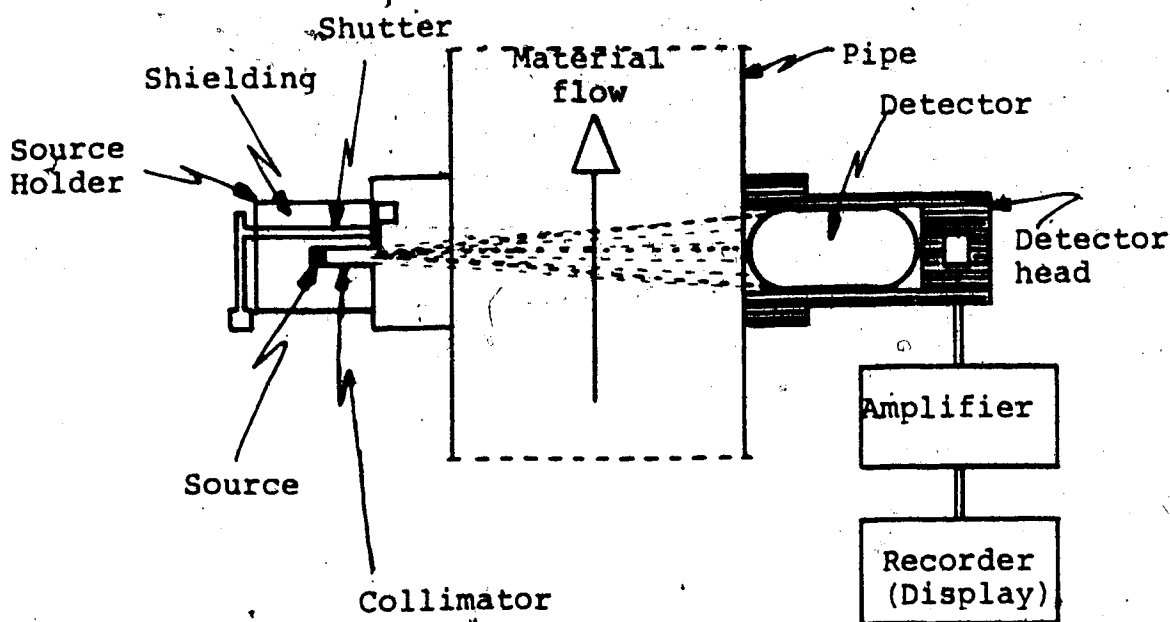
(A) Standard Configuration
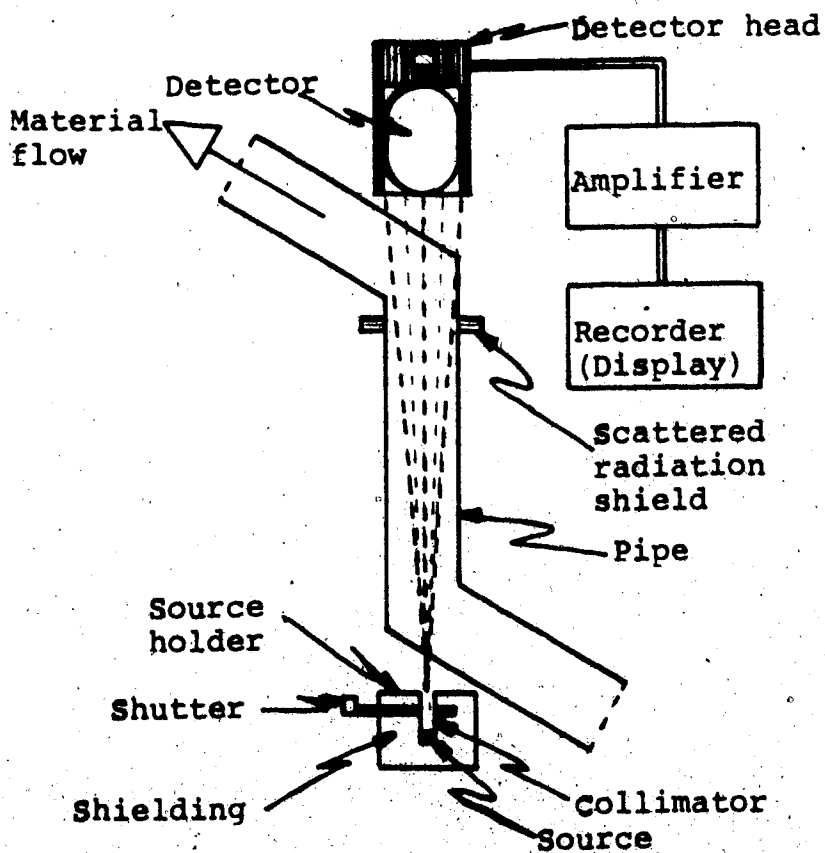
(B) "Z-type" or "Down the Line" configuration

Figure 5.3 Common Geometries of Industrial Nuclear Pulp Density Gauges.

constraints are met, the sample mass absorption coefficient must reflect the elemental composition since $\mu = f(E,Z)$. It can be shown that the mass absorption coefficient for any phase is simply a weighted average of the coefficients for the elemental species present. Using the same approach, if the mass absorption coefficient of each phase is known, the sample mass absorption coefficient is simply the weighted average value, i.e.:

$$\mu = \sum_i \mu_i w_i \qquad \qquad ...(5.3)$$

where: μ_i = the mass absorption coefficient for component i in the sample.
w_i = mass fraction of component i in the sample.

Inspection of Figure 5.1 shows that by choosing a radioisotope of sufficiently high photon energy (e.g. $E \geq 100$ kev for coal), then μ is substantially independent of Z and can be considered constant. That is, $\mu_1 = \mu_2 = ... = \mu$. Under these conditions and for a fixed path length, x, the only variable parameter in the exponential of equation (5.1) is ρ, the pulp density.

This is the basis for the design of nuclear pulp density gauges where variations in the measured value of I are related, in a logarthmic manner, to changes in the sample pulp density. Linearization of equation (5.1) with respect to ρ permits gauge calibration with a minimum of two (I, ρ) points.

Equations (5.1), (5.3) and (5.4) are sufficient to construct a calibration model for Lyman's ASHSCAN decive.

$$\rho = \frac{1}{\sum_i w_i/\rho_i} \qquad \qquad \text{...(5.4)}$$

where: ρ_i = the density of component i in the sample.

This is useful since it serves as an introduction to the construction of semi-empirical calibration models based on nuclear measurement techniques. In addition, it provides a vehicle for theoretically studying the performance characteristics of ASHSCAN. From Figure 4.2 it is apparent that this device employs a pulp density gauge (Cs-137, E≈660 kev→ μ effectively constant) to estimate ρ, and a lower energy photon transmission gauge (Am-241, E≈60 kev→ μ dependent upon composition) to estimate $\rho\mu$. Denoting the two sub-systems as (1) and (2) respectively, then:

$$\rho = \log_e\left[\frac{I(1)}{I_0(1)}\right]\Big/ -\mu(1)x(1) \qquad \qquad \text{...(5.5)}$$

$$\rho\mu(2) = \log_e\left[\frac{I(2)}{I_0(2)}\right]\Big/ -x(2) \qquad \qquad \text{...(5.6)}$$

where: I(j) = the measured intensity of transmitted photons for sub-system j.
I_0(j) = the incident photon intensity for sub-system j.
μ(j) = the mass aborption coefficient corresponding to sub-system j.
x(j) = the radiation path length for sub-system j.

Since the terms on the right hand sides of these equations are either measured or known from the theory or experiments,

they can be used as predictive relationships. Equations (5.5) and (5.4) can be combined to form:

$$\sum_i w_i / \rho_i = -\mu(1)x(1) \bigg/ \log_e\left[\frac{I(1)}{I_0(1)}\right] \qquad \ldots (5.7)$$

Similarly, dividing equation (5.6) by (5.5) and setting the result equal to equation (5.3) yields:

$$\sum_i \mu_i w_i = \frac{\mu(1)x(1)\log_e\left[I(2)/I_0(2)\right]}{x(2)\log_e\left[I(1)/I_0(1)\right]} \qquad \ldots (5.8)$$

Equations (5.7) and (5.8) provide two simultaneous linear equations in the w_i. Assuming a three phase model for the slurry, (1) water, (2) coal organics and (3) mineral matter, and knowing that $\Sigma w_i = 1$, allows construction of the calibration model. In vector-matrix notation:

$$\begin{bmatrix} w_2 \\ w_3 \end{bmatrix} = \begin{bmatrix} (\frac{1}{\rho_1} - \frac{1}{\rho_2}) & (\frac{1}{\rho_1} - \frac{1}{\rho_3}) \\ (\mu_2 - \mu_1) & (\mu_3 - \mu_1) \end{bmatrix}^{-1} \begin{bmatrix} \frac{\mu(1)x(1)}{\log_e\left[I(1)/I_0(1)\right]} + \frac{1}{\rho_1} \\ \frac{\mu(1)x(1)\log_e\left[I(2)/I_0(2)\right]}{x(2)\log_e\left[I(1)/I_0(1)\right]} - \mu_1 \end{bmatrix} \ldots (5.9)$$

The stream attributes are computed from the solution for the right hand side of equation (5.9) as:

$$s = 100\%(w_2 + w_3) \qquad \ldots (5.10)$$

and,

$$a = \frac{100\%}{Rma}\left[\frac{w_3}{w_2 + w_3}\right] \qquad \ldots(5.11)$$

where: s =% solids by weight in the slurry.
a =% ash by weight in the solids.
Rma =mineral matter to ash ratio for the coal.

Using this calibration model, the sensitivity of
ASHSCAN to changes in the mineral matter mineralogy, in
particular the iron concentration, was theoretically
evaluated (i.e. μ_3 was varied). It was shown that for the
McIntyre flotation circuit product streams, variations in
the iron concentration of the mineral matter of ±0.7% will
contribute a 5% relative error in the estimated ash content.
(This was also observed for an OSCAA type system where iron
compensation was excluded.) Since iron concentration does
change, ASHSCAN would be of limited utility unless
frequently recalibrated.

5.3.2 Deviations from Lambert's Law

While the development of the theory underlying the
nuclear pulp density gauge is reasonably straightforward
using Lambert's law, the restrictions for strict compliance
are seldom met in practice. There are potentially three
effects which can serve to complicate the measurement. Under
"normal" circumstances they will seldom render the
previously developed equations invalid, but the reader
should at least be aware of their existence.

5.3.2.1 Filtration

In some special instances the radioisotope chosen for the particular gauging problem will emit photons at two or more distinct energy levels. For example, Gd-153 emits photons with energies of $E_1 \approx 100$ kev and $E_2 \approx 40$ kev. In this case the lower energy photons would be attenuated to a greater extent by the absorbing medium. This phenomenon is known as *filtration*. Accordingly, as the pulp density and hence the $\rho\mu x$ term increase, the total photon attenuation will occur by smaller and smaller fractions. The linearized form of equation (5.1) will show an increasing slope as μ apparently decreases with increasing ρ. If filtration induced curvature is apparent from the calibration exercise, and remains unresolved, then the calibration model will require a series of terms on the right hand side, similar to the right hand side of equation (5.1). That is, one for each photon energy level which is <u>contributing</u> to the measured intensity.

5.3.2.2 Build-up

The build-up factor, B, is defined as;

$$B = \frac{\text{Observed Intensity at the Detector}}{\text{Primary Intensity Expected at the Detector}} \qquad \ldots(5.12)$$

$$= 1 + \frac{\text{Intensity due to Scattered Radiation}}{\text{Primary Intensity}}$$

Build-up results from the multiple scattering of

radiation in the absorber such that some of the photons
report to the detector which otherwise, under narrow
beam conditions, would not. Relaxation of source and
particularly detector collimation will cause the
build-up factor to increase. The multiple scattering
process in "broad beam geometry" is illustrated in
Figure 5.4(A). Figure 5.4(B) illustrates the variation
of B with beam geometry. These results were obtained by
Wyckoff et. al.(40) using concrete as the absorbing
medium. (Note that in Figure 5.4(B), for a particular
abcissa value, the build-up is simply the ratio of the
corresponding untransformed ordinate values.) Since
Compton scattering is the principal attenuation process
for the photon energy levels encountered in nuclear pulp
density gauges, build-up would be expected to affect
measurement. This is particularly true given the broad
beam geometry employed in industrial gauges (see Figure
5.3).

Fano(41) has derived equations which estimate
build-up factors for various absorbers. However, the
assumed system geometry for the published solutions and
the complexity of the calculations make them essentially
useless in this application. This has prompted other
workers to adopt simple empirical models for B such as;

$$...(5.13)$$

$$B=1+\alpha(\rho\mu x)^\beta; \quad (42,43)$$

⊗ Scattering Event

Absorber

Source

Detector
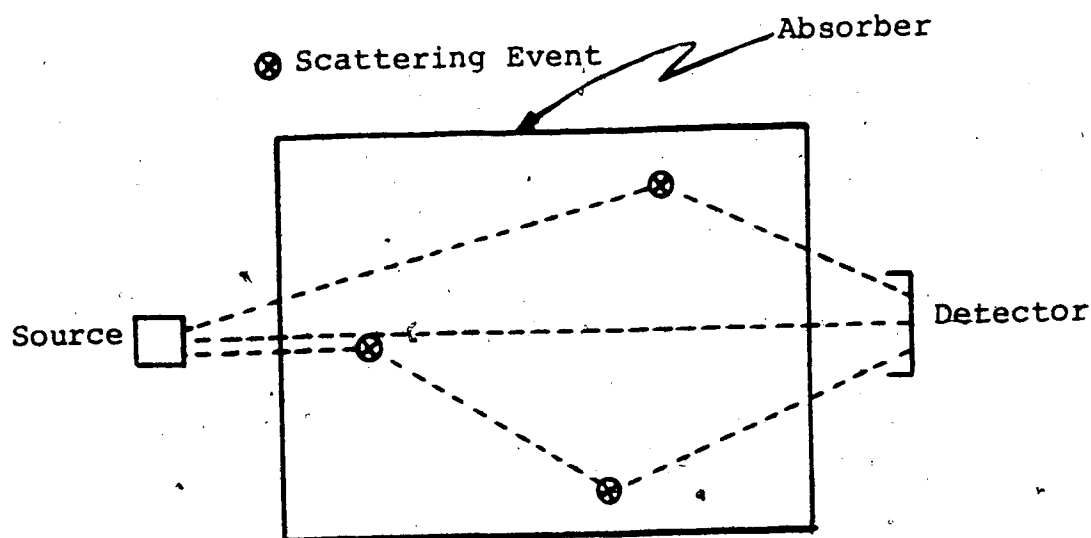
(A) An illustration of broad beam geometry and the scattering processes giving rise to build-up.

○ Narrow Beam

⬡ 13 in. Beam

△ 26 in. Beam

□ 37 in. Beam

800 Kev incident photons

Relative Intensity

Concrete Thickness (ins.)
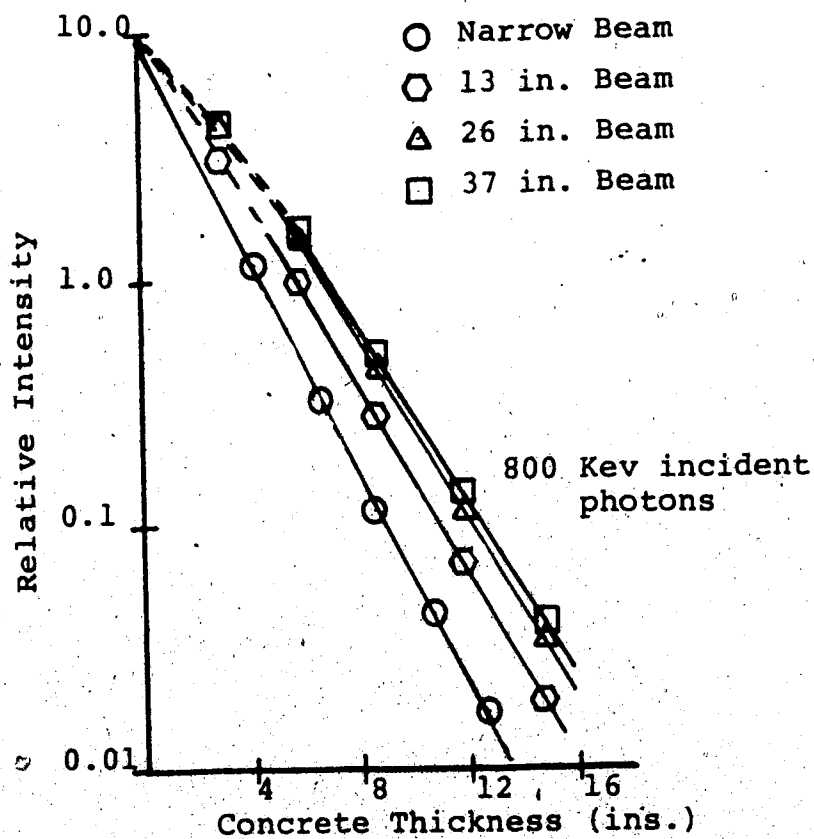
(B) Wyckoff's   experiments with beam geometry

Figure 5.4 The Mechanism and Effect of Build-up.

$$B=1+\alpha(\rho\mu x)+\beta(\rho\mu x)^2 \; ; \; (44)$$

$$B=\sum_{i}^{M} A_i \exp(\alpha_i \rho\mu x) \; ; \; (43)$$

where:

A, α, β are constants.

Lambert's Law is thus modified to include build-up as;

$$I=BI_0 \exp(-\rho\mu x)$$

There are only two means by which build-up can be circumvented and both are largely impractical in an industrial setting. Firstly, narrow beam geometry will virtually eliminate build-up. However, this will also effectively reduce the source strength (I_0) and hence the measured intensity (I) giving rise to poor measurement statistics. (That is, for a Poisson process, the relative error of measurement is proportional to $1/\sqrt{I}$'*.) Secondly, since Compton scattering predominates and because these scattering events are inelastic, the incident photons are always in good geometry. Thus a detection system capable of resolving primary and scattered photon energies could be used to detect only uncollided primary photons. Given the resolution versus photon energy characteristics of the detectors commonly used, this is probably not practical.

'*For a more complete discussion on the statistics of radioisotope emmisions and photon detection the reader is referred to any text on basic X-ray analysis(52,67).

In calibrating the pulp density gauge, if it is judged that build-up creates sufficient non-linearity[1] then simple models for B, of the form given in equations (5.13)-(5.15) must be incorporated in the calibration model (eqn. (5.16)).

5.3.2.3 Broad Beam Geometry

In the design of most density gauges the source is generally collimated to an extent and the detector is left essentially uncollimated. Since the crystal of the scintillation counter (the most common detector) is much larger than the source collimation aperture these gauges operate with broad beam geometry. Neglecting the effects of build-up and considering the source to be in point form, as opposed to disk form[2], the effect of beam divergence can be estimated.

Figure 5.5(A) sets out the geometry of broad beam measurement in spherical coordinates, assuming a point source. The fraction, Ω, of the primary photons which report to a differential element of area on the detector surface, with a source-detector separation of x, and assuming a vacuum is;

$$\Omega = \frac{x^2 \cos\phi \, d\phi \, d\theta}{4\pi x^2} = \frac{\cos\phi \, d\phi \, d\theta}{4\pi} \qquad \qquad ...(5.17)$$

----

[1] A particularly good example of the effect of build-up in a radio-gauging application is given by Gardner and Ely (see (42), pg. 330).
[2] In most cases the path length is long enough to make this a reasonable assumption.

Point
Source

X

lo

ϕ_1

θ_1

Y

Z

Detector

(Plane Parallel
Geometry)
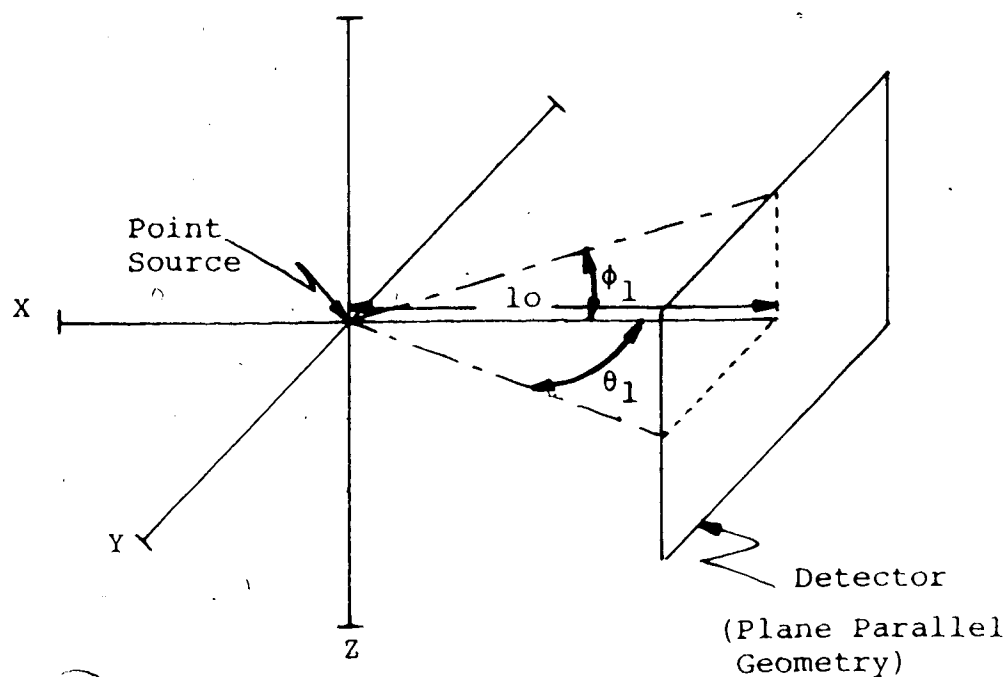
(A) Geometry of the broad beam measurement system.

$\left[\dfrac{N(\rho\mu lo)}{N(\rho\mu lo=1.5)}\right]$

FLUX RATIO

1.0

0.8

0.5

0.3

Equivalent to
Lambert's Law

$\phi_1=\theta_1=5°$
$\phi_1=\theta_1=15°$
$\phi_1=\theta_1=30°$
$\phi_1=\theta_1=40°$

1.5

2.0

2.5

DECAY FUNCTION $(\rho\mu lo)$
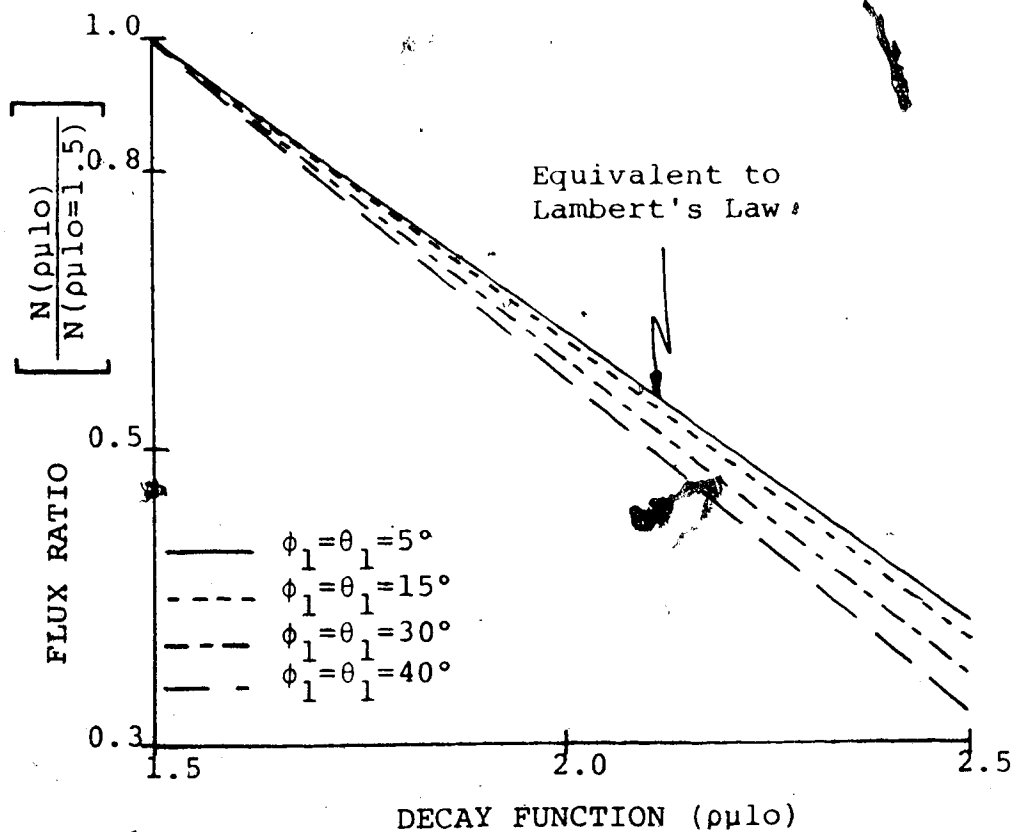
(B) Theoretical attenuation curves for the broad beam.

Figure 5.5 Broad Beam Geometry and its Effect on

Calibration.

where:
    Ω =fraction of photons to the differential element.
    x =source-detector separation.
    θ, ϕ =the angles as defined in Figure 5.5(A).

Accounting for attenuation, the photon flux on this

element of the detector surface, dN, is calculated as;

$$dN=N_0 \Omega \exp(- \frac{\rho\mu x}{\cos\theta\cos\phi}) \qquad ...(5.18)$$

where:
    dN =photon flux to the differential element.
    N_0 =source activity in photons/s.

Integrating over the positive quadrant of the detector,

i.e. $\theta>0$, $\phi>0$, and invoking goemetrical similarity

yields the expression for the flux on the detector, N;

$$N=\frac{N_0}{\pi} \int_0^{\theta_1} \int_0^{\phi_1} \cos\phi \exp(- \frac{\rho\mu x}{\cos\phi\cos\theta})d\phi d\theta \qquad ...(5.19)$$

where:
    θ_1, ϕ_1 define the limits of the detector in the
        positve quadrant.

By inspection of equation (5.19) it is evident that for

very slightly divergent beams, i.e. $\theta_1 \to 0^+$, $\phi_1 \to 0^+$, this

is essentially equivalent to Lambert's law written in

terms of flux rather than intensity. To illustrate the

effect of beam divergence on measured flux suppose that

the detector window is square (ref. Figure 5.5(A), i.e.

$\theta_1=\phi_1$. Choosing a value for θ_1 and some typical $\rho\mu x$

values, the variation in N with $\rho\mu x$ can be studied.

(Note that equation (5.19) requires numerical solution.)

The results of this exercise are shown on Figure 5.5(B)

where the calculated flux values have been reduced by

dividing by the flux corresponding to the lowest $\rho\mu x$
value used. Clearly, the logarithmic relationship
expected from Lambert's law is maintained and the latter
could be applied as the calibration model. In this case,
the apparent source strength would increase with an
increase in beam divergence. The resultant increase in
mean path length would mean a decrease in the slope of
the attenuation curves (slight increase in the apparent
μ, as illustrated in Figure 5.5(B). It can be concluded
from the sample calculation that broad beam geometry
will not introduce curvature in the calibration curves,
within practical limitations.

Thus far build-up effects have been neglected
although they can be very important in broad beam
geometry, In this case build-up has the previously
discussed effect and the calibration model must be
appropriately modified if necessary. This raises the
issue of design compromise where economy of source
requires broad beam irradiation while reduction of
build-up requires narrow beam geometry.

5.4 THE OPTIMIZATION OF PULP DENSITY SUB-SYSTEM DESIGN

A number of authors(44-48) have dealt with the optimal
design of pulp density gauges in varying degrees of
complexity. Apart from Tabor and Lakoski, they have
neglected build-up as well as beam divergence. In all cases
filtration was excluded from the analysis. Consideration of

all of these possible interferences is theoretically
possible but practically very difficult.

Since most of the radioisotopes used in this
application emit only mono-energetic photons, or have
secondary emissions which are of sufficiently low energy to
be totally attenuated in the absorber, filtration can be
reasonably ignored in any analysis. Furthermore, as was
illustrated in Figure 5.5(B), beam divergence does not cause
a departure from Lambert's law other than to increase the
apparent source strength and slightly increase the apparent
mass absorption coefficient. Therefore, beam divergence will
permit the use of Lambert's law in any analysis. However,
the effects of build-up can not be so easily excluded.
Equally unfortunate is the fact that it is impossible to
estimate, *a-priori*, the coefficients of a build-up model.
The design analysis which follows illustrates the methods
using Lambert's law and excluding build-up. General comments
on the expected effect of the latter will be made at the
appropriate points.

The objective in optimizing performance is to design in
such a manner that pulp density accuracy is maximized. In
addition to good installation this includes maximizing
sensitivity. The optimization criterion can be obtained by
application of the Law of Propagation of Errors., i.e.

$$\sigma^2(\rho) = \left[\frac{\delta\rho}{\delta I}\right]^2 \sigma^2(I) \qquad \ldots(5.20)$$

where: $\sigma^2(j)$ = the variance of variable j.

Taking the square root of both sides of equation (5.20) and

dividing by the pulp density yields the expression for the relative error in pulp density measurement''.

$$\frac{\sigma(\rho)}{\rho} = \left|\frac{\delta\rho}{\delta I}\right| \frac{\sigma(I)}{\rho} \qquad \qquad \ldots(5.21)$$

The optimization criterion is simply stated as;

$$\text{MINIMIZE}\left[\left|\frac{\sigma(\rho)}{\rho}\right|\right] \qquad \qquad \ldots(5.22)$$

By appropriate choice of the design parameters, which, with reference to equation (5.1) include, source strength, mass absorption coefficient and path length, optimal design can be achieved. Substitution of equation (5.21) into equation (5.22) with the appropriate expression for $\sigma(I)$, depending upon the nature of the error, allows solution to the minimization problem.

There are several sources of potential error in the intensity measurement. Since the importance of each in a particular application is the subject of careful assessment, they are best treated separately with respect to optimizing gauge design.

5.4.1 Statistical Error

This is the error which is due to variation in the measured radiation intensity at the detector. Since radiation intensity measurement is observed to follow a

''An equivalent expression can be obtained using the classical definition of instrument sensitivity (see (46) for example). Note that the relative error is defined as if the the intensity error were a random variable. This is not necessarily always the case.

Poisson distribution, the expression for $\sigma(I)$ is simply $\sqrt{I}$. The relative error may be written as;

$$\frac{\sigma(\rho)}{\rho} = \frac{-\exp(\frac{\rho\mu x}{2})}{\sqrt{I_0}\rho\mu x} \qquad \qquad \ldots (5.23)$$

and can be minimized by;

a) choosing a large I_0 (source strength) subject to shielding constraints, (and detector saturation)

b) setting $\rho\mu x$ numerically equal to 2. (This is established using calculus for extremum location.) Clearly, the radioisotope (μ) and path length (x) choices are dependent for the given system.

Kawatra(47) obtained the same results with a slightly different approach. His method does not provide any information about the objective function in the neighbourhood of the optimum, which is available from equation (5.23). In fact, the "objective response" is relatively flat in the range $1 \le \rho\mu x \le 3$. The effect of build-up is essentially to translate the the objective reponse to higher values for the optimum of $\rho\mu x$. This is expected since, from Figure 5.4(B), the effect of build-up is to show an apparent decrease in μ. On the other hand, the presence of divergent beam geometry tends to lower the value of this optimal solution as divergence increases. This is also expected since increasing divergence effectively increases the mean path length through the absorber.

5.4.2 Zero Drift Error

This is the error which is due to the electronics employed in the measurement system. While in the strictest sense it is not possible to assign a $\sigma(I)$ value to this error source, the effect can be illustrated by setting,

$$\sigma(I)=K \qquad \qquad ...(5.24)$$

where: K = a constant.

Solving for the relative error yields;

$$\frac{\sigma(\rho)}{\rho} = \frac{-K\exp(\rho\mu x)}{I_0 \ \rho\mu x} \qquad \qquad ...(5.25)$$

and minimization is achieved by;

a)   choosing a large I_0.

b)   setting $\rho\mu x$ numerically equal to 1.

In this case the objective response exhibits pronounced curvature in the neighbourhood of the optimum, however, excursions of $\rho\mu x$ to higher values are more acceptable than the converse. The effects of build-up and beam divergence can be rationalized along the lines of the previous sub-section.

5.4.3 Proportional Error

This is the error which is due to such factors as radioactive decay, mechanical instability, and variations in detector efficiency and amplifier gain. For mathematical convenience the standard deviation of the measured intensity will be defined as;

$$\sigma(I) = KI \qquad \qquad \ldots(5.26)$$

where: K =a constant.

The expression for relative error in pulp density is then given by;

$$\frac{\sigma(\rho)}{\rho} = \frac{-K}{\rho\mu x} \qquad \qquad \ldots(5.27)$$

In this case choosing $\rho\mu x$ as large as is possible will minimize the contribution to measurement error. This statement applies to systems including build-up and beam divergence as well.

5.4.4 Extraneous Absorber

This is the error which is due to solids accumulation in the radiation pathway, variable quantities of entrained air, etc... These errors can only be minimized through the proper considerations in gauge installation and pipeline operation.

5.4.5 More On Entrained Air

In industrial applications air entrainment is something over which the operator may have little control. If significant variations in the air content do not occur, its effect can be removed in the calibration exercise (i.e. air+water=single phase). If significant variations do occur then the pulp density measurement may be virtually meaningless. Where high quality density measurements are required, such as in the OSCAA system, even small variations

in entrained air are unacceptable. Process pulps often contain air and in variable quantity. Kawatra(49) has observed that in flotation pulps it is not unusual to have entrained air contents of from 5% to 20% by volume. Fluctuations of this magnitude can be expected to have profound effects on the attenuation of the incident photons.

The effect of air in estimating the pulp composition can be easily demonstrated considering the ASHSCAN device (see sub-sec. 5.3.1). As was observed above, increasing air content will serve to lower the apparent pulp density. However, the mass absorption coefficient will be largely unaffected by the presence of air (ref. eqn. (5.9)). Thus, in solving the simultaneous linear system, the apparent solids concentration will be lower than expected while the mineral matter (ash) content will be higher. If the device were calibrated about some mean air content then a decrease in this variable would have the opposite effect. This is precisely the reason why Lyman built a high pressure pumping system into the ASHSCAN device.

One possible but often impractical solution to this problem is to make a parallel density measurement on a sample of process water "standard" which is aerated to the same extent. Subsequently, the measured intensity through the pulp can be reduced by dividing by the corresponding reading on the standard which will largely remove the effect of air. Implicit here is that the process water standard sample be can be obtained and that changes in the air

content occur on a relatively long term basis. Both of these requirements are expected to be seldom realized in practice.

There are a number of more direct means of attempting to minimize the air problem, ranging from passive in-line techniques to rather expensive mechanical methods. They can be generally categorized as follows:

a) Passive Methods

These methods typically involve a secondary sample splitting device (cf. On-stream X-ray fluorescence spectrometer systems). Although the primary function of such a device is to extract a small but representative portion of the primary sample for anaysis, it can be designed to provide for fairly quiescent flow thereby promoting deaeration. The system will be in a "distributed" equilibrium and very small bubbles will not have the same probability of escape as the large ones. Therefore, if small bubbles are present in high concentration these methods will prove largely ineffective.

b) Non-Mechanical Centrifugal Methods

These methods have been employed by the nuclear and HVAC industries for the deaeration of process water. In essence, a mechanism is used which imparts a rotational motion to the fluid thus enhancing air removal at the centre by means of centrifugal forces. The nuclear industry in particular(50) has developed the technology to the extent that very little water is lost in the air

take-off stream while very efficient deaeration is
achieved.

c) Mechanical Methods

These methods involve mechanical systems which operate
either on the principles of (b) as, for example,
Autometrics PSM air eliminator(51) or on pressurization
to collapse the air bubbles (cf. ASHSCAN).

The capital and operating costs of the class (c)
methods make them a last resort proposition in the
opinion of this author. Class (b) techniques would
require reasonably careful design and operational
control to avoid sample bias but, if used in conjunction
with class (a) methods would seem to provide an
attractive alternative in both a technical and economic
sense. The class (a) methods represent the simplest
possible solution and a variant was chosen for use in
the OSCAA prototype. It is implicitly assumed that the
slurry flow streams would not contain high
concentrations of very fine air bubbles.

5.4.6 Summary

In the optimal design of nuclear pulp density gauges
the souce strength should be maximized subject to the the
shielding contraints. Depending upon the principal source of
error(s) the optimal value of $\rho\mu x$ can take on different
values. In practice the gauge is usually designed such that;

$$\dots(5.28)$$

$$1 \leq \rho\mu x \leq 3$$

Since ρ is the property to be measured, the radioisotope (μ) and the path length (x) must be chosen to satisfy the equation (5.28). Special care must be taken to minimize the entrained air (especially fluctuations therein) in the pulp, wherever this is possible.

5.5 THE PRINCIPLES OF BACKSCATTER AND FLUORESCENCE RADIATION MEASUREMENT

In this OSCAA sub-system the interaction of the incident radiation with the sample is somewhat more complex than in the transmission measurement, although Lambert's law is the theoretical base. Whereas in transmission gauging, e is simply concerned with the overall photon attenuation passage, the backscatter geometry requires more detailed knowledge. That is, at any particular level in the sample it is necessary to know:

a) the incident photon intensity,

b) the fraction of these photons absorbed in this layer,

c) the fraction of these absorbed photons which interact via the various processes and the spatial distribution of the secondary photons which result,

d) the attenuation of the secondary radiation which is directed toward the sample surface,

e) the sum of all of these factors over all layers in the sample.

While most textbooks on X-ray fluorescence provide some

theoretical background to the subject (see (52); Chap. 4 for example), the mathematical modelling efforts of Rhodes and co-workers (53,54,55) are more easily applied to the present investigation. Although in theory it is possible to account for a continuous particle size distribution(54,55), in practice, and for the purposes of OSCAA, it is sufficient to lump the size distribution into a single average particle diameter(53). The mathematical development which follows is a consolidation of the theory developed by Rhodes et. al.

5.5.1 The Theory of the OSCAA Ash Analysis Sub-System

In developing the theory of operation of similar gauges Rhodes et. al. made the following assumptions;

a) The primary and secondary radiation enter and leave the sample perpendicular to the sample surface. For oblique incidence the terms μ_j in the equations which follow are merely replaced by $\mu_j \cosec\theta$, where θ is the angle the incident beam makes with the surface.

b) All particles have the same average size with an average linear dimension $\bar{d}$, where $\bar{d}$ is defined as;

$$\bar{d} = V / \bar{a} \qquad \qquad \text{...(5.29)}$$

where:
   V = particle volume.
   $\bar{a}$ = particle area presented to the incident radiation averaged over all possible orientations of the particle.

c) In a sample containing more than one type of particle, the distribution of the particles throughout the sample is completely random but, in any horizontal layer of

thickness $\bar{d}$, the average relative volume distribution of the particles is the same as the average over the whole sample. In Figure 5.6(A) the (i+1)th layer represents such a typical "slice" in the sample. Moreover, the physical and chemical properties (ρ, μ, etc...) of each individual particle are homogeneous.

Under the assumptions above, the radiation flux leaving the sample from the (i+1)th layer, N_{i+1}, is;

$$N_{i+1}(t) = I_0' J_i' J_i \bar{a} \sum_j^k \eta_j F_j \qquad \ldots(5.30)$$

where: $N_{i+1}(t)$ =radiation flux of type t arriving at the sample surface from the i+1th layer; t= f for fluorescent radiation and t=b for backscattered radiation.

I_0' =incident intensity of the primary radiation.

η_j =number of j type particles in the i+1th layer where there are a total of k different particle types.

$\bar{a}$ =average particle area presented to the incident radiation.

J_i =average transmission through i layers of the sample for the incident radiation.

J_i' =average transmission through i layers of the sample for the secondary radiation.

F_j =secondary radiation intensity per unit incident intensity for particle type j.

(Implicit in this formulation is that the fluorescent and backscattered radiation are mono-energetic. This is correct for the former when considering a particular line, however, since both inelastic and elastic scattering can occur this assumption is in question for the latter. It will be shown later that, for the OSCAA system, this assumption is indeed reasonable.)

To derive the fluorescent and backscattered radiation models

from equation (5.30), the terms on the right hand side,
other than I_0, are treated individually. To further simplify
the analysis each type of the secondary radiation will be
considered separately.

5.5.1.1 Fluorescent Radiation Model

Transmission Factors: J_i & J_i'

Consider J_i first of all. For generality, suppose
that the sample consists of k types of particles. For a
very narrow photon beam the i layers may be divided into
the set $(n_1, n_2, \ldots, n_k)$ where;

$$\sum_{j}^{k} n_j = i \qquad \ldots (5.31)$$

where:
    n_j =the number of layers in which the incident
        photons encounters the jth type of particle.

Invoking the multinomial distribution, the probability
that the radiation beam will intercept any specific set,
$\underline{n}$, is given by;

$$P(\underline{n}) = \frac{i!}{\prod^{k} n_j!} \prod^{k} \pi_j^{n_j} \qquad \ldots (5.32)$$

where:
    π_j =the probability of encountering the jth particle
        type in the sample. This will be taken as the
        volume fraction of this particular species in
        the entire sample, C_j.

The expected attenuation of the incident photons is then
calculated as;

$$J_i = \sum_{n_1=0}^{i} \sum_{n_2=0}^{i-n_1} \cdots \sum_{n_{k-1}=0}^{i-\sum_{\ell=1}^{k-2} n_\ell} \left[\frac{i!}{\prod^k n_j!} \prod^k \pi_j^{n_j} \exp(-\bar{d}\mu_j n_j \rho_j) \right] \quad \ldots(5.33)$$

$$\text{with: } n_k = i - \sum_{j=1}^{k-1} n_j$$

where:

μ_j, ρ_j = the mass absorption coefficient and density for the jth particle type.

Employing the following change of variable;

$$\omega_j = \pi_j \exp(-\bar{d}\mu_j \rho_j) \quad \ldots(5.34)$$

and the multinomial series identity, the expression for J_i can be written as;

$$J_i = \sum_{n_1=0}^{i} \sum_{n_2=0}^{i-n_1} \cdots \sum_{n_{k-1}=0}^{i-\sum_{\ell=1}^{k-2} n_\ell} \left[\frac{i!}{\prod^k n_j!} \prod^k \omega_j^{n_j} \right] \quad \ldots(5.35)$$

$$= \left[\sum^k \omega_j \right]^i$$

or, with the appropriate substitution;

$$J_i = \left[\sum^k C_j \exp(-\bar{d}\mu_j \rho_j) \right]^i \quad \ldots(5.36)$$

since the fractional attenuation across a layer is constant. By similarity;

$$J_i' = \left[\sum^k C_j \exp(-\bar{d}\mu_j' \rho_j) \right]^i \quad \ldots(5.37)$$

where:

μ_j' = mass absorption coefficient for the fluorescent radiation in the jth particle type.

Number of Particles: η_j

The number of particles of type j, η_j, is

calculated as

$$\eta_j = C_j \frac{A\bar{d}}{\bar{V}} = C_j A / \bar{a} \qquad \ldots(5.38)$$

where:
C_j = volume concentration of the jth particle type in
the sample.
A = cross sectional area of the irradiated sample.

Intensity Factor: F_j

With reference to Figure 5.6(B), consider the

infinitesmal layer dx, located at a depth x below the

surface of the jth particle type. The fraction of the

incident intensity absorbed by this layer is;

$$P_{1j} = -\frac{d}{dx} I_0 \exp(-\mu_j \rho_j x) dx = I_0 \mu_j \rho_j \exp(-\mu_j \rho_j x) dx \qquad \ldots(5.39)$$

where:
P_{1j} = intensity collided in the layer x to x+dx for
particle type j.
μ_j, ρ_j = attributes of jth particle.

The probability that these photons will produce

fluorescent radiation is calculated as;

$$P_{2j} = \frac{\tau_j Y_j w_{xj}}{\mu_j} \qquad \ldots(5.40)$$

where:
P_{2j} = probability that the absorbed photons will
produce fluorescent radiation.
τ_j = photoelectric mass absorption coefficient for
particle type j.
Y_j = fluorescent yield for particle type j.
w_{xj} = mass fraction of the X-ray fluorescent element
of interest in the jth particle.

In particular,

$$\tau_j Y_j = \sum \tau_{\ell j} Y_{\ell j} \qquad \ldots(5.41)$$

is the sum of the individual fluorescence contributions

Primary Photons | Secondary Photons

Surface of area A.

Water

Slurry Sample

Particulate Species

$\bar{d}$ | i+1 th Layer

(A)

Primary Photons | Secondary Photons

$\bar{d}$

Volume = $V = \bar{d}\,\bar{a}$

x

dx
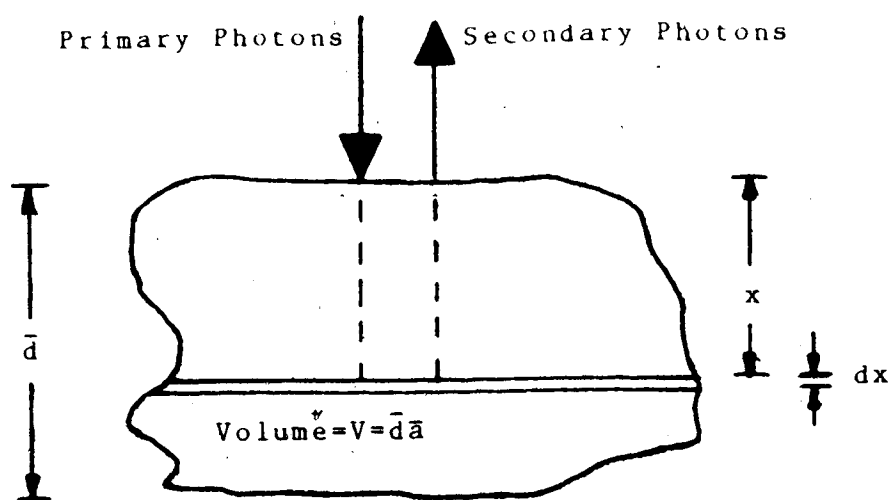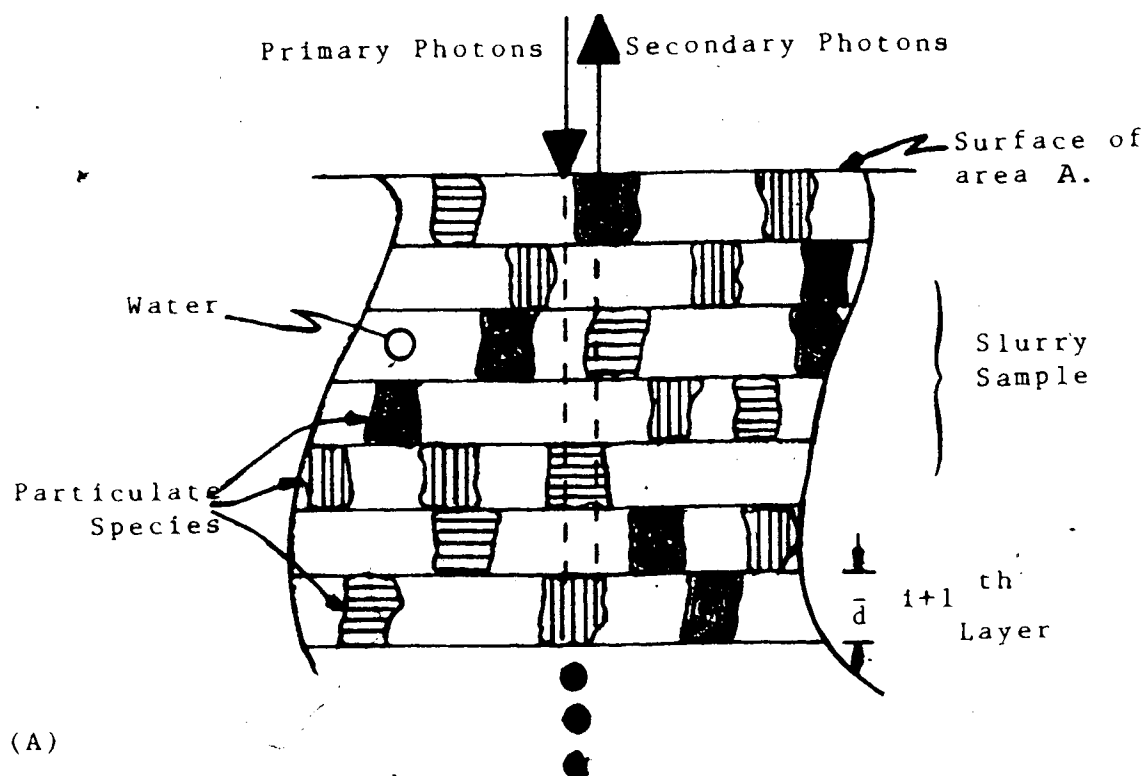
Homogeneous "j-type" Particle

(B)

Figure 5.6 Conceptual Illustrations of the Slurry Sample and an Individual Particle.

from the various shells (K,L and M). In most
applications one is looking specifically for K or L
shell X-rays in which case the appropriate values for
the shell of interest would be input to equation (5.40).
The attenuation of the fluorescent radiation which is
directed toward the particle surface is given by;

$$p_{3j} = G \exp(-\mu_j' \rho_j x) \qquad \ldots (5.42)$$

where:
p_{3j} = fraction of fluorescent photons reaching the
particle surface from a depth x.
G = geometrical factor.

Thus, the total expected fluorescent radiation intensity
at the particle surface is the product of equations
(5.39), (5.40), and (5.41), integrated over the range of
x, i.e.;

$$I_{xj} = \int_0^{\bar{d}} \frac{\tau_j Y_j W_{xj}}{\mu_j} \mu_j \rho_j G I_0 \exp(-\rho_j x(\mu_j + \mu_j')) dx$$

$$= \frac{\tau_j Y_j W_{xj}}{(\mu_j + \mu_j')} G I_0 (1 - \exp(-\rho_j \bar{d}(\mu_j + \mu_j'))) \qquad \ldots (5.43)$$

where:
I_{xj} = intensity of fluorescent radiation at the
surface of a j type particle.

Dividing both sides of equation (5.43) by I_0 gives the
expression for F_j as;

$$F_j = \frac{\tau_j Y_j W_{xj}}{(\mu_j + \mu_j')} G(1 - \exp(-\rho_j \bar{d}(\mu_j + \mu_j'))) \qquad \ldots (5.44)$$

Substitution of equations (5.36), (5.37), (5.38) and
(5.44) into equation (5.30) and summing over all z

layers, where d (z+1) is the sample thickness, yields;

$$N(f)_j = \frac{N_0 C_j \tau_j Y_j w_{xj}}{(\mu_j + \mu_j')} G(1-\exp(-\rho_j \bar{d}(\mu_j+\mu_j'))) \sum_{i=0}^{z} (J_i J_i')^i \quad ...(5.45)$$

where:
   N_0 = incident flux upon the sample, i.e. $N_0 = I_0 A$.
Of particular importance in this work is the case where
$z \to \infty$, i.e. an effectively infinitely thick sample. Using
the convergence properties of infinite series (see
(56);pp. 413-415), the transmission factor product
summation can be written as;

$$\sum_{i=0}^{\infty} (J_i J_i')^i = \frac{1}{(1-JJ')} \quad ...(5.46)$$

and the final expression for fluorescence flux at the
sample surface is;

$$N(f) = \frac{N_0 G}{(1-JJ')} \sum^{k} \left[\frac{C_j \tau_j Y_j w_{xj}}{(\mu_j+\mu_j')} (1-\exp(-\rho_j \bar{d}(\mu_j+\mu_j'))) \right] \quad ...(5.47)$$

This model can be further simplified by allowing
the average particle size to approach zero. Under this
assumption the sample becomes a homogeneous mixture.
Taking the limit of equation (5.47) as $\bar{d} \to 0^+$ gives an
indefinite result as both the denominator and the
numerator vanish. Applying L'Hospital's rule yields;

$$\lim_{\bar{d} \to 0} \left[\frac{N_0 G \sum^{k} \left[\frac{C_j \tau_j Y_j w_{xj}}{(\mu_j + \mu_j{}')} \rho_j(\mu_j + \mu_j{}') \exp(-\bar{d}\rho_j(\mu_j + \mu_j{}')) \right]}{\sum^{k} \sum^{k} (\rho_i \mu_i{}' + \rho_j \mu_j) C_j C_i \exp(-\bar{d}(\rho_i \mu_i{}' + \rho_j \mu_j))} \right] \qquad \ldots (5.48)$$

$$= \frac{N_0 G \sum^{k} \tau_j Y_j w_{xj} C_j \rho_j}{\sum^{k} C_j \rho_j (\mu_j + \mu_j{}')}$$

For a particular sample,

$$\ldots (5.49)$$

$$C_j \rho_j = q w_j$$

where:

q = a constant.

w_j = mass fraction of component j.

and substitution gives;

$$N(f) = \frac{N_0 G \sum^{k} \tau_j Y_j w_{xj} w_j}{\sum^{k} w_j (\mu_j + \mu_j{}')} \qquad \ldots (5.50)$$

Rhodes and Hunter(55) have done a similar exercise in reducing the more general form of the model given by equation (5.45) to the homogeneous sample representation. The difference lies in the fact that equation (5.50) assumes an infinitely thick sample. It will be shown later that this is a reasonable assumption with the OSCAA flow cell design.

Figure 5.7(A) compares equations (5.50), the horizontal line, and (5.47), the curve, as a function of the mean particle diameter, $\bar{d}$. The ordinate data is the predicted reduced iron fluorescence flux typical of the
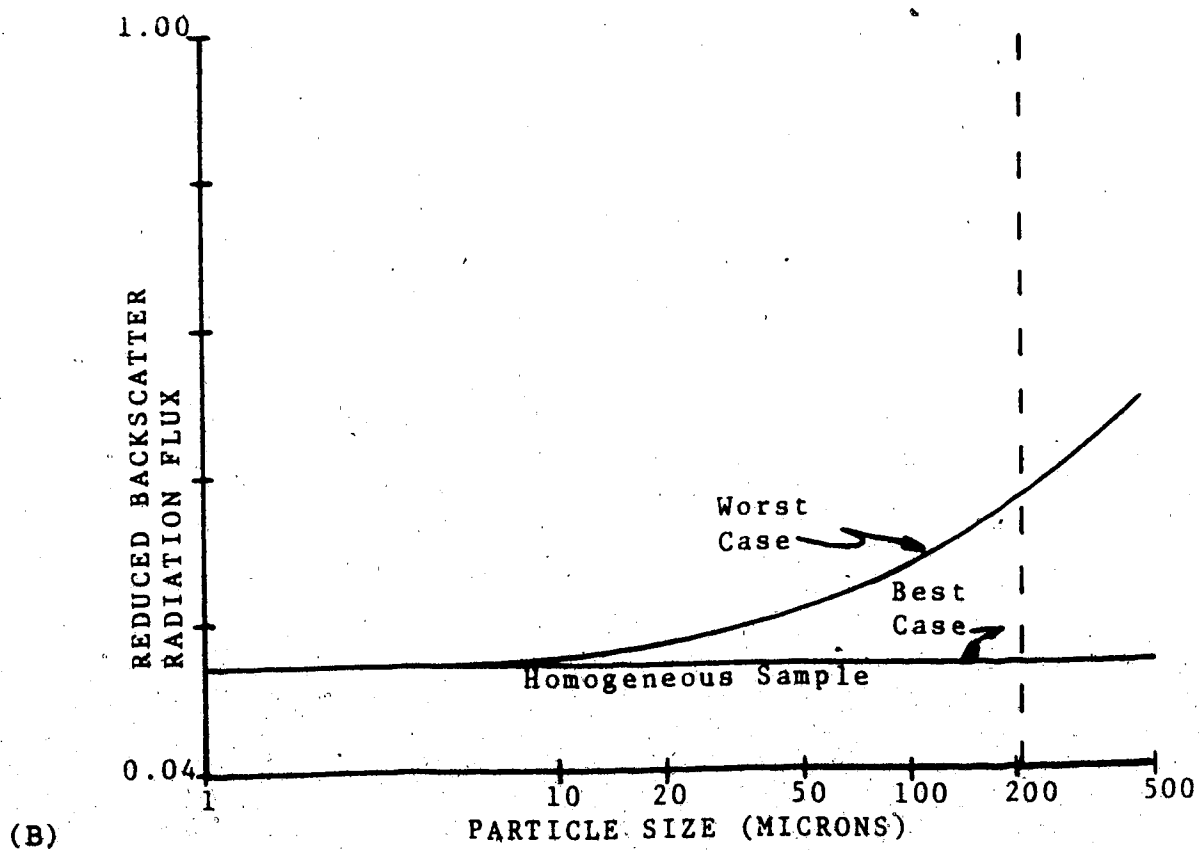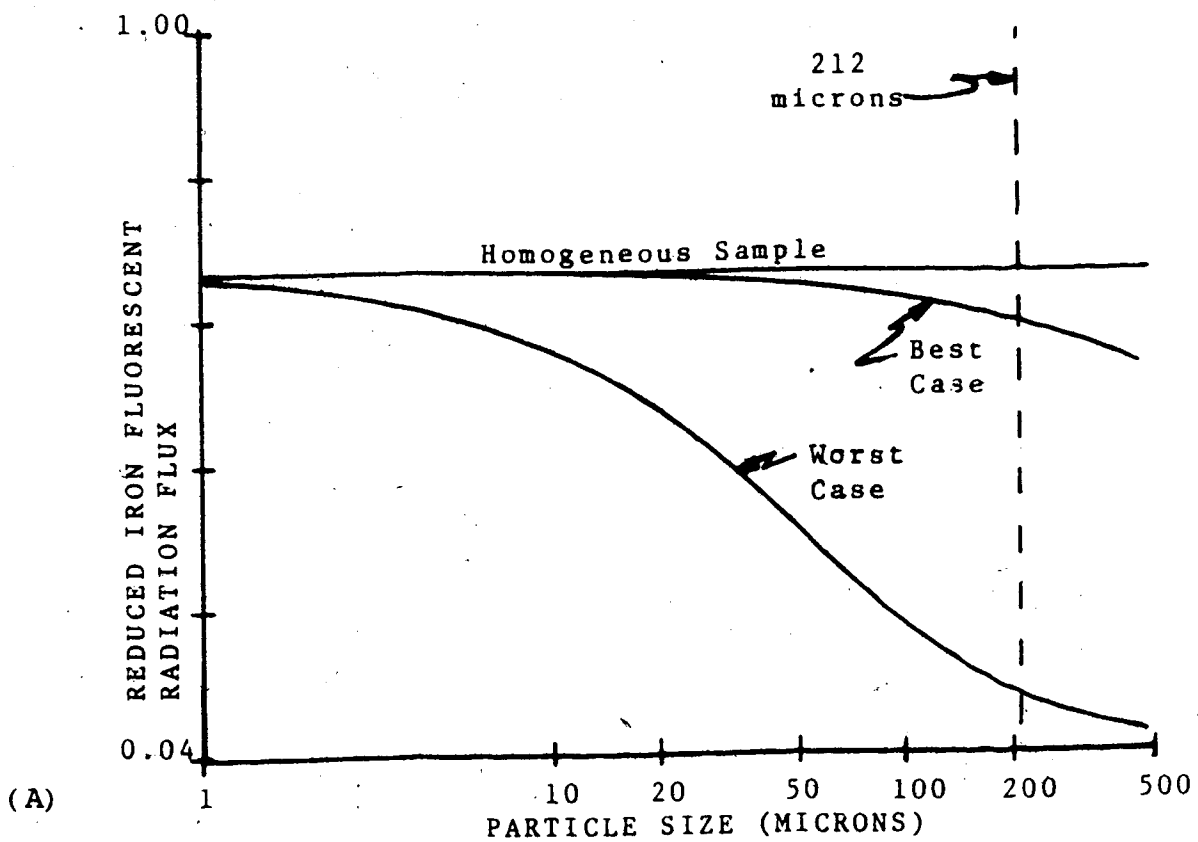
Figure 5.7 Particle Size Effects in Fluorescent and

various flow streams around the McIntyre flotation circuit (ref. Figure 3.1). (Only the curves for the flotation feed are shown, but they are representative of the tailings and concentrate streams as well.) The vertical line at 212 microns represents a typical mean particle diameter derived from screen analysis. For the purposes of this calculation the irradiating isotope was taken to be Cd-109 and the fluorescent radiation of interest was the iron $K\alpha$ X-rays. Since the detailed mineralogy of the solids is unknown a "best case" and "worst case" are presented. The best case assumes that the slurry consists of water and solids particles. The latter are assumed to be homogeneous with constant composition. The worst case assumes that the slurry consists of water and three types of solids particles. These are iron-free coal organics, iron-free mineral matter, and hematite. The method of estimating the component attributes is discussed in detail in Chapter 7.

The results illustrated on Figure 5.7(A) compare with similar calculations done by Rhodes and Hunter (see (54); fig. 3). For a particular flow stream there is considerable difference between the best case and the worst case. As expected, the best case curve is much less sensitive to particle size. From a practical point of view the "real" curve will lie somewhere in between the limiting cases, however, it is expected to lie

closer to the best case curve because of the partially liberated nature of solid phases. This will be especially true for the flotation output streams where, by the selective nature of the process, some homogenization occurs. The slope of the "true" curve at the "true" mean diameter will determine the extent to which changes in particle size will affect the fluorescent radiation flux. It is expected that this will increase in importance in the order of concentrate, to feed, to tailings. The other major point of interest from this figure is the loss in secondary photon flux as $\bar{d}$ increases. This would be expected to have implications for design with respect to the determination of accumulation times.

Despite the differences in predicted photon flux between the homogeneous sample and the best and worst cases, equation (5.50) is proposed for calibrating the OSCAA analyser. Apart from the absence of explicit size dependence (for which there is no means of measurement), the only difference is that the apparent incident photon flux will be lower.

5.5.1.2 Backscattered Radiation Model

Transmission Factors

These are of the same form given in equations (5.36) and (5.37) with the only difference arising in equation (5.37) where, μ_j', is the mass absorption

coefficient for the backscattered radiation.

Number of Particles

This is identical to equation (5.38) given above.

Intensity Factors

Unlike fluorescence, where only one element (iron) in the sample was considered, each component in each particle will scatter some of the incident radiation.

Proceeding as in the previous sub-section with reference to Figure 5.6(B), consider the infinitesmal layer dx, at a depth of x in the jth particle type. The fraction of the incident radiation absorbed in this layer is given by equation (5.39). The probability that these absorbed photon will produce backscattered radiation is calculated as;

$$P_{2j} = \frac{\sigma_j}{\mu_j} \qquad \qquad ...(5.51)$$

where:

p_{2j} =probability that the absorbed photons will produce backscattered radiation in the general direction of the detector.

σ_j =a composite scattering mass absorption coefficient which has contributions from both the Rayleigh and Compton processes. It depends upon incident photon energy, absorber character, system geometry, etc...

The attenuation of the backscattered radiation is given by equation (5.42), with the understanding that μ_j' is now the mass absorption coefficient for the backscattered radiation.

Thus, the expected backscattered radiation at the surface of a j type particle is the product of equations (5.39), (5.42) and (5.51), integrated over the range of

x, i.e.;

$$I_{sj} = \int_0^{\bar{d}} \frac{\sigma_j}{\mu_j} \rho_j \mu_j GI_0 \exp(-\rho_j x (\mu_j + \mu_j')) dx$$

...(5.52)

$$= \frac{\sigma_j GI_0}{(\mu_j + \mu_j')} (1 - \exp(-\rho_j \bar{d} (\mu_j + \mu_j')))$$

where:
   $I_{.j}$ = intensity of backscatter radiation at the surface of a j type particle.

Division of equation (5.52) by I_0 gives the intensity factor F_j as;

$$F_j = \frac{\sigma_j G}{(\mu_j + \mu_j')} (1 - \exp(-\rho_j \bar{d} (\mu_j + \mu_j'))) \qquad ...(5.53)$$

Substitution of the appropriate equations into equation (5.30) and assuming an infinitely thick sample yields the model form of equation (5.54);

$$N(b) = \frac{N_0 G}{(1-JJ')} \sum^k \frac{\sigma_j C_j}{(\mu_j + \mu_j')} (1 - \exp(-\rho_j \bar{d} (\mu_j + \mu_j'))) ...(5.54)$$

Before deriving the homogeneous sample model another simplification can be made to equation (5.54). Rayleigh events produce scattered photons with the same energy as the incident photons whereas Compton events result in an energy loss. The extent of this energy loss depends upon the scattering angle, ψ, and the incident photon energy. Mathematically;

$$\Delta E = E \left[1 - \frac{1}{1 + 0.001957 E (1 - \cos\psi)} \right] \qquad ...(5.55)$$

where:
   ΔE = energy difference between the incident and

scattered photon in kev.

ψ =the scattering angle; $0° \le \psi \le 180°$.

For Cd-109, with E≈22 kev and using ψ=120° and ψ=180°, the respective energy losses are 1.3 kev and 1.7 kev. With such relatively small changes in photon energy one can assume tnat the mass absorption coefficient for the primary and secondary radiation are equivalent, i.e;

$$\mu_j = \mu_j' \qquad \qquad ...(5.56)$$

and equation (5.54) may be rewritten as;

$$N(b) = \frac{N_0 G}{(1-JJ')} \sum^k \frac{\sigma_j C_j}{2\mu_j}(1-\exp(-2\rho_j \bar{d}\mu_j)) \quad ...(5.57)$$

Now, taking the limit as $\bar{d} \to 0^+$, employing L'Hospital's rule gives the model for a homogeneous sample as;

$$N(b) = \frac{N_0 G \sum^k w_j \sigma_j}{2 \sum^k w_j \mu_j} \qquad \qquad ...(5.58)$$

Again, as with equation (5.50), equation (5.58) implicitly assumes an infinitely thick sample which is reasonable for the OSCAA system.

Figure 5.7(B) compares equation (5.58), the horizontal line, and equation (5.57), the curve, to illustrate the particle size effect in backscatter measurement. The ordinate data is the predicted reduced backscatter photon flux. All other conditions are the same as those used in the development of Figure 5.7(A). (For the purposes of clarity, only the flotation feed curves are presented.) The scattering cross sections are computed by the method described in the following subsection. Again, best case and worst case curves are

presented.

The results illustrated on Figure 5.7(B) indicate that the particle size effect is much less pronounced in backscattering than in fluorescence. In particular, the best case curves are very nearly the same as the homogeneous sample model for all three flow streams. It is expected that equation (5.58) would be useful in calibrating an OSCAA type system.

5.5.1.3 Calculation of the Composite Scattering Coefficient

The composite scattering coefficient, σ_j, introduced in equation (5.51) is not simply the sum of the tabulated Rayleigh and Compton coefficients[*] as was assumed by Rhodes et. al. in their work. Both of these events exhibit a strong angular dependence and to avoid bias in the composite coefficient it is necessary to appropriately correct σ_m and σ_{nm}. The method amounts to calculating first order correction factors, r_m and r_{nm} which, when applied to the tabulated values, provide the composite coefficient, σ, i.e.

$$\sigma = r_m \sigma_m + r_{nm} \sigma_{nm} \qquad \ldots (5.59)$$

where:
σ =composite scattering mass absorption coefficient.
σ_m, σ_{nm} =Compton and Rayleigh mass absorption coefficients.
r_m, r_{nm} =correction factors.

For the OSCAA system geometry (see Chap. 6) it is

----

[*]The tabulated values account for scattering in all possible directions.

required to calculate the correction factors for

scattering in the range of $120° \le \psi \le 180°$. The actual

intersection of the detector with this band is accounted

for by a simple factor reflecting the area covered and

it can be lumped into G.

For Compton scattering, the exercise begins with

the Klein-Nishina equation given by Zeigler et. al.(57).

$$\sigma_m' = 3.92 \times 10^{-26} \left[\frac{E'}{E}\right]^2 \left[\frac{E}{E'} + \frac{E'}{E} - \sin^2\psi\right] \quad ...(5.60)$$

where:

σ_m' = the Compton cross-section per electron per unit solid angle, i.e. cm^2 per electron per steradian.

E = the energy of the incident photons.

E' = the energy of the scattered photons which is calculated from equation (5.55) as $E'=E-\Delta E$.

ψ = the scattering angle.

To compute the overall cross-section it is necessary to

integrate equation (5.60) over the spherical surface,

and muliply by the number of electrons per atom, Z;

$$\sigma_m = Z\int_0^{2\pi}\int_0^{\pi} \sigma_m' \sin\psi d\psi d\phi \quad ...(5.61)$$

or,

$$\sigma_m = 2\pi Z\int_0^{\pi} \sigma_m' \sin\psi d\psi \quad ...(5.62)$$

Davisson and Evans(58) provide analytical expressions

which allow this calculation, however, numerical methods

provide equivalent answers and are simpler to use. The

correction factor is computed as;

$$r_m = \frac{2\pi Z \int_{120}^{180} \sigma_m' \sin\psi\, d\psi}{2\pi Z \int_{0}^{180} \sigma_m' \sin\psi\, d\psi} \qquad \ldots(5.63)$$

For Cd-109 with E≈22 kev, numerical solution of equation (5.63) yields $r_m = \underline{0.279}$.

For Rayleigh scattering, Zeigler et. al. have shown that the cross-section is approximately given by;

$$\sigma_{nm}' = k f(\psi) Z^3 / E^3 \qquad \ldots(5.64)$$

where:

σ_{nm}' =the Rayleigh cross-section per atom per unit solid angle, i.e. cm^2 per atom per steradian.

k =a constant.

$f(\psi)$ =a function dependent upon the scattering angle.

The function $f(\psi)$ is shown in Figure 5.8. Using a digitized representation of this curve in the numerical solution of equation (5.65),

$$r_{nm} = \frac{2\pi k Z^3 / E^3 \int_{120}^{180} f(\psi) \sin\psi\, d\psi}{2\pi k Z^3 / E^3 \int_{0}^{180} f(\psi) \sin\psi\, d\psi} \qquad \ldots(5.65)$$

for Cd-109 yields $r_{nm} = \underline{0.053}$.

In both equations (5.63) and (5.65) the denominators representing the total scattering cross-sections were compared to the tabulated values
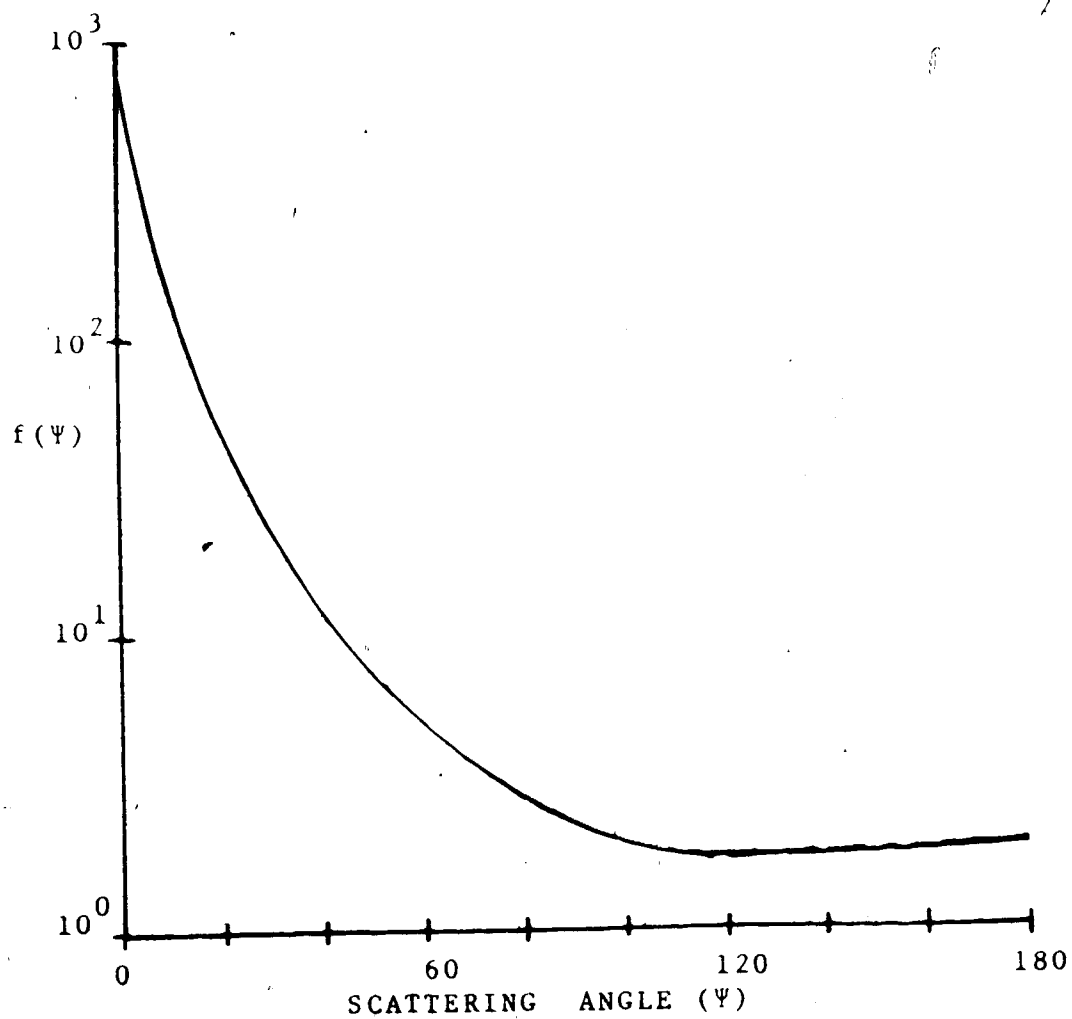
Figure 5.8 The Angular Dependence of the Rayleigh Scattering Cross-Section(Ziegler(57)).

with good agreement. (Before leaving this, and for completeness sake, the mass absorption coefficients are computed from the cross sections above by multiplying by Avogadro's number and subsequently dividing the result by the atomic weight.)

5.6 THEORETICAL IMPLICATIONS IN THE OSCAA SYSTEM DESIGN

To ensure optimal operation of the OSCAA prototype it was important to incorporate the theory in the system design. This minimizes calibration problems to the extent that are dependent upon design.

For the nuclear pulp density gauge, optimal design procedures were outlined in section 5.4. Provided that one has a knowledge of the major potential error sources the design is generally governed by equation (5.28). While this implies that any radioisotope may be used provided that the path length is suitably chosen, there may be practical limitations on the latter. A compromise must therefore be reached. In a recent publication, Kawatra(59) has observed that Gd-153 is better suited for pulp density measurement in coal slurries than Cs-137, which is most commonly employed. Unfortunately, he does not elaborate on the reasons (presumed to be geometric) for this, however, the statement does support the choice of Gd-153 for the OSCAA prototype.

For the ash-analysis sub-system, the optimal design procedures are not nearly so straight forward. Since the technology of flow cell design has been developed and

refined in on-stream XRF applications, this design was direclty adopted. Futhermore, since it was desired to detect both iron Kα fluorescent and backscattered radiation, as well as to intersect a large fraction of this secondary radiation a wide-window proportional counter was selected for detection''. Xenon was chosen as the detector gas to ensure a high probability of detection for both types of secondary photons. The detector window was made of very thin Beryllium to minimize the attenuation of iron X-rays. This leaves the radioisotope as the principal means of optimizing design.

Considering the work of others employing backscatter geometry (see 4.4.2) and the physical constraints of fabricating the source and detector assembly, a single radioisotope was chosen for irradiation purposes. As previously mentioned Cd-109 was selected and the rationale for this choice is discussed below.

A cursory analysis indicated that the best two candidate radioisotopes for this application were Cd-109 (ref. Kawatra(36)) and Pu-238 ($15 \leq E \leq 17$ kev). (ref. SORTEX(11)). Subsequent investigation of their availability indicated that Cd-109 was most easily obtained. (In fact, no source for Pu-238 was found.) Since Cd-109 had previosly been used with reported success and because of the

---

''There was no effort made to evacuate the space between the source and detector assembly and the flow cell window. Under these conditions and with XRF style irradiation and detection equipment the possibility for analysing lighter elements, e.g. $16 \leq Z \leq 25$, would exist (see(60) for example).

availability factor it was chosen for use in the OSCAA prototype.

Retrospectively, it is possible to look at the implications of having made this selection. Boyce et. al.(61) provide the general framework for such an analysis in examining the design of the SORTEX analyser. To simplify the illustrative calculations which follow, several assumptions are made:

a) The homogeneous mixture models for an infinitely thick sample can be applied.

b) The slurry consists of three components, water, coal organics (assumed to be Carbon: $Z=6$), and mineral matter (assumed to be Magnesium: $Z=12$). All of the iron is assumed to be in the mineral matter.

c) The average attributes of the flow streams are given in Figure 3.1 and the mean slurry pulp density is 1.05 g/cm³ in all cases.

In the design of an OSCAA system there are three criteria of major importance:

a) Maximize sensitivity,

b) Maximize flux (minimize accumulation time for a given accuracy),

c) Ensure that sample is representative.

In mathematical terms, instrument sensitivity is defined as;

$$S = \left| \frac{\delta N}{N} \middle/ \frac{\delta a}{a} \right| \qquad \ldots(5.66)$$

where: S = sensitivity.
       N = flux of secondary photons at the sample surface.
       a = attribute to be measured.

The models may be written in the form,

$$N(b) = \frac{(1-s)\sigma_w + s(1-m)\sigma_o + sm\sigma_m}{(1-s)\mu_w + s(1-m)\mu_o + sm\mu_m} \qquad ...(5.67)$$

where: w,o,m =subscripts denoting water, coal organics, and mineral matter respectively.
s =mass fraction of solids in the sample.
m =mass fraction of mineral matter in the solids.

(For the purposes of these calculations the composite scattering coefficients are simply the sum of the tabulated Rayleigh and Compton coefficients.)

$$N(f) = \frac{\tau sm}{(1-s)\bar{\mu}_w + s(1-m)\bar{\mu}_o + sm\bar{\mu}_m} \qquad ...(5.68)$$

where: $\bar{\mu}_j$ =sum of the mass absorption coefficients for the incident and iron Kα photons, i.e. $\bar{\mu}_j = \mu_j + \mu_j'$.

The expression for sensitivity as a function of mineral matter content are:

$$S(b) = \frac{m(bc-ad)}{(c+md)(a+bm)} \qquad ...(5.69)$$

with: $a = (1-s)\sigma_w + s\sigma_o$ $c = (1-s)\mu_w + s\mu_o$
$b = s(\sigma_m - \sigma_o)$ $d = s(\mu_m - \mu_o)$

and,

$$S(f) = \frac{(1-s)\bar{\mu}_w + s\bar{\mu}_o}{(1-s)\bar{\mu}_w + s(1-m)\bar{\mu}_o + sm\bar{\mu}_m} \qquad ...(5.70)$$

With the exception of the iron Kα radiation, the mass absorption coefficients are dependent upon incident photon energy and both flux and sensitivity for each secondary radiation must be calculated. Figures 5.9 and 5.10 illustrate this energy dependence for both backscattered and iron fluorescence radiation respectively. For sensitivity the curves are plotted at extreme values of the mineral
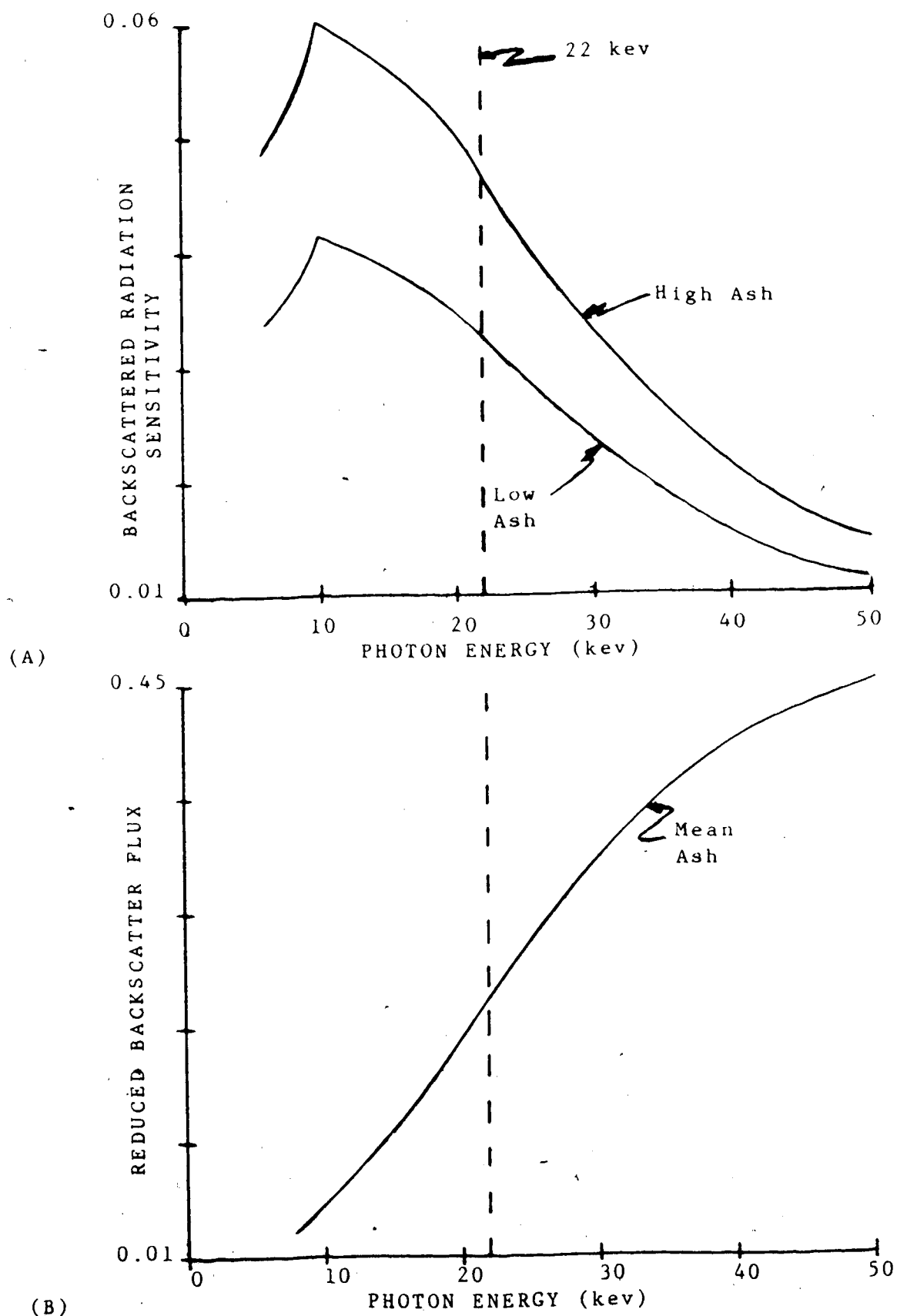
Figure 5.9 Sensitivity and Flux in Backscattered Radiation
Measurement.

(A)

(B)
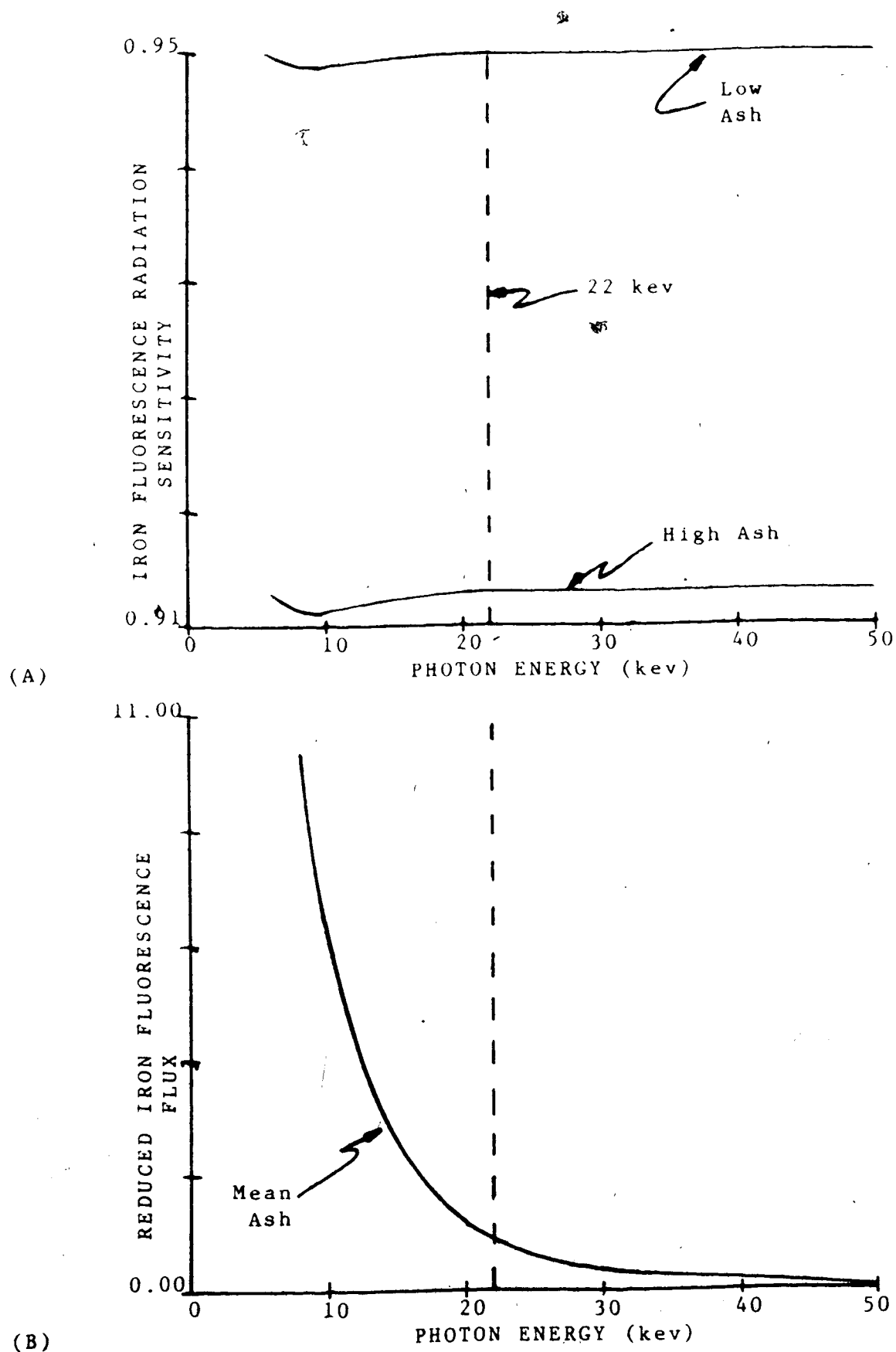
Figure 5.10 Sensitivity and Flux in Iron Fluorescence

Radiation Measurement.

matter concentration, m. The results are consistent with the findings of Boyce et. al. and since the general trends are the same for all flow streams, only the feed stream data is presented. Figure 5.11 is included to demonstrate the relative difficulty in making the measurement on a slurry sample as compared to dry solids. The vertical dashed line represents the Cd-109 photon energy. Pu-238, having principal emissions in the range of 15-17 kev, lies just to the left of the Cd-109 line.

On the basis of Figures 5.9 and 5.10 the following conclusions can be made. For backscattered radiation, Cd-109 sensitivity is somewhat less than that for Pu-238, however the photon flux would be significantly greater, all other things being equal. For iron fluorescent radiation, sensitivity is about the same for both radioisotopes but Pu-238 would provide a significanlty greater flux. In summary, Pu-238 would appear to be a marginally better choice for a primary photon source than Cd-109.

With respect to ensuring a representative sample, this is simply measured by the maximum depth from which secondary radiation will return to the sample surface, i.e. the "thin slice" for analysis. Since sample homogeneity has been assumed, the appropriate expression for calculating this depth is taken from the decay term in equations (5.44) and (5.52). Using Clayton and Cameron's(46) definition of saturation depth as the "depth from which 95% of the total secondary radiation is obtained", the appropriate
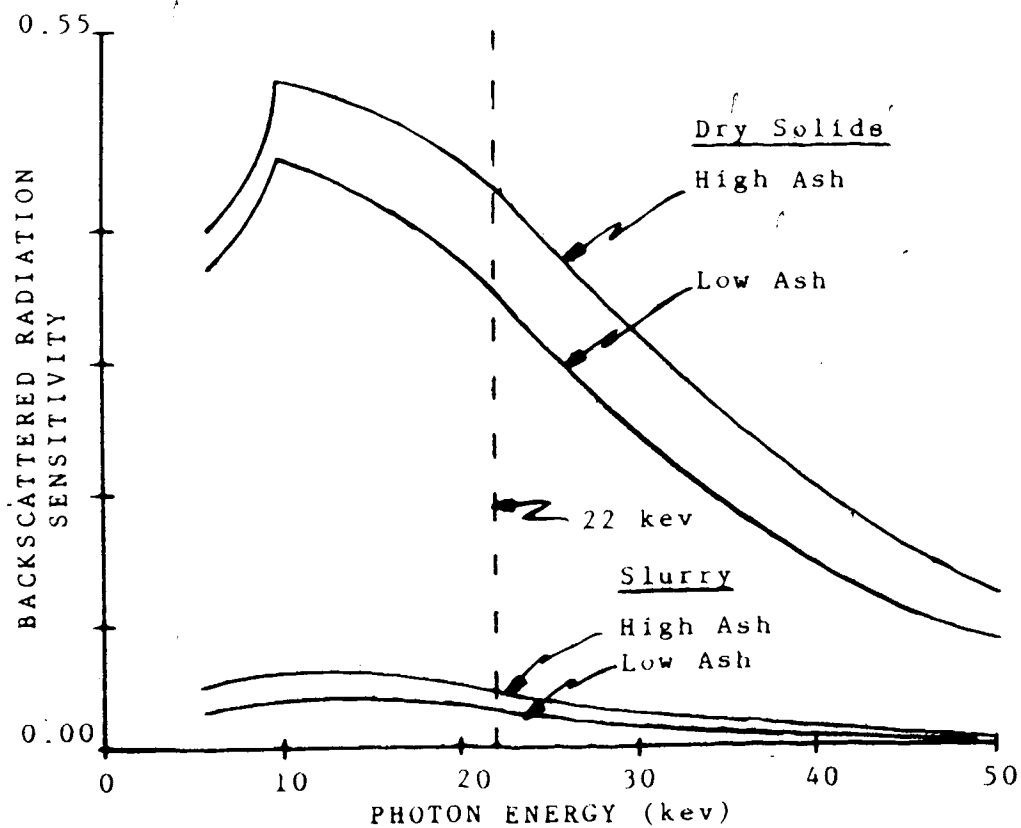
Figure 5.11 Backscatter Sensitivity Differences in Dry and Slurried Solids Samples.

expressions are;

$$d_b(sat.) = \frac{3}{2\rho\{(1-s)\mu_w + s(1-m)\mu_o + sm\mu_m\}} \qquad \ldots(5.71)$$

$$d_f(sat.) = \frac{3}{\rho\{(1-s)\bar{\mu}_w + s(1-m)\bar{\mu}_o + sm\bar{\mu}_m\}} \qquad \ldots(5.72)$$

where: $d_j(sat.)$ =the saturation depth in cm. for secondary radiation type j.

Figure 5.12 illustrates the relationship between saturation depth and photon energy for both types of secondary radiation. From this figure it is evident that a significantly thicker slice of the sample is analysed using Cd-109 for the backscattered radiation. This is true in the case of iron fluorescence as well but to a lesser extent. In this case Cd-109 would be preferred to Pu-238 because of its sampling characteristics. In considering the saturation depths for the secondary radiation in comparison to the flow cell depth of 2.54 cm, the infinitely thick sample assumption in the modelling work is justified.

This semi-quantitative analysis indicates, at least to the author, that there is little to choose between the two radioisotopes. In fact, the final choice would logically be made on the basis of price, availability, half-life, etc...., with the appropriate weighting factors.
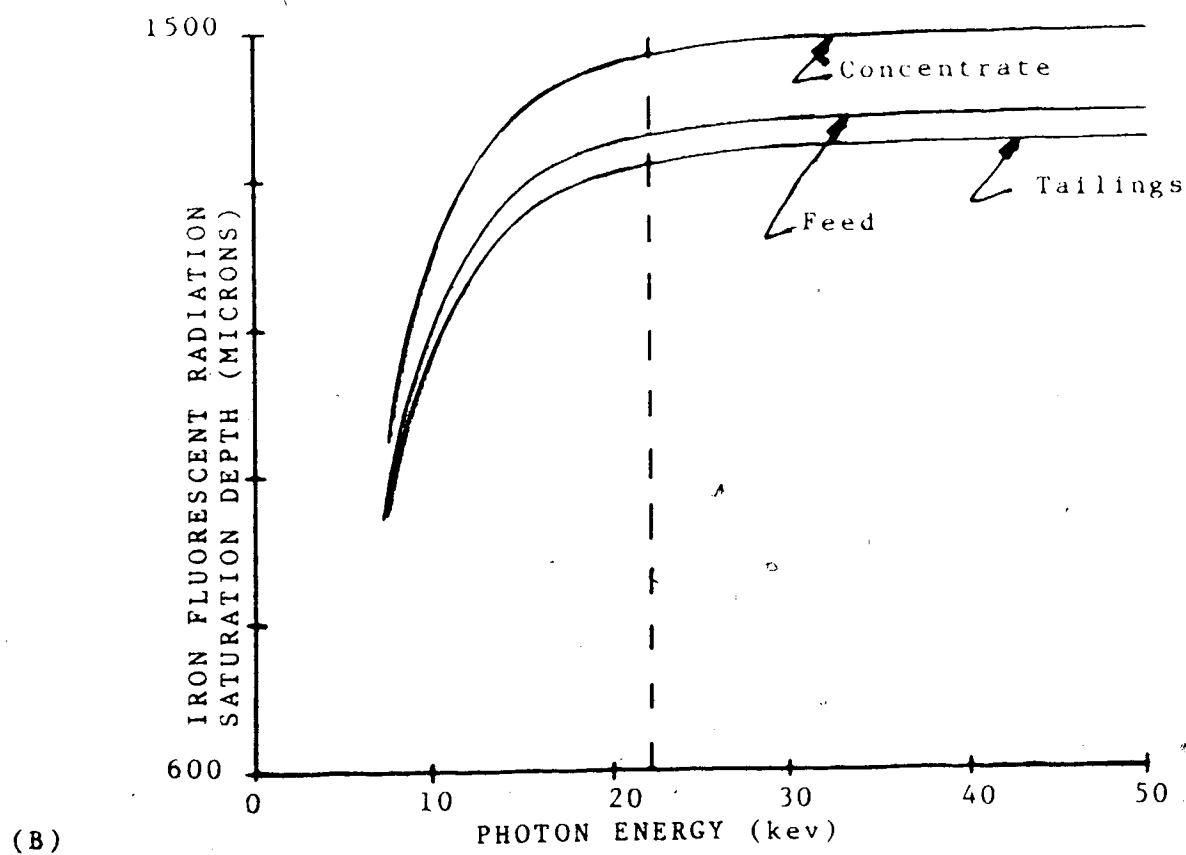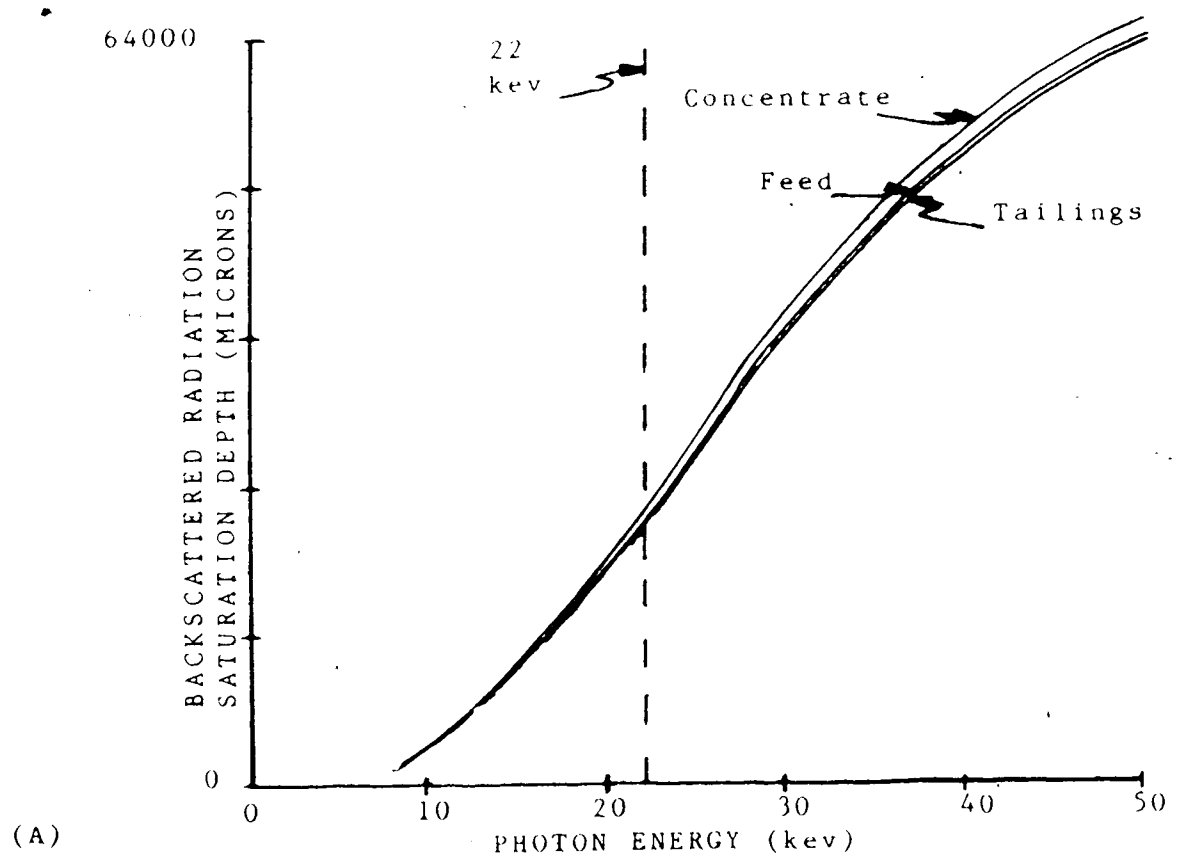
Figure 5.12 Saturation Depth for Secondary Radiation.

5.7 CALIBRATION EQUATIONS

Two types of calibration equations may be used with an OSCAA type system, either a set of semi-empirical equations derived from the theory or a set of empirical equations. For the purposes of process monitoring the most important stream attributes are the solids content of the slurry (% by weight), and the mineral matter content of the solids. The iron content, while important in compensation, does not require to be reported, unless it is on an alarm basis (e.g. tramp heavy medium).

5.7.1 Semi-Empirical Calibration Equations

The physical model of the slurry employed in calibration includes water, iron free coal organics, iron free mineral matter and hematite in an infinitely thick homogeneous mixture. Designating the mass fractions as w_1, w_2, w_3, and w_4 respectively, the necessary models are written in the form;

Pulp Density

$$\log_e \left[{}^{Cp}\!/_{Cw} \right] = A_1 \frac{1}{\sum w_i / \rho_i} + B_1 \qquad \qquad ...(5.73)$$

where: Cp =counts through pulp in the accumulation time,
        Cw =counts through water in an equivalent time
            period.
        w_i =mass fraction of component i in the slurry.
        ρ_i =density of the ith component in g/cm^3.
        A_1, B_1 =calibration constants where, in theory,
            $A_1 = -\mu x$ and $B_1 = \rho_1 \mu x$.

Backscatter

$$Cb = A_2 \frac{\sum w_i \sigma_i}{\sum w_i \mu_i} + B_2 \qquad \qquad \ldots(5.74)$$

where: Cb =backscatter counts in the accumulation time.
σ_i =the composite (see eqn. 5.59) scattering coefficient.
A_2 =calibration constant including incident flux, geometry, etc..
B_2 =calibration constant accounting for offset due to detector choking, radiation leakage, backscatter from flow cell housing, etc...

Iron Fluorescence

$$Cf = A_3 \frac{w_4}{\sum w_i \bar{\mu}_i} + B_3 \qquad \qquad \ldots(5.75)$$

where: Cf =fluorescence counts in accumulation time.
A_3 =similar to A_2.
B_3 =similar to B_2.

From calibration experiments each of the three models can be parameterized (A_i, B_i) using linear regression. The component attributes ρ_i, μ_i, and, σ_i are obtained by experiment, by curve fitting or from published tables.

Subsequent to the individual model calibration exercise, the three equations can be combined to form a linear system which may be used to predict the mass composition of the slurry from the radiation measurements. In vector-matrix notation the system looks like;

$$\begin{bmatrix} w_2 \\ w_3 \\ w_4 \end{bmatrix} = \begin{bmatrix} \left[1 - \frac{1}{\rho_2}\right] & \left[1 - \frac{1}{\sigma_3}\right] & \left[1 - \frac{1}{\rho_4}\right] \\ D(\mu_2 - \mu_1) - (\sigma_2 - \sigma_1) & D(\mu_3 - \mu_1) - (\sigma_3 - \sigma_1) & D(\mu_4 - \mu_1) - (\sigma_4 - \sigma_1) \\ (\bar{\mu}_2 - \bar{\mu}_1) & (\bar{\mu}_3 - \bar{\mu}_1) & (\bar{\mu}_4 - \bar{\mu}_1) - \frac{1}{E} \end{bmatrix}^{-1} \quad \ldots(5.76)$$

$$\bullet \begin{bmatrix} 1 - \frac{1}{H} \\ \sigma_1 - D\mu_1 \\ -\bar{\mu}_1 \end{bmatrix}$$

and,

$$H = \left[\frac{\log_e \left[\frac{Cp}{Cw} \right] - B_1}{A_1} \right] \qquad \ldots (5.77)$$

$$D = \left[\frac{Cb - B_2}{A_2} \right] \qquad \ldots (5.78)$$

$$E = \left[\frac{Cf - B_3}{A_3} \right] \qquad \ldots (5.79)$$

whence;

$$s = 100\% (w_2 + w_3 + w_4) \qquad \ldots (5.80)$$

where: s = % solids in the slurry by weight.

and,

$$m = 10^4 \% \left[\frac{w_3 + w_4}{s} \right] \qquad \ldots (5.81)$$

where: m = % mineral matter in the solids by weight.

and,

$$a = \frac{m}{Rma} \qquad \ldots (5.82)$$

where: a = % ash in the solids by weight.
        Rma = mineral matter to ash ratio for the coal.

5.7.2 Empirical Calibration Equations

Cooper(62) has observed that, in general, calibration of on-stream analysers using semi-empirical models provides better predictive accuracy than the more frequently encountered general polynomial (empirical) calibration equations. Since the latter was entertained in the OSCAA protype calibration work the formulation of Smallbone and

Gurvich(60) is presented here;

$$P = a_0 + \sum_{j=1}^{n} a_j C_j + \sum_{j=1}^{n} \sum_{k=1}^{n} a_{jk} C_j C_k \qquad \ldots(5.83)$$

where: C_j = the counts of the jth radiation type in the
           accumulation time.
         n = the total number of radiation measurements made.
         a_j, a_{jk} = "best fit" coefficients.
         P = the slurry property to be predicted.

Implicit in this formulation is that only those terms which

are statistically significant would be retained in the

calibration equation. Thus, stepwise multiple linear

regression would be a suitable method of parameterizing the

equation.

5.8 SUMMARY

The theory of operation of the OSCAA sub-systems has

been discussed with emphasis on potential sources of error

and complications in the measurements. The theory has been

used in some aspects of the prototype design as well as in

the development of calibration models. The content of this

chapter should equip the reader to understand the operation

of any similar type of on-stream coal ash analyser.

6. OSCAA LABORATORY EQUIPMENT DESIGN AND EXPERIMENTAL PROCEDURE

6.1 INTRODUCTION

The major effort in this thesis project was to design a prototype on-stream ash analyser and study its performance in the laboratory. Based upon the results of this portion of the project a limited plant trial was to be considered.

It is generally observed that equipment of this type will perform better under well controlled laboratory conditions. The measures of performance made in the laboratory are estimates of what can be expected in the field. By attempting to closely simulate "real-world" operating conditions the estimates so obtained are more reasonable expectations of plant performance.

For the purposes of the laboratory investigation four calibration runs were deemed necessary for performance evaluation. These were:

a) Calibration on Flotation Feed,

b) Calibration on Flotation Concentrate,

c) Calibration on Flotation Tailings,

d) Calibration on Flotation Feed With Varying Iron
    Concentration.

The sections which follow describe the final equipment configuration, the experimental design and the pre/post calibration run sample handling methods. The discussion of the results of the calibration tests are treated separately

in Chapter 7.

6.2 EQUIPMENT DESIGN

The OSCAA equipment layout for the laboratory program is illustrated in Figure 6.1. For the purposes of a more detailed explanation it is convenient to consider the system in three parts:

a) The Flow Loop,

b) The Pulp Density Sub-System,

c) The Ash Analysis Sub-System.

These are discussed below.

6.2.1 The Flow Loop

A SALA model SPV 180 3.8 cm (1.5 in.) vertical pump with a 0.028 m³ (1 ft³) sump and a 5 horsepower variable speed drive was used to pump the slurry to the secondary sampling device. The primary sample delivery rate was nominally 9.1 m³/h (40 USGPM), which is typical of most on-stream XRF systems. The primary sample slurry flow rate was estimated from a calibrated "V-notch" weir in the collection launder which delivered the recycled pulp to the sump. The launder also provided for access to the flow streams for sampling purposes.

The pump sheave size was calculated for a primary sample flow rate of 13.6 m³/h (60 USGPM) of water, recognizing that the corresponding delivery of aerated slurry would be somewhat less (ref. (63)). The head for this
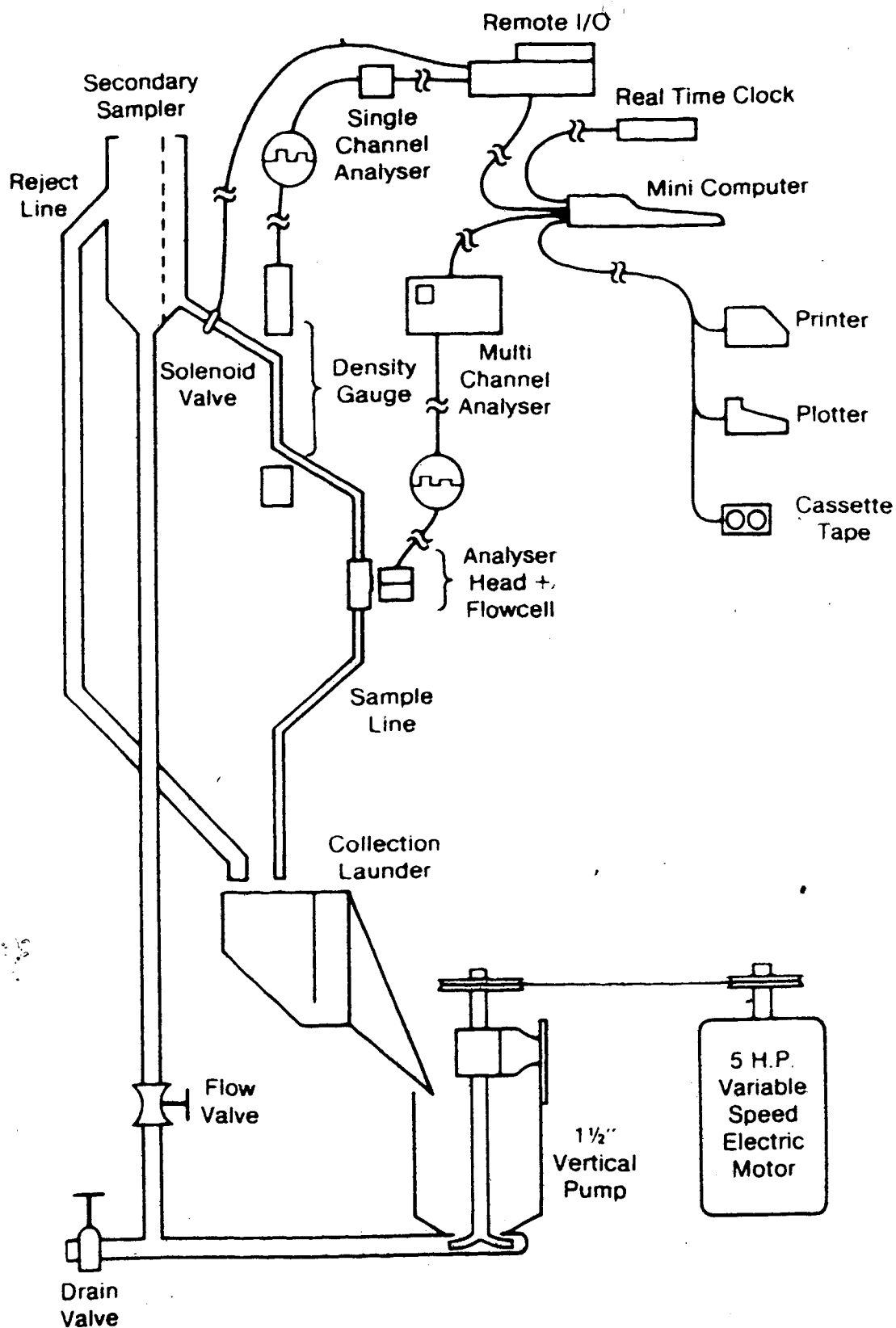
Figure 6.) A Schematic Illustration of the OSCAA Prototype Test Rig.

flow rate was estimated by solving the macroscopic
isothermal energy balance and these two values were used in
conjunction with the manufacturer's pump curves to specify
impeller speed and drive horsepower. A variable speed
controller was included on the drive for fine adjustment of
flow rate.

The function of the secondary sampling device in the
flow loop is threefold:

a) To split a representative secondary sample from the
    primary sample input. This sample was to be provided to
    the OSCAA components at a substantially constant static
    head to prevent window warping in the ash analysis
    sub-system, which would affect measured radiation
    intensity

b) To remove, via a screen, tramp material (e.g. woodchips)
    which may report in the primary sample stream and which
    could potentially block or otherwise disrupt the
    secondary sample flow.

c) To remove, at least in-so-far as was possible, the air
    which was entrained in the primary sample. This was
    required to ensure accuracy in the pulp density
    measurement.

Since the secondary sampler design, although commonly
employed, is not often given in the published literature, a
sketch is included in Figure 6.2.

The secondary sample from such a device is expected to
have a flow rate of nominally 1.6 to 2.3 m³/h (7-10 USGPM).
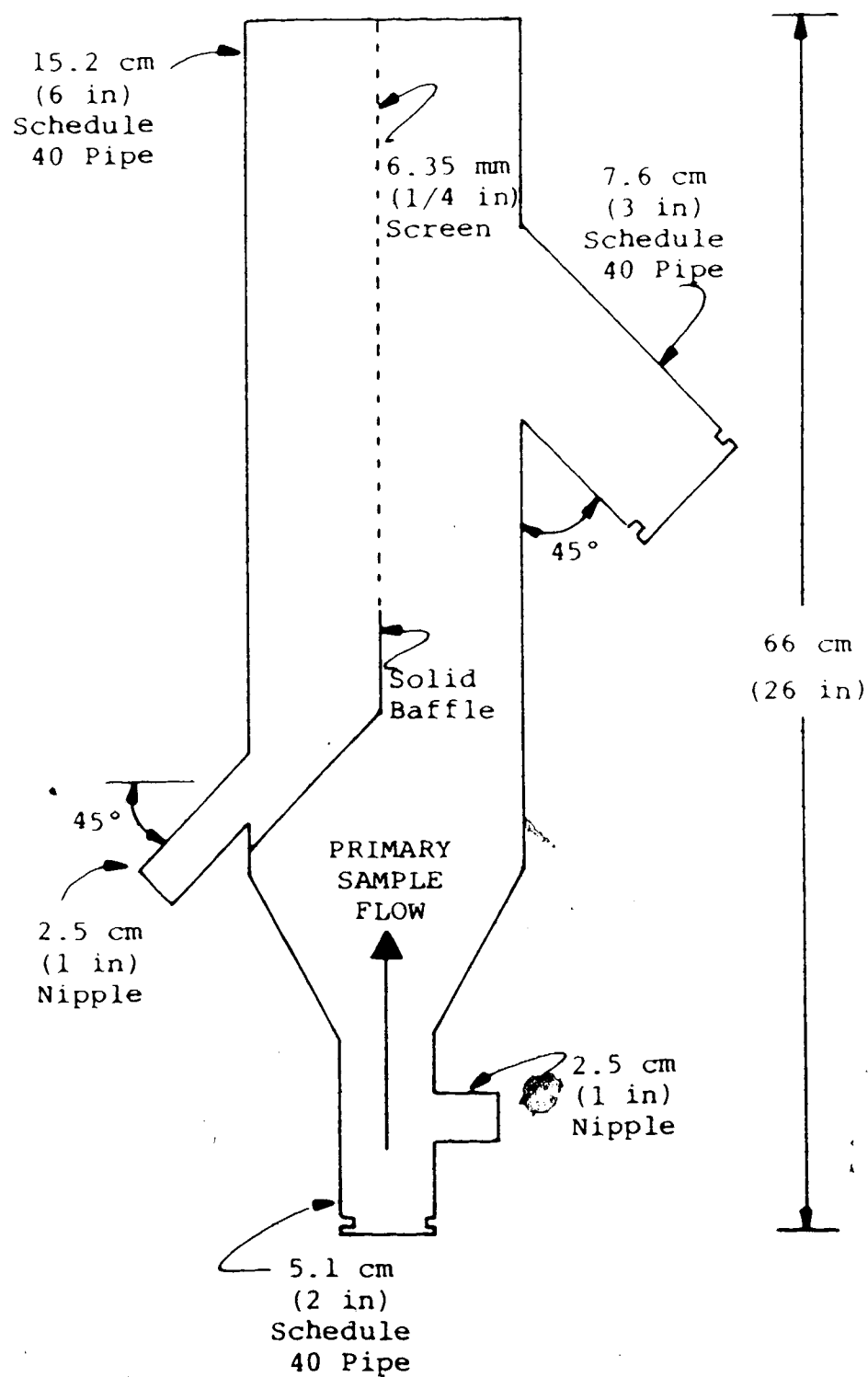
Figure 6.2 A Sketch of the Secondary Sampling Device.

With the configuration of the 2.54 cm (1 in) and 1.3 cm (0.5 in) schedule 40 PVC tubing used in the fabrication of the OSCAA sample line, it was estimated from the macroscopic isothermal energy balance that the flow rate would be approximately 1.7 m^3/h (7.5 USGPM). Subsequent testing of the system in operation proved the typical value to be 1.9 m^3/h (8.4 USGPM), which is good agreement considering the method of analysis.

Since the secondary sample flow in the OSCAA sample line is essentially vertical a homogeneous flow was expected. Using the correlations of Lowenstein(64) it was shown that for all three flotation product streams to be tested, the critical velocity[a] was exceeded by at least a factor of 2.

Finally, size degradation studies were performed by pumping a slurry through the system for an extended period of time. The principal change appeared in the coarsest size fraction where, in a four hour period, the mass frequency retained on a 0.84 mm (20 mesh) sieve decayed from an initial value of 6.57% to a final value of 4.9%. This magnitude of change is expected to have a negligible effect on the backscattered and fluorescent radiation intensity considering the relative mass frequency. In addition, comparisons of sample attributes for various slurry mixtures were made between the reject and secondary sample lines.

---

[a]The critical velocity is the minimum velocity in a slurry pipeline which will ensure homogeneous distribution of the solids in the axial plane.

Good agreement was obtained with a typical result shown in Table 6.1.

6.2.2 The Pulp Density Measurement Sub-System

The equipment used to make the pulp density measurement is illustrated in Figure 6.3 and Plate 6.1.

The radioistope employed in the pulp density gauge was Gd-153 which has a principal photon energy of $\approx$100 kev. This relatively low energy photon source allowed a gauge design with practical length and minimized shielding requirements. The "Z-type" geometry was adopted to provide the path length required for optimal performance while maintaining homogeneous flow. In the design of the pulp density gauge it was assumed that the principal source of error would arise from the statistical fluctuation of the detected radiation. In this case, and as was shown in Chapter 5, $\rho\mu x=2$ provides the minimum relative error in measurement if Lambert's law holds. Depending upon the nature of the slurry, the density may vary in the range of $1.0 \leq \rho \leq 1.1$, which, when substitution for μ is made, yields an optimal path length of 11.4 cm $\leq$ x(optimal) ≤ 12.5 cm. Unfortunately, the physical constraints of fabricating the gauge resulted in a mean path length of 14.5 cm., close to, but not within the theoretical optimum range. (Note that because of beam divergence and minimal detector collimation some build-up would be expected and hence a slightly longer path length is desirable.)

Table 6.1 Comparison of Sample and Reject Line Slurry

Attributes

ATTRIBUTE	REJECT STREAM	SAMPLE STREAM
% Solids	18.3	18.6
% Ash	56.7	55.8
Solids Size Distribution		
+35 mesh	34.6	33.5
-35/+65	21.3	21.8
-65/+150	14.8	14.7
-150/+270	15.6	16.6
-270/+325	3.2	3.4
-325 mesh	10.5	10.0
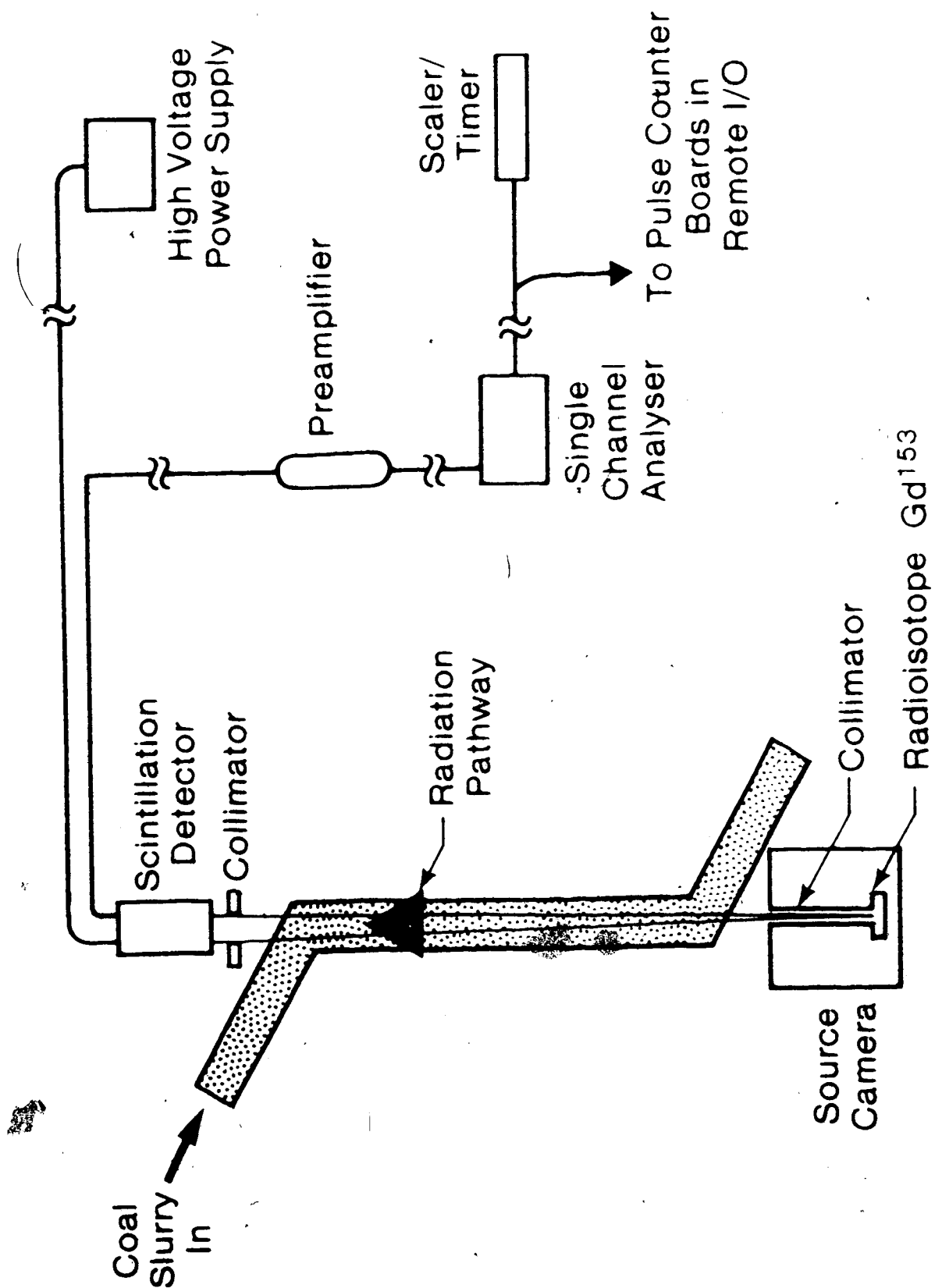
Figure 6.3 A Schematic of the OSCAA Pulp Density Sub-System.

Plate 6.1 The OSCAA Pulp Density Gauge

The scintillation counter and the necessary support electronics are shown on Figure 6.3. A single >channel analyser. (SCA) was used to examine the energy region of interest (ROI) in the amplified detector output (i.e. 50 kev≤E≤100 kev). The SCA provides two parallel output channels. One of these signals was connected to the pulse counter circuitry in the remote I/O interface. The other was connected to a simple scaler for cross-checking purposes. The remote I/O was under the real time control of the computer program supervising data acquisition. (A more complete decription of this equipment is left to the next section.)

The functional specifications of the pulp density sub-system are given in Table 6.2.

6.2.3 The Ash Analysis Measurement Sub-System

The equipment used for ash analysis, or, more properly, to obtain the backscattered and iron fluorescence radiation measurements, is illustrated in Figure 6.4 and Plate 6.2.

The radioisotope employed in this system was Cd-109. This choice was more fully evaluated in chapter 5. The detector was a Xenon filled side window proportional counter. The source detector geometry illustrated in Figure 6.4 is not a conventional configuration (ref. (52) pg. 369 for example). The geometry used in the OSCAA ash analysis gauge was required for a number of reasons which include:

a) size of source and detector relative to flow cell,

Table 6.2 Functional Specifications of the OSCAA Pulp Density Gauge Sub System

CATEGORY	ITEM	DESCRIPTION
Pipeline	Piping	(a) 2.54 cm φ Sch 40 PVC (b) Total Vertical Pass Line Distance Source to Detector 36.8 cm (c) Vertical Pass Line Distance Through Slurry 14.6 cm (d) Inflow/Outflow elbows at 45°
Source Camera	Radio Isotope	(a) Gadolinium 153 (b) Activity when Purchased 130 mCi (c) Half life 241.5 days (d) Principal radiations at 97 Kev (e) Disk Source 15.2 mmφ x 6.3 mm
	Collimator	(a) Length 10.3 cm (b) Diameter 0.95 cm
	Casing	(a) Overall Outside Dimensions 16.3 cm x 12.1 cm x 10.2 cm (b) Outer case Constructed with 1.27 cm Steel Plate (c) Case core is aluminum
Detection	Collimator	(a) 2.15 cm φ in 1.27 cm Steel Plate
	Detector	(a) Model 802.3 Canberra[+] Scintillation Detector (b) Crystal 5.08 cm φ by 5.08 cm
Electrical Hardware	Preamplifier(s)	(a) Model 805 Canberra[+] Scintillation Detector Preamplifier (b) Model 802.5 Canberra Tube Base
	Single Channel Analyser	(a) Model 2015 Canberra[+] Amplifier/Timing Single Channel Analyser
	High Voltage Power Supply	(a) Model 3102 Canberra[+] High Voltage Power Supply
	Scaler/Timer	(a) Model 1776 Canberra[+] Dual Counter

[+]Canberra Industries Inc.
45 Gracey Avenue
Meriden, Connecticut
06450
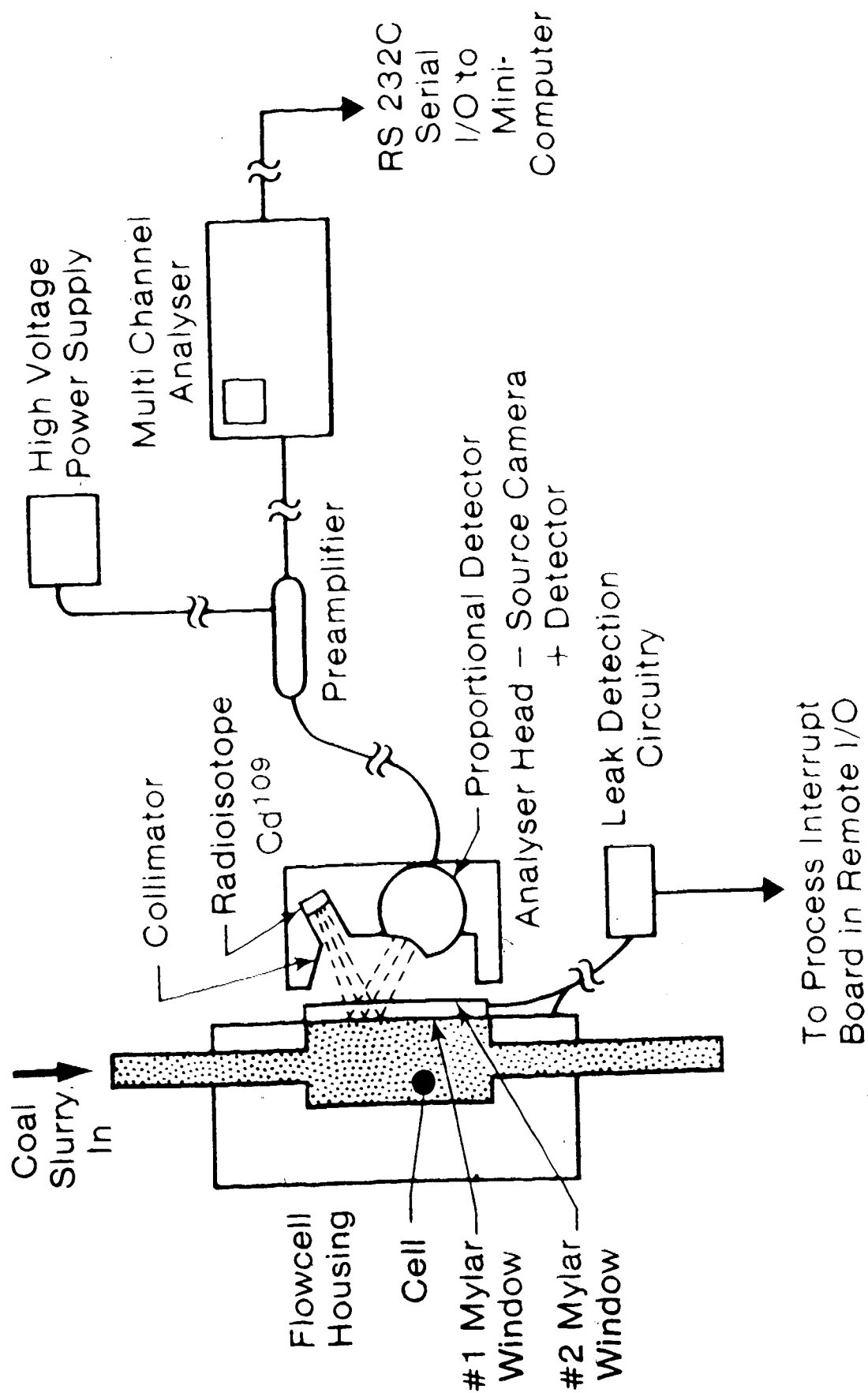
Figure 6.4 A Schematic of the OSCAA Ash Analysis Sub-System.

The Flow Cell
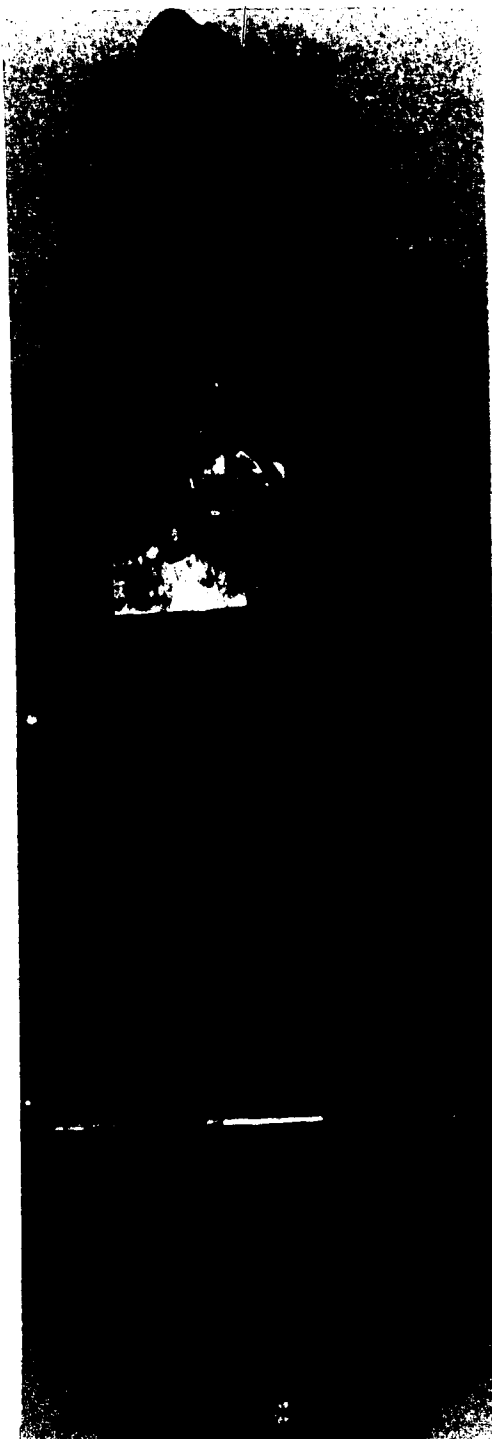
The Assembly For On-Line
Measurement

The Ash Analysis Head

(Source & Detector)

Plate 6.2 The Ash Analysis Gauge

b) the requirement for adequate shielding between the
    source and the detector,

c) the requirement to minimize the distance between the
    detector and the window to prevent excessive air
    attenuation of the iron $K\alpha$ X rays.

Since the geometry is unique a cross sectional sketch
is included in Figure 6.5.

The source and detector housing was equipped with a
rotating four position shutter mechanism. One position
provided for maximum attenuation of the primary photons
required for safe storage. The other three positions
provided for primary photon attenuation by factors of 0.0,
0.5 and 0.75. The latter two positions used aluminum filters
for attenuation purposes. Experience had shown that the 0.5
position was the best from an operating point of view since
it prevented detector choking while maximizing the secondary
photon fluxes.

The flow cell itself was a 3.2 cm (1.25 in) diameter by
2.5 cm (1 in.) cylindrical cavity with the sample flow
perpendicular to the longitudinal axis (ref. fig. 6.5). It
is common practice in XRF applications to provide for leak
detection and thus prevent sample spillage if the thin
window ruptures. For the OSCAA sub-system this was
accomplished by using a dual Mylar™ film covering. Two wires
were placed between the films such that when the inner
window ruptured an electrical circuit was closed which
generated a process interrupt to the remote I/O.
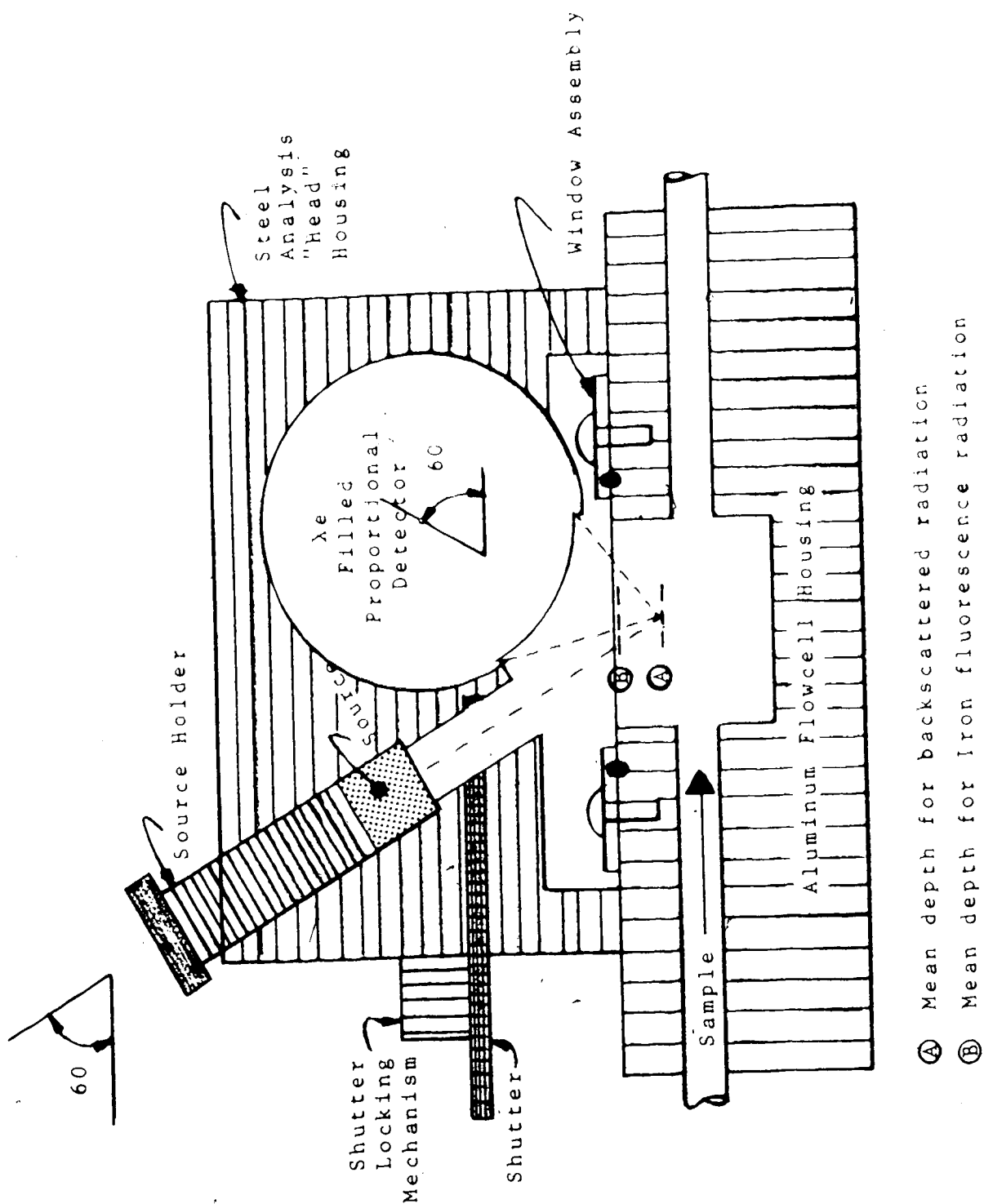
Figure 6.5 A Sketch of the OSCAA Ash Analysis Gauge

Subsequently, the secondary sample flow was stopped by means of a solenoid valve on the secondary sampler discharge. While this circuitry was included in the design it was never used since the operating life of a single window was more than sufficient to complete a given laboratory or plant run. Finally, by proper positioning of the flow cell in the sample line, the window was kept under slight negative pressure thus minimizing warping which could occur with changes in the static head.

The materials of construction of the flow cell and source and detector assembly were aluminum and steel respectively. These were chosen because of their mechanical properties and, in the case of the latter, for its shielding ability. Interference effects which would result from the backscattering of primary photons from the aluminum flow cell housing were minimized through collimation. Similarly, interference effects which could arise by primary photon excitation of the iron in the steel assembly were minimized, but not eliminated, by wrapping the detector in a 3 mm (1/8 in.) lead sheet.

The electronic components required to support the detector and analyse the output are shown on Figure 6.4. A multichannel analyser (MCA), under control of the data acquisition program was used to acquire the secondary photon energy spectrum. When the data acquisition program expired the energy spectrum was transferred to computer memory and thence to cassette tape by means of a high speed serial

interface and a fast buffer. Plate 6.3 shows the primary elements of the electronic support and data acquisition systems for both of the measurement sub-systems.

The functional specifications of the ash analysis sub-system and electronic support equipment are given in Table 6.3.

6.3 EQUIPMENT SETUP AND OPERATION

As mentioned in sub-section 5.1.1, the theory of operation of the nucleonic equipment employed in the OSCAA prototype hardware configuration is adequately described in most textbooks dealing with X-ray analysis. The equipment operating settings, i.e. detector voltages, amplifier gains, etc..., were determined using methods described by Bertin (ref. (52): pp. 330-338). No explicit deadtime corrections were made, these were effectively embodied in the best-fit parameters determined on the calibration models.

6.4 EXPERIMENTAL DESIGN

The raw material used to generate the samples required for the laboratory experimentation was obtained from McIntyre Mines Ltd. The material consisted of two large samples of flotation concentrate and one of flotation tailings. All three of the samples were individually mixed and sub-sampled for bagging and storage. A representative sample of each was analysed for ash content, iron concentration of the ash and solids specific gravity.

Preamplifiers

Interfaces
HP1B/RS232C

Real-Time
Clock

NIM Bin
(Power supplies,
SCA, scalar/
timer)

Multichannel
Analyser

Remote
Input/Output

Printer

Plotter

Cassette
Tape

Control
Computer
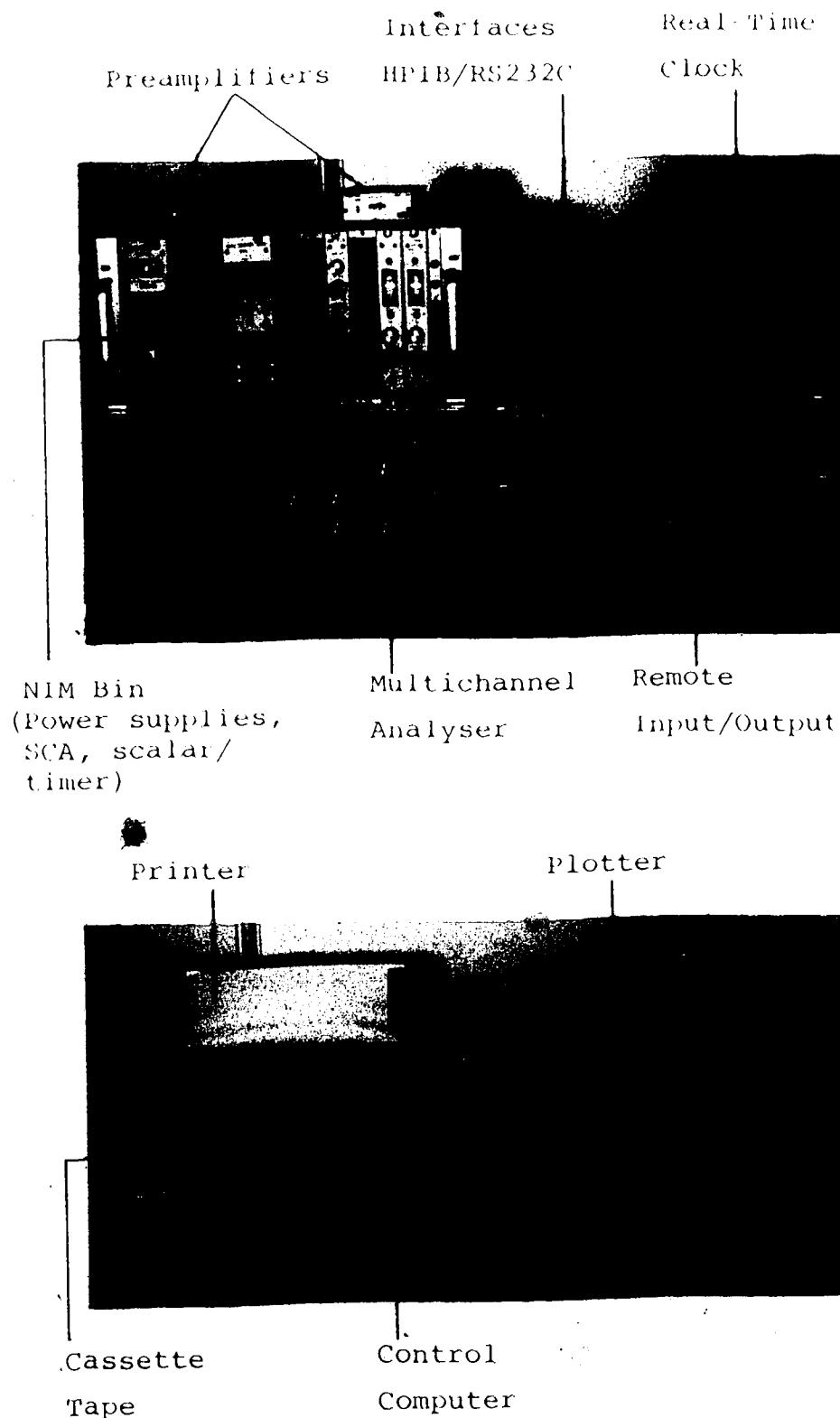
Plate 6.3 The OSCAA Electronic Support and Data Acquisition
Systems

Table 6.3 Functional Specifications of the Ash Analysis

Sub-System and the Electrical Hardware

CATEGORY	ITEM	DESCRIPTION
Pipeline	Piping	(a) 1.27 cm φ Sch. 40 PVC
	Flowcell	(a) 3.18 cmφ x 2.54 cm
		(b) Window Material 10 μ Mylar
Analyser Head Source	Radio-isotope	(a) Cadmium 109
		(b) Activity When Purchased 35 mci
		(c) Half Life 453 days
		(d) Principal radiation at 22-26 kev(Ag k x-rays)
		(e) Disk Source 11.4 mmφ x 3.4 mm
	Collimator	(a) Length 2 cm
		(b) Diameter 0.64 cm
Housing	Casing	A(a) Fabricated from Steel
		(b) Approximate Overall Dimentions 15 cm x 8 cm
Detection	Detector	(a) Model 45415 LND+ Sidewindow Prop. Counter
		(b) Xe Filled at 1 Atmosphere
		(c) Beryllium Window of
		(1) thickness 0.13 mm
		(11) size 2.54 cm x 5.1 cm
Electrical Hardware	Preamp-lifier	(a) Model 1406 Canberra Proportional Counter Preamp.
(Energy Disper-sive Analysis)	Multichannel Analyser	(a) Model 8100 Canberra MCA with Necessary Optional Features
	High Voltage Power Supply	(a) Model 3003 Canberra HVPS
	MCA Control Interface	(a) Model 8100-14 Serial Computer Interface
Electrical Hardware	Computer	(a) Model HP9825 Hewlitt Packard Desk Top Calculator With Necessary Features
(Data Acquis-itions, Stor-age, Presenta-tion and Processing)	Remote Input/Output	(a) Model HP6940B Multiprogrammer with Necessary Optional Features
		(b) Model HP59500A H.P.I.B. Interface To The Multiprogrammer
	Interfaces	(a) Model HP98036A RS232C Serial Interface
		(b) Model HP98034A H.P.I.B. Parallel Interface
	Clock	(a) Model HP59039A ASCII Clock
	Plotter	(a) Model HP9872A Graphicoplotter
	Printer	(a) Model HP9871A 30 Baud Impact Printer
	Mass Storage Medium	(a) Model HP9162-0001 Tape Cartridges

+LND Inc.
Oceanside, New York

For the purposes of organizing a particular performance evaluation on a given product stream, orthogonal design principles were adopted. For the first three runs (feed, concentrate and tailings) a 2-factor (%solids, %ash), 5-level design was used yielding 25 calibration points. The fourth run was a 3-factor (%solids, %ash, %iron), 3-level design yielding 27 calibration points. The advantage of using an orthogonal design is that it provides for the best estimates of calibration model parameters by minimizing covariance among the factors. From an analysis of the preliminary testwork data described in chapter 3 and through discussion with the operators, the design factor levels given in Table 6.4 were identified.

To make maximum use of the the raw coal material which was available it was necessary, wherever possible, to move from point to point on the design by simple "make-up" additions. (By the nature of the experiments there was no need to randomize the order.) Toward this end, an interactive computer program was used to solve the system constraint equations[1] and determine the water, clean coal (concentrate), reject coal (tailings) and magnetite requirements of the slurry. Based on component inventories after sampling for the preceding design point, the incremental additions of the various components were calculated. If negative increments were encountered the

---

[1] The constraint equations included %solids, %ash, %iron and the total system volume. The latter was targetted at 38 litres after the standardization run with water.

Table 6.4 The Orthogonal Design of the Laboratory Runs

RUN	% SOLIDS	% ASH	% IRON IN ASH
1	5,8,11,14, 17	10,13,16,19, 22	N/A
2	20,22.5,25 27.5,30	7.2,8.2,9.2 10.2,11.2	N/A
3	1,2,3,4,5	33,36,39,42,45	N/A
4	7,11,15	12,16,20	6,8,10

component exhibiting the largest relative negative change was fixed at its current level, the volume constraint removed and the additions recalculated. If this calculation provided a slurry volume in excess of 46 litres, a new slurry was mixed for this design point. Calculations for "bleeding" slurry from the system and adding water to reduce only the solids concentration were done by hand since this happened only infrequently.

Having calculated the necessary water and solids additions for each design point in a particular run, the solids components were obtained from the bulk raw samples, mixed in proportion and bagged with appropriate labelling for use in the calibration run. For illustrative purposes the experimental design for the flotation feed calibration is presented in Figure 6.6. The points at which a new slurry was mixed, where the system was bled and the moves involving incremental additions are shown.

6.5 EXPERIMENTAL PROCEDURE

The steps involved in a calibration run may be divided into two parts, operational and sample handling. The former involves all activities up to and including the stream sampling and experimental data storage and the latter involves all subsequent sample handling and analyses.
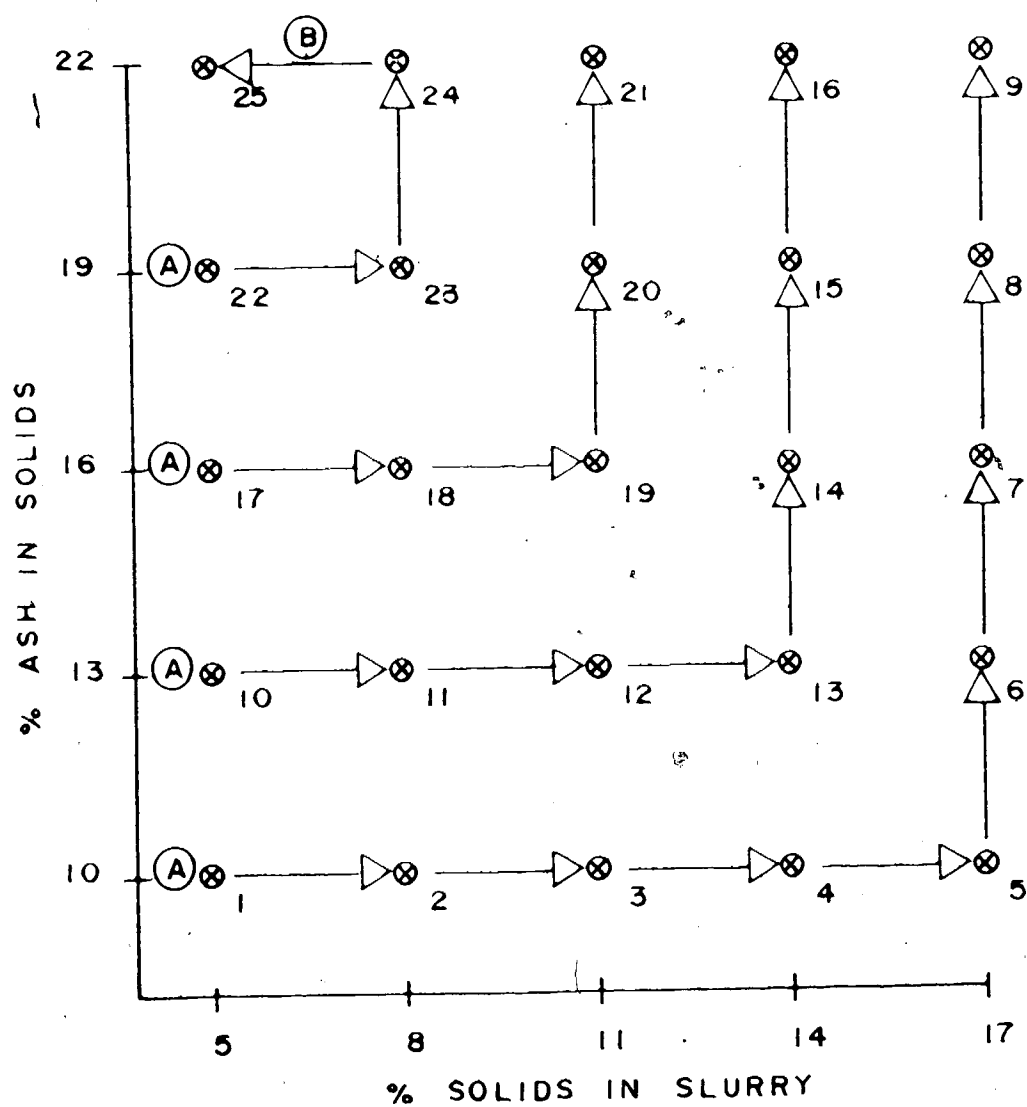
Figure 6.6 The Orthogonal Design for Flotation Feed

6.5.1 Operational Methods

Each run was divided into a series of design points. For example, in Figure 6.6 there are four series of points (labelled as ∅). Each series began with the preparation of a new slurry and testing within a series involved incremental additions and bleeding.

Prior to the start of a new series the system was allowed to "run-in" on 36 litres of water. This provided for instrumentation warm-up, room temperature equilibration etc... Steady state was established by monitoring the the secondary photon counts. When this conditon was achieved, the appropriate readings were taken on the water standard and stored for future reference. Although this particular experiment does not appear in the orthogonal design it was conducted for each series.

Once the water standard had been measured the necessary incremental additions were made to the sump, slowly, to facilitate good mixing. The system was then allowed at least 10 minutes of circulation to ensure slurry homogeneity. Upon completion of this stage, the data acquisition period was initiated by means of the computer program. When the program suspended acquisition and began a transfer and storage operations, a 2 litre sample of the slurry was taken from the secondary sample line. When this was complete the incremental additions for the succeeding test were made and another 10 minute mixing period allowed prior to data acquisition.

The decision to take 2 litres of sample was made on the basis of particle size distribution requirements. Although particle size cannot be explicitly accounted for in the calibration models presented in chapter 5, a knowledge of the relative changes was deemed necessary for possible correlation analysis with calibration results (i.e. analysis of residuals)[11]. Using the flotation feed for design purposes, specifying 95% confidence limits and using Barbery's(65) equations for sample size determination, at least 100 g of solids were required. For a slurry of 5% solids, 2 litres were required to provide this weight. It was decided to fix the sample size at 2 litres for all tests, since, with the exception of some of the design points in the tailings run, the 100 g requirement would always be met. Furthermore, 2 litres of sample is relatively easy to handle and is small enough to ensure the maximum usage of the raw coal resources.

Between each series the system was thoroughly flushed with water. The next series was begun with the addition of 36 litres of water and the warm-up period.

After each calibration run equipment maintenance was performed and the Mylar™ window on the flow cell replaced. The hard copy output and the data tape were removed, labelled and stored for the subsequent analysis.

---

[11]From the theory, modest changes in the particle size distribution were not expected to significantly affect results.

6.5.2 Sample Handling

The 2 litre sample from each design point was obtained in two 1 litre beakers. The wet weight of the slurry was recorded and it was then transferred to a drying pan. Rather than use filtration to expedite drying, evaporation under infra-red lamps was employed to avoid potential sample losses. The dry solids weight was recorded and the solids transferred to a 0.6 mm (28 mesh) sieve. Using hand screening and gentle pressure the fine coal agglomerates were broken down. The solids were then thoroughly mixed and a representative 100 g sample was cut for size, ash and iron analysis. In the special cases of runs 1 and 2, 20 g samples were also cut for specific gravity determinations. Any reject material was then bagged and placed into storage.

The 100 g sample was screen analysed (dry) on the following sieve nest; 0.84 mm, 0.6 mm, 0.42 mm, 0.3 mm, 0.21mm, 0.15mm (20/28/35/48/65/100 mesh). The results were recorded and the screen fractions recombined. Minimal weight losses were observed in this step. (In the case of run 3 where some of the slurry samples contained only ≈20 g, screen analyses were not performed.)

The recombined size fractions were then reduced to -0.1 mm (-150 mesh) in a coffee grinder. (Independent studies had shown no iron contamination from the stainless steel blades.) From this very fine sample, duplicate 3 g cuts were obtained for ash analysis. The ash analysis was performed by heating the coal in a muffle furnace at a temperature of 750

C for a period of approximately 6 hours. Inspection of the uncombusted residue showed no trace of organic (black) substance. The reject was bagged, labelled and placed in storage.

The ash residue from the ash analysis step was weighed and the ash content calculated. Except in the very infrequent case of error, where one sample quite obviously gave incorrect results, the mean of these two assays was reported as the solids ash content.

The duplicate ash residues were combined and submitted for iron analysis. This analytical work was done in a commercial laboratory. Despite the fact that both a method(65) and the equipment for performing these analyses were available, consistent results could not be obtained. (This is thought to be due in large part to the state of repair of the atomic absorption analyser.) Thus, a local laboratory with a plasma spectrometer was chosen to do the work. To reduce analytical costs only selected samples from calibration runs 1, 2 and 3 were submitted. It was argued and later shown (ref. Chapter 7) that, since iron was not independently (externally) controlled in these calibrations, it would be strongly correlated with the ash content. Therefore, a correlation constructed on the basis of a few samples could be used to predict the iron concentrations for those samples not analysed. All of the ash samples for run 4 were submitted for iron analysis.

The results of the attribute analyses were tabulated
and stored for the subsequent calibration studies.

7. THE OSCAA SYSTEM LABORATORY CALIBRATION RESULTS

7.1 INTRODUCTION

This chapter describes the methods employed in reducing the data derived from the laboratory experiments and the results of the subsequent calibration studies. Details on the MCA spectrum analysis, semi-empirical model parameter estimation and data preparation prior to calibration are provided. The criteria for assessing the performance of the OSCAA prototype is defined and finally the results of the calibration studies are presented.

7.2 MCA SPECTRUM ANALYSIS

The MCA spectra acquired for the different experiments were analysed to provide measures of the backscattered and iron fluorescence counts required for the calibration studies. This analysis was complicated by two factors:

a) the position of the spectrum with respect to energy was a function of the count rate. (This is consistent with the count rate effect.)

b) due to the relatively poor resolution of proportional counters and the choice of the detector gas (Xe), there was a background discontinuity which underlay the iron peak.

These effects were only important in the case of the iron peak since peak shift effects were negligible and there were no background discontinuities in the case of the backscatter

peak. A typical MCA spectrum for an experiment is presented in Figure 7.1. It is convenient to consider the methods of peak resolution separately.

7.2.1 Backscatter Peak Resolution

Studies on the nature of the background both on the low energy and on the high energy side of the backscatter peak indicated that it could be modelled via the simple linear expression:

$$B = b_0 + b_1 C$$

...(7.1)

where: B = background counts in channel number C.
C = channel number
b_0, b_1 = coefficients of the linear model.

Since Xe has no absorption edges in the energy region of interest (ROI), there was no reason to suspect a discontinuity. To estimate the linear model coefficients in equation (7.1) a "quick" computation was used rather than the more mathematically (statistically) correct linear regression analysis. The quick method involved the following steps:

a) Define a region on the spectrum to the low energy side of the peak where the contribution of the peak is negligible. Calculate the mean background count for this region and the centroid channel.

b) Repeat the calculations on the high energy side of the peak.

c) Using the two points defined in (a) and (b) above, estimate the coefficients of the background model.
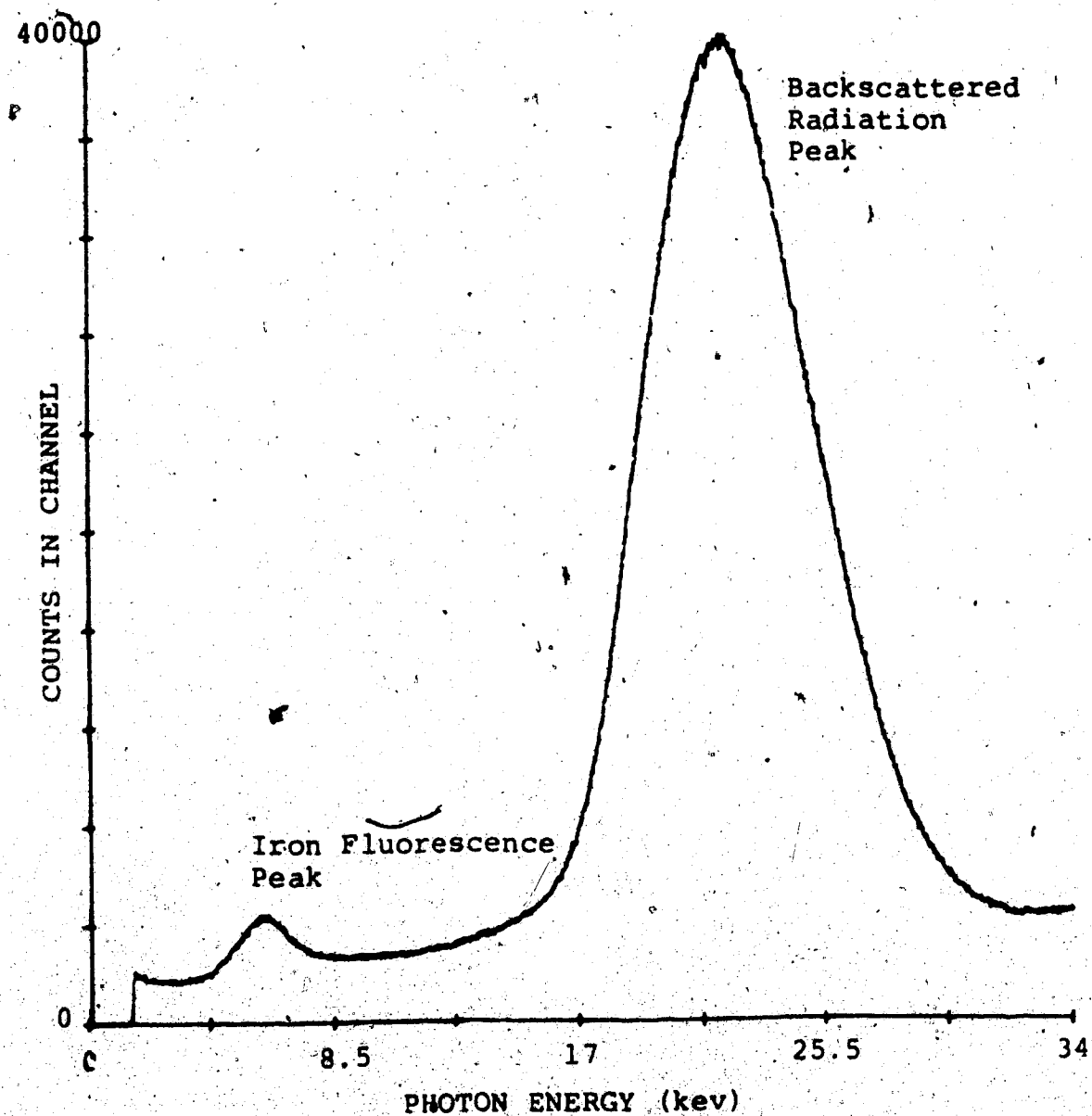
Figure 7.1 A Typical Experimental MCA Spectrum.

The magnitude of the counts in the channels which define the backscatter peak preclude the need of any mathematical manipulation of the raw data such as smoothing. Once the low energy and high energy peak boundary channels were defined, peak integration over the ROI is performed simply by subtracting the predicted background from the observed counts for each channel within the boundaries, and summing the results. This procedure is illustrated schematically in Figure 7.2.

7.2.2 Iron Peak Resolution

The problems associated with analysing the iron peak occur because of spectrum shifting and an underlying background discontinuity.

Peak shifts result when the gross count rate at the detector changes and the resolution of the individual pulses is not complete (ref. (67) pg. 75). Although these shifts generally have a range of only a few channels in the MCA spectrum for a particular stream, they must be accounted for to ensure maximum accuracy in deriving the iron fluorescence count data. This does not represent a particularly difficult problem since all of the peak analysis methods studied were adaptive (i.e. capable of responding to peak movement).

The discontinuity in the background which underlies the iron peak represents the more serious problem in resolution. It was strongly suspected that the discontinuity was correlated with the Xe detector gas absorption edges (ref.
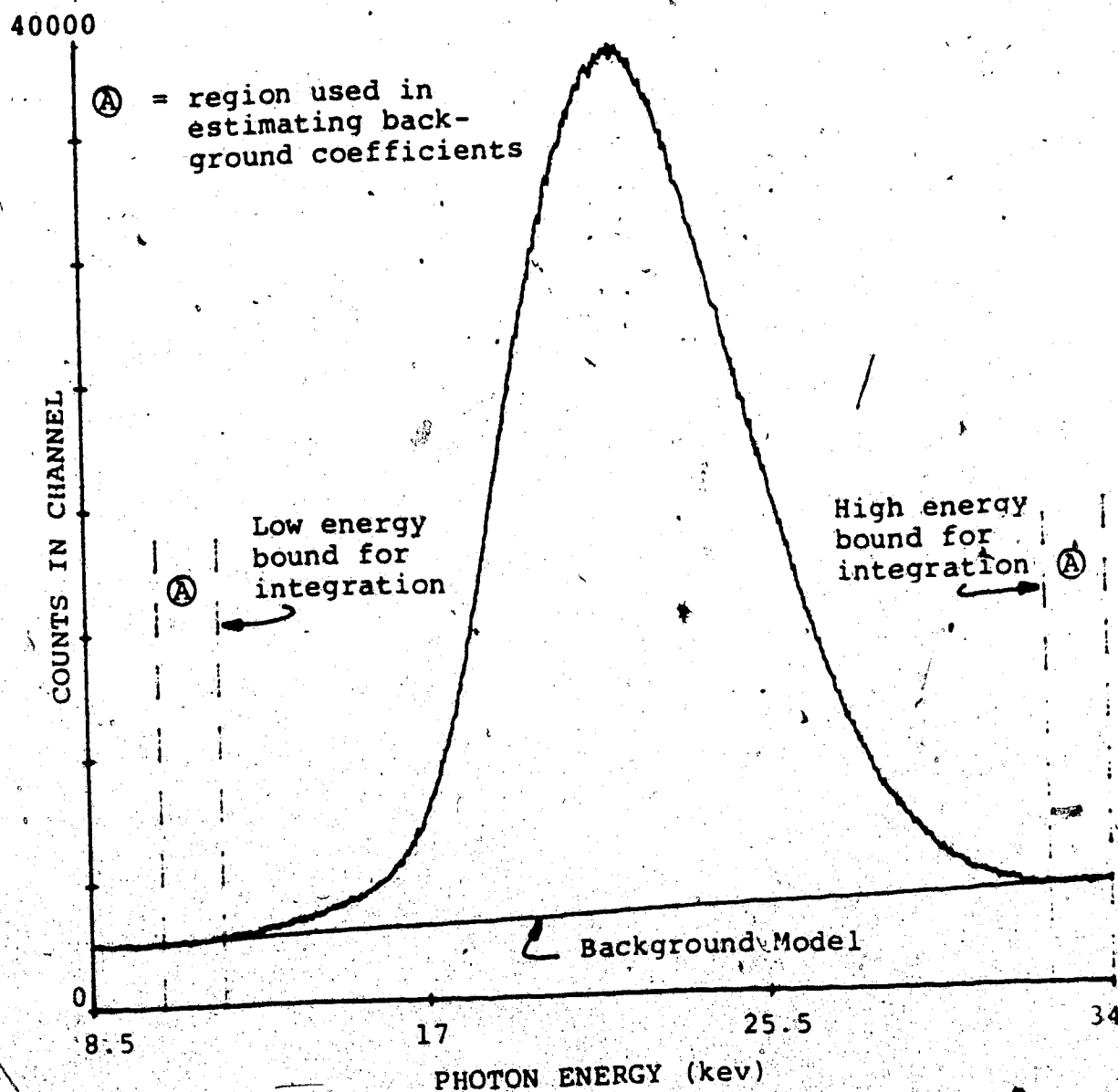
Figure 7.2 A Schematic Representation of the Method Employed in Resolving the Backscatter Peak.

(52) pg. 305). The mass absorption coefficient for Xe over the energy range of interest is shown in Figure 7.3. The principal iron fluorescence peak, Fe Kα at 6.4 kev, is observed to lie just to the high energy side of the Xe L shell absorption edges. Given the resolution of the proportional counter it was expected that there would be some overlap resulting in a discontinuity which would underlie the iron K fluorescent radiation peaks.

A special experiment was designed where it was possible to directly irradiate the detector with the Cd-109 source, both with and without iron fluorescence. A typical result for the experiment is shown in Figure 7.4. It is readily apparent from this figure that overlap does indeed exist. Calculations on the spectral data indicated that the beginning of the discontinuity on the high energy side corresponds to the Xe L1 absorption edge (5.5 kev).

Clearly, the method used to extract the iron fluorescence counts should be somewhat more sophisticated than that which was employed to resolve the backscatter peak. Since it is desirable, from a statistical accuracy viewpoint, to use the area under the peak as a measure of the fluorescence counts a peak modelling approach was intially adopted[1].

The modelling approach, while more mathematically elegant, proved to be less precise than a simple resolution

---

[1] This is the preferred method of measurement in energy dispersive analysis as opposed to the single energy (wavelength) measurement common in wavelength dispersive XRF analysis.
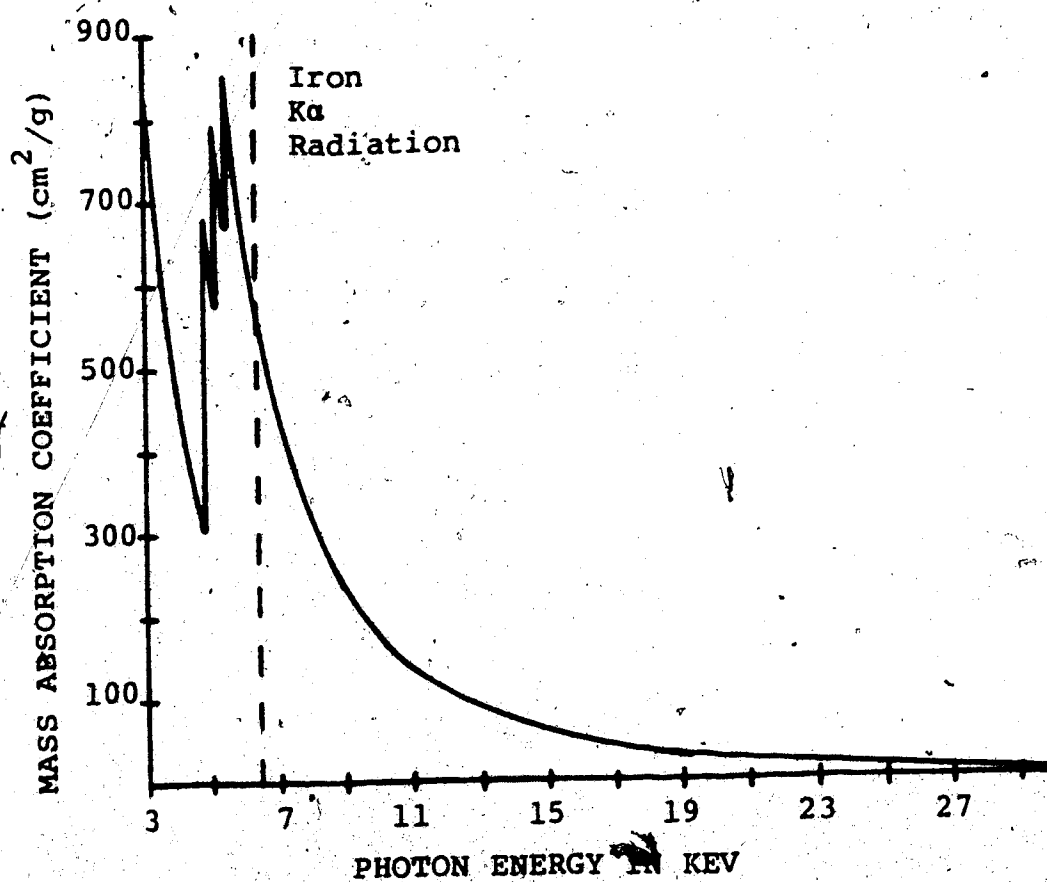
Figure 7.3 The Mass Absorption Coefficient for Xenon as a
Function of Photon Energy.
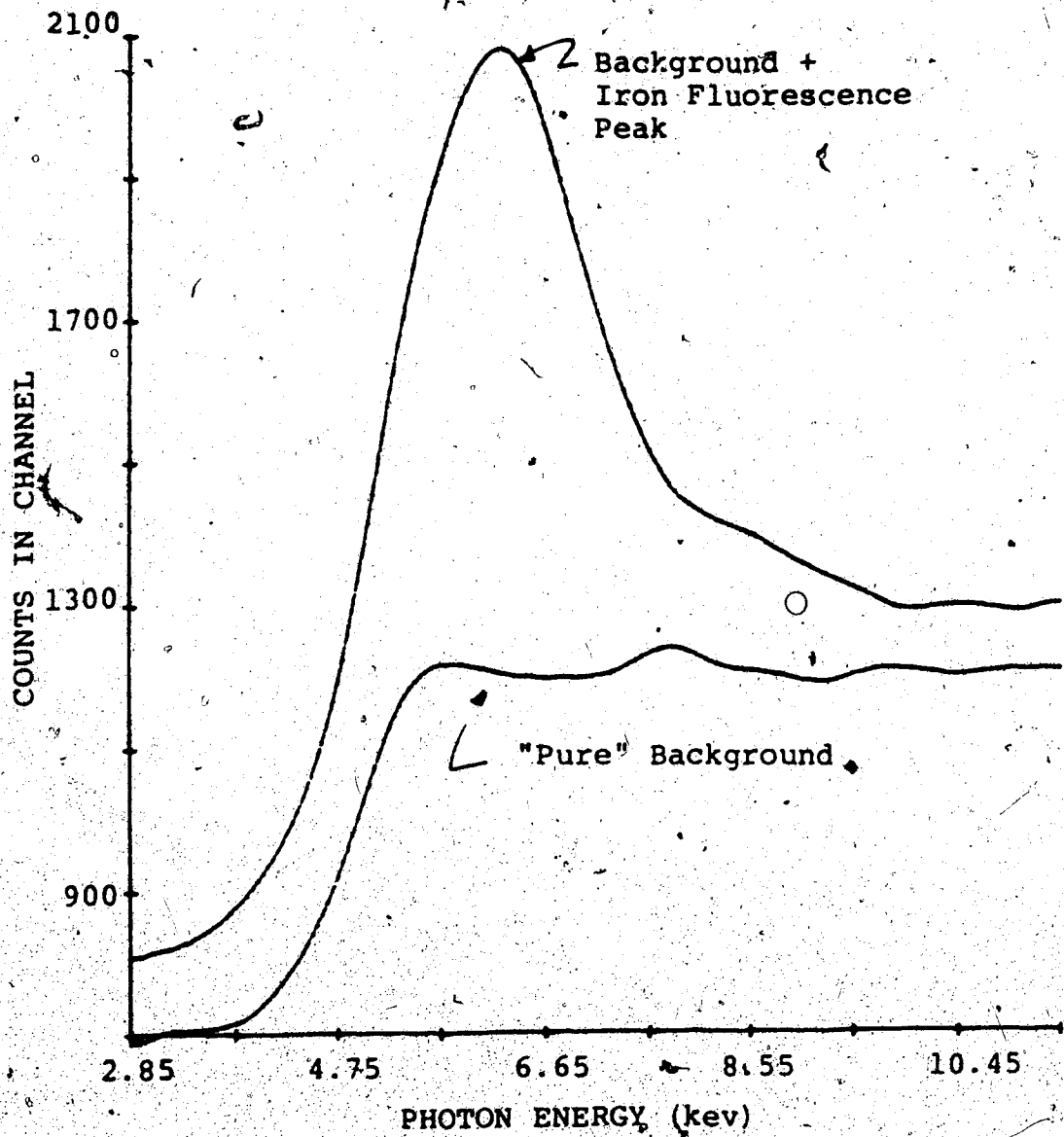
Figure 7.4 Identification of the Discontinuity Underlying the Iron Fluorescence Peak.

technique, and for this reason was not used in the QSCAA studies. However, in view of the potential application of peak-modelling in the next generation of instrument development, the methodology and the results of the resolution studies are described in the text which follows.

7.2.2.1 Modelling the Iron Fluorescence Peaks

The iron fluorescence radiation peak model is given in equation (7.2). The model assumes a double Gaussian function to account for both the $K\alpha$ (6.4 kev) and $K\beta$ (7.05 kev) contributions.

$$\hat{Y}_i = Y' \left\{ \exp\left[-k\left[\frac{i-C\alpha}{W\alpha}\right]^2\right] + R\exp\left[-k\left[\frac{i-C\beta}{W\beta}\right]^2\right] \right\} \qquad \ldots (7.2)$$

where: $\hat{Y}_i$ = iron K fluorescent radiation counts in channel i.
Y' = iron $K\alpha$ fluorescent radiation counts for "α-peak" modal channel.
k = numerical constant ($=4\ln(2)$).
i = channel number.
$C\alpha$ = modal channel for the $K\alpha$ radiation.
$W\alpha$ = full width at half maximum (FWHM) for the $K\alpha$ peak.
$C\beta$ = modal channel number for the $K\beta$ radiation.
R = ratio of the $K\beta$ to $K\alpha$ peak heights.
$W\beta$ = FWHM for the $K\beta$ peak.

The unknown parameter set in the equation (Y', $C\alpha$, $W\alpha$, $C\beta$, R, $W\beta$) can be reduced from the theory. Jenkins and Devries((67) pg. 175) show that R is approximately equal to 0.15. Using a steel sample in a scanning electron microscope equipped with energy dispersive XRF analysis, R was observed to be 0.143. Moreover, since the MCA spectrum was linear in energy (channel number) with a zero intercept, the ratio of $C\beta/C\alpha$ was calculated to be

1.102 and therefore;

$$C\beta = 1.102C\alpha \qquad \qquad \ldots(7.3)$$

In addition, the theory states that;

$$W \propto E^{0.5} \qquad \qquad \ldots(7.4)$$

and, therefore;

$$W\beta = \left[\frac{7.05}{6.4}\right]^{0.5} W\alpha = 1.05W\alpha \qquad \qquad \ldots(7.5)$$

Equation (7.5) was corroborated by the scanning electron microscope work. Substitution of equations (7.3) and (7.5) and the independently obtained value of R into equation (7.2) produced a model in three unknown parameters, namely Y', $C\alpha$, and $W\alpha$.

7.2.2.2 Modelling the Background

The background model was assumed to take on one of two forms. The first form considered the background to be constant on the high energy side of the discontinuity. This meant that only the data in this region of the spectrum could be analysed, however, as shown in Figure 7.4, the fluorescence peak is relatively well defined in this region. It is possible, in principle, to fit the combined background and iron fluorescence models over this region. If Cm is taken as the channel corresponding the maximum counts in the observed spectrum, the constant background model can be estimated as follows;

$$B = \text{MINIMUM} \left\{ \sum_{j=i-n}^{i+n} Y_j \Big/ (2n+1) \right\}; \quad i=1,2,\ldots,250 \quad \ldots(7.6)$$

where: B = estimate of the background counts on the high
    energy side of the discontinuity.
  n = the averaging increment (taken as 2 in this
    work).
  Y_j = observed counts in channel j.
  Cm = modal channel in the observed spectrum.

The second form of the background model was derived from inspection of plots of the first derivative of the "pure" background spectra from the special experiment (ref. fig. 7.4). Since the resulting curve resembled a Gaussian density distribution it was argued that the background could be partially modelled as an integrated form of this function. This required that the background be considered as a three part function. It would be constant both below and above the discontinuity and be equivalent to the integrated Gaussian over the discontinuity (ref. fig. 7.4: "pure background").

Mathematically;

$$BL = MINIMUM \left\{ \sum_{j=i-n}^{i+n} Y_j \Big/ (2n+1) \right\}; \quad i = 60, \ldots, Cm \qquad \ldots(7.7)$$

$$BU = MINIMUM \left\{ \sum_{j=i-n}^{i+n} Y_j \Big/ (2n+1) \right\}; \quad i = Cm, \ldots, 250 \qquad \ldots(7.8)$$

where: BL, BU = constant background on the lower and
    upper energy side of the discontinuity,
    respectively.

Since the total counts under a Gaussian peak, I, is related to the FWHM, Wb, and the counts in the modal channel, Y'', as;

$$I = \frac{Y''Wb\sqrt{2\pi}}{2.35} \qquad \ldots(7.9)$$

where: I = total counts under the background "peak".
   Y'' = counts in the modal channel for the
    background "peak".

Wb =FWHM for the background "peak".

then, if BL and BU are fixed according to equations (7.7) and (7.8);

$$I=BU-BL \qquad \qquad ...(7.10)$$

and combining equations (7.9) and (7.10) with rearrangement yields;

$$Wb=\frac{2.35(BU-BL)}{\sqrt{2\pi}\ Y''} \qquad ...(7.11)$$

Thus the unknown parameters for an integrated Gaussian function describing background would be Cb, the modal channel, and Y'', and the final model for the background is given in equation (7.12).

$$B_i=BL+\sum_{j=\ell}^{i}Y''\exp\left[-k\left[\frac{j-Cb}{Wb}\right]^2\right] \qquad ...(7.12)$$

where: B_i =background counts in the ith channel.
ℓ =channel corresponding to BL.
Cb =modal channel for the background "peak".

7.2.2.3 Modelling the Spectrum

Considering the discussion above, there were two methods of modelling the photon energy spectrum in the region including the iron peak. The first was to examine the spectrum on the high energy side of the discontinuity. In this case equations (7.2) and (7.6) were used, where, for the latter, B was also considered an unknown whose intial estimate was obtained from equation (7.6). This was termed the "1/2 Peak Method" since it examined a little more that one-half of the peak. The other method examined the entire peak using equations (7.2) and (7.12) and was termed the "full peak

method".

For comparative purposes a very simple extraction technique was also studied, analogous to wavelength dispersive XRF analysis. In this case the background was estimated from equation (7.6) and the counts in channel Cm, corrected for background, B, were taken as the iron radiation measurement. This was termed the "simple method".

Parameterization of the models was accomplished using an orthogonal multivariable search algorithm (an adaptation of the Coggin's algorithm; (68)). Initial estimates of the parameters were available from previous work. The objective function minimized in the parameterization exercise was the standard x^2 criterion having the form;

$$x^2 = \sum_{i=a}^{b} \frac{(Y_i - \hat{Y}_i)^2}{Y_i} \qquad \ldots(7.13)$$

where: $\hat{Y}_i$ = predicted counts in channel i.
a, b = channel limits defining the range of fit.

Once the model parameters are known, the area under the iron K fluorescent radiation peak is analytically available from expressions of the form given by equation (7.9) (summing a and β contributions).

With regard to the spectrum itself, the raw data showed considerable statistical fluctuation as was expected at the relatively low count levels. As an alternative to a direct fit on the raw data, a smoothing algorithm was developed as described by Marr(69). The

spectrum smoothing procedure is recommended by Bevington (ref. (70) pg. 250) to improve the fit by reducing the x^2 value, but not without warnings on potential problems related to increased uncertainty on the parameters. Briefly, the smoothing algorithm requires that the raw count data be transformed by taking logarithms. Then, using linear regression[1], and assuming a quadratic relationship, the transformed counts in a particular channel were estimated by fitting the quadratic over (2n+1) points, n on either side of the channel of interest. For this work n was taken to be 12. In accordance with Marr's suggestion, the smoothing operation involved two passes with the algorithm, the results of the second pass were re-transformed to produce the smoothed spectrum.

7.2.2.4 Results of the Resolution Studies

The three extraction methods were then tested on both raw and smoothed spectra to determine which would provide the most precise results (accuracy could not be tested). For the purposes of the extraction methodology testing a series of 4 spectra on pure water samples were used. The water spectrum shows a pronounced iron peak due to the steel used in the fabrication of the source and detector housing. It is, however, the minimum peak height obtainable and thus is most susceptible to

---

[1] The regression is done using convolution integers because of the equispaced channel data.

statistical fluctuations. For this reason the water
spectra make the best test-bed for methodology
evaluation. It was argued that the method selected must
be reliable for all spectra acquired and therefore must
be accurate for any subset, including the pure water
spectra.

A selection of the results of the evaluation
studies is presented in Table 7.1. In Table 7.1, (A) and
(B) compare the "1/2 peak method" on both the raw and
smoothed spectral data. For comparative purposes both Y'
and I are reported. In both cases Y' was a more stable
estimator of the fluorescent counts than I, as reflected
in the relative error of estimation. This is the result
of the additional uncertainty in the FWHM, which is
required in addition to Y' to compute I. It is clear
from the differences in the relative error figures that
the smoothed data gave more stable estimations than did
the raw data. (B) and (C) compare the "1/2 peak method"
and the "full peak method" as applied to smoothed data
demonstrating the superiority of estimation for the
latter. This is thought to be the result of the "full
peak method" including the entire range of the iron
fluorescence peak thereby improving parameter
estimation. Finally, (D) demonstrates the results for
the "simple method" which was judged to be the best
method for resolving iron count data. (The trends shown
here were later substantiated in the calibration

Table 7.1 Results of Iron Peak Resolution Studies

(A) "1/2 Peak Method" on Raw Data

Case #	Y' counts	I counts
1	1387.1	65256.8
2	1411.5	74752.6
3	1317.3	61109.4
4	1396 4	73487.2
Mean	1378.1	68651.5
Std. Dev.	41.7	6557.8
Rel. Err.	3.0%	9.6%

(B) "1/2 Peak Method" on Smoothed Data

Case #	Y' counts	I counts
1	1366.6	60442.9
2	1353.1	62660.2
3	1323.0	61908.6
4	1359.7	67450.2
Mean	1350.6	63115.5
Std. Dev.	19.2	3032.9
Rel. Err.	1.4%	4.8%

(C) "Full Peak Method" on Smoothed Data

Case #	Y' counts	I counts
1	1368.1	58722.6
2	1368.6	59539.0
3	1344.6	61172.9
4	1348.0	62977.7
Mean	1357.3	60602.8
Std. Dev.	12.8	1882.9
Rel. Err.	0.9%	3.1%

(D) "Simple Extraction Method" on Smoothed Data

Case #	Ymax counts
1	1535.4
2	1539.1
3	1533.1
4	1532.1
Mean	1534.9
Std. Dev.	3.1
Rel. Err.	0.2%

exercise for run 1 on flotation feed.)

On the basis of these findings the "simple method" was selected for the subsequent spectral analysis work. Figure 7.5 illustrates the mechanics of the "simple method" for extraction of the iron count data. Briefly, the raw data is first smoothed, the modal channel identified and the background estimated whence the corrected counts in the modal channel, Ymax, is calculated.

It was indeed unfortunate that a reliable estimate of peak area could not be developed within the time frame of this project. A reliable estimator of this form would have provided statistically better estimates of the iron counts.

7.3 PARAMETER ESTIMATION FOR THE SEMI-EMPIRICAL CALIBRATION MODELS

The four component semi-empirical OSCAA calibration model given by equations (5.76) through (5.79) requires that various mass absorption and scattering absorption nuclear coefficients be available for each component in the assumed physical model of the slurry. In addition, estimates of the component densities are required. In principle these parameters could be estimated by including them as unknowns in the model calibration exercise (together with the A_i, B_i). However, it is considerably simpler to calculate the nuclear coefficients from the data available in the literature,
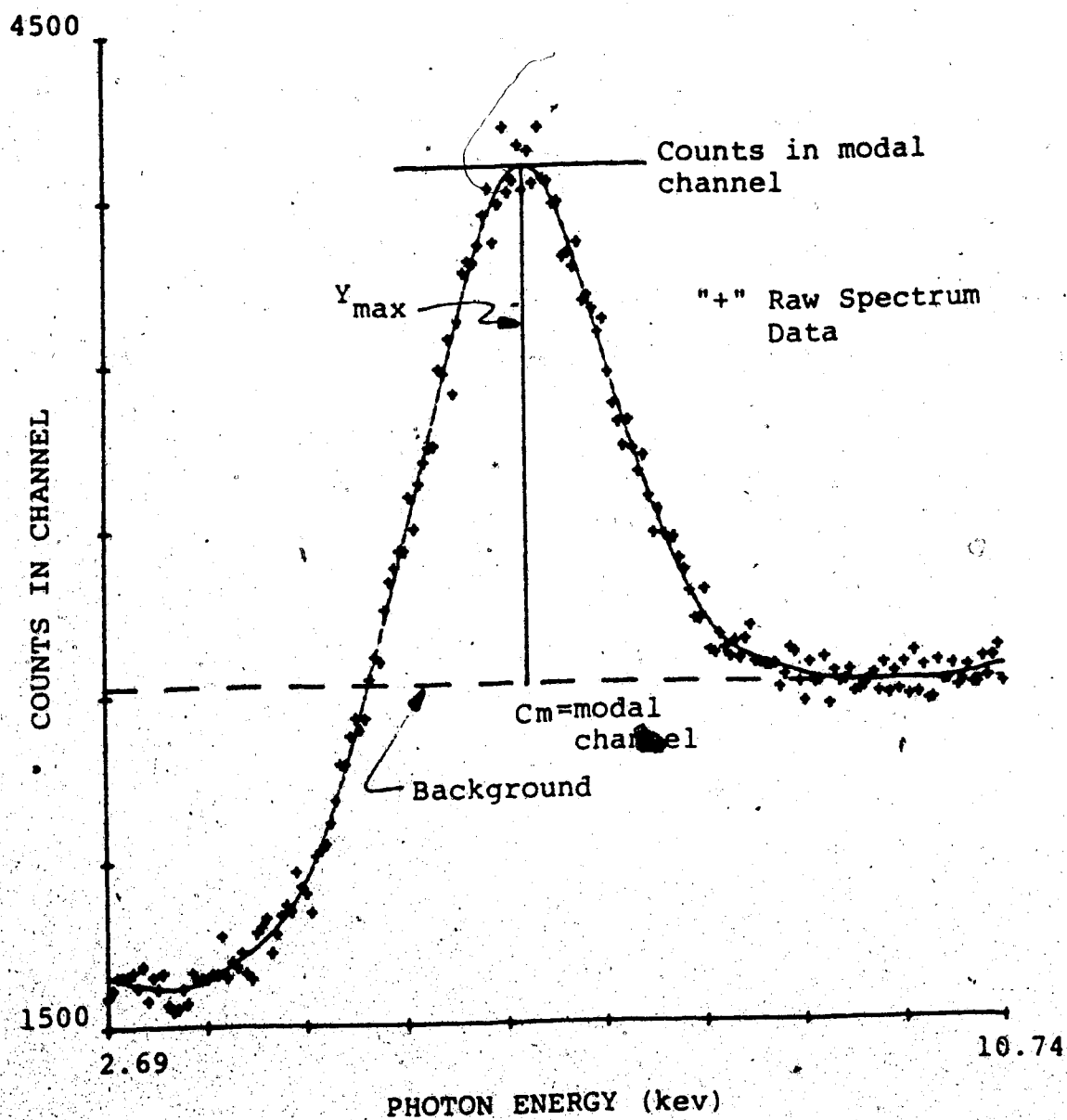
Figure 7.5 Resolution of the Iron Fluorescence Peak by the Simple Method.

knowing the approximate elemental composition of the
components. Furthermore, the densities can be estimated by
fitting the assumed physical model of the coal solids to
actual specific gravity data derived from the analysis of
experimental samples.

7.3.1 Calculation of the Nuclear Coefficients

An interactive computer program was written (Appendix
1) and the appropriate data base constructed from the
tabulated values(39) such that upon entry of:

(i) the ash analysis,

(ii) the ultimate analysis of the coal,

the appropriate nuclear coefficients were estimated from the
elemental composition. Included in the output from this
program were the mass absorption coefficients at 6.4 kev
(principal Fe fluorescence photon energy) and 22 kev
(average principal Cd-109 photon energy), as well as the
combined scattering absorption coefficients. (The later were
estimated by calculating σ_m and σ_{am}, correcting them with
r_m, r_{am} (sub-section 5.5.1.3), and adding the results
together). These various coefficients are computed for:

(i)the organic phase,

(ii)the overall mineral matter phase (including the
iron component),

(iii) the iron free mineral matter phase.

Since the composition of the other two possible components,
namely water and hematite, are fixed, these calculations

were done only once. A sample of the relevant portion of the computer program output is presented in Figure 7.6.

Several ultimate and ash analyses were available on McIntyre Mines Ltd. coal (see, for example, (71), pg. 55). These were done at different times and by different groups and included results obtained on the raw coal samples used in this work. Interestingly, the ultimate analysis changed very little and the most significant differences between the ash analyses were the concentrations of iron, This suggests that, in this particular case at least, the nuclear coefficients will be reasonable for the deposit as a whole thus the four component model assumed for calibration purposes was quite reasonable.

7.3.2 Estimating Solid Component Densities

It was explicitly stated in the discussion in sub-section 5.7.1 that the coal solids were assumed to consist of least two phases, minimally an organic phase and a mineral matter phase. The coal solids density, in terms of these two phases, may be written as;

$$\rho_s = \left[\frac{1}{\frac{(1-m)}{\rho_2} + \frac{m}{\rho_3'}} \right] \qquad ...(7.14)$$

where: ρ_s =coal solids density.
ρ_2, ρ_3' =coal solids organic and mineral matter phase densities.
m =mass fraction of mineral matter in the coal solids.

To estimate ρ_2 and ρ_3', the specific gravity data derived from run 1 was used as it provided the widest range of values. A non-linear regression program(72) was employed to

ORGANIC PHASE CALCULATIONS....

	CARBON	HYDROGEN	NITROGEN	SULFUR	OXYGEN	ASH
WT. % (RAW)	83.70	4.44	1.26	0.49	2.59	7.52
WT. % (ADJ)	90.51	4.80	1.36	0.53	2.80	0.0

TOTAL AC(6.4)= 9.5469 TOTAL AC(22)= 0.4069 INCOH. SCATTER (22)= 0.1704
          COH. SCATTER (22)= 0.0574 TOTAL SCATTER (22)= 0.0506

INORGANIC PHASE CALCULATIONS....

OXIDE OF	WEIGHT % RAW	WEIGHT % ADJUSTED	EXCLUDING HEMATITE
SILICON	52.16	53.98	58.63
ALUMINUM	23.65	24.48	26.58
CALCIUM	3.27	3.38	3.68
MAGNES.	0.74	0.77	0.83
TITANIUM	1.89	1.96	2.12
SODIUM	0.84	0.87	0.94
POTASS.	1.37	1.42	1.54
PHOSPH.	0.97	1.00	1.09
SULFUR	4.08	4.22	4.59
IRON	7.65	7.92	0.0

DATA FOR ASH FORMING MINERALS:

TOTAL AC(6.4)= 79.4664 TOTAL AC(22)= 2.2408 INCOH. SCATTER (22)= 0.1503
          COH. SCATTER (22)= 0.1507 TOTAL SCATTER (22)= 0.0499

OXYGEN FRACTION IN THE IRON FREE INORGANICS IS 49.87 %

DATA FOR MINERAL MATTER:

TOTAL AC(6.4)= 74.0140 TOTAL AC(22)= 2.0941 INCOH. SCATTER (22)= 0.1524
          COH. SCATTER (22)= 0.1443 TOTAL SCATTER (22)= 0.0502

DATA FOR HEMATITE:

TOTAL AC(6.4)= 55.9200 TOTAL AC(22)= 13.8680 INCOH. SCATTER (22)= 0.1301
          COH. SCATTER (22)= 0.3500 TOTAL SCATTER (22)= 0.0549

DATA FOR COMPOSITE MINERAL MATTER:

TOTAL AC(6.4)= 72.5814 TOTAL AC(22)= 3.0263 INCOH. SCATTER (22)= 0.1507
          COH. SCATTER (22)= 0.1606 TOTAL SCATTER (22)= 0.0506

Figure 7.6 Sample Program Output for Calculating Nuclear
Coefficients in the Semi-Empirical Calibration Models.

calculate the estimates. The raw data and the regression results are presented in Table 7.2.

For the purposes of the four component model, where it was necessary to provide a ρ_3 value for the iron free mineral matter, equation (7.14) was used to transform ρ_3';

$$\rho_3 = \left[\frac{(1-\ell)}{\dfrac{1}{\rho_3'} - \dfrac{\ell}{\rho_4}} \right]$$

...(7.15)

where: ρ_3 = density of the iron free mineral matter.
ρ_4 = density of hematite.
ℓ = mass fraction of iron bearing mineral in the mineral matter phase.

7.4 DATA PREPARATION

This section deals with the methods employed to manipulate the raw data prior to performing the calibration studies. It is divided into two sub-sections, the first dealing with slurry attribute analyses and the second with the radiation count data.

7.4.1 Preparation of the Slurry Attribute Data

As described in sub-section 6.4.2, three slurry attributes were measured;

a) % solids in the slurry,

b) % ash in the solids,

c) % iron in the ash.

The analyses for (a) and (b) were done in-house but for (c), the analyses were performed by a commercial laboratory. In order to minimize costs for the latter, in all but run 4, where the iron concentration was independently controlled,

Table 7.2 Estimates of the Solid Phase Densities in the

McIntyre Coal

RAW DATA FOR FLOTATION FEED CALIBRATION RUN

Experiment Number	Mass Fraction of Mineral Matter (m)	Solids[++] Specific Gravity
1	0.1092	1.360
2	0.1100	1.359
3	0.1112	1.362
4	0.1133	1.357
5	0.1136	1.355
6	0.1466	1.374
7	0.1819	1.409
8	0.2230	1.442
9	0.2572	1.4685
10	0.1372	1.3742
11	0.1385	1.3699
12	0.1395	1.3697
13	0.1412	1.3681
14	0.1797	1.4022
15	0.2148	1.4385
16	0.2556	1.4601
17	0.1752	1.4011
18	0.1763	1.3992
19	0.1807	1.4092
20	0.2181	1.4400
21	0.2565	1.4636
22	0.2107	1.4221
23	0.2438	1.4499
24	0.2518	1.4511

[+]Mineral Matter is calculated from ash assuming
R_{ma} = 1.1 (eqn 5.82)

[++]Determined using a pycnometer with varsol as
the diluting medium.

Regression Results (eqn(7.13))

Solid Phase	Density	95% Conf. Limits
Organics	1.28	± 0.01
Mineral Matter	2.47	± 0.10

Index of multiple determination (r^2) = 0.85

Calculated "F" statistic = 588 (viz $F_{2,22,.05}$ = 3.4)

only a few of the selected ash residues were submitted for iron analysis. It was expected that a systematic relationship between iron content and ash would be observed for the simple raw coal blending used in runs 1 through 3.

A quadratic function can be used, over a limited range of ash values, to characterize the iron versus ash relationship. A typical result of this approach is illustrated in Table 7.3 for run 1 and a portion of run 2 where the same raw coal samples were used for blending. The quadratic approximation is a relatively accurate predictor, and through substitution of the ash values for particular samples the corresponding iron content can be estimated. These estimated values were used in the calibration studies. In the cases where the regression was insignificant the model predicted relatively constant iron contents, as would be expected, and these values were used.

Calculation of the mass fractions of the various slurry components was left to the computer programs which perform the calibration model parameterization. Tables 7.4 through 7.7 present the attribute analyses for the four laboratory runs.

7.4.2 Preparation of Radiation Count Data

The backscattered radiation data derived in the manner described in section 7.2 were not manipulated prior to the calibration, however, both the pulp density and iron fluorescence counts were modified. The method of handling

Table 7.3 Estimating Iron Content From Ash

RAW DATA FROM FLOTATION FEED CALIBRATION (RUN #1)
AND FLOTATION CONCENTRATE CALIBRATION (RUN #2)

Experiment Number	Ash (%)	Iron in Ash(%)
1:10	12.47	5.13
1:13	12.84	4.92
1:14	16.34	4.58
1:15	19.53	4.38
1:16	23.24	3.35
1:17	15.93	4.57
1:23	19.15	4.31
1:25	22.89	4.37
2:2	3.36	5.56
2:5	7.34	5.71
2:6	8.39	5.57
2:11	8.25	5.46

Quadratic Relationship:

$$\% \text{ Iron} = b_o + b_1(\%\text{Ash}) + b_2(\%\text{Ash})^2$$

$$\text{with } b_o = 7.156$$
$$b_1 = -0.2397$$
$$b_2 = 5.063 \times 10^{-3}$$

Index of multiple determination $(r^2) = 0.978$

Calculated "F" statistic = 406 (viz $F_{3,9,.05} = 3.86$)

Table 7.4 Slurry Attribute Analyses for Laboratory Run 1

EXPERIMENT NUMBER	% SOLIDS IN SLURRY	% ASH IN SOLIDS	% IRON IN ASH
1	5.23	9.93	5.28
2	8.41	10.00	5.27
3	11.58	10.11	5.25
4	14.79	10.30	5.22
5	17.94	10.33	5.22
6	17.52	13.33	4.86
7	18.05	16.54	4.58
8	18.73	20.27	4.38
9	19.08	23.38	4.32
10	5.14	12.47	4.95
11	8.46	12.59	4.94
12	11.51	12.68	4.93
13	14.75	12.84	4.91
14	14.81	16.34	4.59
15	15.24	19.53	4.41
16	15.42	23.24	4.32
17	5.20	15.93	4.62
18	8.33	16.03	4.61
19	11.59	16.43	4.58
20	11.92	19.83	4.39
21	12.03	23.32	4.32
22	8.60	19.15	4.42
23	8.76	22.10	4.33
24	5.22	22.89	4.32

Table 7.5 Slurry Attribute Analyses for Laboratory Run 2

EXPERIMENT NUMBER	% SOLIDS IN SLURRY	% ASH IN SOLIDS	% IRON IN ASH
1	22.08	7.24	5.69
2	24.54	7.36	5.67
3	27.13	7.38	5.66
4	29.78	7.41	5.66
5	32.46	7.34	5.67
6	32.59	8.39	5.50
7	32.64	9.47	5.34
8	32.66	10.60	5.18
9	32.77	11.73	5.04
10	21.24	8.20	5.53
11	23.73	8.25	5.52
12	26.30	8.34	5.51
13	28.55	8.35	5.51
14	28.11	9.47	5.34
15	28.56	10.38	5.21
16	28.71	11.59	5.06
17	20.96	10.71	3.56
18	23.27	10.37	3.60
19	25.85	10.28	3.61
20	25.74	11.34	3.55
21	25.61	12.33	3.68
22	21.14	11.65	3.57
23	23.77	11.59	3.57
24	23.70	12.61	3.75
25	21.36	12.53	3.73

Table 7.6 Slurry Attribute Analyses for Laboratory Run 3

EXPERIMENT NUMBER	% SOLIDS IN SLURRY	% ASH IN SOLIDS	% IRON IN ASH
1	1.10	32.40	3.90
2	2.15	32.29	3.90
3	3.23	32.92	3.91
4	4.50	32.66	3.91
5	5.63	33.08	3.91
6	1.03	34.09	3.91
7	2.11	34.05	3.91
8	3.29	35.41	3.92
9	4.43	35.98	3.92
10	5.56	35.91	3.92
11	1.11	38.13	3.94
2	2.07	37.21	3.93
13	3.19	37.99	3.94
14	4.41	38.87	3.94
15	5.55	38.85	3.94
16	1.04	39.48	3.95
17	2.21	40.47	3.96
18	3.33	40.91	3.96
19	4.55	41.15	3.97
20	5.68	41.44	3.97
21	1.10	44.39	4.01
22	2.23	43.79	4.00
23	3.29	44.05	4.00
24	4.34	43.71	4.00
25	5.69	44.18	4.00

Table 7.7 Slurry Attribute Analyses for Laboratory Run 4

EXPERIMENT NUMBER	% SOLIDS IN SLURRY	% ASH IN SOLIDS	% IRON IN ASH
1	7.47	12.51	4.17
2	13.04	12.49	4.22
3	16.01	12.69	4.08
4	16.12	16.80	4.64
5	16.82	22.02	4.58
6	7.47	16.57	4.56
7	11.73	16.89	5.69
8	12.13	21.45	5.65
9	7.57	21.09	6.12
10	7.58	12.59	6.99
11	12.01	12.80	7.06
12	16.17	12.65	7.10
13	16.41	17.25	7.42
14	16.89	21.36	7.36
15	7.52	16.57	7.16
16	11.73	16.80	7.41
17	12.01	21.23	7.62
18	7.08	21.08	7.92
19	7.59	12.54	8.70
20	11.95	12.58	9.02
21	16.28	12.59	9.06
22	16.16	17.03	9.16
23	16.78	21.55	9.36
24	7.39	16.39	9.44
25	11.66	16.66	9.16
26	12.23	20.62	9.56
27	7.09	20.82	10.03

the pulp density counts was a two step process.

a) Subtract Background: In this case the background was estimated by closing the source camera shutter, which effectively totally shields the Gd-153 source from the detector. A series of 300 second counts were the recorded and the mean value (typically 40,000 counts) was scaled up to the corresponding data acquisition period and subtracted from the raw count data.

b) Reduction by Standardization: The corrected count values obtained in (a) were divided by the corresponding values for the pure water experiments run prior to each series. The corrected and reduced count data from this process were used in the calibration studies.

For the iron fluorescence count data, each experimental value was corrected by subtracting the corresponding value for the pure water experiments.

In summary, all of the radiation count data was corrected for background at some point or another in the spectral analysis or data preparation stages. It is common to reduce density count information as well as other spectral data, utlizing standards, to account for equipment drift etc... In this case only the density count data was reduced since this has the effect of partially compensating for varying entrained air content between series. The iron count data was corrected from the pure water standards to remove the contribution due to the fluorescence from the steel assembly housing the source and detector in the ash

analysis sub-system. The radiation data used in the calibration studies is presented in Tables 7.8 through 7.11.

7.5 THE CRITERIA FOR ASSESSING CALIBRATION RESULTS

There are a variety of means of assessing the performance of an on-stream analysis device intended for use in process control. It is the opinion of the author that the best criteria for evaluating OSCAA is a modified version of that defined by Howarth et. al.(73). If the unit meets the following criteria for both % solids and % ash prediction it is acceptable for process control applications.

$$100\% \left[\frac{S(y)}{\bar{y}} \right] \leq 10\% \qquad \ldots(7.16)$$

$$\left[\frac{100\% S(y)}{\max(y_i) - \min(y_i)} \right] \leq 10\% \qquad \ldots(7.17)$$

and,

$$S(y) = \left[\sum_{i=1}^{N} \frac{(y_i - \hat{y}_i)^2}{N} \right]^{0.5} \qquad \ldots(7.18)$$

$$\bar{y} = \sum_{i=1}^{N} y_i \Big/ N \qquad \ldots(7.19)$$

where: N = number of experiments.
S(y) = an uncorrected estimate of the standard error of prediction.
$\bar{y}$ = the mean value of the measured attribute.
y_i = measured value of the attribute for experiment i.
$\hat{y}_i$ = predicted value of the attribute for experiment i.

Criterion (1) is the common relative error index of

Table 7.8 Radiation Count Data for Laboratory Run 1

EXPERIMENT NUMBER	REDUCED PULP DENSITY COUNTS	BACKSCATTER COUNTS (X 1 E-06)	CORRECTED IRON COUNTS (X 1 E-02)
1	0.95809	6.117952	1.216
2	0.94000	6.102803	2.115
3	0.91419	6.086581	2.502
4	0.89005	6.075626	3.110
5	0.86558	6.057477	4.123
6	0.85429	6.013170	4.906
7	0.84192	5.961919	6.193
8	0.81751	5.884961	7.236
9	0.80255	5.819540	7.952
10	0.96104	6.094012	1.274
11	0.93173	6.080016	2.133
12	0.90955	6.056673	2.569
13	0.87998	6.038117	3.651
14	0.87161	5.991722	4.490
15	0.86107	5.942789	5.439
16	0.85212	5.889042	6.142
17	0.95244	6.083932	1.452
18	0.91948	6.044457	2.307
19	0.89405	6.010995	3.420
20	0.89014	5.978627	3.587
21	0.87610	5.934969	4.475
22	0.92405	6.031274	3.170
23	0.91716	5.998970	3.657
24	0.95103	6.037998	2.084

Table 7.9 Radiation Count Data for Laboratory Run 2

EXPERIMENT NUMBER	REDUCED PULP DENSITY COUNTS	BACKSCATTER COUNTS (X 1 E-06)	CORRECTED IRON COUNTS (X 1 E-02)
1	0.84267	6.006070	4.083
2	0.83124	5.996590	4.401
3	0.80688	5.991073	4.984
4	0.78777	5.986919	5.215
5	0.77289	5.987024	6.042
6	0.76768	5.954420	6.464
7	0.76403	5.912414	7.308
8	0.76903	5.877636	7.646
9	0.76588	5.837851	8.329
10	0.85075	5.986594	3.759
11	0.83438	5.982572	4.493
12	0.81811	5.967861	4.898
13	0.80539	5.961365	5.403
14	0.80315	5.926213	5.897
15	0.79414	5.898715	6.668
16	0.78765	5.860857	7.428
17	0.83899	5.966444	2.749
18	0.82373	5.948627	3.137
19	0.80551	5.948843	3.810
20	0.80103	5.911218	4.786
21	0.80082	5.882074	5.228
22	0.84226	5.946631	2.926
23	0.82465	5.938064	3.436
24	0.82538	5.907781	4.271
25	0.84476	5.922986	3.456

Table 7.10 Radiation Count Data for Laboratory Run 3

EXPERIMENT NUMBER	REDUCED PULP DENSITY COUNTS	BACKSCATTER COUNTS (X 1 E-06)	CORRECTED IRON COUNTS (X 1 E-02)
1	0.99728	10.550379	0.529
2	0.97853	10.492260	1.696
3	0.97238	10.419597	2.496
4	0.96037	10.351724	3.864
5	0.95048	10.289182	4.790
6	0.98931	10.532543	0.803
7	0.98382	10.462132	2.146
8	0.96922	10.384149	3.041
9	0.96012	10.320749	3.943
10	0.94432	10.232109	5.414
11	0.98750	10.518073	1.090
12	0.98077	10.442373	1.747
13	0.96485	10.349414	3.406
14	0.95217	10.273763	4.450
15	0.93376	10.204092	5.130
16	0.98939	10.508805	1.424
17	0.97214	10.414876	2.854
18	0.96263	10.336678	3.928
19	0.95410	10.236924	5.419
20	0.93917	10.144000	6.652
21	0.99273	10.472705	1.658
22	0.97177	10.381948	2.875
23	0.95486	10.298769	4.226
24	0.94171	10.200385	5.359
25	0.92869	10.102627	6.791

Table 7.11 Radiation Count Data for Laboratory Run 4

EXPERIMENT NUMBER	REDUCED PULP DENSITY COUNTS	BACKSCATTER COUNTS (X 1 E-06)	CORRECTED IRON COUNTS (X 1 E-02)
1	0.96042	10.291798	2.598
2	0.93295	10.264365	3.973
3	0.90574	10.216802	5.889
4	0.89215	10.031330	8.887
5	0.88062	9.833685	11.963
6	0.95239	10.225282	3.809
7	0.92447	10.136001	5.847
8	0.90898	9.986970	8.464
9	0.94512	10.137179	5.507
10	0.96076	10.272513	4.062
11	0.92776	10.205070	6.414
12	0.89902	10.139892	8.898
13	0.89067	9.923238	13.482
14	0.87396	9.717968	17.518
15	0.95232	10.190652	6.664
16	0.90994	10.052209	10.480
17	0.90187	9.916616	12.876
18	0.93977	10.082540	8.074
19	0.94997	10.243785	5.519
20	0.92704	10.162231	8.789
	0.89980	10.086588	12.449
	0.88838	9.859798	17.039
	0.87743	9.630489	22.739
	0.94003	10.144875	7.212
	0.91516	10.000495	12.017
6	0.90851	9.841708	15.749
27	0.94432	10.033064	9.883

performance. The addition of criterion (2), the range error, ensures a reasonable spread of calibration data when compared to the standard error. The modification herein is that the denominator in equation (7.17) does not include a correction for the number of parameters estimated from the experimental data. This was done to facilitate direct comparison of the results obtained with OSCAA to those reported by Lyman(32) for the ASHSCAN system. (To account for coefficients the 10% figure in equations (7.15) and (7.16) should be reduced to approximately 9%: worst case or most coefficients.)

7.6 CALIBRATION STUDIES ON THE LABORATORY DATA

The calibration models entertained in these studies were as follows:

a) The four component model.

This model is described by equations (5.76) through (5.79).

b) The three component model.

This is the model which is the OSCAA analog to the ASHSCAN calibration model, where there is no attempt to correct for varying iron concentration. The calibration equations were a subset of those in (a), with the appropriate algebraic modifications.

c) The Kawatra formulation.

This was somewhat similar to the form stated by Kawatra and Dalton(36) where the % ash attribute is predicted

directly from the radiation measurements via an empirical model. In this case, however, the general Lucas Tooth model (eqn. (5.83)) was employed with a stepwise multiple linear regression program(72) for parameterization.

d) The combined formulation.

Earlier work by the author on a bench scale version of OSCAA had shown that linear expressions, of the form derived from fitting the general Lucas Tooth model, could be obtained for direct prediction of both the % solids and % ash <u>in the slurry.</u> These models can be combined to calculate the % ash in the solids.

For each model, the measures of performance defined in the previous section were computed and reported. Appendix 2 includes the source listing for the four component model calibration computer program and the output for the four laboratory runs.

While the performance criteria were calculated for the iron prediction in the four component model they were not considered to be relevant in evaluating the overall performance of OSCAA. The important process control variables are the % ash, and to a lesser extent, the % solids, and these were used in determining the system utility.

To minimize the amount of descriptive material presented for each of the four laboratory runs, only the four component model performance was illustrated in any

detail. This model was chosen over the other three because it compares favourably with them on a performance basis and because it contains a theoretical component, which makes it a more sound predictive tool. (It is also capable of predicting both of the attributes of interest.) It is worthy of note that, in the author's opinion, the results of the four component model could be improved to some extent if the fixed model parameters (section 7.3) were also treated as unknowns (cf. Lyman's approach). However, for the purposes of this work it was judged unnecessary, and, indeed, the goodness of the calibrations represent experimental support for the model.

The four laboratory tests, because of their independent nature, are discussed separately below.

7.6.1 Run 1 Results: Flotation Feed

For run 1, the data acquisition period was 10 minutes. This period was judged short enough to be acceptable for process control at McIntyre (see sub-section 3.1.3) and long enough to minimize statistical fluctuation in the radiation count data. The results of the calibration studies are summarized in Table 7.12. Figure 7.7 illustrates the predictive accuracy of the four component model for both the % solids and % ash attributes. (The ± 10% relative error envelope is included on the figure to demonstrate the degree of precision and distribution of residuals in the estimation.)

Table 7.12 Summary of Calibration Results for Laboratory Run

1

TEST: Flotation Feed (#1)

Semi-Empirical Models

MODEL	RELATIVE ERROR		RANGE ERROR	
	% Solids	% Ash	% Solids	% Ash
4 Component Model	5.64	5.72	4.88	6.61
3 Component Model	5.79	4.27	5.02	5.13

Empirical Models

MODEL	RELATIVE ERROR		RANGE ERROR	
	% Solids	% Ash	% Solids	% Ash
Kawatra [+] Formulation	N/A	6.5	N/A	7.0
Combined [++] Formulation	3.36	6.31	2.87	7.24

[+]Calibration equation contains 4 "independent" variables

[++]Calibration equations contain 3 "independent" variables
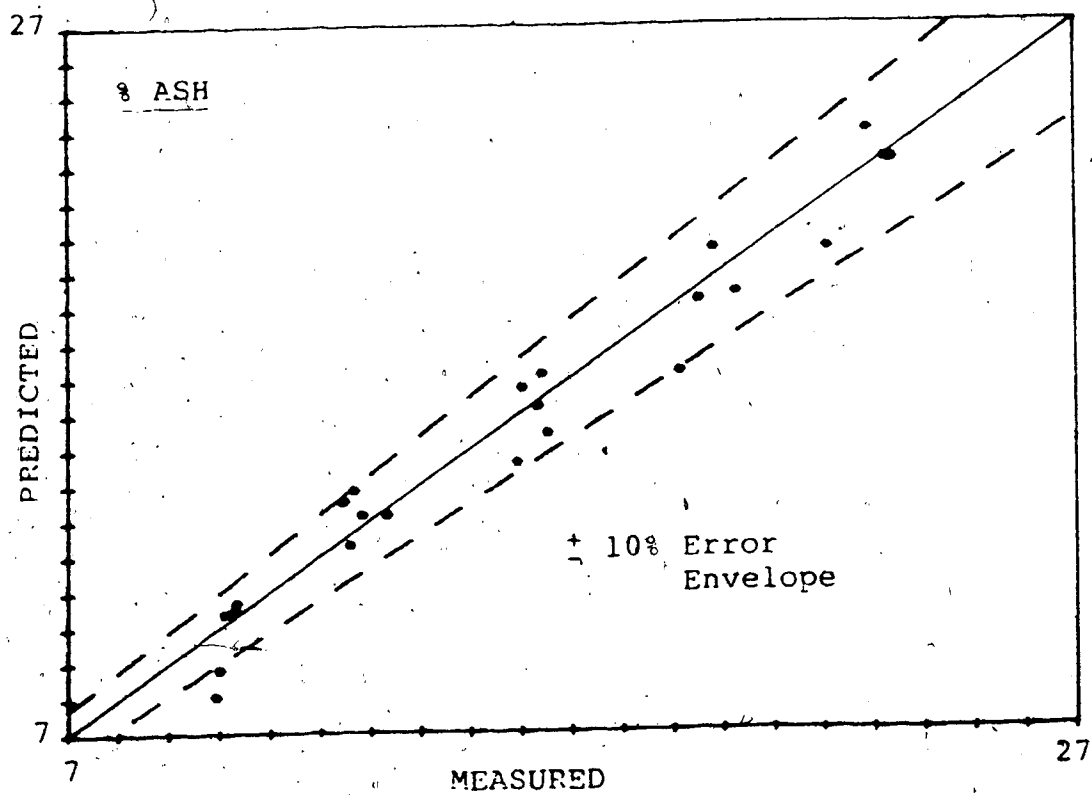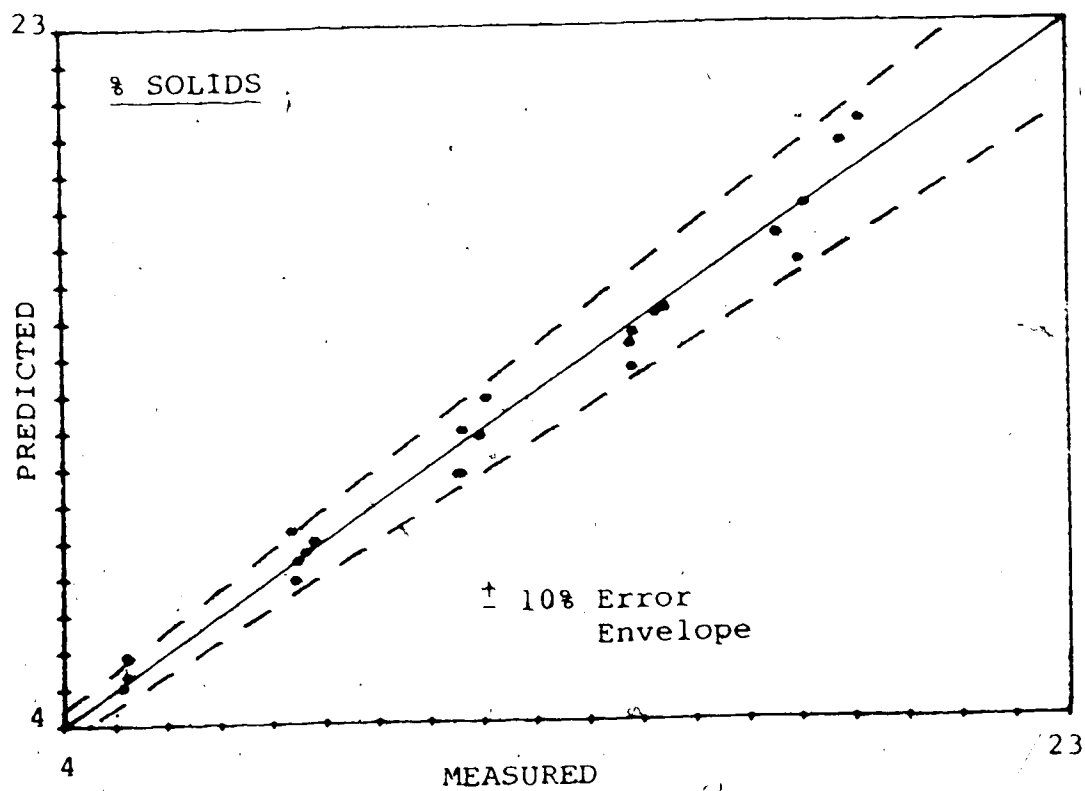
Figure 7.7 The Predictive Accuracy of the Four Component

A rather extensive residuals analysis was performed on the four component model for each calibration run. Since the findings were generally the same for all runs, the nature of the investigation will be summarized for run 1 only. As mentioned above, scatter plots similar to Figure 7.7 provide a graphical representation of this information.

It was mentioned in chapter 6 that size analyses were performed on the coal solids obtained from each experiment, where quantities permitted. Defining the mass fraction passing 0.5mm (35 mesh) as the reference size (reflecting coarse particle concentration), the residuals from the linear regression analysis on equations (5.74) and (5.75) were plotted against size. The range of the size variable was significant, i.e. 68% -0.5mm → 78% -0.5mm. The residuals versus size scatter plots were examined for trends but in both cases random behaviour was apparent. As a further check on the size dependency of the iron and backscatter systems, the residuals associated with the measured and predicted attribute values were plotted against size. Again, random behaviour was apparent. It was concluded from this and comparable studies for the other runs that the error introduced in calibration as a result of changing particle size distribution was insignificant.

The errors quoted in Table 7.12 represent an overall picture of prototype precision. It is important that these values be homogeneous or at least within the acceptable limits over the range of the calibration if the device is to

be of any practical utility. To study the homogeneity the relative errors of prediction for a particular nominal solids concentration or a particular nominal ash quality were computed. The results are presented in Table 7.13. It is evident from this table that, with the exception of the first entries (low attribute value), the errors are approximately homogeneous. The apparent problem in the case of the low % solids value relates to the performance of the density gauge at these levels and will be discussed more fully in section 7.6.3. In the case of the low % ash computation the magnitude of the relative error is due primarily to one very poor predicted ash value in this set. It was concluded from this work that the relative error in prediction is approximately homogeneous, or at least within the acceptable limits, over the range of the attributes studied.

From Table 7.12 it is clear that all of the models meet the performance criteria. With respect to the prediction of the ash attribute, the semi-empirical models are observed to be slightly more precise. Moreover, the three component model exhibits slightly better precision than does the four component model. The latter is thought to arise as a result of the inclusion of the iron count data in the four component model. Since the iron content in the ash is relatively stable, this source of information contains more noise than it does statistically valid information. Nevertheless, the four component model is quite suitable for

Table 7.13 Homogeneity of Relative Error over the Attribute

Range for Run 1

% SOLIDS		% ASH	
MEAN SOLIDS CONTENT	RELATIVE ERROR	MEAN ASH CONTENT	RELATIVE ERROR
5.2%	9.12%	10.1%	9.97%
8.51%	6.63%	12.8%	5.08%
11.73%	5.35%	16.3%	5.42%
15.0%	3.88%	19.7%	5.06%
18.26%	5.38%	23.0%	3.53%

calibration purposes.

By comparison with Table 7.12, the relative errors on % solids and % ash for the ASHSCAN system in similar service were 5% and 11% respectively. While these values were determined on a plant test scale, the ranges of the two variables were about the same. Moreover, since Lyman could not employ a unique, experiment orthogonal design approach under these conditions, there exists the possibilty of multicolinearity[19] and/or repeat experiments in his data. These would be expected to enhance the performance measures to some degree. Finally, Lyman utilizes best fit techniques to calculate all of the parameters in his calibration model which is also expected to enhance precision. In summary, OSCAA compares favourably with ASHSCAN in monitoring a flotation feed stream and provides the potential for adjusting to changes in ash mineralogy (specifically iron concentration) without recalibration.

7.6.2 Run 2 Results: Flotation Concentrate.

For run 2 the data acquistion period was also 10 minutes for the reasons given above. Unfortunately, in the preparation of the solids samples for the experiments two **different** clean coal bulk samples had to be used. While this did not substantially alter the orthogonality of the experimental design with respect to the principal

---

[19]Multicolinearity describes the situation where there is a high degree of correlation between two or more of the independent variables used in designing an experiment or in the construction of a linear model.

attributes, it did produce a change in the iron
concentration of the mineral matter. (See Table 7.5
experiments 1-16 and 17-25.) The net effect was the
introduction of iron as a pseudo-factor in a non-orthogonal
manner. For this reason, the nuclear coefficients used in
the semi-empirical models were taken as the arithmetic
average of those calculated for the two clean·coal samples.
The results of the calibration studies are summarized in
Table 7.14. Figure 7.8 illustrates the predictive accuracy
of the four component model for both the % solids and % ash
attributes. From Table 7.14 it is clear that, with the
exception of the three component model, all other
calibration models meet the performance criteria. However,
in this case the empirical models exhibit slightly better
precision with the combined formulation yielding excellent
results. The failure of the three component model arises
directly as a result of the changing iron concentration in
the mineral matter. This illustrates the necessity of
including iron in the calibration model to preclude frequent
recalibration work. The comparatively poorer performance of
the four component model relative to the empirical models is
thought to be predominantly the result of the compromise in
calculating the nuclear coefficients. However, the results
are still quite good when compared to the performance
criteria and, more importantly, the variation in the
pseudo-factor was reasonably accommodated.

Table 7.14 Results of Calibration Studies for Laboratory Run 2

TEST: Flotation Concentrate (#2)

Semi-Empirical Models

MODEL	RELATIVE ERROR		RANGE ERROR	
	% Solids	% Ash	% Solids	% Ash
4 Component Model	2.72	3.65	6.1	6.7
3 Component Model	3.3	9.44	7.37	17.13

Empirical Models

MODEL	RELATIVE ERROR		RANGE ERROR	
	% Solids	% Ash	% Solids	% Ash
Kawatra [+] Formulation	N/A	3.08	N/A	5.62
Combined [++] Formulation	2.00	2.08	4.49	3.72

[+]Calibration equation contains 2 "independent" variables

[++]Calibration equations contain 5 "independent" variables
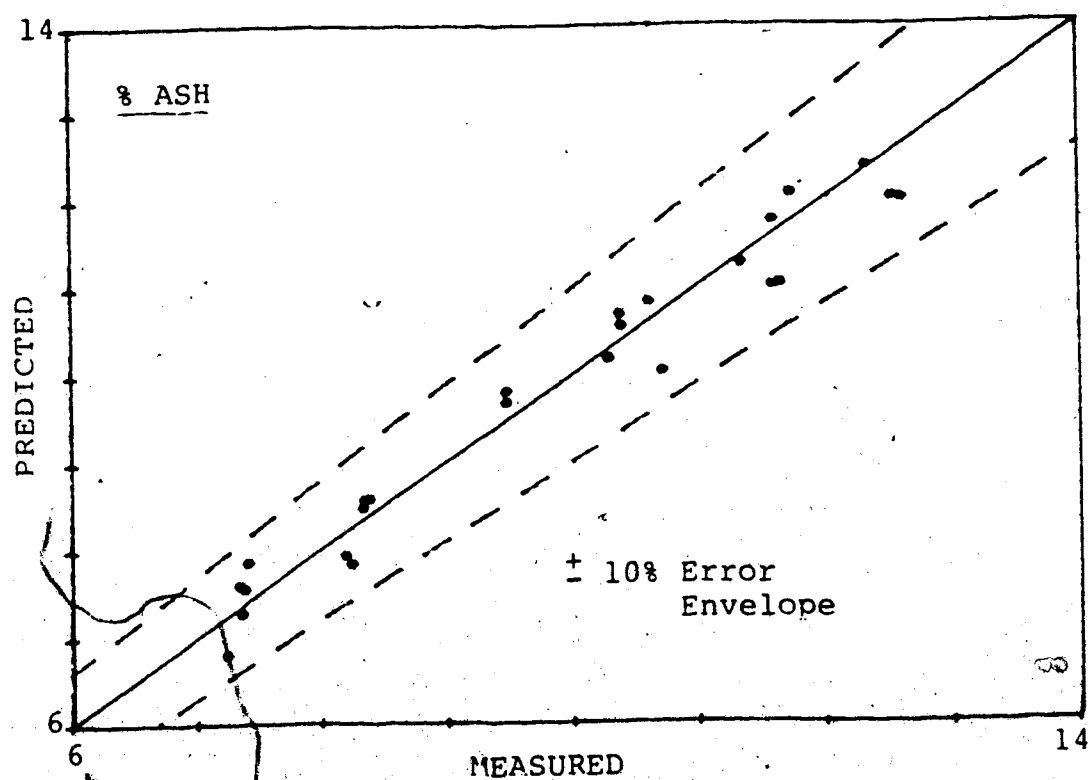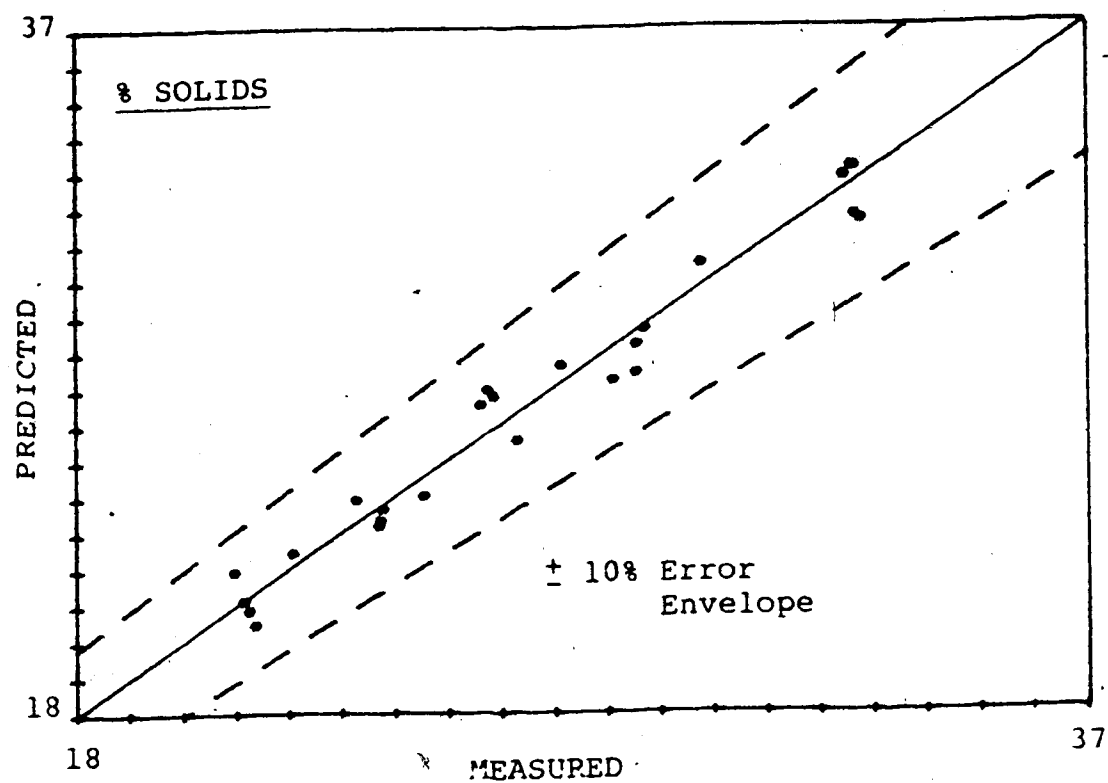
Figure 7.8 The Predictive Accuracy of the Four Component
Model for Laboratory Run 2.

Again, by comparison, the relative errors on % solids

and % ash for the ASHSCAN device in similar service were 3%

and 3.8% respectively, although the ranges were slightly

larger than those in run 2. The same comments on

experimental integrity hold. In summary, OSCAA compares

favourably to ASHSCAN in monitoring a flotation concentrate

stream and has demonstrated its ability to account for

changes in ash mineralogy, something of which ASHSCAN is

incapable.

7.6.3 Run 3 Results: Flotation Tailing

A considerable amount of time (≈ 7 months) elapsed

between the completion of run 2 and the commencement of run

3. As a result of the relatively short half life of the

Gd-153 radioisotope (242 days) the data acquisition period

was doubled to 20 minutes. This provided for approximately

the same number of counts in the pulp density sub-system as

for similar conditions in run 2, but had the effect of

improving the statistical accuracy of the backscatter/iron

count data because of the longer half life of the Cd-109

radioisotope. The results of the calibration studies are

presented in Table 7.15. Figure 7.9 illustrates the

predictive accuracy of the four component model for both the

% solids and % ash attributes.

From Table 7.15 it is clear that none of the

calibration models meet the performance criteria. This was

not totally unexpected since this run included very low

Table 7.15 Results of the Calibration Studies for Laboratory.

Ru

T   tation Tailing (#3): All Data

Se   rical Models

MO L	RELATIVE ERROR		RANGE ERROR	
	% Solids	% Ash	% Solids	% Ash
omponent odel	16.44	40.53	. 11.59	127.7
Component odel	17.27	46.87	12.23	147.7

Emp ical Models

MODEL	RELATIVE ERROR		RANGE ERROR	
	% Solids	% Ash	% Solids	% Ash
Kawatra [+] Formulation	N/A	8.0	N/A	25.21
Combined [++] Formulation	15.53	10.70	10.88	33.75

[+]Calibration equation contains 2 "independent" variables

[++]Calibration equations contain 3 "independent" variables
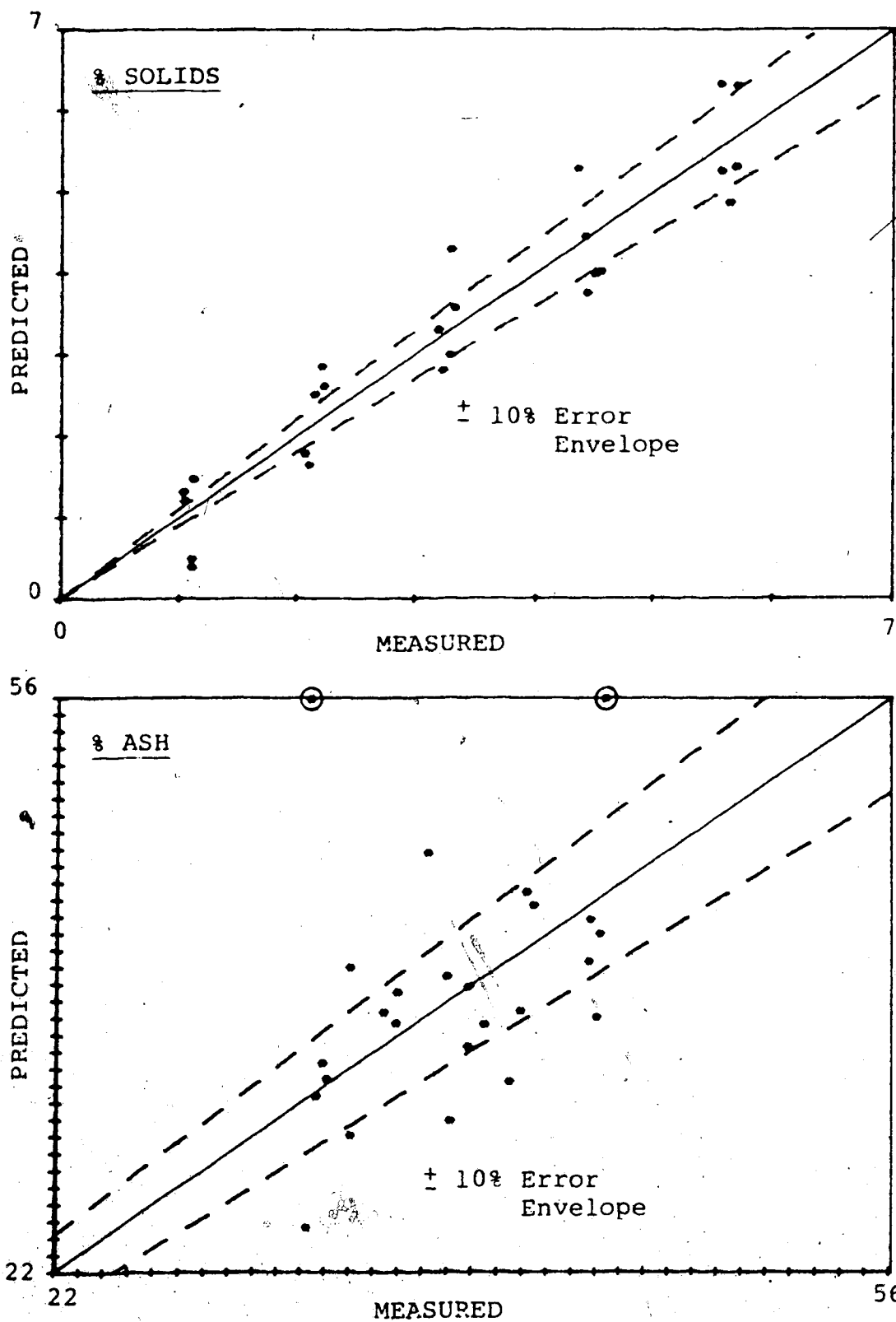
Figure 7.9 The Predictive Accuracy of the Four Component
Model for Laboratory Run 3.

solids concentrations and would thus be prone to large errors in prediction based on radiation statistics alone. This was demonstrated using the theoretical three component model. Equation (5.1) characterizes the pulp density sub-system and equation (5.58) characterizes the ash analysis sub-system. Using the theory and assuming a typical flotation feed pulp composition to estimate the other unknowns in the equations, I_0 and N_0 were calculated to provide total detected counts (excluding background) comparable to those measured in run 1; i.e. $\approx 400,000$ and $\approx 6,000,000$ respectively. Using Monte Carlo techniques a set of simulations were performed at different levels of % solids and % ash, and for each the relative error of prediction for each attribute was calculated. The results of the simulations are summarized in graphical form in Figures 7.10 and 7.11. From the plots it is apparent that as % solids decreases the relative errors increase, this being particularly evident at low levels of the former. Moreover, while the relative error on % solids is effectively independent of the ash content, the relative error on % ash does exhibit a slight dependence on the attribute value. Calculations at very low solids concentrations, $\approx 1\%$, were unstable as expected, however, the relative errors appeared to be in excess of 70% in all cases. This is consistent with the trend of both relative error curves at low solids concentrations. In this light, the values of the performance criteria reported in Table 7.15 seemed quite reasonable.
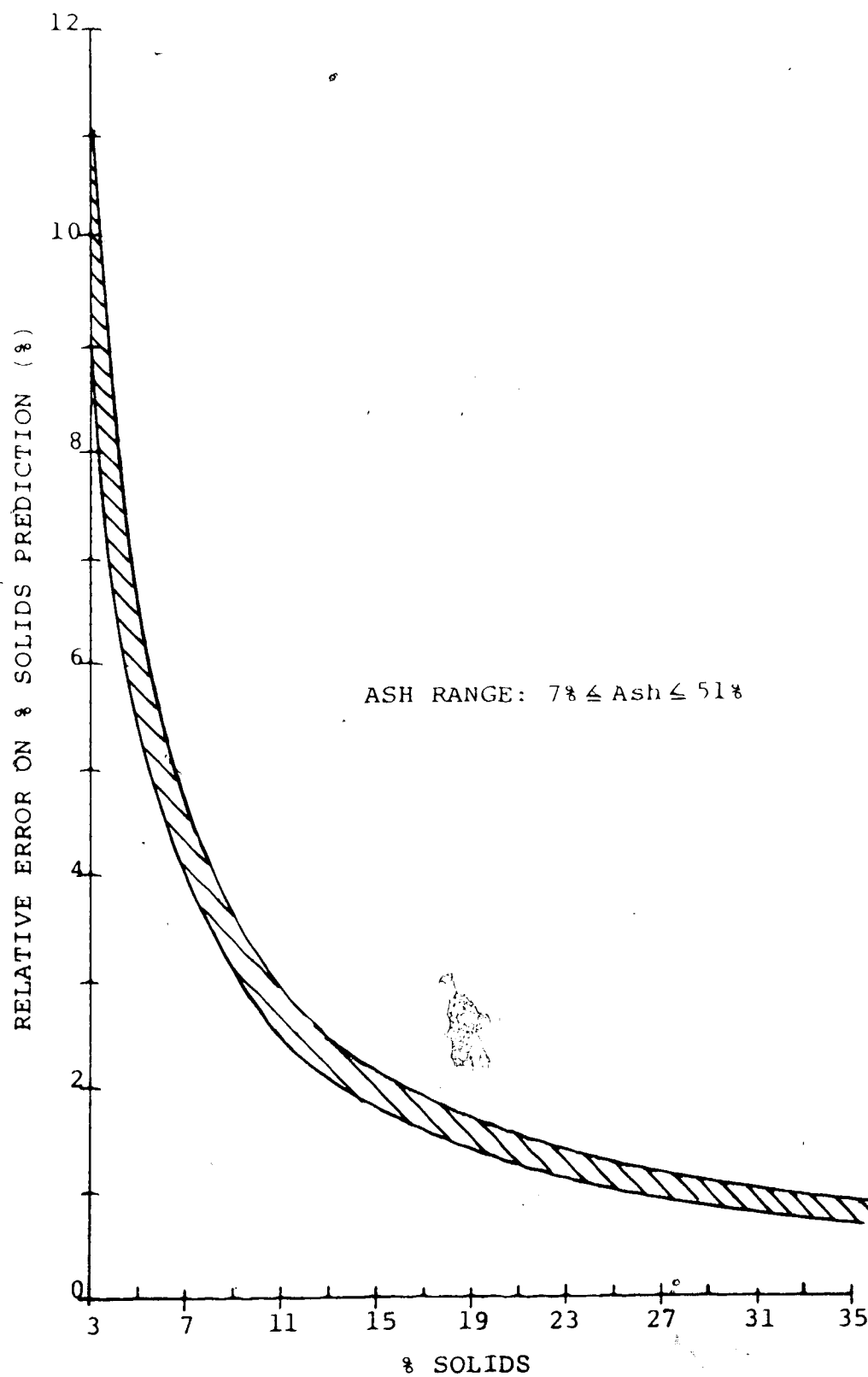
Figure 7.10 Relative Error on % Solids Prediction as a Function of the Attribute Levels.
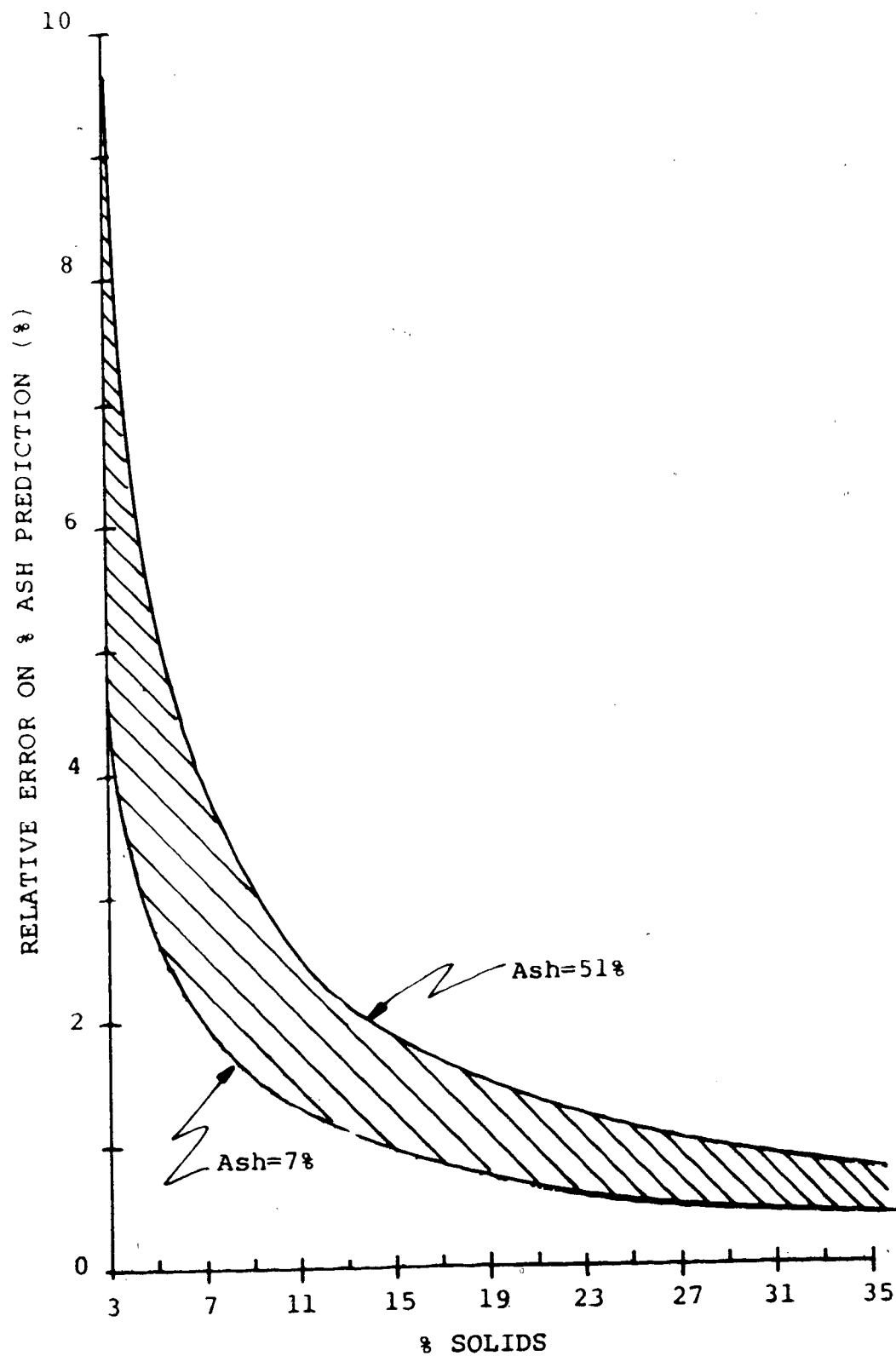
Figure 7.11 Relative Error on % Ash Prediction as a Function of the Attribute Levels.

To partially remove this statistical effect in calibration the data set was modified by excluding all design points at 1% and 2% solids. The modified data set was then re-analysed and the results are summarized in Table 7.16 and Figure 7.12. From Table 7.16 it is apparent that, with the exception of the three component model, the relative error for % ash is met in all cases but the range error is unacceptable. The latter is thought to be the combined effect of statistical fluctuation coupled with sampling and analysis errors. The % solids predictions fail both performance criteria due to statistical fluctuations together with the low mean value of the attribute and the narrow range of study. In examining the results for the three component model it seems evident that, in this case, the iron count information is necessary to stabilize the results.

Considering these results it is recommended that for monitoring a flotation tailings stream of low solids concentration, either extended count times would be required, or preferably, a stronger source be employed to improve upon the statistics. Monte Carlo techniques could be used to obtain a first approximation on source strength using the method described above.

For the sake of completeness, the relative error on the % solids and % ash for the ASHSCAN system in similar service were 9% and 7% respectively. While the comments on experimental integrity are valid here as well, an important

Table 7.16 Results of Calibration Studies for the Modified Data Set in Laboratory Run 3

TEST: Flotation Tailing (#3): Reduced Data Set

Semi-Empirical Models

MODEL	RELATIVE ERROR		RANGE ERROR	
	% Solids	% Ash	% Solids	% Ash
4 Component Model	13.59	8.19	24	27.34
3 Component Model	163.1	76.15	289.6	254.3

Empirical Models

MODEL	RELATIVE ERROR		RANGE ERROR	
	% Solids	% Ash	% Solids	% Ash
Kawatra [+] Formulation	N/A	7.68	N/A	25.69
Combined [++] Formulation	12.54	8.74	22.4	29.17

[+] Calibration equation contains 1 "independent" variables

[++] Calibration equations contain 3 "independent" variables
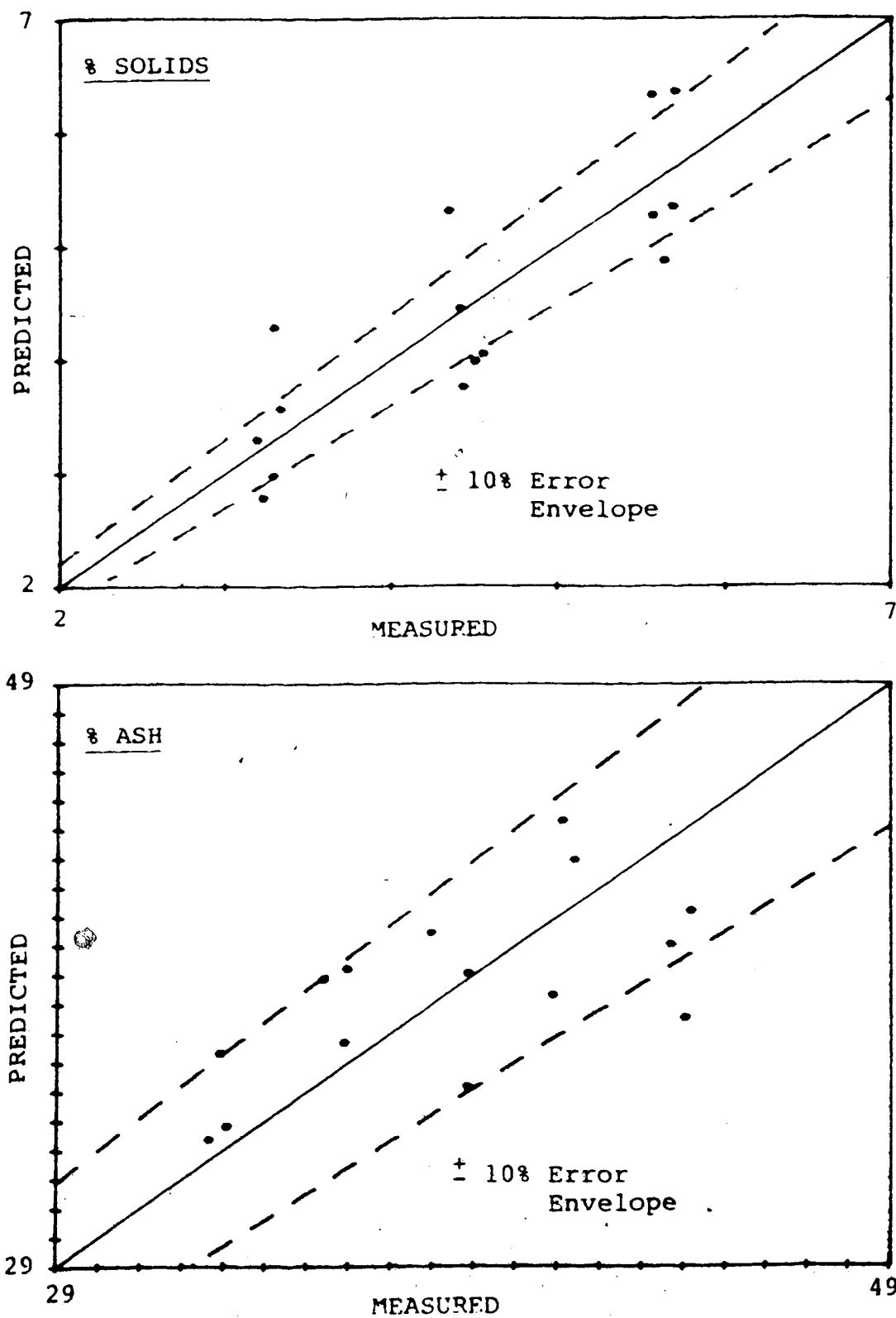
Figure 7.12 The Predictive Accuracy of the Four Component
Model for Laboratory Run 3:Modified Data.

difference was the range of study. The range of solids concentration for ASHSCAN more closely resembled that of the flotation feed stream in run 1. This would be expected to stabilize density gauge performance and hence the overall performance of the OSCAA system. In summary, OSCAA, in its present form, is not well suited to monitoring flotation tailings streams at low solids concentrations. However, increasing the statistical accuracy of the pulp density sub-system together with the minimum value for the solids concentration would be expected to produce results comparable to those reported for ASHSCAN.

7.6.4 Run 4 Results: Flotation Feed with Varying Iron Concentration

The data acquisition period for this run was 20 minutes for the reasons given above. The material used to control the iron content of the ash was fine magnetite, not hematite as assumed in the four component model. This was done to reflect contamination by tramp heavy medium which can occur in those plants which employ heavy medium washing circuits. The results of the calibration studies are summarized in Table 7.17. Figure 7.13 illustrates the predictive accuracy of the four component model for both the % solids and % ash attributes.

From Table 7.17 it is apparent that, with the exception of the three component model, as expected, the other calibration models met or were very close to the performance

Table 7.17 Results of Calibration Studies for Laboratory Run 4

TEST: Flotation Feed with Varying Iron (#4)

Semi-Empirical Models

MODEL	RELATIVE ERROR		RANGE ERROR	
	% Solids	% Ash	% Solids	% Ash
4 Component Model	8.68	5.28	10.6	9.34
3 Component Model	8.51	11.00	10.40	19.52

Empirical Models

MODEL	RELATIVE ERROR		RANGE ERROR	
	% Solids	% Ash	% Solids	% Ash
Kawatra[+] Formulation	N/A	6.16	N/A	10.9
Combined[++] Formulation	6.24	5.35	7.64	9.44

[+]Calibration equation contains 4 "independent" variables

[++]Calibration equations contain 6 "independent" variables
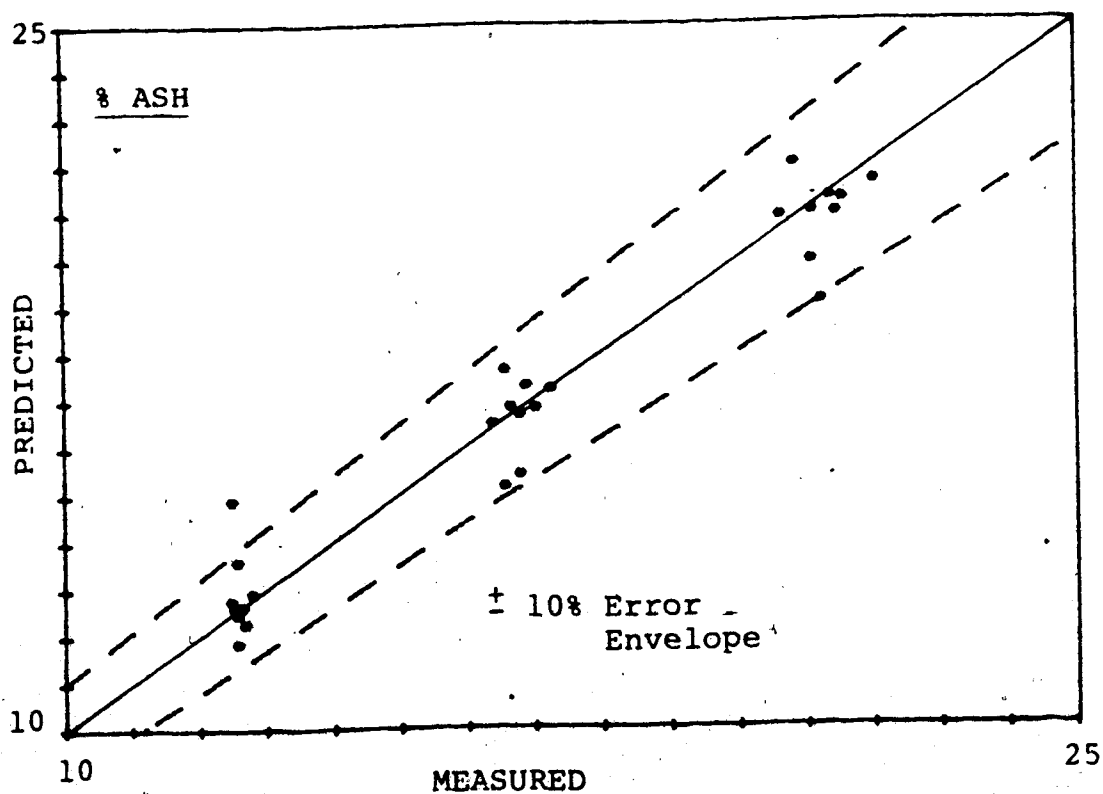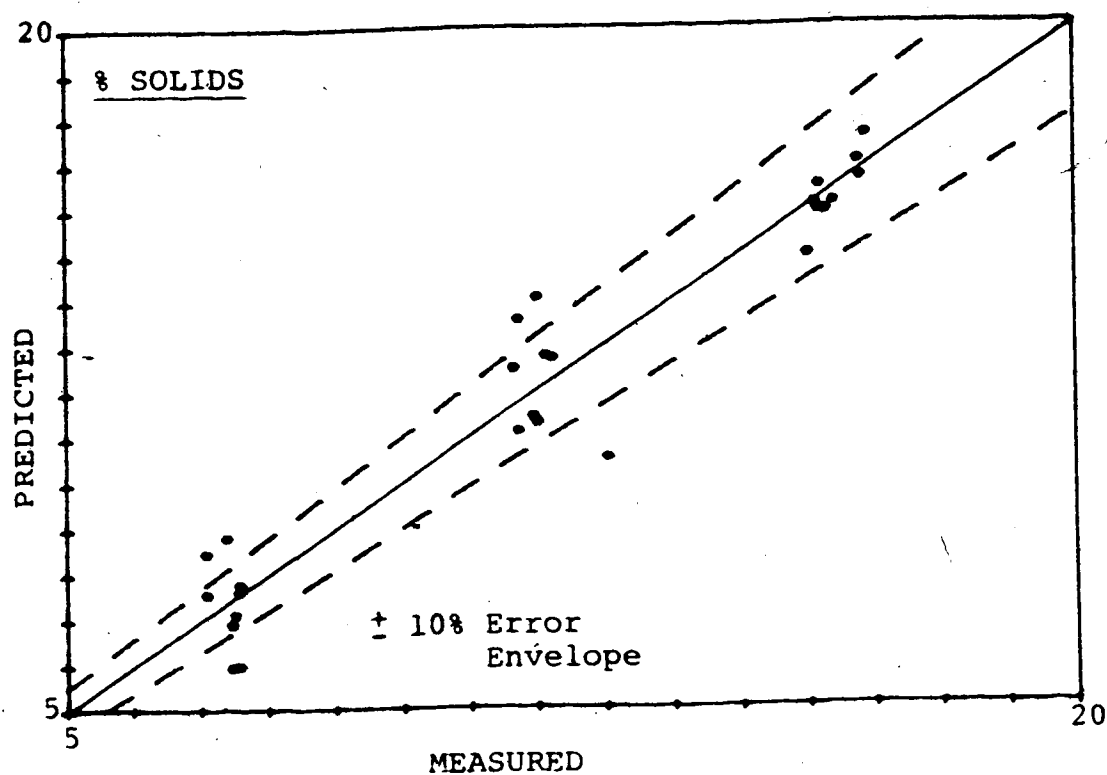
Figure 7.13 The Predictive Accuracy of the Four Component Model for Laboratory Run 4.

criteria. The comparatively poorer performance in % solids prediction for this run when compared to run 1 is due, in large part, to the unexplainable difference in pulp density sub-system performance (see density gauge calibration statistics in appendix 2). Never-the-less, the results for the four component model make it an acceptable predictive tool.

There was no similar test for the ASHSCAN system.

7.7 SUMMARY OF LABORATORY INVESTIGATIONS

From the discussion above it is evident that an OSCAA type system would be feasible for process control purposes in the fine coal circuit at McIntyre Mines Ltd. The tailings stream would have to be excluded from the analysis based on current prototype design. Rather simple design changes would be expected to correct this problem and allow all three process streams to be monitored. Furthermore, it is expected that with improvements in design (specifically more counts in a shorter time), the data acquisition period could be reduced to 5 minutes, which is more in line with the process response time.

It is apparent from run 2 and run 4 where the iron concentration of the mineral matter was a factor that a three component slurry model was not satisfactory for attribute prediction. This is important as evidenced in this project where two clean coals from the same deposit provided significantly different iron values, and in Lyman's work

where he observed that the coal could have an iron concentration in the ash in the range of; $5\% \leq [Fe] \leq 15\%$. This would require frequent instrument recalibration or at the very least frequent updating of the calibration model parameters. This kind of system requirememt is incompatible with the those of the industry.

8. THE OSCAA SYSTEM PLANT CALIBRATION RESULTS

8.1 INTRODUCTION

Upon completion of the laboratory calibration runs it was decided to proceed with a plant trial of the OSCAA prototype device. McIntyre Mines Ltd. personnel agreed in principle to cooperate, pending the finalization of the experimental plan.

Based on the laboratory results and the difficulties attendant to flow stream sampling and multiplexing, a single flow stream was chosen for monitoring, the flotation concentrate. For practical reasons it was necessary to choose the concentrate stream from the number four flotation cell bank. With this general objective in mind a reconnaissance trip was made to the minesite for preliminary design purposes. Subsequently, an experimental plan was developed and the responsibilities of the operating personnel clearly defined. McIntyre agreed to the proposal and installed the necessary piping and valves required for primary sampling. In concert with this work the balance of the materials and equipment were prepared in the University laboratories. One of the paramount concerns was to provide adequate housing for the instrumentation since no facility was available on-site. Toward this end a small trailer was rented, and the required modifications performed including the installation of an air conditioning unit. Provision of the latter is standard practice for industrial on-stream

analytical instrumentation to control airborne dust and the ambient temperature. On June 8, 1981 the OSCAA prototype was transported to the minesite.

8.2 EXPERIMENTAL PROCEDURE

The experimental procedure may be divided into three parts, equipment set-up, data acquisition and sampling and analysis. These are discussed below.

8.2.1 Equipment Set-Up

For a period of 5 days after arrival on the minesite the OSCAA prototype was prepared for the plant calibration work. This included trailer location, installation of the electronic equipment in the trailer, plumbing the sampling system, installing the power lines and situating the analytical facilities.

Plates 8.1 and 8.2 illustrate the installation. The primary sample was obtained from the number four flotation cell bank concentrate collection box and flowed by gravity to the primary sample pump[2]. The sample was then pumped to the secondary sampler where a representative sub-sample was cut for analysis by the OSCAA unit. The reject sample from the secondary sampler and the discharge from the OSCAA sample line were combined in the collection launder. This launder was designed such that either open or closed circuit

---

[2] Pipeline sizing for the primary sample, which would ensure ___ent flow while minimizing the need for valve ___ion was done by solving the appropriate macroscopic ___al energy balance.

OSCAA Sample
Line

Secondary
Sampler

Primary
Sample Input
Line From
#4 Flotation
Cell Bank

Instrumentation
Housing

OSCAA Sample
Return Line

Primary Sample Pump
and Collection
Launder
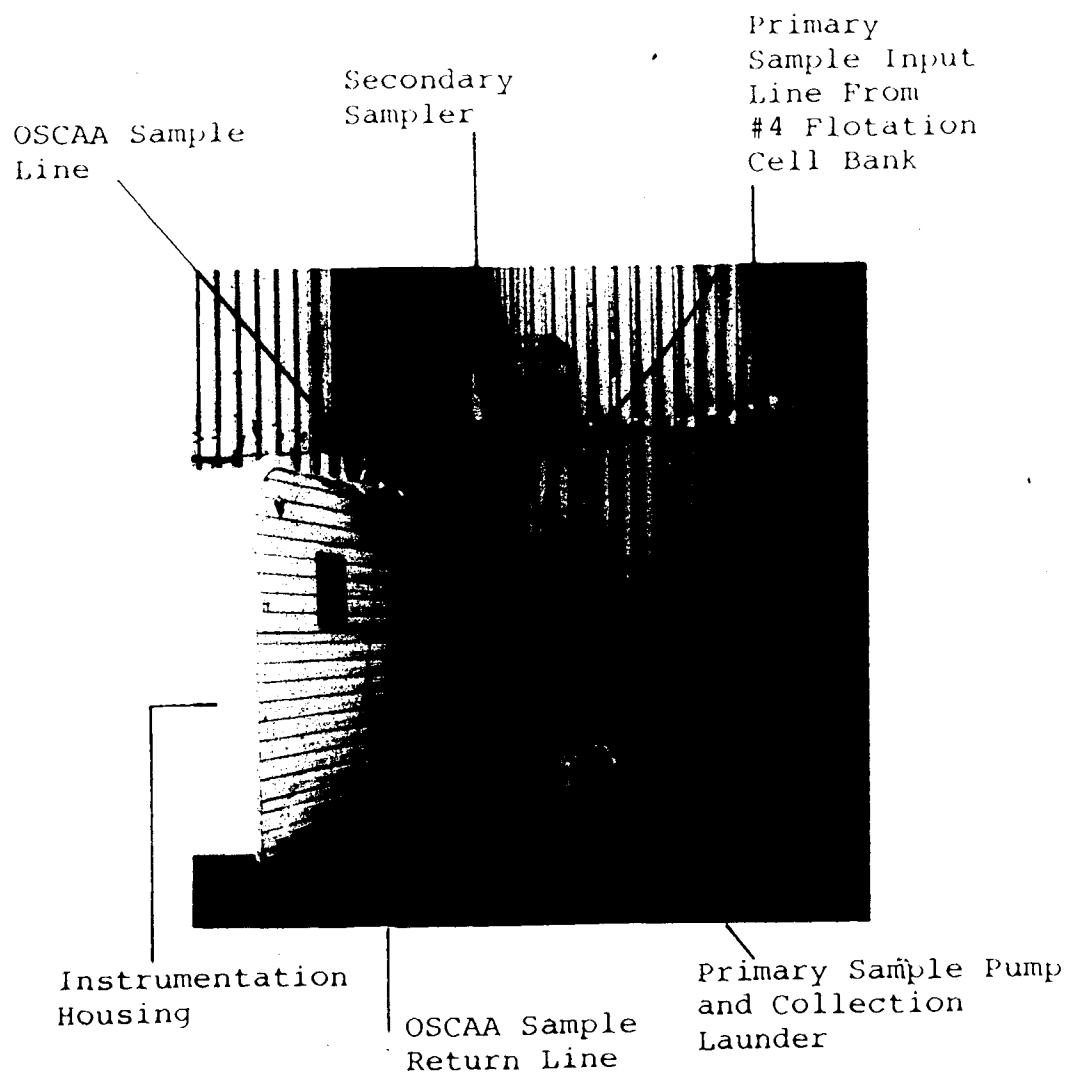
Plate 8.1 An Illustration of the On-Site OSCAA Equipment

Layout

The ash analysis and pulp
density measurement sub-
systems of the OSCAA proto-
type, as installed for the
plant trial.

Plate 8.2 The OSCAA Measurement Sub-Systems for the Plant

Trial

sample flow was possible. In the open circuit mode the launder discharged to the primary sample return line which flowed by gravity to the main sump in the preparation plant basement. Ultimately the primary sample was recirculated to the preparation plant feed. This recirculating load was negligible.

Once the flow loop had been fabricated and tested with water, a batch calibration was attempted using solid samples prepared in the University laboratories. A two factor (% ash, % solids) three level orthogonal design was used which was intended to provide estimates of the calibration equation parameters. It was hoped that by using these estimates it would be possible to provide the operators with on-stream analyses of the concentrate at a relatively high frequency. This would demonstrate the utility of such a device in daily operation. The resultant count data was consistent with previous laboratory findings, however, the samples which were required for attribute analysis were accidentally discarded by a member of the McIntyre quality control laboratory staff. As a result, it was impossible to proceed with the demonstration which had been planned. Notwithstanding this unfortunate circumstance, the equipment appeared to have operated satisfactorily although the ambient conditions at the time of this calibration work were wet and cold, thereby minimizing dust and temperature problems.

One point which is worthy of note here is that it was impossible to obtain a process water standard for data reduction purposes. The only water supply available was the fresh water make-up which is pumped to the plant from the nearby Smoky river. This water was very highly aerated and silty. In practice this source contributes only a small portion to the process water requirements, the bulk consisting of water recirculated from the closed plant dewatering circuit.

8.2.2 Data Acquistion

The data acquisition period was defined to be twenty minutes which was consistent with laboratory calibration runs 3 and 4. The computer programs controlling data acquisition and data processing had to be modified to operate on a continuous basis. Because of the limited fast access memory of the computer an extensive amount of tape transfer was involved to allow the two programs to work in sequence. Output from the programs included the time of day, gross density counts and the corrected backscatter and iron fluorescent radiation counts.

The objective of the plant trial was to run as long as was possible subject to two constraints, namely;

a) the maximum number of samples to be processed should be on the order of 200, and,

b) rental equipment was to be returned by the end of June. Since the operation of the equipment was the responsibility

of the author, daily shift maximum operating periods of from 8 to 12 hours were defined. Moreover, since the biggest changes in attribute values were expected to occur during day shift, experimental work was to take place in the interval of 8:00 am to 8:00 pm. Operating under these constraints together with scheduled and unscheduled plant operating interruptions, calibration work was only possible on five operating days.

8.2.3 Sampling and Analysis

To allow one man to adequately monitor the OSCAA system, obtain the samples and perform the first steps in their analysis, it was necessary to resort to grab sampling over the more accurate composite sampling. On the basis of the fluctuations in the concentrate stream attributes observed in Figures 3.4 and 3.6 this was deemed an acceptable sampling methodology. Furthermore, since the flow stream is relatively high in slurry solids content, only 1 litre of sample was taken from the OSCAA sample line. (While the method was thought to be acceptable it should be noted that the representativity of such a sample is, on the average, about 1 part in 2650, cut at one instant in time. It will be shown later that this method appeared to have contributed significantly to the poor measured performance of the pulp density gauge.)

Samples were cut at approximately the midpoint of the corresponding data acquisition period. In some cases,

sampling was done at both the midpoint and at the end of this interval as a check on the assumptions in the sampling methodology. Duplicate samples were also cut to provide estimates of sampling and analysis error.

Immediately after a sample was cut its wet weight was recorded and the slurry filtered using a portable, vacuum pump driven, Buchner apparatus. The moist filter cakes were bagged, labelled and packaged for shipment to the University laboratories. where they were subsequently dried and weighed. Size analyses were not performed on these samples. A representative 50 g sub-sample was pulverized to -0.15 mm (100 mesh) and duplicate 3 g samples extracted for ash analysis. On the basis of cost and the fact that the iron content of the ash appeared to vary negligibly over the calibration trial, iron analyses were excluded. The latter meant that the four component semi-empirical calibration equation including the iron correction could not be tested on the plant data.

8.3 PROBLEMS ENCOUNTERED IN THE PLANT TRIAL

On the first day of the full calibration testwork the weather was sunny and warm and it quickly became apparent that the air conditioning unit was faulty, although it had successfully completed trial runs at the University. The electrical demand of the air conditioner on start-up was determined to be 35 amps, which, because all instrumentation was on a common circuit, caused some of the nucleonic

instruments to fail. After consultation with the plant electrical department and reference to the appropriate operating manuals it was decided to continue the work without providing air conditioning. It was arranged to record the temperature inside the trailer and make periodic background measurements with the pulp density sub-system (closed shutter). This data would be used in case some instrumentation correction was required although it was not expected.

Another problem which arose was the result of poor communications between plant personnel. The author was to be notified in advance of any scheduled plant shutdowns to facilitate calibration work re-scheduling. Unfortunately, on two occasions, this information was not relayed and, as a result, considerable time was wasted. It should also be noted that at the time of the plant trial, McIntyre was somewhat behind on production commitments and the preparation plant had been running with minimal planned preventive maintenance. This resulted in the plant being in a sub-normal state of repair and frequent short (≈ 1 h) emergency stoppages were experienced.

The calibration work was prematurely halted when it was observed that the density counts obtained on recirculating water were virtually the same as those recorded for the concentrate slurry. This suggested that there was a serious problem in the pulp density measurement (e.g. air entrainment) and effort was then taken to study this. The

net result was that good[¹⁷] data was obtained for only **three** operating days.

8.4 DATA PREPARATION

The data preparation was divided into attribute analyses and radiation count handling, similar to the laboratory calibration runs.

8.4.1 Preparation of the Slurry Attribute Data

While attribute analyses were done for all of the samples taken during the plant trial, only those corresponding to the calibration period are presented. In an effort to obtain better estimates of the> attribute value over the 20 minute period than the point estimate provided by the grab sample, a form of data smoothing was employed. The method was to fit a quadratic to the sample point under consideration and its two nearest neighbours, in time, on either side. From the quadratic, using analytical integration, a mean attribute value was calculated. The procedure is illustrated in Figure 8.1. In cases where one of the neighbours was sufficiently distant (>0.5 h) so as to be potentially unrelated, it was replaced with a dummy point having the same value as the centre point and 0.5 h removed from it. The results of the attribute analyses and the smoothed data are presented in Tables 8.1, 8.2 and 8.3 and

----

[¹⁷]In this context "good" implies complete in the sense that temperature, density background counts and resonable operating times were obtained.

$$(t_b=7.5,7.16)$$

$$a(t) = b_1 + b_2t + b_3t^2$$

$$(7.83,7.04)$$

$$\bar{a} = \dfrac{\displaystyle\int_{t_b}^{t_e} a(t)\ dt}{t_e - t_b} = 6.98$$

$$(t_e=8.25,6.64)$$

MEASURED ASH VALUE (%)

TIME IN HOURS
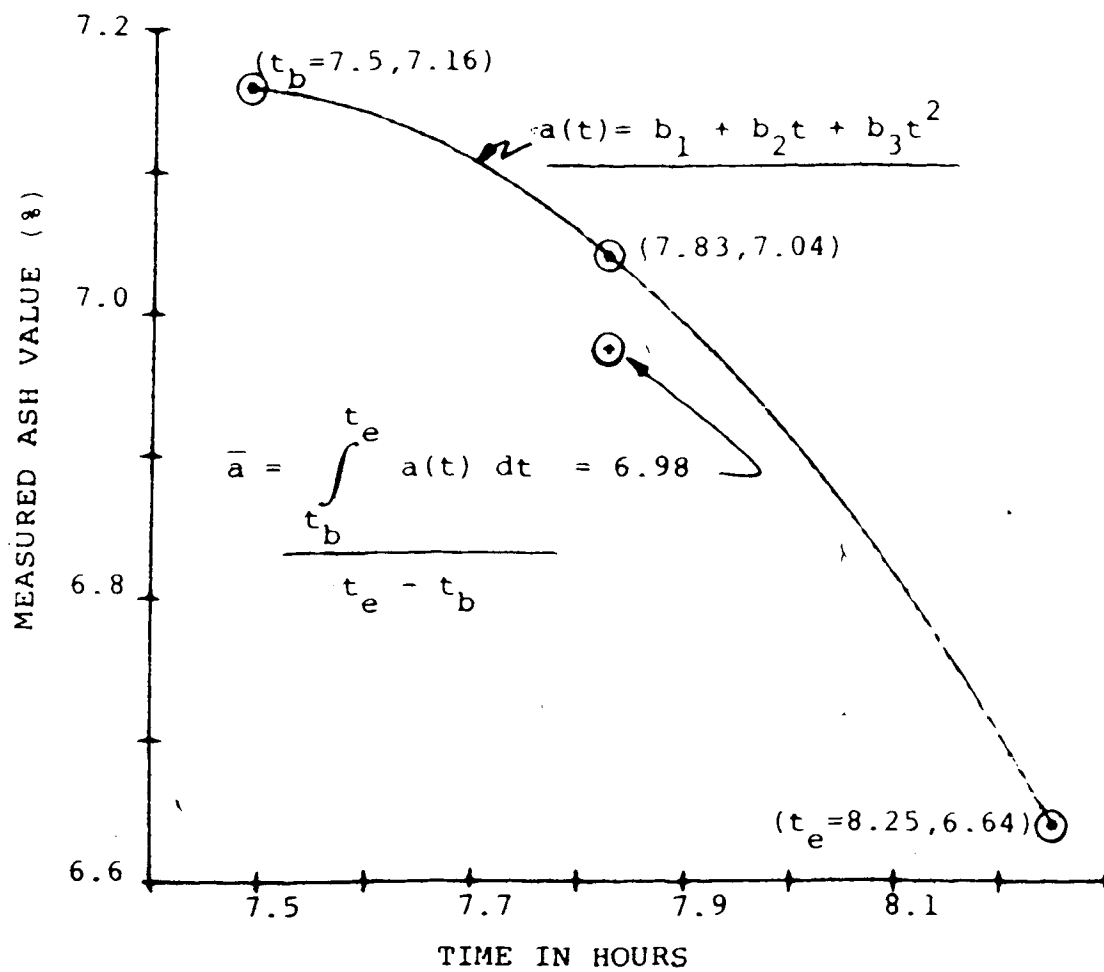
Figure 8.1 An Illustration of the Mechanics of Attribute Smoothing.

the corresponding figures 8.2, 8.3 and 8.4. The effect of the smoothing algorithm is clearly illustrated in the figures where the smoothed data are connected by a solid line. These figures were included to provide further evidence that the trends in Figures 3.4 and 3.6 were typical of process behaviour (i.e. process fluctuations appear amenable to process control).

Not all of the data presented in the tables were used in the calibration equation parameterization exercise. The reasons for this are given in the next section.

8.4.2 Preparation of the Radiation Count Data

Since a process water standard was not available it was impossible to reduce the pulp density counts and correct the iron fluorescence counts in the manner described in the previous chapter[1]. Thus, the data is presented in the form where only background corrections have been made. Furthermore, data which was clearly abnormal was excluded from the calibration data set. Abnormal data was identified by unusually high pulp density counts and correspondingly low backscatter counts. This was the result of a temporary interruption in the primary sample flow generally attributable to an emergency plant stoppage. The calibration data set is presented in Table 8.4. The temperature data included in this table were generated from point estimates

----

[1]Since the thin mylar windows were replaced each day, as a precautionary measure, the absence of standardization would be expected to allow the effect of bias due to window positioning to enter the calibration data.

Table 8.1 Attribute Analyses for June 19, 1981

Time	% Solids Observed	% Solids Estimated	% Ash Observed	% Ash Estimated
8.52	30.30	31.15	7.39	7.24
8.85	32.20	32.23	6.31	6.31
9.29	33.20	32.57	6.11	6.56
9.58	29.70	31.50	7.53	7.03
10.05	35.50	34.17	6.55	6.37
10.49	31.10	32.25	8.23	7.58
10.82	33.50	32.40	7.10	7.42
11.15	32.50	31.33	7.83	6.16
11.58	23.50	24.03	11.13	10.77
11.92	26.60	26.30	11.60	11.63
12.34	26.70	26.21	11.50	11.55
12.50	23.70	23.90	11.43	11.31
12.58	23.20	23.26	11.71	11.73
12.34	23.00	23.32	11.31	11.17
13.10	25.50	25.54	10.53	10.71
13.25	25.70	25.50	10.59	10.54
13.44	24.00	24.71	10.55	10.53
13.55	25.70	25.50	10.34	10.55
13.85	27.00	26.55	9.31	10.15
14.03	23.40	24.17	10.47	10.34
14.20	24.40	24.75	11.32	11.25
14.37	27.50	27.36	11.24	11.35
14.52	23.10	27.75	11.59	11.56
14.79	26.70	26.15	12.45	12.52
14.95	21.80	23.23	13.50	13.21
15.13	25.30	26.74	12.42	12.24
15.39	23.30	27.03	11.13	11.13
15.55	27.90	27.85	11.33	11.43
15.73	27.30	27.33	11.07	11.32
15.39	27.10	26.13	11.73	11.35
16.15	24.40	26.13	12.13	11.91
16.49	26.70	27.22	11.10	10.90
16.91	30.30	30.13	9.40	9.73
17.25	31.90	32.14	9.32	9.18
17.67	33.30	31.94	8.58	9.24
18.01	22.20	24.75	12.62	11.74
18.43	27.60	26.49	10.79	10.90
18.77	31.20	29.31	8.33	9.49
19.19	24.00	25.49	10.40	10.50
19.53	24.50	24.37	10.97	10.95

Table 8.2 Attribute Analyses for June 20, 1981

Time	% Solids Observed	% Solids Estimated	% Ash Observed	% Ash Estimated
7.19	35.10	35.00	7.15	7.13
7.33	35.00	35.06	7.04	6.93
8.25	35.30	35.34	6.54	6.70
8.59	36.10	35.90	6.52	6.55
9.30	31.90	32.00	9.94	10.12
9.54	32.30	32.41	10.57	10.38
10.05	33.10	32.73	9.53	9.31
10.10	31.80	31.59	9.13	9.54
10.32	29.90	30.24	11.07	10.33
11.15	29.50	29.90	11.61	11.33
11.53	30.90	30.46	10.17	10.32
11.75	32.10	32.27	9.37	9.73
11.92	34.30	34.15	8.15	8.51
12.09	35.50	35.44	7.97	7.87
12.34	35.40	35.41	7.31	7.42
12.51	35.00	34.27	6.45	7.19
12.58	30.20	29.12	9.33	9.37
12.35	13.90	23.24	12.92	11.31
13.10	34.10	30.79	6.31	8.15
13.27	34.50	31.55	6.75	6.74
13.44	35.20	34.93	6.57	6.59
13.51	34.30	34.33	7.13	6.99
13.35	34.30	34.35	7.11	6.99
14.03	34.90	34.80	6.73	6.73
14.20	34.90	34.90	6.55	6.59

Table 8.3 Attribute Analyses for June 22, 1981

Time	% Solids Observed	% Solids Estimated	% Ash Observed	% Ash Estimated
7.35	33.10	33.20	5.98	5.93
7.70	32.50	32.55	5.98	5.90
3.12	32.40	32.15	5.57	7.03
3.45	30.10	30.43	9.41	9.24
3.33	30.30	30.15	3.45	9.25
9.22	29.50	24.34	9.43	9.57
9.54	30.70	30.34	3.43	9.20
9.43	30.10	30.15	9.55	9.33
10.40	30.00	29.74	5.35	9.10
10.74	27.30	23.50	3.47	9.03
11.19	27.60	27.52	9.52	9.31
11.35	27.90	23.07	9.79	10.33
11.53	29.20	23.94	13.54	12.35
12.43	24.00	24.29	9.55	9.59
12.50	25.70	25.92	9.37	9.71
12.35	27.40	27.13	9.35	9.45
13.02	23.50	23.52	9.30	9.25
13.19	29.30	29.25	3.42	3.45
13.35	29.70	29.33	3.73	3.34
13.51	30.70	30.41	9.00	3.47
13.73	29.80	30.15	9.20	9.26
13.95	30.00	29.95	9.77	9.75
14.12	29.30	29.73	10.24	10.32
14.37	29.40	29.53	10.79	10.55
14.54	29.90	29.80	11.55	10.47
14.71	29.30	29.37	9.30	9.30
14.33	30.10	30.13	9.57	9.53
15.13	29.40	29.93	10.00	9.37
15.29	29.70	29.75	9.49	9.59
15.47	29.30	29.73	9.67	9.54
15.53	29.30	29.32	9.59	9.73
15.39	29.90	29.35	9.35	9.37
15.39	29.80	29.35	9.30	9.37
15.23	29.70	29.75	10.14	10.01
15.23	29.90	29.75	10.05	10.01
16.55	29.40	29.35	10.02	10.04
16.55	29.90	29.35	9.97	10.04
16.93	29.50	29.67	10.13	10.14
16.93	29.80	29.67	10.14	10.14
17.40	30.10	30.04	10.29	10.31
17.40	30.10	30.04	10.17	10.31
17.74	30.10	29.35	10.55	10.14
17.74	29.90	29.35	10.35	10.14
13.15	23.90	29.19	9.83	10.12
13.15	23.30	29.19	9.90	10.12
13.50	29.50	29.40	10.13	10.11
13.50	29.40	29.40	10.24	10.11
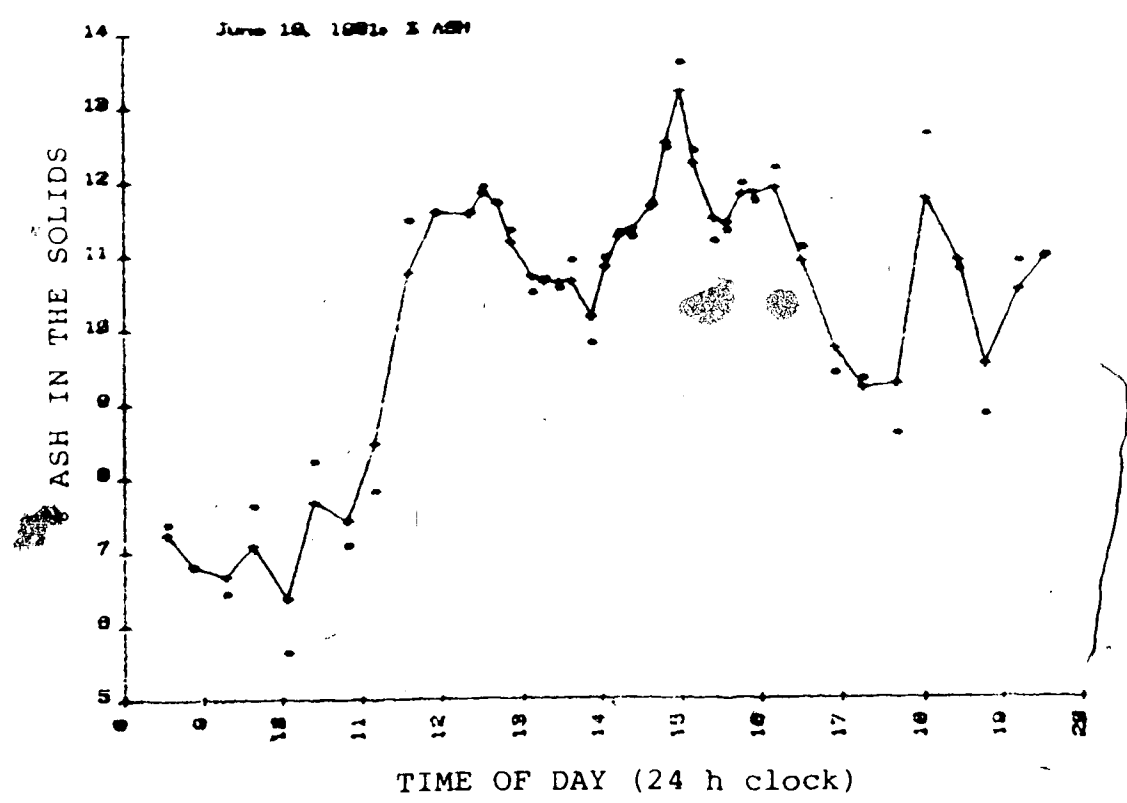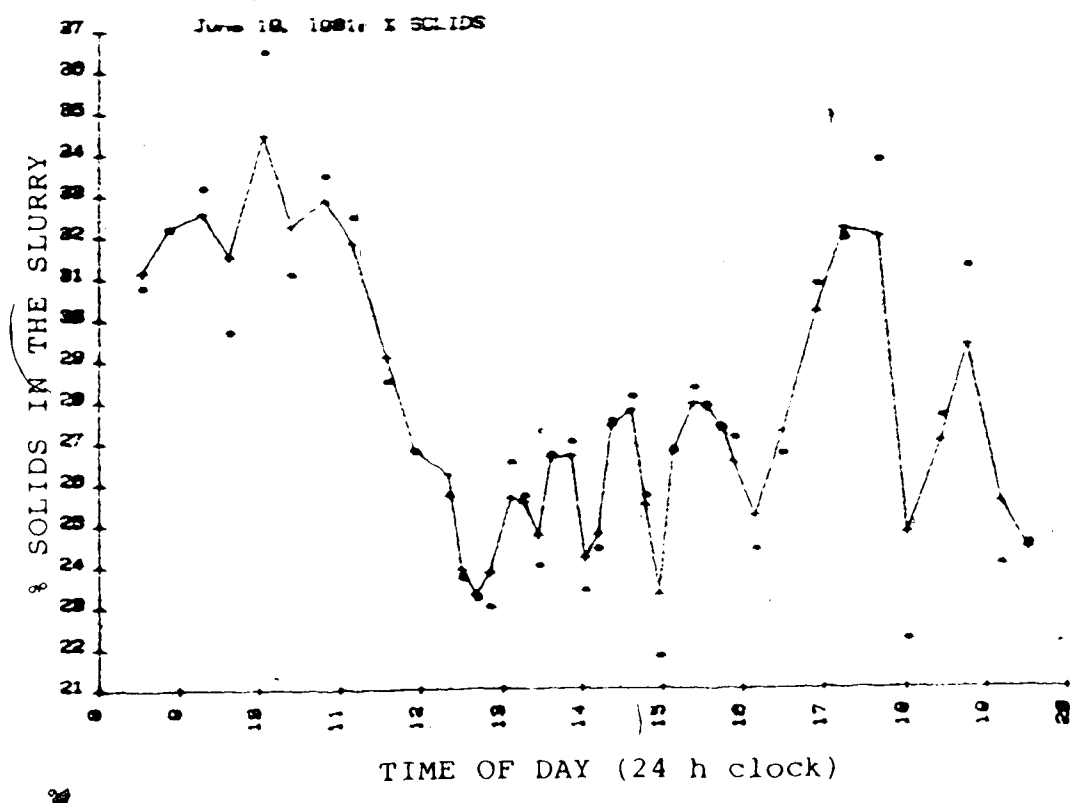
Figure 8.2 Attribute Analyses for June 19, 1981.
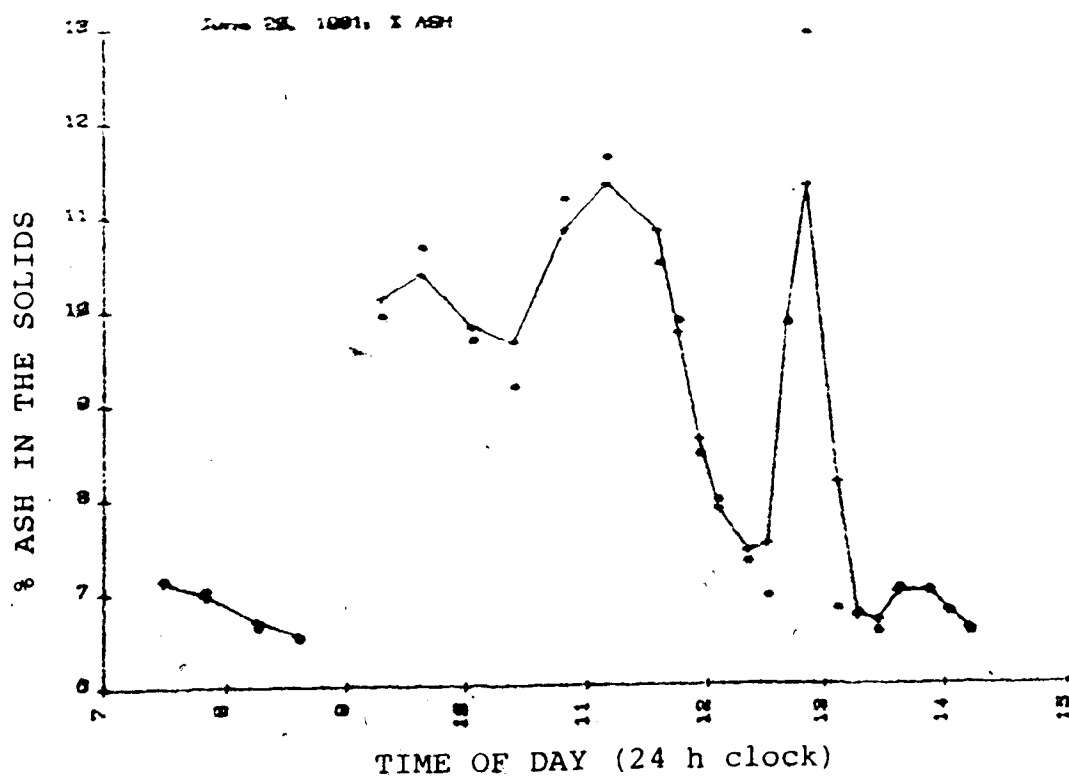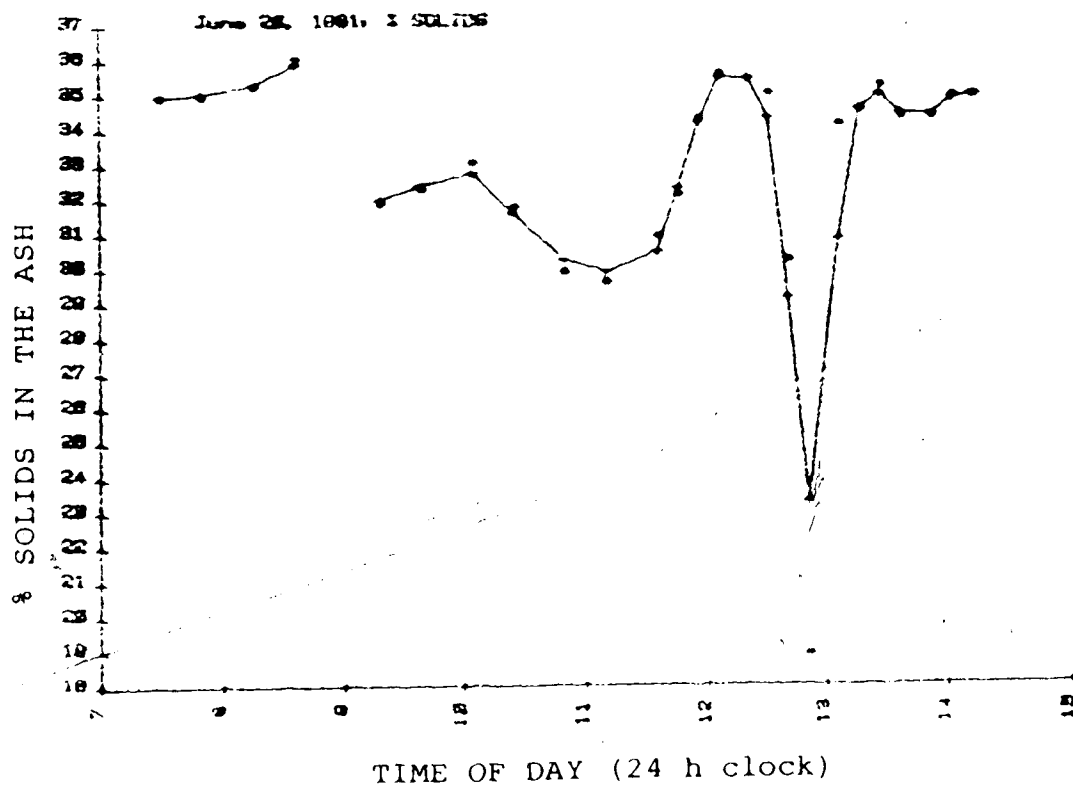
Figure 8.3 Attribute Analyses for June 20, 1981.
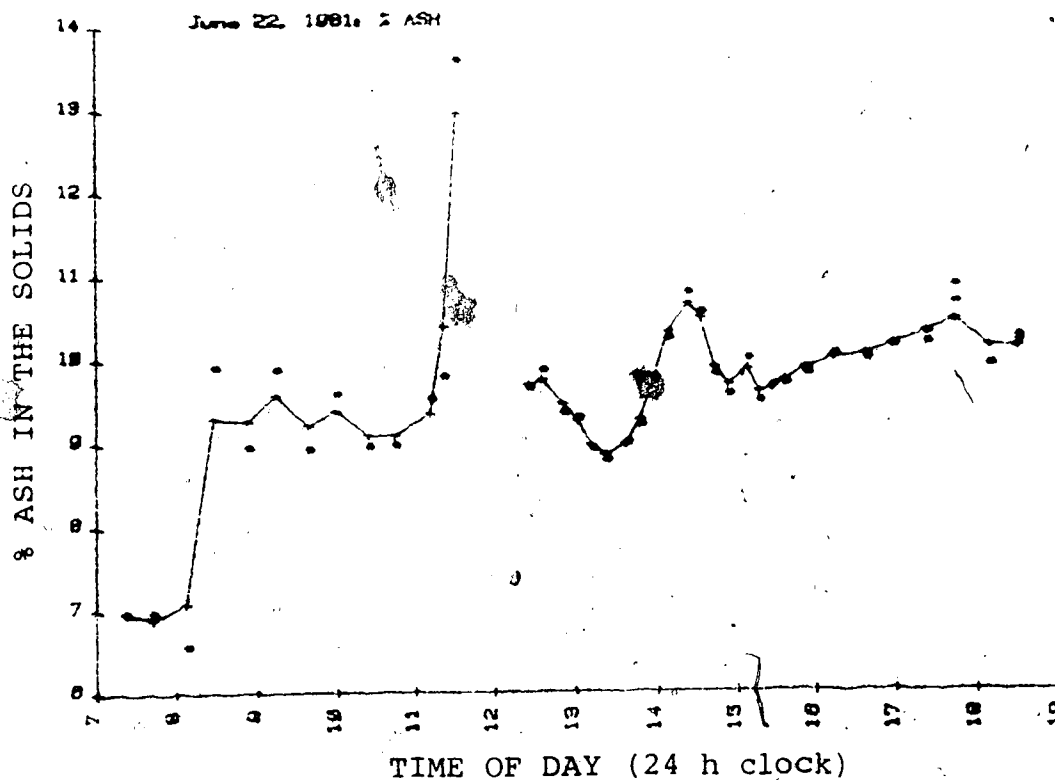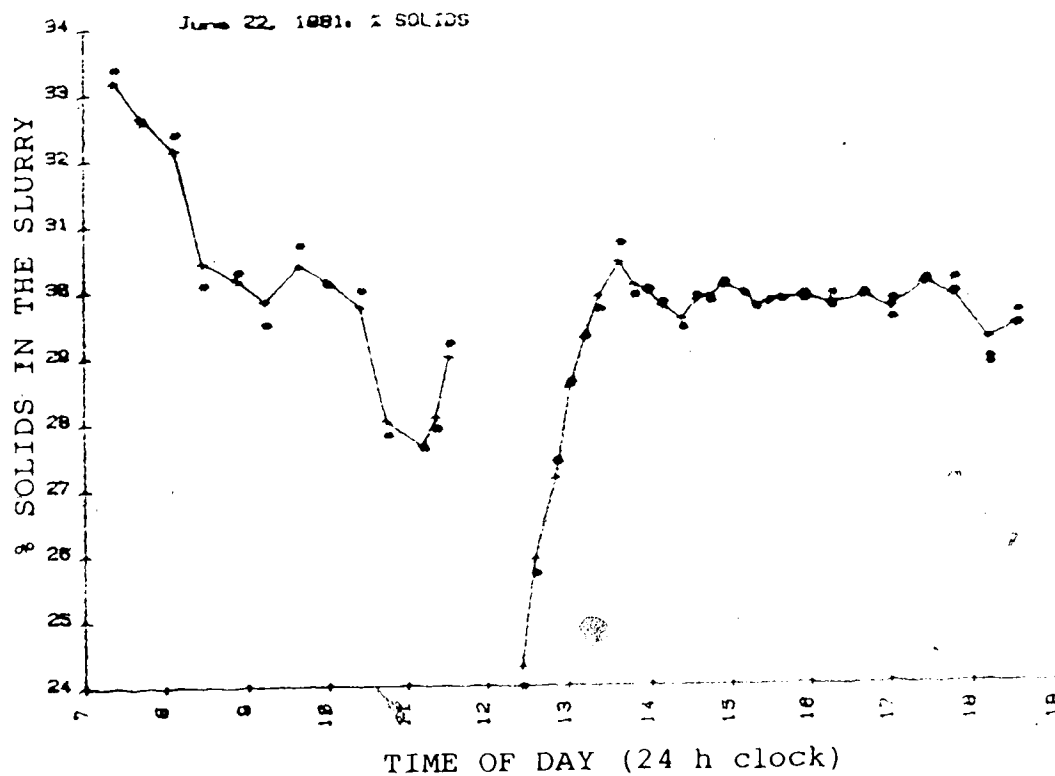
Figure 8.4 Attribute Analyses for June 22, 1981.

Table 8.4 Radiation Count Data for The Plant Calibration Run

Case Number	% Solids	% Ash	Density Counts (1xE-5)	Backscatter Counts (1xE-6)	Iron Counts (1xE-4)	Temperature Deg.F
1	31.15	7.24	4.57343	10.308398	6.3736	92.6
2	32.23	6.81	4.51423	10.400299	7.0382	93.2
3	31.50	7.08	4.73932	10.351318	7.0461	95.4
4	34.47	6.37	4.69215	10.487373	7.0169	96.6
5	32.27	7.68	4.72098	10.355194	6.8174	97.4
6	32.90	7.42	4.68882	10.446918	6.5315	98.1
7	31.58	9.46	4.69010	10.540450	6.7865	98.8
8	29.07	10.72	4.96664	10.112743	7.5537	99.7
9	26.80	11.58	4.95584	10.100175	7.5504	100.3
10	26.21	11.26	5.02019	10.111031	7.7696	101.2
11	23.29	11.69	5.02599	10.114601	6.8410	101.8
12	25.64	10.71	5.01043	10.147506	6.9345	102.3
13	24.76	10.66	5.04442	10.168697	6.9135	103.1
14	26.67	10.16	5.14163	10.152407	6.8779	103.4
15	24.86	11.32	5.17278	10.171855	6.8933	103.7
16	27.26	11.70	5.13515	9.994504	7.4078	103.8
17	23.55	13.25	5.05795	9.962301	7.7018	104.1
18	23.47	11.88	5.31278	10.018292	7.5539	104.6
19	25.19	11.90	5.17665	10.007783	7.6278	104.7
20	27.32	10.90	5.38057	10.027563	7.8258	104.5
21	30.13	9.73	5.24708	10.193346	7.3009	103.5
22	32.16	9.18	5.15765	10.220228	7.1012	103.3
23	31.95	9.24	5.16317	10.242427	7.4758	103.6
24	24.75	11.74	5.15723	10.088490	7.8059	103.5
25	26.99	10.90	5.12223	10.115785	7.3053	103.7
26	29.32	9.50	5.04081	10.163489	7.5243	103.5
27	25.49	10.50	5.07705	10.139630	7.1547	102.6
28	24.26	10.94	5.00054	10.145406	7.1506	102.3
29	35.00	7.13	4.65055	10.412752	7.5252	93.8
30	35.06	6.98	4.58091	10.404745	6.9529	94.0
31	35.34	6.70	4.60607	10.451601	6.8009	94.5
32	32.00	10.12	4.61117	10.179662	7.6086	96.2
33	32.40	10.58	4.61796	10.165187	7.5892	96.7
34	32.78	9.81	4.63606	10.242674	7.0597	97.1
35	31.59	9.64	4.73068	10.241155	7.0142	97.7
36	30.24	10.83	4.71622	10.170563	7.6383	98.5
37	29.89	11.33	4.73850	10.101856	7.5805	99.5
38	30.42	10.82	4.85252	10.111743	7.50e5	100.8
39	34.54	8.64	4.88778	10.330412	6.9058	101.4
40	35.41	7.41	4.93682	10.433425	6.8553	101.2
41	30.77	8.14	5.04219	10.452835	6.4135	100.2
42	34.86	6.67	4.99100	10.448192	6.6087	100.3
43	34.41	7.00	4.99742	10.471340	6.4082	100.0
44	33.20	6.98	4.81606	10.449181	6.8990	97.7
45	32.66	6.90	4.81734	10.428157	6.9521	88.2
46	30.43	9.29	4.81206	10.192773	7.3592	89.8
47	30.16	9.26	4.35408	10.385673	7.5311	90.6
48	29.84	9.52	4.37133	10.204775	7.5288	91.3
49	30.39	9.20	4.36165	10.241688	7.0615	91.8
50	30.16	9.38	4.38158	10.196981	6.9568	92.8
51	29.74	9.09	4.41910	10.140953	7.3172	94.5
52	27.62	9.34	4.64718	10.229708	6.6117	97.2
53	24.24	9.68	5.06700	10.215297	6.5013	100.9
54	27.11	9.45	5.01087	10.241673	7.1188	101.2
55	29.29	8.98	5.06190	10.272856	7.0412	102.2
56	30.45	8.98	4.98296	10.265250	7.0721	103.1
57	30.02	9.72	5.05242	10.194013	6.7295	103.2
58	29.52	10.66	5.05342	10.142591	7.2761	102.6
59	29.93	9.91	5.14169	10.183740	7.4153	102.4
60	29.83	9.86	5.04899	10.179860	7.2129	102.0
61	29.85	9.66	5.13097	10.204108	7.0574	101.9
62	29.83	9.87	5.11235	10.191377	7.1490	101.7
63	29.77	10.01	5.19442	10.180995	7.1969	102.0
64	29.83	10.04	5.05396	10.185493	7.1130	102.9
65	29.69	10.15	5.09794	10.170526	7.3074	103.1
66	30.04	10.31	5.19250	10.175512	7.2500	103.6
67	29.87	10.44	5.14008	10.167977	7.3127	103.7
68	29.19	10.12	5.01656	10.195514	7.0982	103.0
69	29.36	10.15	4.78099	10.190554	7.0374	102.9

and the quadratic smoothing algorithm described in the previous section.

8.5 PLANT CALIBRATION RESULTS

It was evident in conducting this testwork that the electronics section of the pulp density sub-system exhibited a strong dependence on ambient temperature. The extent of this influence was not expected on the basis of the material contained in the operating manuals for this equipment. (This problem was independently addressed in subsequent testwork, the results of which are discussed later.) The net effect is that an accurate pulp density count was not available and the three component semi-empirical calibration model could not be tested on the data set without rather radical modification. However, the Kawatra formulation of an empirical calibration equation was directly tested and the results are presented in Table 8.5 with an illustration of predictive accuracy given in Figure 8.5. The calibration equation had the form shown below:

$$\% \ Ash = b_0 + b_1 (\text{BACKSCATTER COUNTS}) + b_2 \frac{(\text{BACKSCATTER COUNTS}) \cdot}{(\text{TEMPERATURE})} \qquad \ldots (8.1)$$

The contribution of the cross product term is only barely significant and its exclusion has little impact on the evaluation criteria (which become 4.47% and 6.21% respectively.) The presence of temperature in the calibration equation may indicate a slight temperature dependence in the ash analysis sub-system electronics. The

Table 8.5 Results of the Plant Calibration Studies

TEST: IN-PLANT CALIBRATION STUDIES

Semi-Empirical Model

MODEL	RELATIVE ERROR (%)		RANGE ERROR (%)	
	% Solids	% Ash	% Solids	% Ash
Modified 3 Component Model	8.47	4.53	20.75	6.25

Empirical Model

MODEL	RELATIVE ERROR (%)		RANGE ERROR (%)	
	% Solids	% Ash	% Solids	% Ash
Kawatra + Formulation	N/A	4.17	N/A	5.80

+ Calibration equation contains 2 "independent"
   variables.
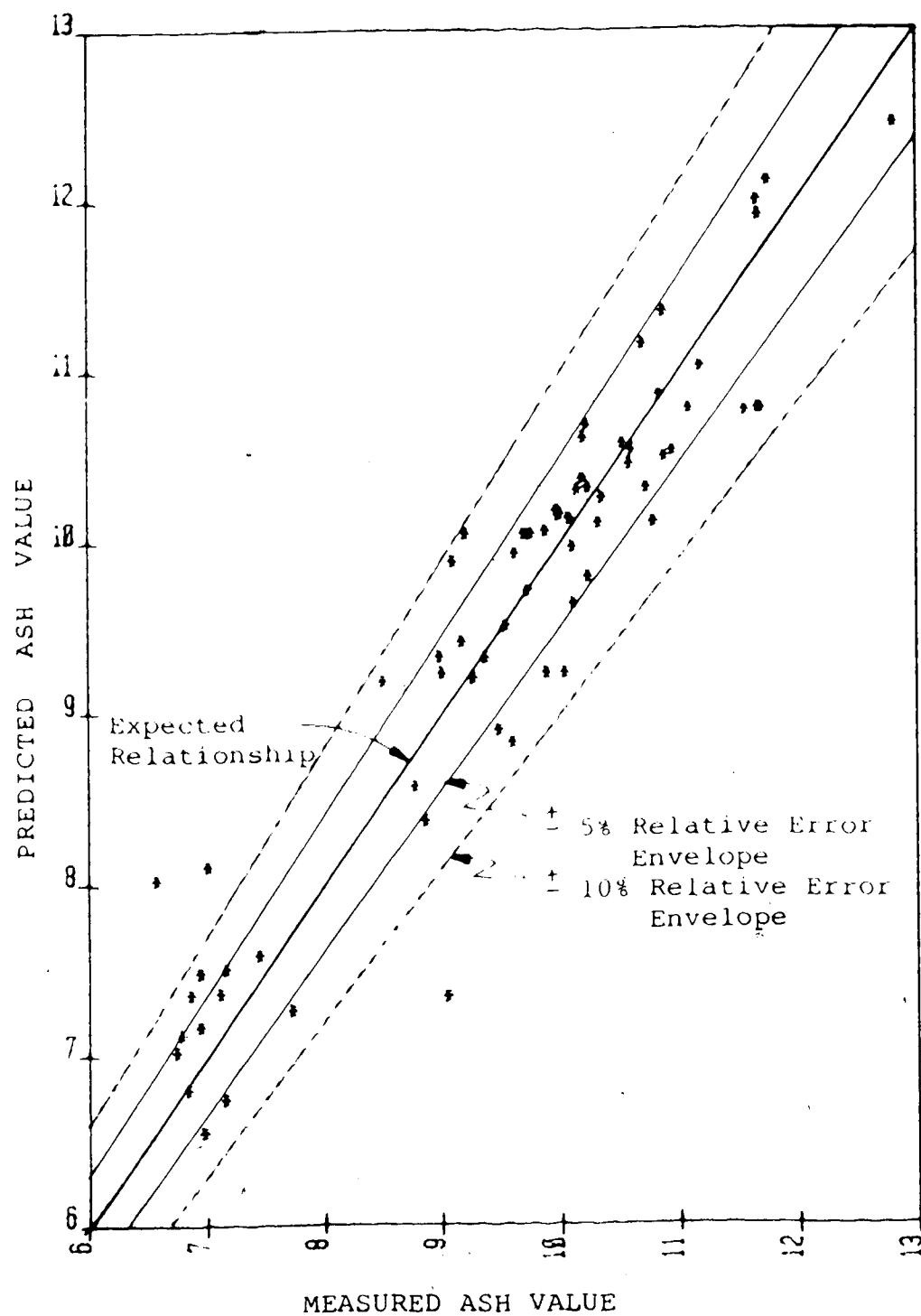
Figure 8.5 The Predictive Accuracy of the Empirical
Calibration Equation.

accuracy provided by this calibration indicates that the
OSCAA unit has definite potential for application as an
industrial process control sensing element.

In connection with the simulation work discussed in
sub-section 7.6.3 (ref. Figures 7.10 & 7.11), a separate set
of Monte Carlo simulations were performed where the error in
obtaining the pulp density count, $\epsilon = \sqrt{I_0}$, was multiplied by
an integer valued variable, m, i.e. mϵ, with m=1,2,...,5,
prior to perturbing the expected counts for computation of
the attribute values (m=1 corresponds to the Poisson
distribution). It was evident from these simulation
calculations that, while the relative error on % solids was
slightly more sensitive to an increase in the pulp density
measurement error than was the relative error on % ash, both
remained within acceptable limits. Accepting that the
prediction of % ash is therefore rather insensitive to the
pulp density, the three component model was modified and the
calibration performed, the results of which are included in
Table 8.5. The modification was to fix the reduced pulp
density counts at a level corresponding to the mean slurry
composition. It is readily apparent from Table 8.5 that, in
so doing, the % solids prediction fails to meet the range
error criterion as expected, however, the % ash prediction
criteria are well within the acceptable limits and do not
differ substantially from those quoted for the empirical
model. A plot of the % ash predictions using the modified
semi-empirical model strongly resembles Figure 8.5 and thus

has been excluded.

Considering the accuracy of the the ash analyses
(empirically smoothed point estimates) the evaluation
criteria are remarkably good. One might not expect such
impressive results for the flotation tailings and feed
streams, however, for initial control activities the
concentrate grade is the most important control variable. In
the opinion of the author, one of the principal reasons that
a pulp density measurement was not required in the
calibration equation was that, in practice, pulp density and
ash in the concentrate stream are broadly correlated (see
also (74) pg. 234). Figure 8.6 illustrates this correlation
for the attribute analyses given earlier. Such colinearity
works in favour of the empirical model which needs only a
single measurement under these circumstances.

It must be kept in mind that, for the period of
testing, the mineralogical composition of the solids species
appeared to be relatively constant and, as such, should
provide for the best calibration results.

8.6 TEMPERATURE DEPENDENCE OF THE SCA

Upon the return of the equipment from the plant trial
the temperature dependence of the pulp density sub-system
was further investigated. Initially, with water in the
density gauge flow line, the various components
sub-system were heated with a hot air gun and
count rate observed. The only component displaying any
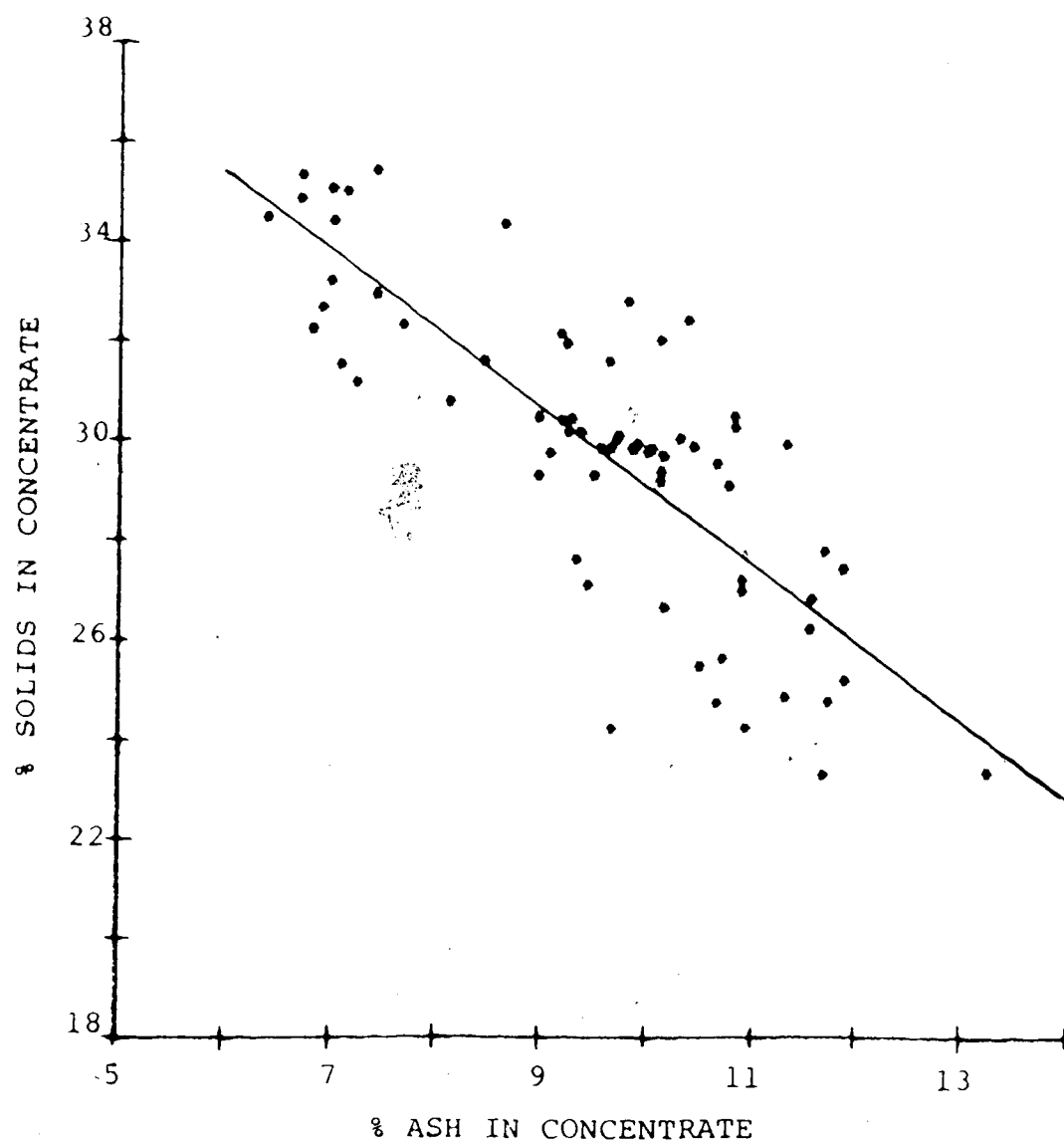
Figure 8.6 The Correlation Between Flotation Concentrate Slurry Attributes.

temperature sensitivity was the single channel analyser (SCA).

The NIM bin, containing the SCA, was placed in a glove box with a heater and a temperature controller. Under these conditions the average count rate through water was obtained as a function of the ambient temperature. The results of this experiment are shown in Figure 8.7. A linear temperature dependence was observed.

Having demonstrated the temperature dependence of the SCA output an effort was made to remove the associated bias from the observed pulp density counts. A model of the form given in equation (8.2) was fitted to the appropriate data from Table 8.4.

$$\hat{C}_0 = D\exp(-C\rho) + AT + B$$

...(8.2)

where: $\hat{C}_0$ = predicted observed pulp density counts.
D = theoretical incident photon intensity (cf. Lambert's Law).
C = the density attenuation coefficient ($=\mu x$).
A = temperature coefficient.
B = background counts.

The constant B in the equation was estimated from closed shutter measurements and was fixed for the purposes of parameterization. The value of ρ was calculated from the ash and solids content assuming a two phase solid (ref. Chap. 7) in water. Using an unweighted least squares objective function and a multivariable search algorithm(75), estimates of the parameters D, C and A were obtained. The values of C and D compared closely to those obtained in the laboratory experimentation. The index of multiple determination for the fit was 0.90 and the temperature effect was observed to make
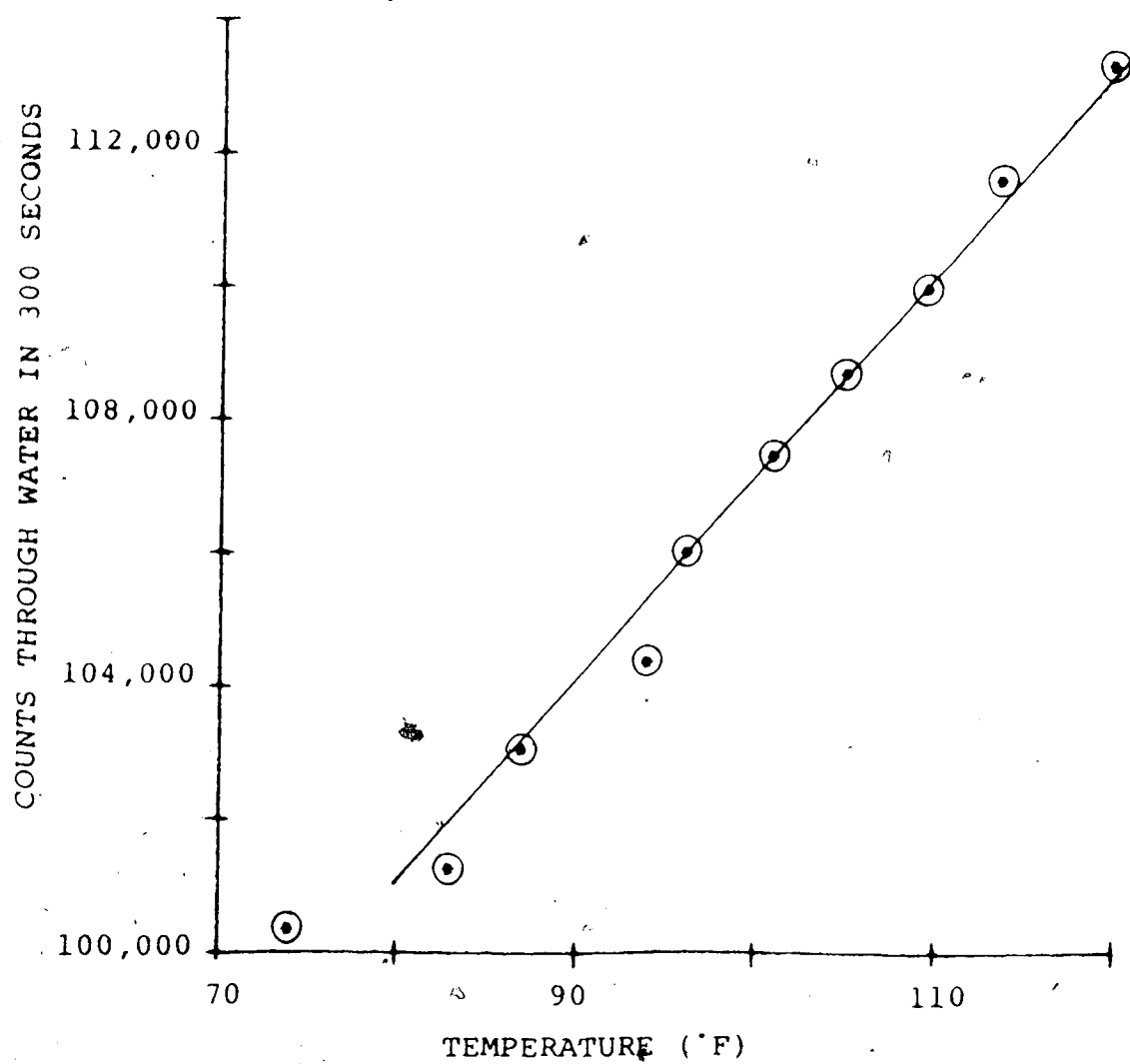
Figure 8.7 The Temperature Dependence of the SCA.

the biggest contribution to the explicable variance in the observed counts. The contribution from the term in equation (8.2) representing Lambert's law was substantially lower. Nevertheless, the "expected observed" counts (temperature bias and background removed) were generated from this term and a modified data set prepared for analysis. Both the empirical (Kawatra) and semi-empirical (three component-unmodified) model were tested on this data set. For the former, no change in model form was discovered. For the latter, the density correlation remained extremely poor and the model was incapable of meeting the performance criteria.

The conclusion which can be drawn from this exercise is that the pulp density measurement was strongly correlated with the ambient temperature of the SCA. However, even when the effects of this bias were removed, there was essentially no correlation between pulp density and the expected radiation counts from the measurement sub-system. While it was impossible to absolutely quantify the contributing factors it was strongly suspected that poor estimates of slurry attribute data over the measurement interval, inadequate source strength/count time, entrained air and electronic noise were the dominant causes of poor sub-system performance. This aspect is treated in more depth in sections 8.7 and 8.8.

8.7 ASSOCIATED PLANT TESTWORK

There were several other tests which were conducted in conjunction with the plant OSCAA calibration trial. These are discussed below.

8.7.1 Estimation of Sampling and Analysis Error

The results of the calibration have shown that the sampling and analysis techniques provided reasonable point estimates. However, quantitative evidence was gathered to demonstrate the reliabilty of the samples.

In order to deduce the error associated with the sampling and subsequent analysis of the material obtained from the OSCAA sample line during the calibration work, duplicate cuts were made for the final 8 calibration points on June 22, 1981. Assuming that these errors are normally distributed and that the variances are homogeneous, the mean attribute value, pooled variance, standard deviation and relative error of measurement are as follows:

% SOLIDS

Mean Value = 29.7%

Pooled Variance = 0.0144%^{2}

Standard Deviation = 0.12%

Relative Error = 0.4%

% ASH

Mean Value = 10.14%

Pooled Variance = 0.004%^{2}

Standard Deviation = 0.063%

Relative Error = 0.6%

The relative errors are considered to be quite good indicating consistency in sampling technique and the subsequent sample preparation and analysis.

8.7.2 Flotation Concentrate Sample Integrity Check

To check on the representativity of the sample delivered to the OSCAA prototype, relative to the slurry in the flotation concentrate collection box, a sampling campaign was conducted. Composite samples were obtained (6 cuts at 5 min. intervals) at three points in the flow system as shown in Figure 8.8. The analytical results for the three points are included in the figure.

Inspection of the sample attributes indicates good agreement between the reject and sample lines in the OSCAA system. However, an apparent bias exists for the solids concentration and particle size attributes between the collection box sample and the other two. The differences are expected because of the flow system design and the sampling technique. It is impossible to make a case for either sample 1 or sample 2/3 being "more correct" and, in fact, the true values of the flotation concentrate attributes are probably some intermediate of those reported.

Sample #1 obtained by dipping a "half-moon" sampler in the pulp.

From Flotation

#4 FLOTATION BANK CONCENTRATE COLLECTION BOX

To Filter

OSCAA Feed Line

Sample #2 obtained by stream diversion in the OSCAA reject line.

Sample #3 obtained by stream diversion in the OSCAA sample line.
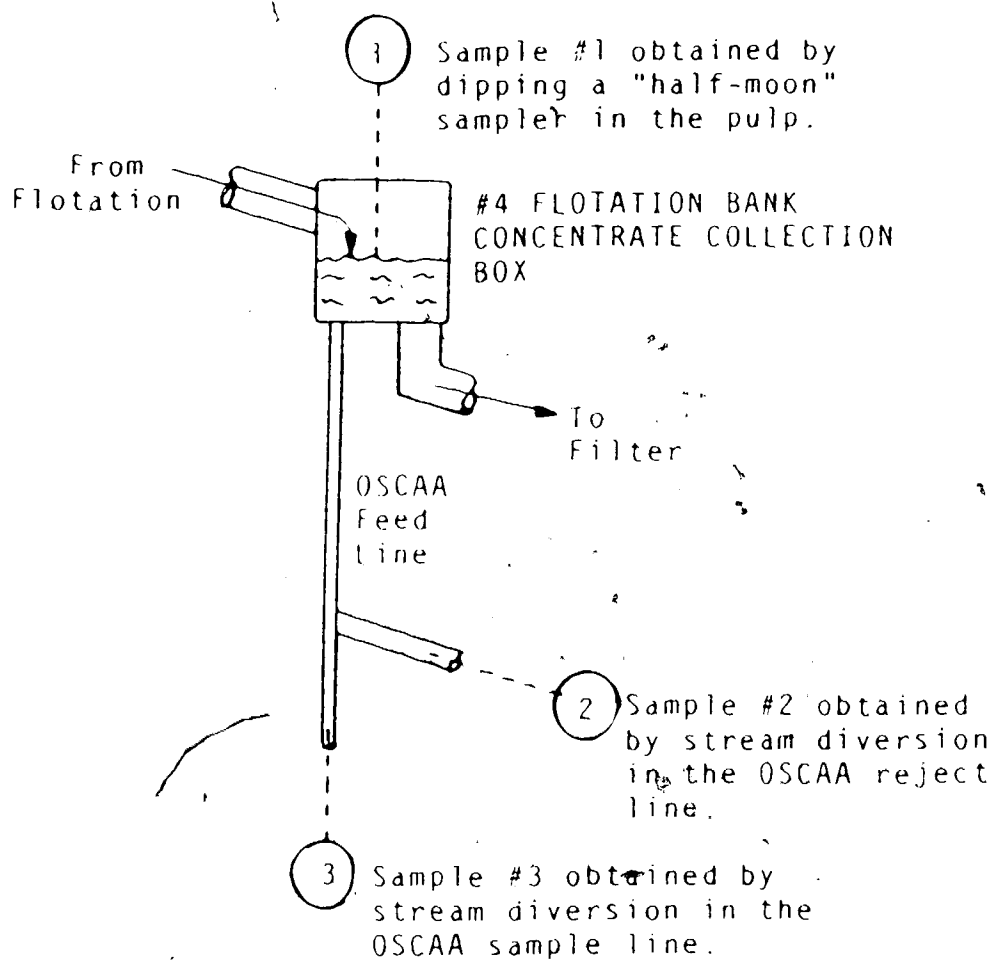
Attribute	Sample #1	Sample #2	Sample #3
% Solids (wt.)	27.8	29.2	29.4
% Ash	10.0	10.1	10.1
% -100 Mesh	47.0	43.4	43.5

Figure 8.8 Concentrate Sample Integrity Check.

8.7.3 Preliminary Studies on Flotation Concentrate Air Entrainment

It was noted earlier that calibration sampling was suspended when it was thought that aeration was playing a significant and variable role in pulp density measurement. In order to try and study this effect an entire day was spent monitoring the concentrate stream attributes, making measurements with the OSCAA system over short intervals (12 min.) and varying the frother concentration in the flotation feed. The effect of increasing frother concentration was expected to stabilize the froth bubbles. It was thought that in so doing more air would be entrained in the primary sample and hence produce interference in the pulp density sub-system. Substantial changes in the frother addition rate were made (minimum=40cc/min; maximum=180cc/min) and essentially no changes were observed in the pulp density counts. Although these results are somewhat inconclusive there is some indication that the degree of aeration of the flotation concentrate pulp is substantially fixed and therefore will not create a measurement problem.

8.8 A FINAL COMMENT ON THE PULP DENSITY MEASUREMENT PROBLEM

In the light of the results described above in section 8.6 and subsection 8.7.3, neither temperature nor entrained air appear to substantially account for the poor performance exhibited by the pulp density measurement sub-system. Since electronic noise was impossible to quantify retrospectively,

but would be assumed to be small, the problem seems due, in large part, to statistical fluctuations in radiation count data and poor interval estimates of the slurry attributes.

Considering the data in Table 8.4, the mean pulp density was calculated to be 1.0842 g/cm^3 with a standard deviation of 0.0081 g/cm^3. Assuming a Gaussian distribution, it is estimated that 95% of the samples would have a pulp density in the range of; $1.068 \leq \rho \leq 1.1$ g/cm^3. Using the estimates of C (=2.8686) and D (=5,648,900) from equation (8.2), the expected difference in counts at these limits, computed from Lambert's law, would be about $D\{\exp(-1.068C)-\exp(-1.1C)\}\approx23,145$, a relatively small range for calibration purposes. Statistical fluctations in the base radiation count data (i.e. ρ=1.0842→ I=251,912) at a 99% confidence interval ($\pm3\sigma$) are approximately 13% of this range and thus would make a minor contribution to the poor pulp density correlation. Given the limitation on counting time, a stronger source would be required to reduce this contribution.

Duplicate sampling has demonstrated that reliable point estimates of the attributes can be made, however, the interval estimate was expected to contain some error despite the smoothing operation. (The value of this error was not measured, an unfortunate oversight in the experimental plan.) Assuming for the moment that all of the variation in pulp density is due to poor attribute estimates and further that the relative error of estimation is the same for both

the % solids and % ash allows a solution for this quantity at 9%. (That is, if the mean attribute values had associated relative errors of 9%, then the expected standard deviation of the calculated pulp density, from the Law of Propagation of Errors, would be 0.0081 g/cm^3.) It is expected that the the relative errors of estimation were less than this value but may have been as high as 5% and thus poor interval attribute estimation can make a significant contribution to masking the expected pulp density correlation. Furthermore, errors in the estimation of attribute values at extreme points (most distant from mean) can have a disproportionately large impact on on the calibration by the nature of the parameterization method (linear regression). Referring to Figures 8.2, 8.3 and 8.4 it is evident that the smoothing operation tends to minimize these fluctuations.

The failure of the pulp density measurement sub-system to provide reliable results for calibration purposes is a function of all of the contributing factors previously mentioned. It is the opinion of the author that, of these factors, poor interval attribute estimation in conjunction with a narrow calibration range was the most significant. Perhaps more importantly, and with regard to OSCAA design, entrained air did not appear to play an important role in the plant trial.

8.9 SUMMARY

The plant trial was judged to be a success since a calibration was obtained which met the performance criteria. However, only one of the three process streams was monitored and for this stream the mineralogical composition appeared to remain relatively constant.

The results indicated areas for improvement in the OSCAA system design (pulp density sub-system) as well as in experimental methods (attribute estimation).

9. CONCLUSIONS AND FUTURE WORK

9.1 CONCLUSIONS

The conclusions which can be drawn from the work completed in this project are presented below.

For western Canadian coal preparation plants, the steady state optimization objective is to have each circuit within the plant producing a product having the same incremental ash value, such that the overall ash specification is met for each shipment from the plant. This will maximize production from the coal reserves, which, in turn, should maximize before tax operating profit, since the operating costs associated with the additional production are expected to be small. The difficulty in measuring the incremental ash content precludes the direct implementation of this philosophy. In general, the operator selects circuit product ash set points which (hopefully) correspond to the optimal operating scenario. Short term fluctuations around these set points result in production losses. Experimental evidence from McIntyre Mines Ltd. and communication from other operators indicates that these fluctuations do indeed occur. Moreover, they occur in a manner which should make them amenable to simple regulatory feedback control systems. Spectral analysis of experimental data can be used to help the operator assess the technical and economic potential of such simple control systems. Better control of both intrinsic and especially extrinsic disturbances will reduce

direct and indirect production losses and should allow closer adherence to the steady state optimization objective in the longer term.

Thusfar the sensors required for the development of these process control systems have received relatively little attention. In particular, ash sensors have only recently been commissioned for on-line process monitoring of essentially dry coal solids. Development projects for the on-stream ash analysis of fine coal slurries have recently been completed in Australia (ASHSCAN) and in Canada (OSCAA). The introduction of these sensors into the plant should provide the operator with an useful tool both in improving his process understanding as well as in forming the basis for the development of process control schemes.

The laboratory calibration of the OSCAA prototype was a qualified success. A set of four orthogonally designed calibration experiments were conducted on simulated flotation product flow streams for the McIntyre flotation circuit, including one in which the iron concentration of the mineral matter was independently controlled. A semi-empirical calibration model, derived from the theory, was used for data reduction. In all but one case, the performance criteria for range error and for relative error in attribute (% solids, % ash) prediction were met. The one exception was the flotation tailings stream where a combination of low accumulated density counts from the pulp density system (high relative error) coupled with a low

solids concentration in the slurry prevented successful calibration. It is felt that some relatively simple instrument design modifications would correct this problem. The performance of OSCAA in the laboratory compared very favourably with ASHSCAN in roughly equivalent service.

The plant calibration exercise was also a qualified success. An acceptable calibration was obtained for the flotation concentrate flow stream, even though the pulp density sub-system failed to operate properly. Entrained air did not appear to be a major source of calibration error in this work. On the basis of the laboratory and plant testwork which has been completed, OSCAA seems to be an acceptable instrument design for application in process monitoring and process control of fine coal preparation circuits.

The OSCAA instrument design is superior to that of its chief competetor, ASHSCAN, because it is capable of accommodating changes in the mineral matter mineralogy (specifically iron concentration) without requiring recalibration. Moreover, it is compatible with existing on-stream XRF equipment used in the base metal industry and therefore could be supported by vendors currently marketing in this area. From the author's discussions with representatives of both the coal industry as well the XRF vendor companies it is clear that there is considerable interest on both sides in continuing OSCAA development.

9.2 FUTURE WORK

The work envisaged for the immediate future of this project may be broken into two stages, second generation equipment design and evaluation strategy.

Second Generation Equipment Design

It is recommended that the OSCAA prototype design be modified prior to further evaluation testwork. The minimum set of modifications is given below; however, other modifications may also be included (e.g. computer hardware, dual isotope - dual detector ash analysis sub-system,...).

a) include a passive air eliminator in the secondary sampling device.

b) provide for flow stream multiplexing or multi-stream measurements.

c) modify both measurememt sub-system source and detector designs to enhance statistical precision, simplify spectral analysis (iron peak) and reduce the analysis time.

Succesful modifications in these areas should appreciably improve system performance and render it suitable for a more rigorous evaluation in the plant environment.

Evaluation Strategy

To more fully evaluate the second generation of instrument design it should be tested for a fairly long period of time in the operating plant environment, in what might be imagined as normal service. One of western Canada's more complex fine coal preparation circuits would be

preferred since this should adequately identify multiplexing problems, particle size effects, etc..., while giving industry a fair indication of instrument utility. For the purposes of this evaluation simple process monitoring should be undertaken with efforts in process control being reserved for late in this evaluation program or for some subsequent evaluation program.

It is the opinion of the author that there are two reasonable means of reaching the end of this stage. The first would be to encourage a major manufacturer of on-stream XRF equipment to pursue the development using the information generated from this project and in-house expertise. Given the experience of these manufacturers and the performance of the first generation prototype it is expected that the evaluation could be completed quite quickly, barring political problems between the parties concerned. The second route would be to have some reserach organization, such as the Coal Mining Research Centre, carry out the second generation design and evaluation. This would probably mean a longer time to completion of these second generation activities, but it would allow a more equitable and complete transfer of the technology of on-stream ash analysis to the industry.

10. REFERENCES

1) Patching T.H., Beck R.A.D., Harrison I., Mackay I.
   Western Canada's Coal:"The Sleeping Giant"
   Canada West Foundation, Calgary, Nov., 1980

2) Barron K.
   Technology of Coal Mining-Present and Future
   CMRC Report 80/3, Mar., 1980
   Coal Mining Research Centre, Edmonton

3) Berkowitz N.
   Prognoses for Alberta Thermal and Metallurgical Coal
   CIM Bull., Aug., 1982, pg. 110

4) Butcher S.G.,Wright P.L.
   The Purpose and Practice of Coal Preparation in Canada
   CMRC Report 81/19-T, Apr., 1980
   Coal Mining Research Centre, Edmonton

5) Hahn G.J.
   Process Improvement Using Evolutionary Operation
   ChemTech., Mar., 1970, pg. 204

6) Hahn G.J.
   Process Improvement Through Simplex EVOP
   ChemTech., May, 1970, pg. 343

7) Leonard J.W., Ed.
   Coal Preparation: 4th Edition
   AIME, New York, 1979

8) Gottfried B.S., Cierpisz S.
   Theoretical Aspects of Coal Washer Performance
   Int. J. Min. Proc., Vol. 4, 1977, pg. 261

9) Bird B.M., Marshall S.M.
   Jigging, Classification, Tabling and Flotation of Coals
   Presenting Difficult Washing Problems
   USBM Bull. 337, 1931

10) Butcher S.G., Beninger B.L.

Optimization of Proceeds in Changing Market and Mining Conditions
CIM Bull., July, 1979, pg. 143

11) Cammack P., Balint A.
On-Stream Ash in Coal Monitoring for Profit
SME/SAIME Trans., Vol. 260, Dec., 1976, pg. 361

12) Wells C.H.
Control Systems in Coal Preparation
Envirotech Corp., Instrument and Controls Group
Menlo Park, California

13) Rayner J.N.
An Introduction to Spectral Analysis
Pion Press Ltd., London, 1971

14) Plitt L.R., Flintoff B.C.
A Preliminary Study of the Flotation Circuit at McIntyre Mines Ltd.
Int. Report, Dept. of Min. Engng., Univ. Alberta.

15) McIntyre A.
A Laboratory Investigation of Coal Flotation
M. Sc. Thesis, Dept. Min. Engng., Univ. Alberta, 1981

16) Laguitton D., Flintoff B.C., Plitt L.R.
SPOC and the Canadian Coal Industry
Proc. 2nd Tech. Conf. West. Can. Coals
Univ. Alberta, June, 1982

17) Clayton C.G.
Applications of Nuclear Techniques in the Coal Industry
Paper SM-216/101, Proc. Symp. Nucl. Tech. Min. Res.
Vienna, 1977, IAEA Vienna, 1977

18) Crosland R., Hall D.A., Laverick M.K.
Continuous Ash Monitoring and Coal Blending Processes
In "Mineral Processing and Extractive Metallurgy"
M. Jones Ed.
IMM, London, 1970

19) Mikhail M.W., Homeniuk O.E.
Automatic In-Line Ash Monitor for Coal Slurries
Proc 3rd IFAC Symp., Montreal, Aug., 1980, pg. 389

20) Rogers R.S.C., Bozorgmanesh H., Gozani T., Brown T.
Continuous On-Line Nuclear Analyser of Coal
Paper Pres., Am. Min. Cong. Int'l. Coal Show, Chicago,
May, 1980

21) Sowerby B.D.
Measurement of Specific Energy, Ash and Moisture in Bulk
Coal Samples by a Combined Neutron and Gamma Ray Method
Nucl. Inst. Meth., Vol. 160, 1979, pg. 173

22) Bochenin V.I.
A Reduction of the Error in Determining the Ash Content
of Coal by the Radioisotope Method
Khimiya Tverdgo Topliva, Vol. 10, No. 5, 1976, pg. 173

23) Ailwood C.R., Bunch K., Fookes R.A., Gravitis V.L., Watt
J.S.
Determination of Combustible Volatile Matter in Coal
Mine Roadway Dusts by Backscatter of X-Rays from a
Radioisotope Source
Proc. Aust. IMM, No. 261, Mar., 1977, pg. 47

24) Pendey H.D., Hague R., Ramaswamy V.
Use of Compton Scattering in X-Ray Fluorescence for
Determination of Ash in Indian Coal
Adv. X-Ray Anal., Vol. 24, 1981, pg. 323

25) Renault J.
Rapid Determination of Ash in Coal by Compton
Scattering, Ca and Fe Fluorescence
Adv. X-Ray Anal., Vol. 23, 1980, pg. 45

26) Brown F.V., Jones S.A.
On-Site Determination of Ash in Coal Utilizing a
Portable XRF Analyser
Adv. X-Ray Anal., Vol. 23, 1980, pg. 110

27) Cooper J.A., Wheeler B.D., Wolfe W.J., Bartlett D.M.,
Schlafke D.B.
Determination of Sulfur, Ash and Trace Element Content
of Coal, Coke and Fly Ash Using Multi-Element Tube
Excited X-Ray Fluorescence Analysis
Adv. X-Ray Anal., Vol. 20, 1977, pg. 431

28) Starnes P., Clarke P.W.
The Contiuous Automatic Analysis of Dry Powders and

Aqueous Suspensions Using Radioisotope Techniques
Paper SM-68/14, Proc. Symp. Rad. Instr. Ind. Geophys.
Warsaw, Oct., 1965
IAEA Vienna, Vol. 1, 1966

29) Nagy M., Varga K.
Determination of Ash Content of Coals by Gamma Ray
Transmission Method
Paper SM-68/23, Proc. Symp. Rad. Instr. Ind. Geophys.
Warsaw, Oct., 1965
IAEA Vienna, Vol. 1, 1966

30) Fushimi H.
Coal Ash Measurement with Two Radioisotopic Radiation
Sources
Nucl. Engng. (Tokyo), Vol. 31.13, No. 6, 1967, pg. 47

31) Fookes R.A., Gravitis V.L., Watt J.S.
Determination of Ash Content of Coal by Mass Absorption
Coefficient Measurements at Two X-Ray Energies
Paper SM-216/5, Proc. Symp. Nucl. Tech. Min. Res.
IAEA Vienna, 1977

32) Lyman G.J., Chesher R.J.
On-Stream Analysis for Ash in Coal Slurries
Paper Pres. ICCR, Dusseldorf, Sept., 1980

33) Churchill T.R., Dalton J.L., Dibbs H.P.
The Determination of Lead in Ore Slurries by Gamma-Ray
Attenuation
CANMET Report CM 75-3, Ottawa, 1975

34) Dijkstra H., Sieswerda B.S.
Apparatus for Continuous Determination of the Ash
Content of Coal
Proc. 3rd Int. Coal Prep. Cong., Brussels, 1958, pg. 645

35) Hardth L.
Experiences with an Isotope Instrument for the
Continuous and Rapid Determination of Ash Content in
Coking Coal
Gluakkauf, May, 1965, pg. 653

36) Kawatra S.K., Dalton J.L.
The On-Line Measurement of Ash in Coal Slurries
Can. J. Spectr., Vol. 21, No. 2, Mar., 1976, pg. 58

37) Kawatra S.K., Laurila M.J., Larsen D.
On-Line Analysis of Coal Ash in Flotation Slurries:A
Laboratory Investigation
Proc. 17th APCOM, AIME, New York, 1982, pg. 87

38) Fano U.
Gamma-Ray Attenuation-Part 1: Basic Processes
Nucleonics, Vol. 11, No. 8, Aug. 1953, pg. 9

39) Plechety E.F., Terrel J.A.
Photon Cross Sections: 1 kev to 100 Mev
Lawrence Radiation Laboratories, Livermore, Ca.,
UCRL-50400, Vol. VI

40) Wyckoff H.O., Kennedy R.J., Bradford W.R.
Broad and Narrow Beam Attenuation of 500-1400 kev X-Rays
in Lead and Concrete
Nucleonics, Vol. 3, Nov., 1948, pg. 62

41) Fano U.
Gamma Ray Attenuation-Part 2: Analysis of Penetration
Nucleonics, Vol. 11, No. 9, Sept., 1953, pg. 55

42) Gardner R.P., Ely R.L.
Radioisotope Measurement and Applications in Engineering
Reinhold Pub. Co., New York, 1967

43) Eichholz G.G.
Radioisotope Engineering
Marcel Dekker Inc., New York, 1972

44) Tabor P., Lakoski L.
High Accuracy Fluid Density Gauge
Paper SM-68/46, Proc. Symp. Rad. Inst. Ind. Geophys.
Warsaw, Oct., 1965
IAEA Vienna, Vol. 1, 1966

45) Cameron J.F.
Fluid Density Measurement in Enclosed Systems
Unknown

46) Clayton C.G., Cameron J.F.
A Review of the Design and Applications of Radioisotope
Instruments in Industry
Paper SM-68/2, Proc. Symp. Rad. Instr. Ind. Geophys.

Warsaw, Oct., 1965
IAEA Vienna, Vol. 1, 1966

47) Kawatra S.K.
The Influence of Flow Cell and Strength of Source on the
Performance of a Gamma Density Gauge
Int. J. Min. Proc., Vol. 3, 1976, pg. 167

48) Lyman G.J.
Optimal Path Length in Radiation Transmission
Measurements
Int. J. Min. Proc., Vol. 8, 1981, pg. 223

49) Kawatra S.K.
Effect of Variation of Entrained Air in Flotation
Slurries on the On-Stream Determination of Copper by
Radioisotope X-Ray Fluorescence Analysis
Can. J. Spectr., Vol. 21, No. 1, Feb., 1970, pg. 5

50) Bradfute J.O.
ISHR Gas Separator
USAEC Report ORNL-CF-52-5-235

51) Klee B.J.
The Economic Value of Precise Particle Size Control
Min. Engng., Nov., 1970, pg. 35

52) Bertin E.P.
Principles and Practice of X-Ray Spectrometric Analysis
Plenum Press, New York, 1975

53) Berry P.F., Furuta T., Rhodes J.R.
Particle Size Effects in Radioisotope Spectrometry
Adv. X-Ray Anal., Vol. 12, 1969, pg. 612

54) Hunter C.B., Rhodes J.R.
Particle Size Effects in X-Ray Emission Analysis:
Formula for Continuous Size Distributions
X-Ray Spectr., Vol. 1, 1972, pg. 107

55) Rhodes J.R., Hunter C.B.
Particle Size Effects in X-Ray Emission Analysis:
Simplified Formulae for Certain Practical Cases
X-Ray Spectr., Vol. 1, 1972, pg. 113

56) Johnson R.E., Kiokemeister F.L.
Calculus with Analytic Geometry: 3rd Ed.
Allyn and Bacon, Boston, 1965

57) Ziegler C.A., Bird L.L., Chleck D.J.
X-Ray Rayleigh Scattering Method for Analysis of Heavy
Atoms in Low Z Media
Anal. Chem., Vol. 31, No. 11, Nov., 1959, pg. 1795

58) Davisson C.M., Evans R.D.
Gamma Absorption Coefficients
Rev. Mod. Phys., Vol. 24, No. 2, Apr., 1952, pg. 79

59) Kawatra S.K.
A Coal Ash Monitor for Coal Cleaning Processes
In "Fine Particle Processing"
P. Somasundaran Ed.
SAIME, New York, 1980, Chap. 30

60) Smallbone A.H., Gurvich Y.M.
On-Line Determination of Light Elements to Improve the
Assay of Cu, Mo, Pb, Zn and Ni in Various Slurries
Can. Res., May, 1978, pg. 53

61) Boyce I.S., Clayton C.G., Page D.
Some Considerations Relating to Accuracy of Measuring
the Ash Content of Coal by X-Ray Scattering
Paper SM-216/43, Proc. Symp. Nucl. Tech. Min. Res.
IAEA Vienna, 1977

62) Cooper H.R.
On-Stream X-Ray Analysis
In "Flotation: A.M. Gaudin Memorial Volume"
AIME, Vol. 2, 1976, Chap. 30

63) Lindkvist L.
Froth Pumping
CIM Trans., Vol. LXXVI, 1973, pg. 25

64) Lowenstein J.G.
Design So Solids Can't Settle Out
Chem. Engng., Vol. 66, No. 1, Jan., 1959, pg. 133

65) Barbery G.
Derivation of a Formula to Estimate the Mass of a Sample

For Size Analysis
Trans. IMM (C), Vol. 81, No. 784, Mar., 1972, pg. C49

66) Bernas B.
A New Method for Decomposition and Comprehensive
Analysis of Silcates by Atomic Absorption Sepctrometry
Anal. Chem., Vol. 40, No. 11, Sept., 1968, pg. 1682

67) Jenkins R., DeVries J.L.
Practical X-Ray Spectrometry
Springer-Verlag, New York, 1967

68) Box M.J., Davies D., Swann W.H.
Non-Linear Optimization Techniques
Imperial Chemical Industries, London, 1969

69) Marr H.E.
Mathematical Smoothing of Digitized X-Ray Spectra
USBM Info. Circ. 8553, 1972

70) Bevington P.R.
Data Reduction and Error Analysis for the Physical
Sciences
McGraw Hill, Toronto, 1969

71) Tibbets T.
Evaluation of Canadian Commercial Coals
CANMET Report 76-41, 1976

72) Dixon W.J., Brown M.B.
BMDP-77 Biomedical Computer Programs, P-Series
Univ. Ca. Press, Berkely Ca., 1977

73) Howarth W.J., Wenk G.J., Wilkinson L.R.
Radioisotope On-Stream Analysis
CIM Bull., Sept. 1973, pg. 76

74) Lynch A.J., Johnson N.W., Manlapig E.V., Thorne C.G.
Mineral and Coal Flotation Circuits: Their Simulation
and Control
Elsevier, New York, 1981

75) Nelder J.A., Mead R.
A Simplex Method for Function Minimization

Comp. J., Vol. 7, 1965, pg. 308

11.1 PROGRAM FOR CALCULATING NUCLEAR COEFFICIENTS

```
      DOUBLE PRECISION ORG(5,4), DIRT(9,5), VM(4), FEO(4)
      DOUBLE PRECISION R(6),R1(6),SUM1,SUM2,SUM3,SUM4,SUM5,FRAC
      DOUBLE PRECISION U(10), U1(10), U2(10)
      REAL*8 NAME(16)/'CARBON','HYDROGEN','NITROGEN','SULFUR','OXYGEN',
     1'ASH','SILICON','ALUMINUM','CALCIUM','MAGNES.','TITANIUM',
     2'SODIUM','POTASS.','PHOSPH.','SULFUR','IRON'/
C
C     THIS PROGRAM COMPUTES THE TOTAL MASS ABSORPTION
C     COEFFICIENTS FOR PHOTON ENERGIES OF 6.4 AND 22 KEV.
C     IN ADDITION TO A SCATTERING COEFFICIENT UNIQUE TO
C         THE GEOMETRY OF THIS EXPERIMENT.
C
C
C     B.C. FLINTOFF              SEPTEMBER 15, 1981
C
C
C     (1) Read in the necessary data to perform the calculations
C         from data file attached to device 7
C
C
      DO 20 I = 1, 5
      READ (7,10) (ORG(I,J),J=1,4)
   10 FORMAT (5F10.2)
   20 CONTINUE
      DO 30 I = 1, 9
      READ (7,10) (DIRT(I,J),J=1,5)
   30 CONTINUE
      READ (7,10) (VM(I),I=1,4)
      READ (7,10) (FEO(I),I=1,4)
C
C     (2) Read in the ultimate analysis
C
      WRITE (6,40)
   40 FORMAT (' -...'(1) THE ORGANIC PHASE:')
      DO 60 I = 1, 6
      IF (I .EQ. 5) GO TO 60
      WRITE (6,50) NAME(I)
   50 FORMAT (' ', 'ENTER THE WEIGHT PERCENT FOR ', A8)
      READ (5,10) R(I)
   60 CONTINUE
```

```
41  C
42  C   (3) Read in the ash analysis
43  C
44
45      WRITE (6,70)
46  70  FORMAT ('-', '(2) THE INORGANIC PHASE:')
        DO 80 I = 1, 10
47      WRITE (6,80) NAME(6 + I)
48  80  FORMAT (' ', 'ENTER THE WEIGHT % FOR THE OXIDE OF ', A8)
49      READ (5,10) U(I)
50  80  CONTINUE
51  C
52  C   (4) Perform the calculations for the organic phase
53  C       (a) compute oxygen fraction by difference
54  C       (b) adjust C,H,N,S,& O assays for exclusion of ash
55  C       (c) using the coefficient data from ORG compute
56  C           the organic phase absorption coefficients
57  C       (d) output this information
58  C
59      SUM1 = 0.
60      DO 100 I = 1, 6
61      IF (I .EQ. 5) GO TO 100
62      SUM1 = SUM1 + R(I)
63  100 CONTINUE
64      R(5) = 100. - SUM1
65      SUM1 = 0.
66      DO 110 I = 1, 5
67      SUM1 = SUM1 + R(I)
68  110 CONTINUE
69      R1(5) = 0.
70      DO 120 I = 1, 5
71      R1(I) = 100. * R(I) / SUM1
72  120 CONTINUE
73      SUM1 = 0.
74      SUM2 = 0.
75      SUM3 = 0.
76      SUM4 = 0.
77      DO 120 I = 1, 5
78      SUM1 = SUM1 + R1(I) * ORG(I,1) / 100.
79      SUM2 = SUM2 + R1(I) * ORG(I,2) / 100.
80      SUM3 = SUM3 + R1(I) * ORG(I,3) / 100.
```

```
         SUM4 = SUM4 + R1(I) * ORG(I,4) / 100.
130   CONTINUE
      WRITE (6,140)
140   FORMAT ('-','ORGANIC PHASE CALCULATIONS......')
      WRITE (6,150) (NAME(I),I=1,6)
150   FORMAT ('-',15X,6(A8,2X))
      WRITE (6,160) (R(I),I=1,6)
160   FORMAT (' ','WT. % (RAW)',4X,6(F5.2,5X))
      WRITE (6,170) (R1(I),I=1,6)
170   FORMAT (' ','WT. % (ADJ)',4X,6(F5.2,5X))
      SUM5 = 0.2799 * SUM3 + 0.05322 * SUM4
      WRITE (6,180) SUM1, SUM2, SUM3, SUM4, SUM5
180   FORMAT ('-','TOTAL AC(6,4)=',F9.4,'.TOTAL AC(22)=',F8.4,
     1 '.INCOH. SCATTER (22)=',F8.4/10X,'COH. SCATTER (22)=',F8.4,
     2 '.TOTAL SCATTER (22)=',F8.4,//)
C
C     (B) Perform the inorganic phase calculations
C         (a) adjust the raw data to total 100 %
C         (b) calculate weight % for iron free ash
C         (c) calculate the absorption coefficients
C             for the ash forming minerals
C         (d) calculate the absorption coefficients
C             for the iron free mineral matter
C         (e) calculate the absorption coefficients for
C             the composite mineral matter
C         (f) output the results
C
      SUM1 = 0.
      DO 190 I = 1, 10
      SUM1 = SUM1 + U(I)
190   CONTINUE
      SUM2 = 0.
      DO 200 I = 1, 10
      U1(I) = 100. * U(I) / SUM1
      IF (I .LE. 9) SUM2 = U1(I) + SUM2
200   CONTINUE
      DO 210 I = 1, 9
      U2(I) = 100. * U1(I) / SUM2
210   CONTINUE
      U2(10) = 0.
```

```
121         SUM1 = 0.
122         SUM2 = 0.
123         SUM3 = 0.
124         SUM4 = 0.
125         SUM5 = 0.
126         DO 220 I = 1, 9
127         FRAC = DIRT(I,1) * U2(I) / 100.
128         SUM5 = SUM5 + FRAC
129         SUM1 = SUM1 + FRAC * DIRT(I,2)
130         SUM2 = SUM2 + FRAC * DIRT(I,3)
131         SUM3 = SUM3 + FRAC * DIRT(I,4)
132         SUM4 = SUM4 + FRAC * DIRT(I,5)
133   220   CONTINUE
134         FRAC = 1. - SUM5
135         SUM1 = SUM1 + FRAC * ORG(5,1)
136         SUM2 = SUM2 + FRAC * ORG(5,2)
137         SUM3 = SUM3 + FRAC * ORG(5,3)
138         SUM4 = SUM4 + FRAC * ORG(5,4)
139         WRITE (6,230)
140   230   FORMAT ('-', 'INORGANIC PHASE CALCULATIONS....')
141         WRITE (6,240)
142   240   FORMAT ('-', 'OXIDE OF', 2X, 'WEIGHT %', 2X, 'WEIGHT %', 2X,
143        1 'EXCLUDING', /, '10X', 'RAW', 7X, 'ADJUSTED', 2X, 'HEMATITE',
144        2 /, '', 40('-'))
145         DO 250 I = 1, 10
146         WRITE (6,250) NAME(6 + I), U(I), U1(I), U2(I)
147   250   FORMAT ('', A6, 2X, 3(F5.2,5X))
148   260   CONTINUE
149         WRITE (6,270)
150   270   FORMAT ('-', 'DATA FOR ASH FORMING MINERALS:', /, '', 30('-'))
151         SUM5 = .2769 * SUM3 + .0322 * SUM4
152         WRITE (6,180) SUM1, SUM2, SUM3, SUM4, SUM5
153         FRAC = 100. * FRAC
154         WRITE (6,280) FRAC
155   280   FORMAT ('-', 'OXYGEN FRACTION IN THE IRON FREE INORGANICS',
156        1 ' IS', F5.2, ' %')
157         WRITE (6,290)
158   290   FORMAT ('-', 'DATA FOR MINERAL MATTER:', /, '', 23('-'))
159         SUM1 = .001 - 19.55 + .909 * SUM1
160         SUM2 = .001 - .625 + .909 * SUM2
```

```
161      SUM3 = .091 * .174 + .909 * SUM3
162      SUM4 = .091 * .09 + .909 * SUM4
163      SUM5 = .2789 * SUM3 + .05322 * SUM4
164      WRITE (6,180) SUM1, SUM2, SUM3, SUM4, SUM5
165      WRITE (6,300)
166  300 FORMAT ('-',.'DATA FOR HEMATITE:'// ' ', 18('-'))
167      R(1) = .2789 * FEB(3) + .05322 * FEO(4)
168      WRITE (6,180) (FEO(I),I=1,4),R(1)
169      WRITE (6,310)
170  310 FORMAT ('-','DATA FOR COMPOSITE MINERAL MATTER:'// ' ',35('-'))
171      FRAC = 1. - U1(10) / 100.
172      SUM1 = FRAC * SUM1 + (1. - FRAC) * FEO(1)
173      SUM2 = FRAC * SUM2 + (1. - FRAC) * FEO(2)
174      SUM3 = FRAC * SUM3 + (1. - FRAC) * FEO(3)
175      SUM4 = FRAC * SUM4 + (1. - FRAC) * FEQ(4)
176      SUM5 = .2789 * SUM3 + .05322 * SUM4
177      WRITE (6,180) SUM1, SUM2, SUM3, SUM4, SUM5
178      STOP
179      END
```

End of file

290

```
 1   8.603,  .3737,  .1611,  .0578
 2    .4012,  .3665,  .3614,  .0056
 3   14.244,  .4752,  .1585,  .0720
 4  174.086, 4.8737, .14,  .2523
 5   22.314,  .6712,  .1555,  .0891
 6    .467, 122.279, 3.288, .1428, .2104
 7  529.97, 23.2.8203, .1395,  .1544
 8  718.213.848, 9.566, .1354,  .3403
 9  603.78.7557, 2.0675, .1446, .1669
10  589.369.1669, 11.8357, .1221, .3567
11  742.56.35, .1.5703, .1421, .1463
12   83.279.0154, 8.1641, .3112, .1327
13  436.145.9354, 4.0102, .1372, .2242
14    4.174.086, 4.8737, 0.14, .2523
15   18.55, 628, .174, .08
16   55.92.13.666, .1301, .35

End of File
```

12.1 4 COMPONENT MODEL CALIBRATION PROGRAM

```
C
C
C
C     PROGRAM:  4 COMPONENT SEMI-EMPIRICAL OSCAA CALIBRATION
C               ANALYSIS
C
C     METHOD:   THE PROGRAM ESTIMATES THE CALIBRATION CONSTANTS
C               (AI,BI) I=1,2,3 AS DEFINED IN EQUATIONS 5.73,
C               5.74 AND 5.75. EACH SET OF (AI,BI) IS OBTAINED
C               BY UNWEIGHTED LINEAR LEAST SQUARES ANALYSIS ON
C               A SUITABLY TRANSFORMED DATA SET.
C
C               TO PROVIDE AN ESTIMATE OF THE OVERALL GOODNESS
C               OF FIT FOR THE CALIBRATION MODEL THE ATTRIBUTE
C               ANALYSES ARE BACK-CALCULATED FROM THE RADIATION
C               COUNT DATA AND THE CALIBRATION CONSTANTS ABOVE.
C               USING EQUATIONS 5.76 THRU 5.82.
C
C               ALL INPUT DATA IS ECHOED. THE DETAILS OF THE
C               LINEAR REGRESSION OUTPUT TOGETHER WITH THE
C               RESULTS OF THE BACK-CALCULATIONS INCLUDING A
C               STATISTICAL ANALYSIS OF THE GOODNESS OF FIT.
C
C     INPUT
C     FILES:    5=NUCLEAR AND PHYSICAL PARAMETERS FOR THE MODEL
C               7=NUMBER OF CASES AND THE ATTRIBUTE ANALYSES
C               8=RADIATION COUNT DATA
C
C     SUBROUTINES:
C               LINREG (LINEAR REGRESSION ANALYSIS)
C
C     REMARKS:  IN THE BACK CALCULATION SEQUENCE THE CONDITION
C               NUMBER OF THE MATRIX (SEE EQUATION 5.76), BASED
C               ON EUCLIDEAN NORMS, IS ALSO OUTPUT AS A CHECK
C               ON THE NUMERICAL CONDITION OF THE SOLUTION.
C
C
      DOUBLE PRECISION ANAL(50,3),COUNTS(50,3),PARAM(3,4),RHO(3),
     1    D(27,2),COEFF(6),WEIGHT(50,4),CALC(50,3),
     2    SOLN(3,7),SUM(9),RMAX(3),RMIN(3)
      DOUBLE PRECISION SUM1,SUM2,RES1,RES2,RES3,COND,F,T
      DIMENSION MAP(3)
C
C     INITIALLIZE ROW DIMENSION OF ARRAY TRANSFERRING DATA TO
C     THE LINEAR REGRESSION SUBROUTINE
C
      NMAIN=27
C
C     READ IN THE NUCLEAR AND PHYSICAL PARAMETERS
```

```
      C
         READ(5,10)((PARAM(I,J),J=1,4),I=1,3)
   10    FORMAT(4F12.1)
         READ(5,10)(RHO(I),I=1,3)
      C
      C     READ IN THE NUMBER OF CASES AND THE ATTRIBUTE ANALYSES
      C
         READ(7,20)NUMBER
   20    FORMAT(I2)
         DO 30 I=1,NUMBER
         READ(7,10)(ANAL(I,J),J=1,3)
   30    CONTINUE
      C
      C     READ IN THE RADIATION COUNT DATA
      C
         DO 40 I=1,NUMBER
         READ(8,10)(COUNTS(I,J),J=1,3)
   40    CONTINUE
      C
      C     ECHO ALL INPUT INFORMATION
      C
         WRITE(6,50)
   50    FORMAT(1H1,'INPUT INFORMATION:'/,18('*')))
         WRITE(6,55)
   55    FORMAT('-',17('-')))
         WRITE(6,60)
   60    FORMAT('0','SPECIES',8X,'SPECIFIC',2X,'SCATTERING',5X,
        1'TOTAL MASS ABSORPTION COEFFICIENT'/',15X,'GRAVITY',3X,
        2'COEFFICIENT',4X,'AT 22 KEV',6X,'AT 6.4 KEV'/',25X,
        33('CM**2/G',8X)/',70('-'))
         WRITE(6,70)(PARAM(J,1),J=1,3)
   70    FORMAT('WATER',10X,'1.00',6X,3(F8.4,7X))
         WRITE(6,80)RHO(1),(PARAM(J,2),J=1,3)
   80    FORMAT('ORGANICS',7X,F4.2,6X,3(F8.4,7X))
         WRITE(6,85)
   85    FORMAT('MINERAL')
         WRITE(6,90)RHO(2),(PARAM(J,3),J=1,3)
   90    FORMAT('MATTER',9X,F4.2,6X,3(F8.4,7X))
         WRITE(6,100)RHO(3),(PARAM(J,4),J=1,3)
  100    FORMAT('IRON MINERALS',2X,F4.2,6X,3(F8.4,7X)/',70('-'))
         WRITE(6,105)
  105    FORMAT('-','SAMPLE ANALYSES:'/',15('-'))
         WRITE(6,110)
  110    FORMAT('0','CASE NUMBER',4X,'% SOLIDS BY',4X,'% ASH BY WT.',3X,
        1'% IRON BY WT.'/',15X,'WT. IN PULP',4X,'IN SOLIDS',6X,
        2'IN ASH SOLIDS'/',60('-'))
         DO 120 I=1,NUMBER
         WRITE(6,130)I,(ANAL(I,J),J=1,3)
```

```
 97   130 FORMAT(' ',2X,I2,14X,F5.2,10X,F5.2,10X,F5.2)
 98   120 CONTINUE
 99       WRITE(6,150)
100   150 FORMAT(' ',60('-')/' ','RADIATION MEASUREMENTS:'/' ',23('-'))
101       WRITE(6,160)
102   160 FORMAT(' ','CASE NUMBER',4X,'REDUCED',8X,'BACKSCATTER',
103      14X,'IRON FLUORESCENCE'/' ',15X,'DENSITY',8X,'COUNTS',9X,
104      2'COUNTS'/' ',30X,'(X 1E-06)',6X,'(X 1E-04)'/' ',60('-'))
105       DO 170 I=1,NUMBER
106       WRITE(6,180)I,(COUNTS(I,J),J=1,3)
107   180 FORMAT(' ',2X,I2,10X,3(F9.6,6X))
108   170 CONTINUE
109       WRITE(6,190)
110   190 FORMAT(' ',60('-'))
111   C
112   C
113   C
114   C     ****** BEGIN THE CALCULATIONS *******
115   C
116   C     COMPUTE THE MASS FRACTION OF THE FOUR COMPONENTS
117   C
118       DO 200 I=1,NUMBER
119       WEIGHT(I,1)=1.DO-ANAL(I,1)/100.DO
120       WEIGHT(I,2)=ANAL(I,1)/100.DO*(1.DO-1.1DO*ANAL(I,2)/100.DO)
121       WEIGHT(I,3)=1.DO-WEIGHT(I,1)-WEIGHT(I,2)
122       WEIGHT(I,4)=WEIGHT(I,3)*ANAL(I,3)/(1.1DO*69.9DO)
123       WEIGHT(I,3)=WEIGHT(I,3)-WEIGHT(I,4)
124   200 CONTINUE
125   C
126   C     GENERATE THE DATA REQUIRED FOR CALIBRATION OF THE
127   C     PULP DENSITY GAUGE (VIZ. EQUATION 5.73). PERFORM
128   C     THE CALIBRATION.
129   C
130       DO 210 I=1,NUMBER
131       D(I,2)=DLOG(COUNTS(I,1))
132       D(I,1)=1.DO/(WEIGHT(I,1)+WEIGHT(I,2)/RHO(1)+WEIGHT(I,3)/RHO(2)+
133      1 WEIGHT(I,4)/RHO(3))
134   210 CONTINUE
135       WRITE(6,220)
136   220 FORMAT('1','CALIBRATION OF DENSITY GAUGE:'/' ',29('-'))
137       F=0.DO
138       T=0.DO
139       CALL LINREG(D,NUMBER,NMAIN,T,F,O,COEFF(1),COEFF(2))
140   C
141   C     GENERATE THE DATA NECESSARY TO CALIBRATE THE BACKSCATTER
142   C     PORTION OF THE ASH ANALYSIS GAUGE (VIZ EQUATION 5.74).
143   C     PERFORM THE CALIBRATION.
144   C
          DO 230 I=1,NUMBER
```

```fortran
145       D(I,2)=COUNTS(I,2)
146       SUM1=0.DO
147       SUM2=0.DO
148       DO 240 J=1,4
149       SUM1=SUM1+WEIGHT(I,J)*PARAM(1,J)
150       SUM2=SUM2+WEIGHT(I,J)*PARAM(2,J)
151   240 CONTINUE
152       D(I,1)=SUM1/(2.DO*SUM2)
153   230 CONTINUE
154       WRITE(6,250)
155   250 FORMAT('1','CALIBRATION OF BACKSCATTER GAUGE:'//' ',33('-'))
156       F=0.DO
157       T=0.DO
158       CALL LINREG(D,NUMBER,NMAIN,T,F,O,COEFF(3),COEFF(4))
159  C
160  C    GENERATE THE DATA NECESSARY TO CALIBRATE THE IRON
161  C    FLUORESCENCE PORTION OF THE ASH ANALYSIS GAUGE (VIZ
162  C    EQUATION 5.75). PERFORM THE CALIBRATION.
163  C
164       DO 260 I=1,NUMBER
165       D(I,2)=COUNTS(I,3)
166       SUM1=0.DO
167       DO 270 J=1,4
168       SUM1=SUM1+WEIGHT(I,J)*(PARAM(2,J)+PARAM(3,J))
169   270 CONTINUE
170       D(I,1)=WEIGHT(I,4)/SUM1
171   260 CONTINUE
172       WRITE(6,280)
173   280 FORMAT('1','CALIBRATION OF IRON GAUGE:'//' ',26('-'))
174       F=0.DO
175       T=0.DO
176       CALL LINREG(D,NUMBER,NMAIN,T,F,O,COEFF(5),COEFF(6))
177  C
178  C    BACK-CALCULATE THE ATTRIBUTE ANALYSES FOR THE PURPOSES
179  C    OF ASSESSING THE GOODNESS OF FIT.
180  C
181       WRITE(6,290)
182   290 FORMAT('1','BACK-CALCULATION OF CALIBRATION DATA:'//' ',
183       137('-'))
184       WRITE(6,295)
185   295 FORMAT('-','CASE',17X,'% SOLIDS',24X,'% ASH',24X,'% IRON',
186       112X,'CONDITION'/' ','NUMBER',4X,'OBS.',6X,'PRED.',5X,'RESIDUAL',
187       22X,'OBS.',6X,'PRED.',5X,'RESIDUAL',2X,'OBS.',6X,'PRED.',5X,
188       3'RESIDUAL',2X,'NUMBER'/' ',110('-'))
189  C
190  C    (1) CALCULATE THE ELEMENTS OF THE MATRIX ON THE LEFT
191  C        HAND SIDE OF EQUATION 5.76. AUGMENT WITH THE COLUMN
192  C        VECTOR ALSO SHOWN ON THE LEFT HAND SIDE OF EQUATION
```

```
C
C
          5.76
          RMAX(1)=-999999.
          RMAX(2)=-999999.
          RMAX(3)=-999999.
          RMIN(1)=999999.
          RMIN(2)=999999.
          RMIN(3)=999999.
          DO 300 I=1,NUMBER
          PULP=(DLOG(COUNTS(I,1))-COEFF(1))/COEFF(2)
          SOLN(1,1)=1.DO-1.DO/RHO(1)
          SOLN(1,2)=1.DO/RHO(1)-1.DO/RHO(2)
          SOLN(1,3)=1.DO/RHO(2)-1.DO/RHO(3)
          SOLN(1,4)=1.DO-1.DO/PULP
          SUM1=2.DO*(COUNTS(I,2)-COEFF(3))/COEFF(4)
          SOLN(2,1)=SUM1*(PARAM(2,2)-PARAM(2,1))-(PARAM(1,2)-PARAM(1,1))
          SOLN(2,2)=SUM1*(PARAM(2,3)-PARAM(2,2))-(PARAM(1,3)-PARAM(1,2))
          SOLN(2,3)=SUM1*(PARAM(2,4)-PARAM(2,3))-(PARAM(1,4)-PARAM(1,3))
          SOLN(2,4)=PARAM(1,1)-SUM1*PARAM(2,1)
          SUM1=(COUNTS(I,3)-COEFF(5))/COEFF(6)
          SOLN(3,1)=(PARAM(2,2)+PARAM(3,2))-(PARAM(2,1)+PARAM(3,1))
          SOLN(3,2)=(PARAM(2,3)+PARAM(3,3))-(PARAM(2,2)+PARAM(3,2))
          SOLN(3,3)=(PARAM(2,4)+PARAM(3,4))-(PARAM(2,3)+PARAM(3,3))
     1    -1.DO/SUM1
          SOLN(3,4)=-(PARAM(2,1)+PARAM(3,1))
C
C  (2) SCALE THE ROWS IN THE MATRIX TO IMPROVE NUMERICAL
C         CONDITION
C
          DO 310 K=1,3
          SUM1=SOLN(K,1)
          DO 320 J=2,3
          IF(DABS(SOLN(K,J)).GT.DABS(SUM1))SUM1=SOLN(K,J)
  320     CONTINUE
          DO 330 J=1,4
          SOLN(K,J)=SOLN(K,J)/SUM1
  330     CONTINUE
  310     CONTINUE
C
C  (3) CALCULATE THE EUCLIDEAN NORM OF THE MATRIX TO BE
C         INVERTED
C
          SUM1=0.DO.
          DO 340 K=1,3
          DO 340 J=1,3
          SUM1=SUM1+SOLN(K,J)*SOLN(K,J)
  340     CONTINUE
          SUM1=DSQRT(SUM1)
```

```
241  C
242  C     (4) AUGMENT THE MATRIX FORMED ABOVE WITH THE IDENTITY
243  C         MATRIX TO ALLOW CALCULATION OF THE INVERSE
244  C
245        DO 350 K=1,3
246        DO 350 J=5,7
247        SOLN(K,J)=0.DO
248        IF(K.EQ.J-4)SOLN(K,J)=1.DO
249  350 CONTINUE
250  C
251  C     (5) SOLVE FOR THE RIGHT HAND SIDE OF EQUATION 5.76
252  C         USING GAUSS-JORDAN ELIMINATION WITH PARTIAL
253  C         PIVOTING
254  C
255        MAP(1)=0
256        MAP(2)=0
257        MAP(3)=0
258        DO 360 J=1,3
259        L=MAP(J)
260        IF (J.EQ.3)GOTO 400
261        SUM2=0.DO
262        DO 370 K=1,3
263        IF (DABS(SOLN(K,J)).LE.DABS(SUM2))GOTO 370
264        IF(MAP(1).EQ.K.OR.MAP(2).EQ.K.OR.MAP(3).EQ.K)GOTO 370
265        SUM2=SOLN(K,J)
266        L=K
267  370 CONTINUE
268        MAP(J)=L
269        IF(J.EQ.1)GOTO 400
270        DO 380 K=1,3
271        IF(SOLN(K,1).EQ.0.DO.AND.SOLN(K,2).EQ.0.DO)GOTO 390
272  380 CONTINUE
273  390 MAP(3)=K
274  400 DO 410 M=1,3
275        IF(M.EQ.L)GOTO 410
276        JPLUS1=J+1
277        DO 420 K=JPLUS1,7
278        SOLN(M,K)=SOLN(M,K)-SOLN(L,K)*SOLN(M,J)/SOLN(L,J)
279  420 CONTINUE
280        SOLN(M,J)=0.DO
281  410 CONTINUE
282  360 CONTINUE
283        DO 430 J=1,3
284        L=MAP(J)
285        JPLUS1=J+1
286        DO 440 K=JPLUS1,7
287        SOLN(L,K)=SOLN(L,K)/SOLN(L,J)
288  440 CONTINUE
```

```
289          SOLN(L,J)=1.DO
290      430 CONTINUE
291    C
292    C    (6) CALCULATE THE EUCLIDEAN NORM OF THE INVERSE AND
293    C        THE CONDITION NUMBER
294    C
295          SUM2=0.DO
296          DO 450 K=1,3
297          DO 450 J=5,7
298          SUM2=SUM2+SOLN(K,J)*SOLN(K,J)
299      450 CONTINUE
300          SUM2=DSQRT(SUM2)
301          COND=SUM1*SUM2
302    C
303    C    (7) CALCULATE THE PREDICTED ATTRIBUTE ANALYSES AND
304    C        THE RESIDUALS. UPDATE THE VARIABLES TO BE USED
305    C        IN THE STATISTICAL ANALYSIS OF FIT
306    C
307          CALC(I,1)=SOLN(1,4)*100.DO
308          CALC(I,2)=SOLN(2,4)*100.DO/(1.1DO*SOLN(1,4))
309          CALC(I,3)=SOLN(3,4)*69.9DO*1.1DO/(SOLN(2,4))
310          RES1=ANAL(I,1)-CALC(I,1)
311          RES2=ANAL(I,2)-CALC(I,2)
312          RES3=ANAL(I,3)-CALC(I,3)
313          IF (ANAL(I,1).GT.RMAX(1))RMAX(1)=ANAL(I,1)
314          IF (ANAL(I,2).GT.RMAX(2))RMAX(2)=ANAL(I,2)
315          IF (ANAL(I,3).GT.RMAX(3))RMAX(3)=ANAL(I,3)
316          IF (ANAL(I,1).LT.RMIN(1))RMIN(1)=ANAL(I,1)
317          IF (ANAL(I,2).LT.RMIN(2))RMIN(2)=ANAL(I,2)
318          IF (ANAL(I,3).LT.RMIN(3))RMIN(3)=ANAL(I,3)
319          SUM(1)=SUM(1)+ANAL(I,1)
320          SUM(2)=SUM(2)+ANAL(I,2)
321          SUM(3)=SUM(3)+ANAL(I,3)
322          SUM(4)=SUM(4)+RES1
323          SUM(5)=SUM(5)+RES2
324          SUM(6)=SUM(6)+RES3
325          SUM(7)=SUM(7)+RES1*RES1
326          SUM(8)=SUM(8)+RES2*RES2
327          SUM(9)=SUM(9)+RES3*RES3
328    C
329    C    (8) OUTPUT THE DATA FOR A PARTICULAR CASE
330    C
331          WRITE(6,460)I,ANAL(I,1),CALC(I,1),RES1,ANAL(I,2),CALC(I,2),RES2,
332         1       ANAL(I,3),CALC(I,3),RES3,COND
333      460 FORMAT('  ',2X,I2,6X,9(F6.2,4X),F10.2)
334      300 CONTINUE
335    C
336    C    (9) OUTPUT THE RESULTS OF THE STATISTICAL ANALYSIS
```

```
337   C
338   C        OF FIT
339   C
340   500   WRITE(6,500)
341         FORMAT(' ',110('-')/'-','RESIDUAL ANALYSIS:'//' ',16('-'))
342         RNUM=FLOAT(NUMBER)
343         WRITE(6,510)
344   510   FORMAT('0','VARIABLE',2X,'MEAN',10X,'RESIDUAL',8X,'RELATIVE',
345        1 2X,'RANGE'/' ',10X,'VALUE',5X,'MEAN',5X,'STD DEV',4X,
346        2 'ERROR',5X,'ERROR'/' ',60('-'))
347         DO 520 J=1,3
348         L=J+3
349         K=J+6
350         SUM1=SUM(L)/RNUM
351         SUM2=((SUM(K)-SUM(L)*SUM(L)/RNUM)/(RNUM-1.D0))**0.5
352         RES1=SUM(J)/RNUM
353         RES2=100.D0*SUM2/RES1
354         RNG=100.*SUM2/(RMAX(J)-RMIN(J))
355         IF(J.EQ.1)WRITE(6,530)RES1,SUM1,SUM2,RES2,RNG
356         IF(J.EQ.2)WRITE(6,540)RES1,SUM1,SUM2,RES2,RNG
357         IF(J.EQ.3)WRITE(6,550)RES1,SUM1,SUM2,RES2,RNG
358   530   FORMAT(' ','% SOLIDS',2X,5(F5.2,5X))
359   540   FORMAT(' ','% ASH',5X,5(F5.2,5X))
360   550   FORMAT(' ','% IRON',4X,5(F5.2,5X)/' ',60('-'))
361   520   CONTINUE
362   C------------------------------------------------------------
363   C
364   C        PROCESSING IS COMPLETE
365   C
366         STOP
            END
```

End of file

```
      SUBROUTINE LINREG(D, N, NMAIN, T, F, IFLAG, B0, B1)
C
C
C     SUBROUTINE LINREG
C
C     AUTHOR: B. C. FLINTOFF
C
C     LAST UPDATE: NOVEMBER 22, 1981
C
C     PURPOSE: TO COMPUTE THE SLOPE AND INTERCEPT VALUES
C              IN A SIMPLE TWO VARIABLE LINEAR REGRESSION
C              PROBLEM.
C
C                    Y = B0 + B1 * X
C
C
C            THIS SUBPROGRAM WAS DESIGNED SPECIFICALLY
C            FOR USE WITH A CALLING PROGRAM WHICH
C            REQUIRES VALUES FOR THE LINEAR MODEL
C            COEFFICIENTS. IN ADDITION TO COMPUTING THESE
C            VALUES, THE SUBPROGRAM OUTPUTS THE STANDARD
C            INFORMATION ASSOCIATED WITH REGRESSION ANALYSIS.
C            THE CALCULATIONS ARE DONE IN DOUBLE PRECISION
C
C
C     USAGE: CALL LINREG(D,N,NMAIN,T,F,IFLAG,B0,B1)
C
C     PARAMETER LIST:
C
C       D - AN (N X 2) MATRIX WHICH CONTAINS THE OBSERVED
C           X VALUES IN THE FIRST COLUMN AND THE OBSERVED
C           Y VALUES IN THE SECOND COLUMN. THE MATRIX
C           MUST BE DECLARED DOUBLE PRECISION IN THE
C           CALLING PROGRAM
C
C       N - THE NUMBER OF JOINT OBSERVATIONS (CASES) OF
C           X AND Y AND N IS LESS THAN 1000
C
C       NMAIN = THE ROW DIMENSION OF "D" IN THE MAIN PROGRAM
C
C       T - THE T STATISTIC USED IN CALCULATING CONFIDENCE
C           INTERVALS. THE USER IS EXPECTED TO INPUT THIS
C           STATISTIC FROM A TWO SIDED TABLE. TYPICALLY THIS
C           WOULD BE THE T(.05, N-2) VALUE TO GENERATE
C           95% CONFIDENCE LIMITS. IF THE T VALUE IS ZERO OR
C           LESS, A DEFAULT OF T(.05, 25)=2.06 IS USED
C
C       F - THE F STATISTIC USED IN TESTING THE SIGNIFICANCE
C           OF THE REGRESSION. THE USER IS EXPECTED TO INPUT
C           THIS STATISTIC. TYPICALLY THIS WOULD BE THE
```

```
C      F(.05 , 1 , N-2 ) VALUE TO TEST THE NULL HYPOTHESES.
C      B1=0. AT THE .05 LEVEL OF SIGNIFICANCE. IF THE
C      F VALUE IS ZERO OR LESS, A DEFAULT OF
C      F(.05 , 1 , 25)=4.24 IS USED. THE UTILITY OF
C      THE MODEL FOR PREDICTION IS EVALUATED BY COMPARING
C      THE CALCULATED F RATIO WITH 4 * F. IF F CALCULATED
C      EXCEEDS 4 * F. THE MODEL WILL BE USEFUL IN
C      PREDICTION
C
C      IFLAG = A USER SET FLAG WHICH REFLECTS WHETHER EITHER
C              OR BOTH OF THE INPUT VARIABLES HAS UNDERGONE
C              TRANSFORMATION.
C              IFLAG=0   NO TRANSFORMATION
C              IFLAG=1   TRANSFORMATION (AN APPROPRIATE
C                        MESSAGE IS OUTPUT)
C
C      B0 = THE CALCULATED INTERCEPT RETURNED BY THIS
C           SUBPROGRAM
C
C      B1 = THE CALCULATED SLOPE RETURNED BY THIS SUBPROGRAM.
C
C      SUBPROGRAMS AND FUNCTIONS REQUIRED: NONE
C
C      REMARKS: NONE
C
C-------------------------------------------------------
C
       DOUBLE PRECISION D(NMAIN,2), SUM(5), R(2,2), SDC(3), CONFB(2)
       DOUBLE PRECISION SSXAM,SSYAM,SSXYAM,SDX,SDY,XMEAN,YMEAN,BO
      1 B1, S2, R2, FC, CORR, YPRED, RES, ERR, T, F
       INTEGER IOUT(2), SIGNIF(2) /'YES', 'NO'/
       WRITE (6,90)
       WRITE (6,100)
       WRITE (6,110) N
       IF (T .LE. 0.DO) GO TO 20
       WRITE (6,120) T
10     IF (F .LE. 0.DO) GO TO 30
       WRITE (6,130) F
       GO TO 40
20     T = 2.060
       WRITE (6,140) T
       GO TO 10
30     F = 4.24
       WRITE (6,150) F
40     IF (IFLAG .NE. 0) WRITE (6,160)
       DO 50 I = 1, 5
```

```
 97         SUM(1) = 0.D0
 98  50  CONTINUE
 99      DO 60 I = 1, N
100         SUM(1) = SUM(1) + D(I,1)
101         SUM(2) = SUM(2) + D(I,2)
102         SUM(3) = SUM(3) + D(I,1) * D(I,1)
103         SUM(4) = SUM(4) + D(I,2) * D(I,2)
104         SUM(5) = SUM(5) + D(I,1) * D(I,2)
105  60  CONTINUE
106      REALN = FLOAT(N)
107      SSXAM = SUM(3) - (SUM(1)*SUM(1)) / REALN
108      SSYAM = SUM(4) - (SUM(2)*SUM(2)) / REALN
109      SSXYAM = SUM(5) - (SUM(1)*SUM(2)) / REALN
110      R(1,1) = 1.D70
111      R(1,2) = -1.D-70
112      R(2,1) = 1.D70
113      R(2,2) = -1.D-70
114      DO 70 I = 1, N
115         IF (D(I,1) .LT. R(1,1)) R(1,1) = D(I,1)
116         IF (D(I,1) .GT. R(1,2)) R(1,2) = D(I,1)
117         IF (D(I,2) .LT. R(2,1)) R(2,1) = D(I,2)
118         IF (D(I,2) .GT. R(2,2)) R(2,2) = D(I,2)
119  70  CONTINUE
120      SDX = (SSXAM/(REALN - 1.)) ** 0.5
121      SDY = (SSYAM/(REALN - 1.)) ** 0.5
122      XMEAN = SUM(1) / REALN
123      YMEAN = SUM(2) / REALN
124      WRITE (6,170)
125      WRITE (6,180) XMEAN, SDX, R(1,1), R(1,2)
126      WRITE (6,190) YMEAN, SDY, R(2,1), R(2,2)
127      WRITE (6,200)
128      B1 = SSXYAM / SSXAM
129      B0 = YMEAN - B1 * XMEAN
130      S2 = (SSYAM - B1*SSXYAM) / (REALN - 2.)
131      SDC(1) = (S2*SUM(3)/(REALN*SSXAM)) ** 0.5
132      SDC(2) = (S2/SSXAM) ** 0.5
133      SDC(3) = (-S2*XMEAN/SSXAM)
134      CONFB(1) = T * SDC(1)
135      CONFB(2) = T * SDC(2)
136      IOUT(1) = SIGNIF(1)
137      IF ((B0 - CONFB(1)) .LT. O.D0 .AND. (B0 + CONFB(1)) .GT. O.D0)
138  1IOUT(1) = SIGNIF(2)
139      IOUT(2) = SIGNIF(1)
140      IF ((B1 - CONFB(2)) .LT. O.D0 .AND. (B1 + CONFB(2)) .GT. O.D0)
141  1IOUT(2) = SIGNIF(2)
142      WRITE (6,210) B0, SDC(1), CONFB(1), IOUT(1)
143      WRITE (6,220) B1, SDC(2), CONFB(2), IOUT(2)
144      WRITE (6,230) SDC(3)
```

```
145       WRITE (6,240)
146       WRITE (6,250)
147       CORR = SUM(4) - SSYAM
148       K = 1
149       WRITE (6,260) CORR, K
150       CORR = B1 * SSXAM
151       WRITE (6,270) CORR, K, CORR
152       CORR = SSYAM - B1 * SSXAM
153       K = N - 2
154       WRITE (6,280) CORR, K, S2
155       K = N - 1
156       WRITE (6,290) SSYAM, K
157       WRITE (6,300) SUM(4), N
158       R2 = 1 - (S2*REALN) / SSYAM
159       FC = R2 - SSYAM / S2
160       IOUT(1) = SIGNIF(1)
161       IF (FC .LT. F) IOUT(1) = SIGNIF(2)
162       IOUT(2) = SIGNIF(1)
163       IF (FC .LT. (4.*F)) IOUT(2) = SIGNIF(2)
164       WRITE (6,310) R2
165       WRITE (6,320) FC, IOUT(1), IOUT(2)
166       WRITE (6,330)
167       IPLUS = 0
168       IMINUS = 0
169       DO 80 I = 1, N
170       IOUT(1) = SIGNIF(2)
171       YPRED = BO + B1 * D(I,1)
172       RES = D(I,2) - YPRED
173       IF (RES .LT. 0.D0) IMINUS = IMINUS + 1
174       IF (RES .GE. 0.D0) IPLUS = IPLUS + 1
175       ERR = (1/REALN + (D(I,1) - XMEAN)*(D(I,1) - XMEAN)/SSXAM) * S2
176       ERR = ERR ** 0.5
177       CORR = T * ERR
178       IF (DABS(RES) .GT. CORR) IOUT(1) = SIGNIF(1)
179       WRITE (6,340) I, D(I,2), YPRED, D(I,1), RES, ERR, CORR, IOUT(1)
180    80 CONTINUE
181       WRITE (6,350) IPLUS, IMINUS
182       WRITE (6,360)
183       RETURN
184    90 FORMAT('0',20X,'TWO VARIABLE LINEAR REGRESSION ANALYSIS'//,
185      1 20X,39('*'))
186   100 FORMAT('0',27X,'MODEL FORM:  Y = BO + B1*X',/',27X,25('-'))
187   110 FORMAT('0','INPUT INFORMATION:'/,'NUMBER OF CASES IS ', I3)
188   120 FORMAT(' ','USER SUPPLIED "T" STATISTIC IS ', F6.2)
189   130 FORMAT(' ','USER SUPPLIED "F" STATISTIC IS ', F7.2)
190   140 FORMAT(' ','DEFAULT "T" (.05,25) STATISTIC IS ', F5.2)
191   150 FORMAT(' ','DEFAULT "F" (.05,1,25) STATISTIC IS ', F5.2)
192   160 FORMAT(' ','***INPUT VARIABLES HAVE BEEN TRANSFORMED***')
```

```
170 FORMAT('-','VARIABLE',9X,'MEAN',11X,'STD. DEV.',6X,'MINIMUM',
    1  'VALUE',2X,'MAXIMUM VALUE'/',75('-'))
180 FORMAT('  ',4X,'X',10X,4(D14.7,1X))
190 FORMAT('  ',4X,'Y',10X,4(D14.7,1X)/',75('-'))
200 FORMAT('-','COEFFICIENT',6X,'ESTIMATE',7X,'STD. ERR. B',4X,
    1  'CONF. INT.',5X,'SIGNIFICANT'/',75('-'))
210 FORMAT('  ',3X,'BO',10X,3(D14.7,1X),3X,A4)
220 FORMAT('  ',3X,'B1',10X,3(D14.7,1X),3X,A4/',75('-'))
230 FORMAT('  ',5X,'(COVARIANCE(BO,B1)=',D14.7,')',',')
240 FORMAT('-',20X,'ANALYSIS OF VARIANCE'/)
250 FORMAT('  ','SOURCE',16X,'SUM OF',9X,'DEGREES OF',5X,'MEAN',
    1  'SQUARE',/',22X,'SQUARES',8X,'FREEDOM'/',',
    2  65('-'))
260 FORMAT('  ','REGRESSION(BO)',6X,D14.7,4X,I1)
270 FORMAT('  ','REGRESSION(B1/BO)',3X,D14.7,4X,I1,11X,D14.7)
280 FORMAT('  ','RESIDUAL',12X,D14.7,5X,I3,8X,D14.7/',',
    1  65('-'))
290 FORMAT('  ','TOTAL (CORR.)',7X,D14.7,5X,I3)
300 FORMAT('  ','TOTAL (UNCORR.)',5X,D14.7,5X,I3/',65('-'))
310 FORMAT('O','COEFFICIENT OF MULTIPLE DETERMINATION(R**2) IS ',
    1  F6.4)
320 FORMAT('O','SIGNIFICANCE OF REGRESSION AND PREDICTOR UTILITY',
    1  /',CALC. F RATIO=',F9.2,4X,'REGRESSION SIGNIFICANT:',A4)
    2  A4,4X,'EQUATION CAN BE USED FOR PREDICTION:',A4)
330 FORMAT('-','OBSERV. #',2X,'Y(OBS.)',8X,'Y(PRED.)',7X,'X(OBS.)',
    1  8X,'RESIDUAL',7X,'STD. ERR. Y',4X,'CONF. LIMIT',4X,
    2  'OUTLIER'/',115('-'))
340 FORMAT('  ',1X,I3,6X,6(D14.7,1X),2X,A4)
350 FORMAT('  ',115('-')/'-','RESIDUAL ANALYSIS: # OF POSITIVE',
    1  'VALUES=',I3,'; # OF NEGATIVE VALUES=',I3)
360 FORMAT('-','*********RUN COMPLETE********')
    END
```

End of file

12.2 RESULTS FOR CALIBRATION RUN 1

INPUT INFORMATION:
****

MODEL PARAMETERS:

SPECIES	SPECIFIC GRAVITY	SCATTERING COEFFICIENT CM**2/G	TOTAL MASS ABSORPTION COEFFICIENT	
			AT 22 KEV CM**2/G	AT 6.4 KEV CM**2/G
WATER	1.00	0.0540	0.6374	19.8080
ORGANICS	1.28	0.0506	0.4069	9.5469
MINERAL MATTER	2.37	0.0502	2.0941	74.0140
IRON MINERALS	5.10	0.0549	13.8680	55.9200

SAMPLE ANALYSES:

CASE NUMBER	% SOLIDS BY WT. IN PULP	% ASH BY WT. IN SOLIDS	% IRON BY WT. IN ASH SOLIDS
1	5.23	9.93	5.28
2	8.41	10.00	5.27
3	11.58	10.11	5.25
4	14.79	10.30	5.22
5	17.94	10.33	5.22
6	17.52	13.33	4.86
7	18.05	16.54	4.58
8	18.73	20.27	4.38
9	19.08	23.38	4.32
10	5.14	12.47	4.95
11	8.46	12.59	4.94
12	11.51	12.68	4.93
13	14.75	12.84	4.91
14	14.81	16.34	4.59
15	15.24	19.53	4.41
16	15.42	23.24	4.32
17	5.20	15.93	4.62
18	8.33	16.03	4.61
19	11.59	16.43	4.58
20	11.92	19.83	4.39
21	12.03	23.32	4.32
22	8.60	19.15	4.42
23	8.76	22.10	4.33

24.   5.22   22.89   4.32

RADIATION MEASUREMENTS:

CASE NUMBER	REDUCED DENSITY	BACKSCATTER COUNTS (X 1E-06)	IRON FLUORESCENCE COUNTS (X 1E-04)
1	0.958090	6.117952	1.216000
2	0.940000	6.102803	2.115000
3	0.914190	6.086581	2.502000
4	0.890050	6.075626	3.110000
5	0.865580	6.057477	4.123000
6	0.854290	6.013170	4.906000
7	0.841920	5.961919	6.193000
8	0.817510	5.884961	7.236000
9	0.802550	5.819540	7.952000
10	0.961040	6.094012	1.274000
11	0.931730	6.080016	2.133000
12	0.909550	6.056673	2.569000
13	0.879980	6.038117	3.651000
14	0.871610	5.991722	4.490000
15	0.861070	5.942789	5.439000
16	0.852120	5.889042	6.142000
17	0.952440	6.083932	1.452000
18	0.919480	6.044457	2.307000
19	0.894050	6.010895	3.420000
20	0.890140	5.978627	3.587000
21	0.876100	5.934969	4.475000
22	0.824050	6.031274	3.170000
23	0.917160	5.998970	3.657000
24	0.951030	6.037998	2.084000

CALIBRATION OF DENSITY GAUGE:

TWO VARIABLE LINEAR REGRESSION ANALYSIS
****

MODEL FORM: Y = BO + B1*X

INPUT INFORMATION:
NUMBER OF CASES IS 24
DEFAULT "T" (.05,25) STATISTIC IS 2.06
DEFAULT "F" (.05,1,25) STATISTIC IS 4.24

VARIABLE	MEAN	STD. DEV.	MINIMUM VALUE	MAXIMUM VALUE
X	0.1036032E+01	0.1487179E-01	0.1013858E+01	0.1064132E+01
Y	-0.1123072E+00	0.4970354E-01	-0.2199611E+00	-0.100C000E-69

COEFFICIENT	ESTIMATE	STD. ERR. B	CONF. INT.	SIGNIFICANT
BO	0.3320280E+01	0.9693076E-01	0.1996773E+00	YES
B1	-0.3313206E+01	0.9355039E-01	0.1927138E+00	YES

(COVARIANCE(BO,B1)=-0.9067016E-02)

ANALYSIS OF VARIANCE

SOURCE	SUM OF SQUARES	DEGREES OF FREEDOM	MEAN SQUARE
REGRESSION(BO)	0.3027098E+00	1	0.5584075E-01
REGRESSION(B1/BO)	0.5584075E-01	1	0.4451902E-04
RESIDUAL	0.9794184E-03	22	
TOTAL (CORR.)	0.5682017E-01	23	
TOTAL (UNCORR.)	0.3595300E+00	24	

COEFFICIENT OF MULTIPLE DETERMINATION(R**2) IS 0.9812

SIGNIFICANCE OF REGRESSION AND PREDICTOR UTILITY   EQUATION CAN BE USED FOR PREDICTION:YES
CALC. F RATIO= 1252.31   REGRESSION SIGNIFICANT:YES

OBSERV. #	Y(OBS.)	Y(PRED.)	X(OBS.)	RESIDUAL	STD. ERR. Y	CONF. LIMIT	OUTLIER
1	-0.4281356E-01	-0.3884122E-01	0.1013858E+01	-0.3972340E-02	0.2481515E-02	0.5111919E-02	NO
2	-0.6187540E-01	-0.6746939E-01	0.1022499E+01	0.5593989E-02	0.1859509E-02	0.3830587E-02	YES
3	-0.8971685E-01	-0.9626680E-01	0.1031299E+01	0.6909950E-02	0.1432125E-02	0.2950177E-02	YES
4	-0.1164776E+00	-0.1269406E+00	0.1040449E+01	0.1046294E-01	0.1423236E-02	0.2931922E-02	YES
5	-0.1443555E+00	-0.1569765E+00	0.1049514E+01	0.1262098E-01	0.1856272E-02	0.3823919E-02	YES
6	-0.1574846E+00	-0.1607239E+00	0.1050645E+01	0.3239368E-02	0.1929729E-02	0.3975241E-02	NO
7	-0.1720703E+00	-0.1746876E+00	0.1054860E+01	0.2617296E-02	0.2226501E-02	0.4586590E-02	YES
8	-0.2014921E+00	-0.1924289E+00	0.1060214E+01	-0.9063251E-02	0.2640623E-02	0.5439682E-02	YES
9	-0.2199611E+00	-0.2054080E+00	0.1064132E+01	-0.1455313E-01	0.2960629E-02	0.6098894E-02	NO
10	-0.3973925E-01	-0.3984310E-01	0.1014161E+01	0.1038545E-03	0.2457916E-02	0.5063307E-02	NO
11	-0.7071221E-01	-0.7100360E-01	0.1023566E+01	0.2913970E-03	0.1793058E-02	0.3693698E-02	YES
12	-0.9480531E-01	-0.1002106E+00	0.1032381E+01	0.5405260E-02	0.1404144E-02	0.2892535E-02	YES
13	-0.1278561E+00	-0.1320186E+00	0.1041981E+01	0.4162454E-02	0.1471299E-02	0.3030875E-02	NO
14	-0.1374132E+00	-0.1401724E+00	0.1044442E+01	0.2759181E-02	0.1572895E-02	0.3240162E-02	NO
15	-0.1495795E+00	-0.1517905E+00	0.1047949E+01	0.2210998E-02	0.1760061E-02	0.3625724E-02	YES
16	-0.1600279E+00	-0.1622399E+00	0.1051103E+01	0.2211961E-02	0.1960285E-02	0.4038187E-02	YES
17	-0.4872817E-01	-0.4288249E-01	0.1015078E+01	-0.5845680E-02	0.2388951E-02	0.4917118E-02	YES
18	-0.8394699E-01	-0.7380231E-01	0.1024410E+01	-0.1014467E-01	0.1742694E-02	0.3589949E-02	NO
19	-0.1119936E+00	-0.1072040E+00	0.1034492E+01	-0.4789551E-02	0.1369570E-02	0.2821313E-02	YES
20	-0.1163765E+00	-0.1164121E+00	0.1037271E+01	0.3553536E-04	0.1366892E-02	0.2815796E-02	NO
21	-0.1322750E+00	-0.1236900E+00	0.1039468E+01	-0.8584997E-02	0.1399378E-02	0.2882717E-02	YES
22	-0.7898910E-01	-0.8027594E-01	0.1026364E+01	0.1286848E-02	0.1634912E-02	0.3367919E-02	NO
23	-0.8647334E-01	-0.8561149E-01	0.1027975E+01	-0.8618479E-03	0.1556640E-02	0.3206677E-02	NO
24	-0.5209967E-01	-0.4811313E-01	0.1016657E+01	-0.2096544E-02	0.2267229E-02	0.4670491E-02	NO

RESIDUAL ANALYSIS: # OF POSITIVE VALUES= 15 , # OF NEGATIVE VALUES= 9

********RUN COMPLETE********

CALIBRATION OF BACKSCATTER GAUGE:

TWO VARIABLE LINEAR REGRESSION ANALYSIS
****

MODEL FORM: Y = BO + B1*X

INPUT INFORMATION:
NUMBER OF CASES IS 24
DEFAULT "T" (.05,25) STATISTIC IS 2.06
DEFAULT "F" (.05,1,25) STATISTIC IS 4.24

VARIABLE	MEAN	STD. DEV.	MINIMUM VALUE	MAXIMUM VALUE
X	0.4051928E-01	0.1201585E-02	0.3763705E-01	0.4207439E-01
Y	0.6013901E+01	0.7678190E-01	0.5819540E+01	0.6117952E+01

COEFFICIENT	ESTIMATE	STD. ERR. B	CONF. INT.	SIGNIFICANT
BO	0.3429862E+01	0.3485716E-01	0.7180572E-01	YES
B1	0.6377308E+02	0.8598988E+00	0.1771391E+01	YES

(COVARIANCE(BO,B1)=-0.2996100E-01)

ANALYSIS OF VARIANCE

SOURCE	SUM OF SQUARES	DEGREES OF FREEDOM	MEAN SQUARE
REGRESSION(BO)	0.8680081E+03	1	0.1350554E+00
REGRESSION(B1/BO)	0.1350554E+00	1	0.2454454E-04
RESIDUAL	0.5401999E-03	22	
TOTAL (CORR.)	0.1355956E+00	23	
TOTAL (UNCORR.)	0.8681437E+03	24	

COEFFICIENT OF MULTIPLE DETERMINATION(R**2) IS 0.9957

SIGNIFICANCE OF REGRESSION AND PREDICTOR UTILITY
CALC F RATIO= 5498.22   REGRESSION SIGNIFICANT:YES   EQUATION CAN BE USED FOR PREDICTION:YES

SERY #	Y(OBS)	Y(PRED.)	X(OBS)	RESIDUAL	STD ERR Y	CONF LIMIT	OUTLIER
1	0.6117952E+01	0.6113075E+01	0.4207439E+01	0.4876863E-02	0.1676697E-02	0.3453994E-02	YES
2	0.6102803E+01	0.6101462E+01	0.4189229E+01	0.1340716E-01	0.1554686E-02	0.3202652E-02	NO
3	0.6086581E+01	0.6090034E+01	0.4169740E+01	-0.2452653E-02	0.143578E-02	0.2949050E-02	NO
4	0.6075626E+01	0.6074605E+01	0.4147115E+01	0.1021044E-02	0.130182E-02	0.2680435E-02	YES
5	0.6057477E+01	0.6062110E+01	0.4127522E+01	-0.4632800E-02	0.1202353E-02	0.2476846E-02	NO
6	0.6013170E+01	0.6011896E+01	0.4048784E+01	0.1273745E-02	0.1011848E-02	0.2084406E-02	YES
7	0.5961919E+01	0.5954472E+01	0.3958740E+01	0.7446548E-02	0.1290432E-02	0.2658289E-02	NO
8	0.5884961E+01	0.5886041E+01	0.3851435E+01	-0.1079500E-02	0.1998850E-02	0.4117630E-02	YES
9	0.5819540E+01	0.5830092E+01	0.3763705E+01	-0.1055239E-01	0.2676881E-02	0.5514373E-02	YES
10	0.6080016E+01	0.6099899E+01	0.4186778E+01	-0.5886891E-02	0.1538738E-02	0.3169800E-02	NO
11	0.6056673E+01	0.6078872E+01	0.4153806E+01	0.1144070E-02	0.1338122E-02	0.2756532E-02	YES
12	0.6038117E+01	0.6059317E+01	0.4123142E+01	0.2643639E-02	0.1182416E-02	0.2435775E-02	NO
13	0.5991722E+01	0.6037290E+01	0.4086604E+01	0.8265272E-03	0.1059514E-02	0.2182598E-02	YES
14	0.5942789E+01	0.5987598E+01	0.4010683E+01	0.4123990E-02	0.107863E-02	0.2208037E-02	YES
15	0.5889042E+01	0.5938933E+01	0.3943374E+01	0.3855994E-02	0.1430006E-02	0.2945814E-02	NO
16	0.6083932E+01	0.5885048E+01	0.3849879E+01	0.3994069E-02	0.2010405E-02	0.4144303E-02	NO
17	0.6044457E+01	0.6081456E+01	0.4157858E+01	0.2476329E-02	0.1361795E-02	0.2804041E-02	YES
18	0.6010995E+01	0.6051407E+01	0.4110740E+01	0.6950155E-02	0.1130868E-02	0.2329582E-02	YES
19	0.5978627E+01	0.6016793E+01	0.4056462E+01	0.5797739E-02	0.1012238E-02	0.2085210E-02	YES
20	0.5934969E+01	0.5975538E+01	0.3991172E+01	0.3089371E-03	0.1360830E-02	0.2803000E-02	NO
21	0.6031274E+01	0.5934730E+01	0.3927784E+01	0.2386479E-02	0.1470609E-02	0.3029454E-02	YES
22	0.6022936E+01	0.6022936E+01	0.4066095E+01	0.8338467E-02	0.1018796E-02	0.2098720E-02	YES
23	0.5998970E+01	0.5960013E+01	0.4023878E+01	0.2957454E-02	0.1039848E-02	0.2142087E-02	YES
24	0.6037998E+01	0.6045006E+01	0.4100702E+01	-0.7008036E-02	0.1094994E-02	0.2255688E-02	YES

RESIDUAL ANALYSIS   # OF POSITIVE VALUES= 15   # OF NEGATIVE VALUES= 9

**********RUN COMPLETE**********

CALIBRATION OF IRON GAUGE

TWO VARIABLE LINEAR REGRESSION ANALYSIS

MODEL FORM Y = B0 + B1*X

INPUT INFORMATION:
NUMBER OF CASES IS 24
DEFAULT "T" (.05,25) STATISTIC IS 2.06
DEFAULT "F" (.05,1,25) STATISTIC IS 4.24

VARIABLE	MEAN	STD DEV	MINIMUM VALUE	MAXIMUM VALUE
X	0.6275709E-04	0.2894018E-04	0.1935122E-04	0.1272105E-03
Y	0.3716792E+01	0.1849845E+01	0.1216000E+01	0.7952000E+01

COEFFICIENT	ESTIMATE	STD ERR B	CONF INT	SIGNIFICANT
B0	-0.2494984E+00	0.1403399E+00	0.2891000E+00	NO
B1	0.6320067E+05	0.2038178E+04	0.4198645E+04	YES

(COVARIANCE(B0,B1)=-0.2607035E+03)

ANALYSIS OF VARIANCE

SOURCE	SUM OF SQUARES	DEGREES OF FREEDOM	MEAN SQUARE
REGRESSION(B0)	0.3315490E+03	1	
REGRESSION(B1/B0)	0.7694379E+02	1	0.7694379E+02
RESIDUAL	0.1760504E+01	22	0.8002289E-01
TOTAL (CORR.)	0.7870430E+02	23	
TOTAL (UNCORR.)	0.4102533E+03	24	

COEFFICIENT OF MULTIPLE DETERMINATION(R^{2}) IS 0.9756

SIGNIFICANCE OF REGRESSION AND PREDICTOR UTILITY
CALC. F RATIO= .959.52   REGRESSION SIGNIFICANT: YES   EQUATION CAN BE USED FOR PREDICTION: YES

OBSERV. #	Y(OBS.)	Y(PRED.)	X(OBS.)	RESIDUAL	STD. ERR. Y	CONF. LIMIT	OUTLIER
1	0.1216000E+01	0.9735115E+00	0.1935122E-04	0.2424885E+00	0.1056458E+00	0.2176302E+00	YES
2	0.2115000E+01	0.1737158E+01	0.3143410E-04	0.3778418E+00	0.8608172E-01	0.1773283E+00	YES
3	0.2502000E+01	0.2518513E+01	0.4379777E-04	-0.1651253E-01	0.6948107E-01	0.1431310E+00	NO
4	0.3110000E+01	0.3346321E+01	0.5689527E-04	-0.2363207E+00	0.5896633E-01	0.1214706E+00	YES
5	0.4123000E+01	0.4145094E+01	0.6953395E-04	-0.2209389E-01	0.5937230E-01	0.1230469E+00	NO
6	0.4906000E+01	0.4806701E+01	0.8000231E-04	0.9929873E-01	0.6759975E-01	0.1392555E+00	NO
7	0.6193000E+01	0.5719541E+01	0.9444581E-04	0.4734593E+00	0.8663602E-01	0.1784702E+00	YES
8	0.7236000E+01	0.6833224E+01	0.1120672E-03	0.4027760E+00	0.1159098E+00	0.2387742E+00	YES
9	0.7952000E+01	0.7790294E+01	0.1272105E-03	0.1617062E+00	0.1434982E+00	0.2956062E+00	NO
10	0.1274000E+01	0.1158801E+01	0.2228298E-04	0.1151991E+00	0.1006948E+00	0.2074313E+00	NO
11	0.2133000E+01	0.2090794E+01	0.3702954E-04	0.4220629E-01	0.7799972E-01	0.1607794E+00	YES
12	0.2569000E+01	0.2956269E+01	0.5072363E-04	-0.3872691E+00	0.6273617E-01	0.1292365E+00	YES
13	0.3651000E+01	0.3898889E+01	0.6563834E-04	-0.2478890E+00	0.5804113E-01	0.1195647E+00	NO
14	0.4490000E+01	0.4615706E+01	0.7698026E-04	-0.1257060E+00	0.6461168E-01	0.1331000E+00	NO
15	0.5439000E+01	0.5401699E+01	0.8941673E-04	0.3730089E-01	0.7928938E-01	0.1633361E+00	NO
16	0.6142000E+01	0.6284836E+01	0.1039303E-03	-0.1428357E+00	0.1009606E+00	0.2079788E+00	NO
17	0.1452000E+01	0.1438489E+01	0.2670838E-04	0.1351054E-01	0.9344873E-01	0.1925043E+00	YES
18	0.2307000E+01	0.2460536E+01	0.4287983E-04	-0.1535358E+00	0.7053808E-01	0.1453084E+00	YES
19	0.3420000E+01	0.3577084E+01	0.6054654E-04	-0.1570839E+00	0.5791879E-01	0.1193127E+00	YES
20	0.3587000E+01	0.4238445E+01	0.7101101E-04	-0.6514453E+00	0.6014398E-01	0.1238966E+00	YES
21	0.4475000E+01	0.4915906E+01	0.8173022E-04	-0.4409063E+00	0.6949606E-01	0.1431619E+00	YES
22	0.3170000E+01	0.2924672E+01	0.5022369E-04	0.2453275E+00	0.6314150E-01	0.1300715E+00	YES
23	0.3657000E+01	0.3372185E+01	0.5730450E-04	0.2848154E+00	0.5880300E-01	0.1211342E+00	YES
24	0.2084000E+01	0.1998332E+01	0.3556656E-04	0.8566296E-01	0.8003478E-01	0.1648716E+00	NO

RESIDUAL ANALYSIS   # OF POSITIVE VALUES= 13   # OF NEGATIVE VALUES= 11

••••••••RUN COMPLETE••••••••

BACK-CALCULATION OF CALIBRATION DATA

CASE NUMBER	% SOLIDS OBS	% SOLIDS PRED	RESIDUAL	% ASH OBS	% ASH PRED	RESIDUAL	% IRON OBS	% IRON PRED	RESIDUAL	CONDITION NUMBER
1	5.23	5.84	-0.61	9.93	8.08	1.85	5.28	6.94	-1.66	29.72
2	8.41	7.92	0.49	10.00	8.83	1.17	5.27	7.53	-2.26	29.53
3	11.58	10.78	0.80	10.11	10.42	-0.31	5.25	5.46	-0.21	29.45
4	14.79	13.63	1.16	10.30	10.54	-0.24	5.22	5.19	0.03	29.33
5	17.94	16.51	1.43	10.33	10.72	-0.39	5.22	5.46	-0.24	29.12
6	17.52	17.23	0.29	13.33	13.17	0.16	4.86	5.09	-0.23	28.97
7	18.05	18.06	-0.01	16.54	15.46	1.08	4.58	5.25	-0.67	28.72
8	18.73	19.75	-1.02	20.27	19.42	0.85	4.38	4.56	-0.18	28.54
9	19.08	20.37	-1.29	23.38	23.16	0.22	4.32	4.18	0.14	28.42
10	5.14	5.05	0.09	12.47	13.55	-1.08	4.95	5.03	-0.08	29.71
11	8.46	8.46	-0.00	12.59	12.32	0.27	4.94	5.14	-0.20	29.53
12	11.51	10.77	0.74	12.68	13.88	-1.20	4.93	4.26	0.67	29.45
13	14.75	14.26	0.49	12.84	13.19	-0.35	4.91	4.66	0.25	29.22
14	14.81	14.57	0.24	16.34	16.23	0.11	4.59	4.57	0.02	29.06
15	15.24	15.10	0.14	19.53	19.21	0.32	4.41	4.55	0.14	28.88
16	15.42	15.24	0.18	23.24	23.21	0.03	4.32	4.28	0.04	28.76
17	5.20	5.91	-0.71	15.93	14.66	1.27	4.62	4.44	0.18	29.68
18	8.33	9.26	-0.93	16.03	16.77	-0.74	4.61	3.75	0.86	29.51
19	11.59	11.95	-0.36	16.43	17.16	-0.73	4.58	4.09	0.49	29.28
20	11.92	11.80	0.12	19.83	20.69	-0.86	4.39	3.65	0.74	29.25
21	12.03	12.83	-0.80	23.32	23.18	0.14	4.32	3.73	0.59	29.08
22	8.60	8.69	-0.09	19.15	17.21	1.94	4.42	5.21	-0.79	29.33
23	8.76	8.99	-0.23	22.10	20.70	1.40	4.33	4.84	-0.51	29.23
24	5.22	5.34	-0.12	22.89	24.03	-1.14	4.32	4.19	0.13	29.56

RESIDUAL ANALYSIS

VARIABLE	MEAN VALUE	RESIDUAL MEAN	RESIDUAL STD DEV	RELATIVE ERROR	RANGE ERROR
% SOLIDS	12.01	0.00	0.68	5.64	4.86
% ASH	16.23	0.16	0.93	5.72	6.91
% IRON	4.71	-0.13	0.71	15.03	73.71

12.3 RESULTS FOR CALIBRATION RUN 2

INPUT INFORMATION:
****

MODEL PARAMETERS:

SPECIES	SPECIFIC GRAVITY	SCATTERING COEFFICIENT CM**2/G	TOTAL MASS ABSORPTION COEFFICIENT AT 22 KEV CM**2/G	AT 6.4 KEV CM**2/G
WATER	1.00	0.0540	0.6374	19.8080
ORGANICS	1.28	0.0506	0.4089	9.6260
MINERAL MATTER	2.37	0.0502	2.0560	72.8270
IRON MINERALS	5.10	0.0549	13.8680	55.9200

SAMPLE ANALYSES:

CASE NUMBER	% SOLIDS BY WT. IN PULP	% ASH BY WT. IN SOLIDS	% IRON BY WT. IN ASH SOLIDS
1	22.08	7.24	5.69
2	24.54	7.36	5.67
3	27.13	7.38	5.66
4	29.78	7.41	5.66
5	32.46	7.34	5.67
6	32.59	8.39	5.50
7	32.64	9.47	5.34
8	32.66	10.60	5.18
9	32.77	11.73	5.04
10	21.24	8.20	5.53
11	23.73	8.25	5.52
12	26.30	8.34	5.51
13	28.55	8.35	5.51
14	28.11	9.47	5.34
15	28.56	10.38	5.21
16	28.71	11.59	5.06
17	20.96	10.71	3.56
18	23.27	10.37	3.60
19	25.85	10.28	3.61
20	25.74	11.34	3.55
21	25.61	12.33	3.68
22	21.14	11.65	3.57
23	23.77	11.59	3.57

24	23.70	12.61	3.75
25	21.36	12.53	3.73

RADIATION MEASUREMENTS:

CASE NUMBER	REDUCED DENSITY	BACKSCATTER COUNTS (X 1E-06)	IRON FLUORESCENCE COUNTS (X 1E-04)
1	0.842670	6.006070	4.083000
2	0.831240	5.996590	4.401000
3	0.806880	5.991073	4.984000
4	0.787770	5.986919	5.215000
5	0.772890	5.987024	6.042000
6	0.767680	5.954420	6.464000
7	0.764030	5.912414	7.308000
8	0.769030	5.877636	7.646000
9	0.766680	5.837851	8.129000
10	0.850750	5.986594	3.759000
11	0.834380	5.982572	4.493000
12	0.818110	5.967861	4.898000
13	0.805390	5.961365	5.403000
14	0.803150	5.926213	5.897000
15	0.794140	5.895715	6.668000
16	0.787650	5.860857	7.428000
17	0.838990	5.966444	2.749000
18	0.823730	5.948627	3.137000
19	0.805510	5.948843	3.810000
20	0.801030	5.911218	4.786000
21	0.800820	5.882074	5.228000
22	0.842260	5.946631	2.926000
23	0.824650	5.938064	3.436000
24	0.825380	5.907781	4.271000
25	0.844760	5.922986	3.456000

CALIBRATION OF DENSITY GAUGE:

TWO VARIABLE LINEAR REGRESSION ANALYSIS
****

MODEL FORM: Y = BO + B1*X

INPUT INFORMATION:
NUMBER OF CASES IS 25
DEFAULT "T" (.05,25) STATISTIC IS 2.06
DEFAULT "F" (.05,1,25) STATISTIC IS 4.24

VARIABLE	MEAN	STD. DEV.	MINIMUM VALUE	MAXIMUM VALUE
X	0.1074344E+01	0.1192961E-01	0.1057101E+01	0.1096538E+01
Y	-0.2133101E+00	0.3392100E-01	-0.2691482E+00	-0.1000000E-69

COEFFICIENT	ESTIMATE	STD. ERR. B	CONF. INT.	SIGNIFICANT
BO	0.2790913E+01	0.1154609E+00	0.2378493E+00	YES
B1	-0.2796331E+01	0.1074646E+00	0.2213771E+00	YES

(COVARIANCE(BO,B1)=-0.1240723E-01)

ANALYSIS OF VARIANCE

SOURCE	SUM OF SQUARES	DEGREES OF FREEDOM	MEAN SQUARE
REGRESSION(BO)	0.1137530E+01	1	0.2670798E-01
REGRESSION(B1/BO)	0.2670798E-01	1	0.3944526E-04
RESIDUAL	0.9072411E-03	23	
TOTAL (CORR.)	0.2761522E-01	24	
TOTAL (UNCORR.)	0.1165145E+01	25	

COEFFICIENT OF MULTIPLE DETERMINATION(R**2) IS 0.9643

SIGNIFICANCE OF REGRESSION AND PREDICTOR UTILITY
CALC. F RATIO= 675.08   REGRESSION SIGNIFICANT:YES   EQUATION CAN BE USED FOR PREDICTION:YES

OBSERV. #	Y(OBS.)	Y(PRED.)	X(OBS.)	RESIDUAL	STD. ERR. Y	CONF. LIMIT	OUTLIER
1	-0.1711799E+00	-0.1690740E+00	0.1058525E+01	-0.2105891E-02	0.2113736E-02	0.4354296E-02	NO
2	-0.1848367E+00	-0.1888826E+00	0.1065609E+01	0.4045841E-02	0.1568149E-02	0.3230385E-02	YES
3	-0.2145803E+00	-0.2097299E+00	0.1073064E+01	-0.4850470E-02	0.1263623E-02	0.2603062E-02	YES
4	-0.2385491E+00	-0.2314188E+00	0.1080820E+01	-0.7130337E-02	0.1436010E-02	0.2958179E-02	YES
5	-0.2576185E+00	-0.2532545E+00	0.1088629E+01	-0.4364092E-02	0.1983505E-02	0.4086020E-02	YES
6	-0.2643823E+00	-0.2589672E+00	0.1090672E+01	-0.5415107E-02	0.2157900E-02	0.4445272E-02	YES
7	-0.2691482E+00	-0.2641709E+00	0.1092533E+01	-0.4977290E-02	0.2323427E-02	0.4786259E-02	YES
8	-0.2626253E+00	-0.2693543E+00	0.1094386E+01	0.6728971E-02	0.2493332E-02	0.5136263E-02	NO
9	-0.2672298E+00	-0.2753696E+00	0.1096538E+01	0.8639867E-02	0.2695544E-02	0.5552820E-02	YES
10	-0.1616370E+00	-0.1650928E+00	0.1057101E+01	0.4100162E-02	0.1657593E-02	0.3414641E-02	YES
11	-0.1810663E+00	-0.1851665E+00	0.1064280E+01	0.5582171E-02	0.1284348E-02	0.2645756E-02	YES
12	-0.2007585E+00	-0.2063406E+00	0.1071852E+01	0.8488377E-02	0.1332959E-02	0.2745895E-02	YES
13	-0.2164286E+00	-0.2249170E+00	0.1078495E+01	0.6220249E-02	0.1339739E-02	0.2759862E-02	YES
14	-0.2192138E+00	-0.2326844E+00	0.1081273E+01	0.2188910E-02	0.1460202E-02	0.3008015E-02	NO
15	-0.2304955E+00	-0.2385953E+00	0.1083387E+01	-0.1061031E-03	0.1588100E-02	0.3271486E-02	NO
16	-0.2387015E+00	-0.1691917E+00	0.1058567E+01	-0.6364749E-02	0.2110098E-02	0.4346800E-02	YES
17	-0.1755565E+00	-0.1874152E+00	0.1065084E+01	-0.6497261E-02	0.1602544E-02	0.3301239E-02	YES
18	-0.1939125E+00	-0.2087625E+00	0.1072718E+01	-0.7517198E-02	0.1268209E-02	0.2612510E-02	YES
19	-0.2162797E+00	-0.2113764E+00	0.1073653E+01	-0.1048045E-01	0.1258306E-02	0.2592109E-02	YES
20	-0.2218569E+00	-0.2136145E+00	0.1074453E+01	-0.8504571E-02	0.1256164E-02	0.2587697E-02	YES
21	-0.2221191E+00	-0.1732110E+00	0.1060004E+01	0.1544460E-02	0.1988113E-02	0.4095511E-02	NO
22	-0.1716665E+00	-0.1953205E+00	0.1067911E+01	0.2524317E-02	0.1433797E-02	0.2953622E-02	NO
23	-0.1927962E+00	-0.1979042E+00	0.1068835E+01	0.5992794E-02	0.1388648E-02	0.2860615E-02	YES
24	-0.1919114E+00	-0.1775043E+00	0.1061540E+01	0.8801568E-02	0.1863141E-02	0.3838069E-02	YES
25	-0.1687027E+00						

RESIDUAL ANALYSIS: # OF POSITIVE VALUES= 13   # OF NEGATIVE VALUES= 12

*********RUN COMPLETE*********

CALIBRATION OF BACKSCATTER GAUGE:

TWO VARIABLE LINEAR REGRESSION ANALYSIS
****

MODEL FORM: Y = BO + B1*X

INPUT INFORMATION:
NUMBER OF CASES IS 25
DEFAULT "T" (.05,25) STATISTIC IS 2.06
DEFAULT "F" (.05,1,25) STATISTIC IS 4.24

VARIABLE	MEAN	STD. DEV.	MINIMUM VALUE	MAXIMUM VALUE
X	0.4121446E-01	0.6706199E-03	0.3976665E-01	0.4217482E-01
Y	0.5940274E+01	0.4549026E-01	0.5837851E+01	0.6006070E+01

COEFFICIENT	ESTIMATE	STD. ERR. B	CONF. INT.	SIGNIFICANT
BO	0.3196331E+01	0.1116725E+00	0.2300453E+00	YES
B1	0.6657718E+02	0.2709203E+01	0.5580956E+01	YES

(COVARIANCE(BO,B1)=-0.3025051E+00)

ANALYSIS OF VARIANCE

SOURCE	SUM OF SQUARES	DEGREES OF FREEDOM	MEAN SQUARE
REGRESSION(BO)	0.8821713E+03	1	0.4784261E-01
REGRESSION(B1/BO)	0.4784261E-01	1	0.7922223E-04
RESIDUAL	0.1822111E-02	23	
TOTAL (CORR.)	0.4966473E-01	24	
TOTAL (UNCORR.)	0.8822209E+03	25	

COEFFICIENT OF MULTIPLE DETERMINATION(R**2) IS 0.9601

SIGNIFICANCE OF REGRESSION AND PREDICTOR UTILITY   EQUATION CAN BE USED FOR PREDICTION:YES
CALC. F RATIO= 601.90   REGRESSION SIGNIFICANT:YES

OBSERV. #	Y(OBS.)	Y(PRED.)	X(OBS.)	RESIDUAL	STD. ERR. Y	CONF. LIMIT	OUTLIER
1	0.6006070E+01	0.6004211E+01	0.4217482E-01	0.1858551E-02	0.3152498E-02	0.6494143E-02	NO
2	0.5996590E+01	0.5999465E+01	0.4210353E-01	-0.2874984E-02	0.2995078E-02	0.6169859E-02	NO
3	0.5991073E+01	0.5997129E+01	0.4206843E-01	-0.6055625E-02	0.2919167E-02	0.6013483E-02	YES
4	0.5986919E+01	0.5994115E+01	0.4202317E-01	-0.7196324E-02	0.2822976E-02	0.5815329E-02	YES
5	0.5987024E+01	0.5994693E+01	0.4203185E-01	-0.7668876E-02	0.2841255E-02	0.5852984E-02	YES
6	0.5954420E+01	0.5956442E+01	0.4145732E-01	-0.2022486E-02	0.1897838E-02	0.3909546E-02	NO
7	0.5912414E+01	0.5918647E+01	0.4088963E-01	-0.6233239E-02	0.1985788E-02	0.4090723E-02	YES
8	0.5877636E+01	0.5880869E+01	0.4032204E-01	-0.3222834E-02	0.3002398E-02	0.6184939E-02	NO
9	0.5837851E+01	0.5843882E+01	0.3976665E-01	-0.6031326E-02	0.4307467E-02	0.8873380E-02	NO
10	0.5986594E+01	0.5981802E+01	0.4183823E-01	0.4791862E-02	0.2454519E-02	0.5056307E-02	YES
11	0.5982572E+01	0.5976448E+01	0.4175781E-01	0.6123665E-02	0.2309935E-02	0.4758465E-02	NO
12	0.5967861E+01	0.5969437E+01	0.4165250E-01	-0.1575559E-02	0.2139435E-02	0.4407235E-02	NO
13	0.5961365E+01	0.5965069E+01	0.4158690E-01	-0.3704378E-02	0.2046210E-02	0.4215192E-02	NO
14	0.5926213E+01	0.5932061E+01	0.4109111E-01	-0.5847869E-02	0.1811237E-02	0.3731147E-02	YES
15	0.5898715E+01	0.5903848E+01	0.4066734E-01	-0.5132541E-02	0.2316470E-02	0.4771927E-02	YES
16	0.5860857E+01	0.5868366E+01	0.4013439E-01	-0.7508531E-02	0.3425076E-02	0.7055656E-02	YES
17	0.5966444E+01	0.5951899E+01	0.4138907E-01	0.1454541E-01	0.1841919E-02	0.3794351E-02	YES
18	0.5948627E+01	0.5952335E+01	0.4139563E-01	-0.3708161E-02	0.1846561E-02	0.3803915E-02	NO
19	0.5948843E+01	0.5947503E+01	0.4132306E-01	0.1339547E-02	0.1804284E-02	0.3716825E-02	NO
20	0.5911218E+01	0.5921001E+01	0.4092498E-01	-0.9782626E-02	0.1945243E-02	0.4007200E-02	YES
21	0.5882074E+01	0.5893168E+01	0.4050693E-01	-0.1109398E-01	0.2615956E-02	0.5388868E-02	YES
22	0.5946631E+01	0.5930781E+01	0.4107188E-01	0.1629668E-01	0.1821565E-02	0.3752423E-02	YES
23	0.5938064E+01	0.5921767E+01	0.4093650E-01	0.1376711E-01	0.1932876E-02	0.3981723E-02	YES
24	0.5907781E+01	0.5894014E+01	0.4051964E-01	0.1376711E-01	0.2590839E-02	0.5337127E-02	YES
25	0.5922986E+01	0.5907899E+01	0.4072820E-01	0.1508665E-01	0.2214594E-02	0.4562062E-02	YES

RESIDUAL ANALYSIS: # OF POSITIVE VALUES= 9   # OF NEGATIVE VALUES= 16

*********RUN COMPLETE*********

CALIBRATION OF IRON GAUGE:

TWO VARIABLE LINEAR REGRESSION ANALYSIS
****

MODEL FORM: Y = BO + B1*X

INPUT INFORMATION:
NUMBER OF CASES IS 25
DEFAULT "T" (.05,25) STATISTIC IS 2.06
DEFAULT "F" (.05,1,25) STATISTIC IS 4.24

VARIABLE	MEAN	STD. DEV.	MINIMUM VALUE	MAXIMUM VALUE
X	0.8977685E-04	0.2335487E-04	0.5757050E-04	0.1402499E-03
Y	0.5072680E+01	0.1566846E+01	0.2749000E+01	0.8329000E+01

COEFFICIENT	ESTIMATE	STD. ERR. B	CONF. INT.	SIGNIFICANT
BO	-0.8481121E+00	0.2377549E+00	0.4897749E+00	YES
B1	0.6595010E+05	0.2566237E+04	0.5286448E+04	YES

(COVARIANCE(BO,B1)=-0.5912321E+03)

ANALYSIS OF VARIANCE

SOURCE	SUM OF SQUARES	DEGREES OF FREEDOM	MEAN SQUARE
REGRESSION(BO)	0.6433021E+03	1	0.5693731E+02
REGRESSION(B1/BO)	0.5693731E+02	1	0.8621042E-01
RESIDUAL	0.1982840E+01	23	
TOTAL (CORR.)	0.5892015E+02	24	
TOTAL (UNCORR.)	0.7022222E+03	25	

COEFFICIENT OF MULTIPLE DETERMINATION(R**2) IS 0.9634

SIGNIFICANCE OF REGRESSION AND PREDICTOR UTILITY
CALC. F RATIO= 658.45   REGRESSION SIGNIFICANT:YES   EQUATION CAN BE USED FOR PREDICTION:YES

OBSERV. #	Y(OBS.)	Y(PRED.)	X(OBS.)	RESIDUAL	STD. ERR. Y	CONF. LIMIT	
1	0.4083000E+01	0.3603024E+01	0.6749249E-04	0.4799755E+00	0.8196807E-01	0.1688542E+00	YES
2	0.4401000E+01	0.4191718E+01	0.7641885E-04	0.2092816E+00	0.6799648E-01	0.1400727E+00	YES
3	0.4984000E+01	0.4767165E+01	0.8514434E-04	0.2168346E+00	0.5991447E-01	0.1234238E+00	YES
4	0.5215000E+01	0.5383531E+01	0.9449028E-04	-0.1685314E+00	0.5995602E-01	0.1235094E+00	NO
5	0.6042000E+01	0.5947506E+01	0.1030418E-03	0.9449370E-01	0.6787644E-01	0.1398254E+00	NO
6	0.6464000E+01	0.6622806E+01	0.1132814E-03	-0.1588063E+00	0.8418256E-01	0.1734160E+00	NO
7	0.7308000E+01	0.7245979E+01	0.1227305E-03	0.6202091E-01	0.1029563E+00	0.2120899E+00	NO
8	0.7646000E+01	0.7827815E+01	0.1315529E-03	-0.1818152E+00	0.1222367E+00	0.2518076E+00	NO
9	0.8329000E+01	0.8401385E+01	0.1402499E-03	-0.7238465E-01	0.1422160E+00	0.2929648E+00	NO
10	0.3759000E+01	0.3819289E+01	0.7077172E-04	-0.6028948E-01	0.7633541E-01	0.1572509E+00	NO
11	0.4493000E+01	0.4417424E+01	0.7984122E-04	0.7557566E-01	0.6401971E-01	0.1318806E+00	YES
12	0.4898000E+01	0.5071345E+01	0.8975661E-04	-0.1733451E+00	0.5872324E-01	0.1209698E+00	YES
13	0.5403000E+01	0.5618739E+01	0.9805674E-04	-0.2157391E+00	0.6244918E-01	0.1286453E+00	YES*
14	0.5897000E+01	0.6062553E+01	0.1047863E-03	-0.1655527E+00	0.7022843E-01	0.1446705E+00	NO
15	0.6668000E+01	0.6596066E+01	0.1128759E-03	0.7193418E-01	0.8344017E-01	0.1718867E+00	YES
16	0.7428000E+01	0.7167718E+01	0.1215439E-03	0.2602823E+00	0.1004699E+00	0.2069680E+00	YES
17	0.2749000E+01	0.2948668E+01	0.5757050E-04	-0.1996678E+00	0.1013869E+00	0.2088569E+00	NO
18	0.3137000E+01	0.3304443E+01	0.6296511E-04	-0.1674433E+00	0.9045763E-01	0.1863427E+00	NO
19	0.3810000E+01	0.3759692E+01	0.6986803E-04	0.5030838E-01	0.7783753E-01	0.1603453E+00	NO
20	0.4786000E+01	0.4079531E+01	0.7471776E-04	0.7064686E+00	0.7029843E-01	0.1448147E+00	YES
21	0.5228000E+01	0.4627382E+01	0.8302481E-04	0.6006180E+00	0.6122625E-01	0.1261260E+00	YES
22	0.2926000E+01	0.3300624E+01	0.6290721E-04	-0.3746245E+00	0.9057072E-01	0.1865756E+00	YES
23	0.3436000E+01	0.3808147E+01	0.7060277E-04	-0.3721472E+00	0.7661314E-01	0.1578230E+00	YES
24	0.4271000E+01	0.4412043E+01	0.7975962E-04	-0.1410427E+00	0.6410340E-01	0.1320530E+00	YES
25	0.3456000E+01	0.3832404E+01	0.7097057E-04	-0.3764039E+00	0.7601038E-01	0.1565813E+00	YES

RESIDUAL ANALYSIS: # OF POSITIVE VALUES= 11   # OF NEGATIVE VALUES= 14

********RUN COMPLETE********

BACK-CALCULATION OF CALIBRATION DATA:

CASE NUMBER	% SOLIDS OBS.	% SOLIDS PRED.	% SOLIDS RESIDUAL	% ASH OBS.	% ASH PRED.	% ASH RESIDUAL	% IRON OBS.	% IRON PRED.	% IRON RESIDUAL	CONDITION NUMBER
1	22.08	22.49	-0.41	7.24	6.81	0.43	5.69	6.55	-0.86	29.77
2	24.54	24.05	0.49	7.36	7.28	0.08	5.67	6.09	-0.42	29.71
3	27.13	27.65	-0.52	7.38	7.56	-0.18	5.66	5.63	0.03	29.55
4	29.78	30.44	-0.66	7.41	7.86	-0.45	5.66	5.10	0.56	29.38
5	32.46	32.85	-0.39	7.34	7.60	-0.26	5.67	5.50	0.17	29.31
6	32.59	33.13	-0.54	8.39	8.58	-0.19	5.50	5.18	0.32	29.15
7	32.64	33.11	-0.47	9.47	9.68	-0.21	5.34	5.20	0.14	29.09
8	32.66	31.78	0.88	10.60	10.83	-0.23	5.18	5.12	0.06	28.97
9	32.77	31.65	1.12	11.73	12.06	-0.33	5.04	5.06	-0.02	29.84
10	21.24	20.89	0.35	8.20	7.94	0.26	5.53	5.73	-0.20	29.69
11	23.73	23.37	0.36	8.25	7.84	0.41	5.52	5.97	-0.45	29.61
12	26.30	25.56	0.74	8.34	8.48	-0.14	5.51	5.43	0.08	29.51
13	28.55	27.43	1.12	8.35	8.57	-0.22	5.51	5.43	0.08	29.43
14	28.11	27.23	0.88	9.47	9.81	-0.34	5.34	5.22	0.12	29.28
15	28.56	28.22	0.34	10.38	10.56	-0.18	5.21	5.24	-0.03	29.14
16	28.71	28.64	0.07	11.59	11.76	-0.17	5.06	5.17	-0.11	30.06
17	20.96	21.96	-1.00	10.71	10.04	0.67	3.56	3.41	0.15	29.98
18	23.27	23.94	-0.67	10.37	10.70	-0.33	3.60	3.26	0.34	29.84
19	25.85	26.78	-0.93	10.28	10.19	0.09	3.55	3.89	-0.06	29.65
20	25.74	26.97	-1.23	11.34	11.27	0.07	3.68	3.92	-0.34	29.57
21	25.61	26.55	-0.94	12.33	12.38	-0.05	3.57	3.41	-0.24	30.03
22	21.14	21.16	-0.02	11.65	11.04	0.61	3.57	3.45	0.16	29.92
23	23.77	23.68	0.09	11.59	11.02	0.57	3.75	3.89	-0.12	29.76
24	23.70	23.21	0.49	12.61	12.01	0.60	3.75	3.89	-0.14	29.92
25	21.36	20.48	0.88	12.53	12.03	0.50	3.73	3.72	-0.01	29.92

RESIDUAL ANALYSIS:

VARIABLE	MEAN VALUE	RESIDUAL MEAN	RESIDUAL STD DEV	RELATIVE ERROR	RANGE ERROR
% SOLIDS	26.53	0.00	0.72	2.72	6.11
% ASH	9.80	0.04	0.36	3.65	6.65
% IRON	4.79	-0.02	0.29	6.09	13.63

12.4 RESULTS FOR CALIBRATION RUN 3: ALL DATA

INPUT INFORMATION:
****

MODEL PARAMETERS:

SPECIES	SPECIFIC GRAVITY	SCATTERING COEFFICIENT CM**2/G	TOTAL MASS ABSORPTION COEFFICIENT AT 22 KEV CM**2/G	AT 6.4 KEV CM**2/G
WATER *	1.00	0.0540	0.6374	19.8080
ORGANICS	1.28	0.0507	0.4344	10.6070
MINERAL MATTER	2.37	0.0506	2.0950	74.3310
IRON MINERALS	5.10	0.0549	13.8680	55.9200

SAMPLE ANALYSES:

CASE NUMBER	% SOLIDS BY WT IN PULP	% ASH BY WT IN SOLIDS	% IRON BY WT IN ASH SOLIDS
1	1.10	32.40	3.90
2	2.15	32.29	3.90
3	3.23	32.92	3.91
4	4.50	32.66	3.91
5	5.63	33.08	3.91
6	1.03	34.09	3.91
7	2.11	34.05	3.91
8	3.29	35.41	3.92
9	4.43	35.98	3.92
10	5.56	35.91	3.92
11	1.11	38.13	3.93
12	2.07	37.21	3.94
13	3.19	37.99	3.94
14	4.41	38.87	3.94
15	5.55	38.85	3.95
16	1.04	39.48	3.96
17	2.21	40.47	3.96
18	3.33	40.91	3.96
19	4.55	41.15	3.97
20	5.68	41.44	3.97
21	1.10	44.39	4.01
22	2.23	43.79	4.00
23	3.29	44.05	4.00

24	4.34	43.71	4.00
25	5.69	44.18	4.00

RADIATION MEASUREMENTS:

CASE NUMBER	REDUCED DENSITY	BACKSCATTER COUNTS (x 1E-06)	IRON FLUORESCENCE COUNTS (x 1E-04)
1	0.997280	10.550379	0.529000
2	0.978530	10.482260	1.696000
3	0.972380	10.419597	2.496000
4	0.960370	10.351724	3.864000
5	0.950480	10.289182	4.790000
6	0.989310	10.532543	0.803000
7	0.983820	10.462132	2.146000
8	0.969220	10.384149	3.041000
9	0.960120	10.320749	3.943000
10	0.944320	10.232708	5.414000
11	0.987500	10.516073	1.090000
12	0.980770	10.442373	1.747000
13	0.964850	10.349414	3.406000
14	0.952170	10.273763	4.450000
15	0.933760	10.204092	5.130000
16	0.989390	10.508805	1.424000
17	0.972140	10.414876	2.854000
18	0.962630	10.336678	3.928000
19	0.954100	10.236924	5.419000
20	0.939170	10.144000	6.652000
21	0.992730	10.472705	1.658000
22	0.971770	10.381948	2.875000
23	0.954860	10.298769	4.226000
24	0.941710	10.200385	5.359000
25	0.928690	10.102627	6.791000

CALIBRATION OF DENSITY GAUGE:

TWO VARIABLE LINEAR REGRESSION ANALYSIS

MODEL FORM Y = BO + B1*X

INPUT INFORMATION:
NUMBER OF CASES IS 25
DEFAULT "T" (.05,25) STATISTIC IS 2.06
DEFAULT "F" (.05,1,25) STATISTIC IS 4.24

VARIABLE	MEAN	STD. DEV	MINIMUM VALUE	MAXIMUM VALUE
X	0.1012667E+01	0.6431188E-02	0.1003712E+01	0.1023301E+01
Y	-0.3552853E-01	0.2013392E-01	-0.7398029E-01	-0.1000000E-69

COEFFICIENT	ESTIMATE	STD. ERR B	CONF INT	SIGNIFICANT
BO	0.3038099E+01	0.1620259E+00	0.3337733E+00	YES
B1	-0.3035180E+01	0.1599961E+00	0.3295918E+00	YES

(COVARIANCE(BO,B1)=-0.2592300E-01)

ANALYSIS OF VARIANCE

SOURCE	SUM OF SQUARES	DEGREES OF FREEDOM	MEAN SQUARE
REGRESSION(BO)	0.3155691E-01	1	0.9144555E-02
REGRESSION(B1/BO)	0.9144555E-02	1	0.2541044E-04
RESIDUAL	0.5844401E-03	23	
TOTAL (CORR.)	0.9728995E-02	24	
TOTAL (UNCORR.)	0.4128590E-01	25	

COEFFICIENT OF MULTIPLE DETERMINATION($R**2$) IS 0.9347

SIGNIFICANCE OF REGRESSION AND PREDICTOR UTILITY
CALC. F RATIO= 357.87   REGRESSION SIGNIFICANT:YES   EQUATION CAN BE USED FOR PREDICTION:YES

OBSERV. #	Y(OBS.)	Y(PRED.)	X1(OBS.)	RESIDUAL	STD ERR	CONF LIMIT	OUTLIER
1	-0.2723706E-02	-0.8885402E-02	0.1003889E+01	0.8161696E-02	0.7288535E-02	0.3561435E-02	YES
2	-0.2170383E-01	-0.2020940E-01	0.1007620E+01	-0.1494437E-02	0.2917713E-02	0.2660929E-02	NO
3	-0.2800860E-01	-0.3221855E-01	0.1011577E+01	0.4209947E-02	0.1023162E-02	0.2107143E-02	YES
4	-0.4043665E-01	-0.4610904E-01	0.1016153E-01	0.5672385E-02	0.1152168E-02	0.2373465E-02	YES
5	-0.5078816E-01	-0.5897382E-01	0.1020392E+01	0.8185666E-02	0.1594944E-02	0.3285584E-02	NO
6	-0.1074755E-01	-0.8348030E-02	0.1007312E+01	-0.2399519E-02	0.175 942E-02	0.3609000E-02	YES
7	0.1631233E-01	-0.2024140E-01	0.1007631E+00	0.3929070E-02	0.1290659E-02	0.2658758E-02	YES
8	-0.3126365E-01	-0.3391453E-01	0.1012135E+01	0.2650870E-02	0.1017759E-02	0.2084223E-02	YES
9	-0.4069700E-01	-0.4720857E-01	0.1016515E+01	0.6511569E-02	0.1813 5E-02	0.2430508E-02	NO
10	-0.5729019E-01	-0.6021116E-01	0.1020799E+00	0.2920971E-02	0.1646002E-02	0.3397763E-02	NO
11	-0.1257878E-01	-0.9785340E-02	0.1004186E+00	-0.2793442E-01	0.169054 E-01	0.3482513E-01	NO
12	-0.1941730E-01	-0.2061945E-01	0.1007755E+01	-0.1202151E-02	0.12783 1E-02	0.2633321E-02	NO
13	-0.3578263E-01	-0.3382346E-01	0.1012105E+01	0.1959166E-02	0.1012174E-02	0.2085078E-02	NO
14	-0.4901169E-01	-0.4860654E-01	0.1016976E+01	-0.4051517E-03	0.122 343E-02	0.25 5967E-02	YES
15	-0.6853583E-01	-0.6219754E-01	0.1021454E+01	0.6338293E-01	0.12996 E-02	0.3563 09E-02	YES
16	-0.1066669E-01	-0.9155968E-02	0.1003978E+01	0.1510719E-02	0.17 286E-02	0.3537609E-02	NO
17	-0.2825545E-01	-0.2313079E-01	0.1008583E+01	0.5124665E-02	0.120 467E-02	0.2475021E-02	YES
18	-0.3808616E-01	-0.3668932E-01	0.1013050E+01	0.1396841E-02	0.1010903E-02	0.2080662E-02	NO
19	-0.4698679E-01	-0.5160185E-01	0.1017963E+01	0.4615057E-02	0.1319903E-02	0.27 2881E-02	YES
20	-0.6275877E-01	-0.6565959E-01	0.1022595E+01	0.2900820E-02	0.188 2 4E-02	0.3875424E-02	NO
21	-0.7296555E-02	-0.1053034E-01	0.1004431E+01	0.3233781E-02	0.1659182E-02	0.3419715E-02	NO
22	-0.2863613E-01	-0.2430186E-01	0.1008968E+01	-0.4334268E-02	0.1169006E-02	0.2408214E-02	YES
23	-0.4619055E-01	-0.3752113E-01	0.1013324E+01	0.8669419E-01	0.1036024E-01	0.2088082E-01	YES
24	-0.6005791E-01	-0.5046675E-01	0.1017589E+01	-0.959 160E-02	0.1279256E-02	0.2635268E-02	YES
25	-0.7398029E-01	-0.6780339E-01	0.1023301E+01	0.6 76902E-02	0.1977 2 E-02	0.4073880E-02	YES

RESIDUAL ANALYSIS   # OF POSITIVE VALUES= 12   # OF NEGATIVE VALUES= 13

••••••••RUN COMPLETE••••••••

CALIBRATION OF BACKSCATTER GAUGE

TWO VARIABLE LINEAR REGRESSION ANALYSIS
••••••••••••••••••••••••••••••

MODEL FORM Y = BO + B1*X

INPUT INFORMATION:
NUMBER OF CASES IS 25
DEFAULT "T" (.05, 25) STATISTIC IS 2.06
DEFAULT "F" (.05, 1, 25) STATISTIC IS 4.24

VARIABLE	MEAN	STD DEV	MINIMUM VALUE	MAXIMUM VALUE
X	0.4069973E-01	0.8481360E-03	0.3907020E-01	0.4189713E-01
Y	0.1035681E+02	0.1259268E+00	0.1010263E+02	0.1055038E+02

COEFFICIENT	ESTIMATE	STD ERR B	CONF INT	SIGNIFICANT
BO	0.4365859E+01	0.1648732E+00	0.3396386E+00	YES
B1	0.1471988E+03	0.4050121E+01	0.8343247E+01	YES

(COVARIANCE(BO,B1)=-0.6676171E+00)

ANALYSIS OF VARIANCE

SOURCE	SUM OF SQUARES	DEGREES OF FREEDOM	MEAN SQUARE
REGRESSION(BO)	0.2681588E+04	1	0.3740682E+00
REGRESSION(B1/BO)	0.3740682E+00	1	0.2831902E-03
RESIDUAL	0.6513374E-02	23	
TOTAL (CORR)	0.3805816E+00	24	
TOTAL (UNCORR)	0.2681969E+04	25	

COEFFICIENT OF MULTIPLE DETERMINATION(R**2) IS 0.9814

SIGNIFICANCE OF REGRESSION AND PREDICTOR UTILITY   EQUATION CAN BE USED FOR PREDICTION YES
CALC F RATIO= 1318.91   REGRESSION SIGNIFICANT YES

OBSERV. #	Y(OBS)	Y(PRED)	X(OBS)	RESIDUAL	STD ERR Y	CONF LIMIT	OUTLIER
1	0.1055038E+02	0.1053297E+02	0.4189645E-01	0.1741231E-01	0.5900835E-02	0.1215572E-01	YES
2	0.1049226E+02	0.1046974E+02	0.4146691E-01	0.2252183E-01	0.4580624E-02	0.9436083E-02	YES
3	0.1041960E+02	0.1040087E+02	0.4099906E-01	0.1872552E-01	0.3577338E-02	0.7369315E-02	YES
4	0.1035172E+02	0.1032801E+02	0.4050408E-01	0.2371334E-01	0.3457676E-02	0.7122810E-02	YES
5	0.1028918E+02	0.1025777E+02	0.4002691E-01	0.3140932E-01	0.4330489E-02	0.8920805E-02	YES
6	0.1053254E+02	0.1053307E+02	0.4189713E-01	-0.5237964E-03	0.5903097E-02	0.1216038E-01	NO
7	0.1046213E+02	0.1046338E+02	0.4142369E-01	-0.1244541E-02	0.4463744E-02	0.9195310E-02	NO
8	0.1038415E+02	0.1037849E+02	0.4084698E-01	0.5663617E-02	0.3418081E-02	0.7041246E-02	NO
9	0.1032075E+02	0.1029923E+02	0.4030853E-01	0.2152322E-01	0.3719943E-02	0.7663081E-02	YES
10	0.1023211E+02	0.1022744E+02	0.3982082E-01	0.4673420E-02	0.4898882E-02	0.1009169E-01	NO
11	0.1051807E+02	0.1051701E+02	0.4178802E-01	0.1066938E-02	0.5545780E-02	0.1142430E-01	NO
12	0.1044237E+02	0.1045050E+02	0.4136623E-01	-0.8129099E-02	0.4239476E-02	0.8733319E-02	YES
13	0.1034941E+02	0.1036604E+02	0.4076242E-01	-0.1662377E-01	0.3375214E-02	0.6952939E-02	YES
14	0.1027376E+02	0.1027201E+02	0.4012363E-01	0.1753601E-02	0.4095330E-02	0.8436378E-02	NO
15	0.1020409E+02	0.1019248E+02	0.3958333E-01	0.1161391E-01	0.5636658E-02	0.1161151E-01	NO
16	0.1050880E+02	0.1051885E+02	0.4180055E-01	-0.1004489E-01	0.5586187E-02	0.1150754E-01	NO
17	0.1041488E+02	0.1042353E+02	0.4115302E-01	-0.8658078E-02	0.3838806E-02	0.7897639E-02	YES
18	0.1033668E+02	0.1033388E+02	0.4054397E-01	0.2794824E-02	0.3424260E-02	0.7053973E-02	NO
19	0.1023692E+02	0.1023872E+02	0.3989750E-01	-0.1799764E-02	0.4678065E-02	0.9636812E-02	NO
20	0.1014400E+02	0.1015140E+02	0.3930427E-01	-0.7399687E-02	0.6578024E-02	0.1355073E-01	NO
21	0.1047270E+02	0.1050092E+02	0.4167878E-01	-0.2821992E-01	0.5201049E-02	0.1071416E-01	YES
22	0.1038195E+02	0.1040437E+02	0.4102282E-01	-0.2242019E-01	0.3611078E-02	0.7438818E-02	YES
23	0.1029877E+02	0.1031305E+02	0.4040241E-01	-0.1427670E-01	0.3574580E-02	0.7363633E-02	YES
24	0.1020039E+02	0.1022960E+02	0.3983550E-01	-0.2921251E-01	0.4855830E-02	0.1000301E-01	YES
25	0.1010263E+02	0.1011695E+02	0.3907020E-01	-0.1431890E-01	0.7408420E-02	0.1526134E-01	NO

RESIDUAL ANALYSIS: # OF POSITIVE VALUES= 12   # OF NEGATIVE VALUES= 13

••••••••RUN COMPLETE•••••••••

CALIBRATION OF IRON GAUGE

TWO VARIABLE LINEAR REGRESSION ANALYSIS
....

MODEL FORM Y = BO + B1*X

INPUT INFORMATION.
NUMBER OF CASES IS 25
DEFAULT "T" (.05,25) STATISTIC IS 2.06
DEFAULT "F" (.05,1,25) STATISTIC IS 4.24

VARIABLE	MEAN	STD. DEV	MINIMUM VALUE	MAXIMUM VALUE
X	0.3386683E-04	0.1723289E-04	0.9534574E-05	0.6626513E-04
Y	0.3429240E+01	0.1797135E+01	0.5290000E+00	0.6791000E+01

COEFFICIENT	ESTIMATE	STD ERR B	CONF INT	SIGNIFICANT
BO	-0.5783425E-01	0.1305544E+00	0.2689420E+00	NO
B1	0.1029643E+06	0.3449941E+04	0.7106876E+04	YES

(COVARIANCE(BO,B1)=-0.4030861E+03)

ANALYSIS OF VARIANCE

SOURCE	SUM OF SQUARES	DEGREES OF FREEDOM	MEAN SQUARE
REGRESSION(BO)	0.2939822E+03	1	
REGRESSION(B1/BO)	0.7556156E+02	1	0.7556156E+02
RESIDUAL	0.1951096E+01	23	0.8483027E-01
TOTAL (CORR.)	0.7751266E+02	24	
TOTAL (UNCORR)	0.3715048E+03	25	

COEFFICIENT OF MULTIPLE DETERMINATION(R**2) IS 0.9726

SIGNIFICANCE OF REGRESSION AND PREDICTOR UTILITY   EQUATION CAN BE USED FOR PREDICTION YES
CALC. F RATIO= 888.74   REGRESSION SIGNIFICANT.YES

OBSERV. #	Y(OBS.)	Y(PRED.)	X(OBS.)	RESIDUAL	STD. ERR. Y	CONF. LIMIT	OUTLIER
1	0.5290000E+00	0.9362163E+00	0.9654322E-05	-0.4072163E+00	0.1018369E+00	0.2097840E+00	YES
2	0.1696000E+01	0.1865137E+01	0.1876609E-04	-0.1691368E+00	0.7835635E-01	0.1614140E+00	YES
3	0.2496000E+01	0.2872053E+01	0.2845537E-04	-0.3760534E+00	0.6116984E-01	0.1260098E+00	NO
4	0.3864000E+01	0.3958888E+01	0.3901082E-04	-0.9488774E-01	0.6089457E-01	0.1254428E+00	YES
5	0.4790000E+01	0.4990303E+01	0.4902803E-04	-0.2003026E+00	0.7828825E-01	0.1612737E+00	NO
6	0.8030000E+00	0.9238865E+00	0.9534574E-05	-0.1208865E+00	0.1021761E+00	0.2104826E+00	YES
7	0.2146000E+01	0.1935301E+01	0.1935753E-04	0.2106994E+00	0.7680387E-01	0.1582159E+00	NO
8	0.3041000E+01	0.3150118E+01	0.3115597E-04	-0.1091183E+00	0.5899726E-01	0.1215343E+00	YES
9	0.3943000E+01	0.4289818E+01	0.4222485E-04	-0.3468176E+00	0.6499730E-01	0.1338944E+00	NO
10	0.5414000E+01	0.5341810E+01	0.5241191E-04	0.7218996E-01	0.8660157E-01	0.1783992E+00	NO
11	0.1090000E+01	0.1132051E+01	0.1155629E-04	-0.4205079E-01	0.9652771E-01	0.1988470E+00	YES
12	0.1747000E+01	0.2085699E+01	0.2081821E-04	-0.3386987E+00	0.7361885E-01	0.1516548E+00	NO
13	0.3406000E+01	0.3289414E+01	0.3250883E-04	0.1165856E+00	0.5843937E-01	0.1203851E+00	YES
14	0.4450000E+01	0.4622251E+01	0.4545348E-04	-0.1722514E+00	0.7064752E-01	0.1455339E+00	YES
15	0.5130000E+01	0.5771710E+01	0.5661714E-04	-0.6417102E+00	0.9774179E-01	0.2013480E+00	YES
16	0.1424000E+01	0.1099553E+01	0.1124066E-04	0.3244473E+00	0.9739819E-01	0.2006402E+00	YES
17	0.2854000E+01	0.2441084E+01	0.2426976E-04	0.4129156E+00	0.6700327E-01	0.1380267E+00	YES
18	0.3928000E+01	0.3707064E+01	0.3656508E-04	0.2209359E+00	0.5899038E-01	0.1215202E+00	YES
19	0.5419000E+01	0.5068880E+01	0.4979118E-04	0.3501199E+00	0.8007124E-01	0.1649467E+00	YES
20	0.6652000E+01	0.6316119E+01	0.6190450E-04	0.3358807E+00	0.1129140E+00	0.2326028E+00	YES
21	0.1658000E+01	0.1336106E+01	0.1353809E-04	0.3218940E+00	0.9116929E-01	0.1878087E+00	YES
22	0.2875000E+01	0.2690632E+01	0.2669339E-04	0.1843680E+00	0.6329037E-01	0.1303781E+00	YES
23	0.4226000E+01	0.3975202E+01	0.3916926E-04	0.2507983E+00	0.6105611E-01	0.1257755E+00	YES
24	0.5359000E+01	0.5166595E+01	0.5074020E-04	0.1924046E+00	0.8235208E-01	0.1696452E+00	YES
25	0.6791000E+01	0.6765109E+01	0.6626513E-04	0.2589114E-01	0.1260406E+00	0.2596437E+00	NO

RESIDUAL ANALYSIS: # OF POSITIVE VALUES= 13   # OF NEGATIVE VALUES= 12

*********RUN COMPLETE*********

BACK-CALCULATION OF CALIBRATION DATA

CASE NUMBER	% SOLIDS OBS	PRED	RESIDUAL	% ASH OBS	PRED	RESIDUAL	% IRON OBS	PRED	RESIDUAL	CONDITION NUMBER
1	1.10	0.39	0.71	32.40	63.01	-30.61	3.90	3.33	0.57	31.10
2	2.15	2.51	-0.36	32.29	24.65	7.64	3.90	3.98	-0.08	30.94
3	3.23	2.80	0.43	32.92	34.39	-1.47	3.91	3.76	0.15	30.84
4	4.50	3.99	0.51	32.66	32.44	0.22	3.91	4.32	-0.41	30.66
5	5.63	4.87	0.76	33.08	33.45	-0.37	3.91	4.27	-0.36	30.55
6	1.03	1.31	-0.28	34.09	30.13	3.96	3.91	3.05	0.86	31.06
7	2.11	1.64	0.47	34.05	40.08	-6.03	3.91	4.73	-0.82	30.89
8	3.29	2.99	0.30	35.41	37.43	-2.02	3.92	3.94	-0.02	30.77
9	4.43	3.75	0.68	35.98	38.59	-2.61	3.92	3.96	-0.04	30.66
10	5.56	5.26	0.30	35.91	36.75	-0.84	3.92	4.10	-0.18	30.47
11	1.11	1.47	-0.36	38.13	30.97	7.16	3.94	3.54	0.40	31.03
12	2.07	1.78	0.29	37.21	46.85	-9.64	3.93	3.06	0.87	30.94
13	3.19	3.30	-0.11	37.99	39.52	-1.53	3.94	3.79	0.15	30.73
14	4.41	4.45	-0.04	38.87	38.89	-0.02	3.94	3.76	0.18	30.59
15	5.55	6.33	-0.78	38.85	35.36	3.49	3.94	3.38	0.56	30.51
16	1.04	1.20	-0.16	39.48	36.68	2.80	3.95	4.71	-0.76	30.98
17	2.21	2.85	-0.64	40.47	33.28	7.19	3.96	4.34	-0.38	30.79
18	3.33	3.57	-0.24	40.91	37.49	3.42	3.96	4.26	-0.30	30.66
19	4.55	4.02	0.53	41.15	44.52	-3.37	3.97	4.43	-0.46	30.47
20	5.68	5.31	0.37	41.44	43.75	-2.31	3.97	4.24	-0.27	30.32
21	1.10	0.49	0.61	44.39	112.32	-67.93	4.01	4.36	-0.35	30.95
22	2.23	2.61	-0.38	43.79	42.92	0.87	4.00	3.74	0.26	30.80
23	3.29	4.29	-1.00	44.05	37.14	6.91	4.00	3.87	0.13	30.62
24	4.34	5.29	-0.95	43.71	40.43	3.28	4.00	3.70	0.30	30.48
25	5.69	6.31	-0.62	44.18	42.09	2.09	4.00	3.81	0.19	30.30

RESIDUAL ANALYSIS:

VARIABLE	MEAN VALUE	RESIDUAL MEAN	RESIDUAL STD DEV	RELATIVE ERROR	RANGE ERROR
% SOLIDS	3.31	0.00	0.54	16.44	11.68
% ASH	38.14	-3.19	15.45	40.53	*****
% IRON	3.94	0.01	0.45	11.36	*****

12.5 RESULTS FOR CALIBRATION RUN 3: PARTIAL DATA

INPUT INFORMATION:
****

MODEL PARAMETERS:

SPECIES	SPECIFIC GRAVITY	SCATTERING COEFFICIENT CM**2/G	TOTAL MASS ABSORPTION COEFFICIENT AT 22 KEV CM**2/G	AT 6.4 KEV CM**2/G
WATER	1.00	0.0540	0.6374	19.8080
ORGANICS	1.28	0.0507	0.4344	10.6070
MINERAL MATTER	2.37	0.0506	2.0950	74.3310
IRON MINERALS	5.10	0.0549	13.8680	55.9200

SAMPLE ANALYSES:

CASE NUMBER	% SOLIDS BY WT. IN PULP	% ASH BY WT. IN SOLIDS	% IRON BY WT. IN ASH SOLIDS
1	3.23	32.92	3.91
2	4.50	32.66	3.91
3	5.63	33.08	3.91
4	3.29	35.41	3.92
5	4.43	35.98	3.92
6	5.56	35.91	3.92
7	3.19	37.99	3.94
8	4.41	38.87	3.94
9	5.55	38.85	3.94
10	3.33	40.91	3.96
11	4.55	41.15	3.97
12	5.68	41.44	3.97
13	3.29	44.05	4.00
14	4.34	43.71	4.00
15	5.69	44.18	4.00

RADIATION MEASUREMENTS:

CASE NUMBER	REDUCED DENSITY	BACKSCATTER COUNTS	IRON FLUORESCENCE COUNTS

		(X 1E-06)	(X 1E-04)
1	0.972380	10.419597	2.496000
2	0.960370	10.351724	3.864000
3	0.950480	10.289182	4.790000
4	0.969220	10.384149	3.041000
5	0.960120	10.320748	3.943000
6	0.844320	10.232109	5.414000
7	0.964850	10.349414	3.406000
8	0.952170	10.273763	4.450000
9	0.933760	10.204092	5.130000
10	0.962630	10.336678	3.928000
11	0.954100	10.236924	5.419000
12	0.939170	10.144000	6.652000
13	0.954860	10.298769	4.226000
14	0.941710	10.200385	5.359000
15	0.928690	10.102627	6.791000

CALIBRATION OF DENSITY GAUGE:

TWO VARIABLE LINEAR REGRESSION ANALYSIS
****

MODEL FORM: Y = B0 + B1*X

INPUT INFORMATION:
NUMBER OF CASES IS   15
DEFAULT "T" (.05,25) STATISTIC IS 2.06
DEFAULT "F" (.05,1,25) STATISTIC IS 4.24

VARIABLE	MEAN	STD. DEV.	MINIMUM VALUE	MAXIMUM VALUE
X	0.1017062E+01	0.4009780E-02	0.1011577E+01	0.1023301E+01
Y	-0.4865832E-01	0.1360321E-01	-0.7398029E-01	-0.1000000E-69

COEFFICIENT	ESTIMATE	STD. ERR. B	CONF. INT	SIGNIFICANT
B0	0.3084191E+01	0.4010061E+00	0.8260724E+00	YES
B1	-0.3080294E+01	0.3942761E+00	0.8122086E+00	YES

(COVARIANCE(B0,B1)=-0.1581060E+00)

ANALYSIS OF VARIANCE

SOURCE	SUM OF SQUARES	DEGREES OF FREEDOM	MEAN SQUARE
REGRESSION(B0)	0.3551449E-01	1	
REGRESSION(B1/B0)	0.2135765E-02	1	0.2135765E-02
RESIDUAL	0.4548974E-03	13	0.3499211E-04
TOTAL (CORR.)	0.2590663E-02	14	
TOTAL (UNCORR.)	0.3810515E-01	15	

COEFFICIENT OF MULTIPLE DETERMINATION(R**2) IS 0.7974

SIGNIFICANCE OF REGRESSION AND PREDICTOR UTILITY   EQUATION CAN BE USED FOR PREDICTION:YES
CALC. F RATIO=   59.04   REGRESSION SIGNIFICANT:YES

OBSERV. #	Y(OBS.)	Y(PRED.)	X(OBS.)	RESIDUAL	STD. ERR. Y	CONF. LIMIT	OUTLIER
1	-0.2800860E-01	-0.3176240E-01	0.1011577E+01	0.3753799E-02	0.2647631E-02	0.5454118E-02	NO
2	-0.4043665E-01	-0.4585935E-01	0.1016153E+01	0.5422701E-02	0.1568809E-02	0.3231746E-02	YES
3	-0.5078816E-01	-0.5891536E-01	0.1020392E+01	0.8127201E-02	0.2014076E-02	0.4148995E-02	YES
4	-0.3126365E-01	-0.3348358E-01	0.1012135E+01	0.2219930E-02	0.2470945E-02	0.5090144E-02	NO
5	-0.4069700E-01	-0.4697523E-01	0.1016515E+01	0.6278229E-02	0.1542472E-02	0.3177491E-02	YES
6	-0.5729019E-01	-0.6017108E-01	0.1020799E+01	0.2880897E-02	0.2123354E-02	0.4372048E-02	NO
7	-0.3578263E-01	-0.3339117E-01	0.1012105E+01	-0.2391458E-02	0.2480254E-02	0.5109322E-02	NO
8	-0.4901169E-01	-0.4839398E-01	0.1016976E+01	-0.6177136E-03	0.1527728E-02	0.3147118E-02	YES
9	-0.6853583E-01	-0.6218699E-01	0.1021454E+01	-0.6348841E-02	0.2308996E-02	0.4756531E-02	NO
10	-0.3808616E-01	-0.3629962E-01	0.1013050E+01	-0.1786538E-02	0.2198918E-02	0.4529770E-02	YES
11	-0.4698679E-01	-0.5143381E-01	0.1017963E+01	0.4447016E-02	0.1568125E-02	0.3230337E-02	NO
12	-0.6275877E-01	-0.6570050E-01	0.1022595E+01	0.2941730E-02	0.2662944E-02	0.5485664E-02	YES
13	-0.4619055E-01	-0.3714379E-01	0.1013324E+01	-0.9046751E-02	0.2122511E-02	0.4372372E-02	YES
14	-0.6005791E-01	-0.5028184E-01	0.1017589E+01	-0.9776072E-02	0.1541425E-02	0.3175335E-02	YES
15	-0.7398029E-01	-0.6787616E-01	0.1023301E+01	-0.6104127E-02	0.2895477E-02	0.5964681E-02	YES

RESIDUAL ANALYSIS: # OF POSITIVE VALUES= 8   # OF NEGATIVE VALUES= 7

*********RUN COMPLETE*********

CALIBRATION OF BACKSCATTER GAUGE:

TWO VARIABLE LINEAR REGRESSION ANALYSIS
•••••••••••••••••••••••••••••••••••••••

MODEL FORM: Y = BO + B1*X

INPUT INFORMATION:
NUMBER OF CASES IS 15
DEFAULT "T" (.05,25) STATISTIC IS 2.06
DEFAULT "F" (.05,1,25) STATISTIC IS 4.24

VARIABLE	MEAN	STD. DEV.	MINIMUM VALUE	MAXIMUM VALUE
X	0.4013531E-01	0.5629729E-03	0.3907020E-01	0.4099906E-01
Y	0.1027628E+02	0.8930058E-01	0.1010263E+02	0.1041960E+02

COEFFICIENT	ESTIMATE	STD. ERR. B	CONF. INT.	SIGNIFICANT
BO	0.4016881E+01	0.3223903E+00	0.6641239E+00	YES
B1	0.1559574E+03	0.8031849E+01	0.1654561E+02	YES

(COVARIANCE(BO,B1)=-0.2589153E+01)

ANALYSIS OF VARIANCE

SOURCE	SUM OF SQUARES	DEGREES OF FREEDOM	MEAN SQUARE
REGRESSION(BO)	0.1584028E+04	1	
REGRESSION(B1/BO)	0.1079232E+00	1	0.1079232E+00
RESIDUAL	0.3721152E-02	13	0.2862425E-03
TOTAL (CORR.)	0.1116443E+00	14	
TOTAL (UNCORR.)	0.1584140E+04	15	

COEFFICIENT OF MULTIPLE DETERMINATION(R**2) IS 0.9615

SIGNIFICANCE OF REGRESSION AND PREDICTOR UTILITY
CALC. F RATIO= 375.03   REGRESSION SIGNIFICANT:YES   EQUATION CAN BE USED FOR PREDICTION:YES

OBSERV. #	Y(OBS.)	Y(PRED.)	X(OBS.)	RESIDUAL	STD. ERR. Y	CONF. LIMIT	OUTLIER
1	0.1041960E+02	0.1041099E+02	0.4099906E-01	0.8611007E-02	0.8198301E-02	0.1688850E-01	NO
2	0.1035172E+02	0.1033379E+02	0.4050408E-01	0.1793416E-01	0.5277851E-02	0.1087237E-01	YES
3	0.1028918E+02	0.1025937E+02	0.4002691E-01	0.2980939E-01	0.4454300E-02	0.9175855E-02	YES
4	0.1038415E+02	0.1038727E+02	0.4084698E-01	-0.3118889E-02	0.7194160E-02	0.1481997E-01	NO
5	0.1032075E+02	0.1030329E+02	0.4030853E-01	0.1745678E-01	0.4584589E-02	0.9444251E-02	YES
6	0.1023211E+02	0.1022723E+02	0.3982082E-01	0.4878602E-02	0.5046107E-02	0.1039498E-01	NO
7	0.1034941E+02	0.1037408E+02	0.4076242E-01	-0.2466563E-01	0.6667277E-02	0.1373459E-01	YES
8	0.1027376E+02	0.1027446E+02	0.4012363E-01	-0.6934251E-03	0.4369397E-02	0.9009955E-02	NO
9	0.1020409E+02	0.1019019E+02	0.3958333E-01	0.1389912E-01	0.6223962E-02	0.1282136E-01	YES
10	0.1033668E+02	0.1034001E+02	0.4054397E-01	-0.3333784E-02	0.5464116E-02	0.1125608E-01	NO
11	0.1023692E+02	0.1023919E+02	0.3989750E-01	-0.2266245E-02	0.4767698E-02	0.9821455E-02	NO
12	0.1014400E+02	0.1014667E+02	0.3930427E-01	-0.2670256E-02	0.7977212E-02	0.1643305E-01	YES
13	0.1029877E+02	0.1031793E+02	0.4040241E-01	-0.1916545E-01	0.4866759E-02	0.1002552E-01	YES
14	0.1020039E+02	0.1022952E+02	0.3983550E-01	-0.2913596E-01	0.4988103E-02	0.1027549E-01	YES
15	0.1010263E+02	0.1011017E+02	0.3907020E-01	-0.7539415E-02	0.9605565E-02	0.1978746E-01	NO

RESIDUAL ANALYSIS: # OF POSITIVE VALUES= 6   # OF NEGATIVE VALUES= 9

*******RUN COMPLETE*********

CALIBRATION OF IRON GAUGE:

TWO VARIABLE LINEAR REGRESSION ANALYSIS

MODEL FORM: Y = BO + B1*X

INPUT INFORMATION:
NUMBER OF CASES IS 15
DEFAULT "T" (.05,.25) STATISTIC IS 2.06
DEFAULT "F" (.05,1.25) STATISTIC IS 4.24

VARIABLE	MEAN	STD DEV	MINIMUM VALUE	MAXIMUM VALUE
X	0.4542212E-04	0.1123801E-04	0.2845537E-04	0.6626513E-04
Y	0.4593933E+01	0.1227870E+01	0.2496000E+01	0.6791000E+01

COEFFICIENT	ESTIMATE	STD ERR B	CONF INT	SIGNIFICANT
BO	-0.2331465E+00	0.3287548E+00	0.6772347E+00	NO
B1	0.1062716E+06	0.7039472E+04	0.1450731E+05	YES

(COVARIANCE(BO,B1)=-0.2250855E+04)

ANALYSIS OF VARIANCE

SOURCE	SUM OF SQUARES	DEGREES OF FREEDOM	MEAN SQUARE
REGRESSION(BO)	0.3165634E+03	1	0.1996829E+02
REGRESSION(B1/BO)	0.1996829E+02	1	0.8761668E-01
RESIDUAL	0.1139017E+01	13	
TOTAL (CORR.)	0.2110731E+02	14	
TOTAL (UNCORR.)	0.3376707E+03	15	

COEFFICIENT OF MULTIPLE DETERMINATION(R**2) IS 0.9377

SIGNIFICANCE OF REGRESSION AND PREDICTOR UTILITY
CALC. F RATIO= 225.91   REGRESSION SIGNIFICANT YES   EQUATION CAN BE USED FOR PREDICTION YES

OBSERV. #	Y(OBS.)	Y(PRED.)	X(OBS.)	RESIDUAL	STD ERR Y	CONF LIMIT	OUTLIER
1	0.2496000E+01	0.2790851E+01	0.2845537E-04	-0.2948507E+00	0.1417966E+00	0.2921010E+00	YES
2	0.3864000E+01	0.3912595E+01	0.3910082E-04	-0.4859484E-01	0.8875822E-01	0.1828419E+00	NO
3	0.4790000E+01	0.4977139E+01	0.4928803E-04	-0.1871393E+00	0.8053226E-01	0.1658964E+00	YES
4	0.3041000E+01	0.3077847E+01	0.3115597E-04	-0.3684722E-01	0.1262003E+00	0.2599726E+00	NO
5	0.3943000E+01	0.4254154E+01	0.4224485E-04	-0.3111544E+00	0.7967234E-01	0.1641250E+00	YES
6	0.5414000E+01	0.5339937E+01	0.5244191E-04	0.7406263E-01	0.9101107E-01	0.1874827E+00	NO
7	0.3406000E+01	0.3221618E+01	0.3250883E-04	0.1843823E+00	0.1187620E+00	0.2446497E+00	NO
8	0.4450000E+01	0.4597266E+01	0.4545348E-04	-0.1472661E+00	0.7642749E-01	0.1574406E+00	YES
9	0.5130000E+01	0.5783646E+01	0.5661714E-04	-0.6536461E+00	0.1097801E+00	0.2261469E+00	YES
10	0.3928000E+01	0.3652683E+01	0.3656508E-04	0.2753175E+00	0.9863310E-01	0.2031841E+00	YES
11	0.5419000E+01	0.5058241E+01	0.4979118E-04	0.3607592E+00	0.8238348E-01	0.1697099E+00	YES
12	0.6652000E+01	0.6345542E+01	0.6190450E-04	0.3064580E+00	0.1389368E+00	0.2862098E+00	YES
13	0.4226000E+01	0.3929433E+01	0.3916926E-04	0.2965671E+00	0.8819631E-01	0.1816843E+00	YES
14	0.5359000E+01	0.5159095E+01	0.5074020E-04	0.1999052E+00	0.8510350E-01	0.1753132E+00	YES
15	0.6791000E+01	0.6808953E+01	0.6626513E-04	-0.1795335E-01	0.1654358E+00	0.3407976E+00	NO

RESIDUAL ANALYSIS: # OF POSITIVE VALUES = 7   # OF NEGATIVE VALUES = 8

********RUN COMPLETE********

BACK-CALCULATION OF CALIBRATION DATA

CASE NUMBER	% SOLIDS OBS	PRED	RESIDUAL	% ASH OBS	PRED	RESIDUAL	% IRON OBS	PRED	RESIDUAL	CONDITION NUMBER
1	3.23	2.79	0.44	32.92	36.34	-3.42	3.91	3.71	0.20	30.83
2	4.50	3.98	0.52	32.66	33.37	-0.71	3.91	4.27	-0.36	30.66
3	5.63	4.87	0.76	33.08	33.83	-0.75	3.91	4.25	-0.34	30.54
4	3.29	2.98	0.31	35.41	38.89	-3.48	3.92	3.90	0.02	30.76
5	4.43	3.76	0.67	35.98	39.23	-3.25	3.92	3.94	-0.02	30.65
6	5.56	5.27	0.29	35.91	36.70	-0.79	3.92	4.10	-0.18	30.47
7	3.19	3.30	-0.11	37.99	40.48	-2.49	3.94	3.77	0.17	30.72
8	4.41	4.45	-0.04	38.87	39.08	-0.21	3.94	3.76	0.18	30.59
9	5.55	6.33	-0.78	38.85	35.17	3.68	3.96	4.40	-0.54	30.51
10	3.33	3.57	-0.24	40.91	38.33	2.58	3.97	4.22	-0.26	30.65
11	4.55	4.05	0.50	41.15	44.35	-3.20	3.97	4.42	-0.45	30.47
12	5.68	5.35	0.33	41.44	43.00	-1.56	4.00	4.25	-0.28	30.62
13	3.29	4.29	-1.00	44.05	37.56	6.49	4.00	3.86	0.14	30.32
14	4.34	5.31	-0.97	43.71	40.10	3.61	4.00	3.71	0.29	30.48
15	5.68	6.36	-0.67	44.18	41.24	2.94	4.00	3.83	0.17	30.31

RESIDUAL ANALYSIS

VARIABLE	MEAN VALUE	RESIDUAL MEAN	RESIDUAL STD DEV	RELATIVE ERROR	RANGE ERROR
% SOLIDS	4.44	0.00	0.60	13.59	24.16
% ASH	38.47	-0.04	3.15	8.19	27.36
% IRON	3.95	-0.01	0.29	7.25	*****

340

12.6 RESULTS FOR CALIBRATION RUN 4

INPUT INFORMATION:
• • • • • • • • • • • • • •

MODEL PARAMETERS:
• • • • • • • • • • •

SPECIES	SPECIFIC GRAVITY	SCATTERING COEFFICIENT CM**2/G	TOTAL MASS ABSORPTION COEFFICIENT AT 22 KEV CM**2/G	AT 6.4 KEV CM**2/G
WATER	1.00	0.0540	0.6374	19.8080
ORGANICS	1.28	0.0506	0.4109	9.7020
MINERAL MATTER	2.37	0.0506	2.0564	74.8860
IRON MINERALS	5.10	0.0549	13.8680	55.9200

SAMPLE ANALYSES:
• • • • • • • • • • •

CASE NUMBER	% SOLIDS BY WT. IN PULP	% ASH BY WT IN SOLIDS	% IRON BY WT IN ASH SOLIDS
1	7.47	12.51	4.17
2	13.04	12.49	4.22
3	16.01	12.69	4.08
4	16.12	16.80	4.64
5	16.82	22.02	4.58
6	7.47	16.57	4.56
7	11.73	16.89	5.69
8	12.13	21.45	5.65
9	7.57	21.09	6.12
10	7.58	12.59	6.99
11	12.01	12.80	7.06
12	16.17	12.65	7.10
13	16.41	17.25	7.42
14	16.89	21.36	7.36
15	7.52	16.57	7.16
16	11.73	16.80	7.41
17	12.01	21.23	7.62
18	7.08	21.08	7.92
19	7.59	12.54	8.70
20	11.95	12.58	9.02
21	16.28	12.59	9.06
22	16.18	17.03	9.16
23	16.78	21.55	9.36

24	7.39	16.39	9.44
25	11.66	16.66	9.16
26	12.23	20.62	9.56
27	7.09	20.82	10.03

RADIATION MEASUREMENTS:

CASE NUMBER	REDUCED DENSITY	BACKSCATTER COUNTS (X 1E-06)	IRON FLUORESCENCE COUNTS (X 1E-04)
1	0.960420	10.291798	2.598000
2	0.932950	10.264365	3.973000
3	0.905740	10.216802	5.889000
4	0.892150	10.031330	8.887000
5	0.880620	9.833685	11.963000
6	0.952390	10.225282	3.809000
7	0.924470	10.136001	5.847000
8	0.908980	9.986970	8.464000
9	0.945120	10.137179	5.507000
10	0.960760	10.272513	4.062000
11	0.927760	10.205070	6.414000
12	0.899020	10.139892	8.898000
13	0.890670	9.923238	13.482000
14	0.873960	9.717968	17.518000
15	0.952320	10.190652	6.664000
16	0.909940	10.052209	10.480000
17	0.901870	9.916616	12.876000
18	0.939770	10.082540	8.074000
19	0.949970	10.243785	5.519000
20	0.927040	10.162231	8.789000
21	0.899800	10.086588	12.449000
22	0.888380	9.859798	17.039000
23	0.877430	9.630489	22.739000
24	0.940030	10.144875	7.212000
25	0.915160	10.000495	12.017000
26	0.908510	9.841708	15.749000
27	0.944320	10.033064	9.883000

CALIBRATION OF DENSITY GAUGE:

TWO VARIABLE LINEAR REGRESSION ANALYSIS
****

MODEL FORM: Y = B0 + B1*X

INPUT INFORMATION:
NUMBER OF CASES IS 27
DEFAULT "T" (.05,25) STATISTIC IS 2.06
DEFAULT "F" (.05,1,25) STATISTIC IS 4.24

VARIABLE	MEAN	STD. DEV.	MINIMUM VALUE	MAXIMUM VALUE
X	0.1036213E+01	0.1206776E-01	0.1020701E+01	0.1055229E+01
Y	-0.8501305E-01	0.2900404E-01	-0.1347207E+00	-0.1000000E-69

COEFFICIENT	ESTIMATE	STD. ERR. B	CONF. INT.	SIGNIFICANT
B0	0.2334498E+01	0.1180560E+00	0.2431954E+00	YES
B1	-0.2334957E+01	0.1139229E+00	0.2346811E+00	YES

(COVARIANCE(B0,B1)=-0.1344841E-01)

ANALYSIS OF VARIANCE

SOURCE	SUM OF SQUARES	DEGREES OF FREEDOM	MEAN SQUARE
REGRESSION(B0)	0.1951349E+00	1	0.2064356E-01
REGRESSION(B1/B0)	0.2064356E-01	1	0.4914156E-04
RESIDUAL	0.1228539E-02	25	
TOTAL (CORR.)	0.2187210E-01	26	
TOTAL (UNCORR.)	0.2170070E+00	27	

COEFFICIENT OF MULTIPLE DETERMINATION(R**2) IS 0.9393

SIGNIFICANCE OF REGRESSION AND PREDICTOR UTILITY   EQUATION CAN BE USED FOR PREDICTION:YES
CALC. F RATIO= 418.08   REGRESSION SIGNIFICANT:YES

OBSERV. #	Y(OBS.)	Y(PRED.)	X(OBS.)	RESIDUAL	STD ERR	CONF LIMIT	OUTLIER
1	-0.4038459E-01	-0.4879438E-01	0.1020701E+01	0.8409793E-02	0.2223230E-02	0.4579852E-02	YES
2	-0.6940367E-01	-0.8613889E-01	0.1036695E+01	0.1673522E-01	0.1350213E-02	0.2781438E-02	YES
3	-0.9900299E-01	-0.1068495E+00	0.1045565E+01	0.7846532E-02	0.1719054E-02	0.3541250E-02	YES
4	-0.1141210E+00	-0.1146429E+00	0.1048902E+01	0.5191195E-03	0.1977359E-02	0.4073359E-02	NO
5	-0.1277291E+00	-0.1291263E+00	0.1055105E+01	0.1997261E-02	0.2540163E-02	0.5232734E-02	NO
6	-0.4878066E-01	-0.5183944E-01	0.1022005E+01	0.3058776E-02	0.2107071E-02	0.4340564E-02	NO
7	-0.7853468E-01	-0.8273061E-01	0.1035235E+01	0.4195928E-02	0.1353683E-02	0.2788587E-02	YES
8	-0.9543219E-01	-0.9135968E-01	0.1038931E+01	-0.4072512E-02	0.1384176E-02	0.2851401E-02	NO
9	-0.5644338E-01	-0.5615364E-01	0.1023853E+01	-0.2897390E-03	0.1950045E-02	0.4017092E-02	YES
10	-0.4003064E-01	-0.4979256E-01	0.1021129E+01	0.9761923E-02	0.2184720E-02	0.4500521E-02	YES
11	-0.7498220E-01	-0.7987304E-01	0.1034011E+01	0.4890837E-02	0.1372206E-02	0.2826743E-02	NO
12	-0.1064500E+00	-0.1084038E+00	0.1046230E+01	0.1953756E-02	0.1767053E-02	0.3640129E-02	YES
13	-0.1157813E+00	-0.1182301E+00	0.1050439E+01	0.2448808E-02	0.2108699E-02	0.4343920E-02	NO
14	-0.1347207E+00	-0.1293490E+00	0.1055200E+01	-0.5371654E-02	0.2549375E-02	0.5251712E-02	YES
15	-0.4885417E-01	-0.5244599E-01	0.1022265E+01	0.3591819E-02	0.2084425E-02	0.4293914E-02	NO
16	-0.9437662E-01	-0.8289542E-01	0.1035306E+01	-0.1148120E-01	0.1353046E-02	0.2787273E-02	YES
17	-0.1032849E+00	-0.9055981E-01	0.1038588E+01	-0.1272508E-01	0.1375971E-02	0.2834500E-02	YES
18	-0.6212011E-01	-0.5267258E-01	0.1023362E+01	-0.9447531E-02	0.2076009E-02	0.4276578E-02	YES
19	-0.5132487E-01	-0.4994842E-01	0.1021195E+01	-0.1376455E-02	0.2178744E-02	0.4488211E-02	NO
20	-0.7575856E-01	-0.7942690E-01	0.1033820E+01	0.3668336E-02	0.1376350E-02	0.2835281E-02	YES
21	-0.1055828E+00	-0.1093997E+00	0.1046657E+01	0.3816926E-02	0.1798819E-02	0.3705565E-02	YES
22	-0.1183557E+00	-0.1165129E+00	0.1049703E+01	0.1842758E-02	0.2045012E-02	0.4212723E-02	NO
23	-0.1307581E+00	-0.1291158E+00	0.1055229E+01	-0.1342301E-01	0.2552140E-02	0.5257408E-02	NO
24	-0.6184349E-01	-0.5160968E-01	0.1021907E+01	-0.1023381E-01	0.2115694E-02	0.4358328E-02	YES
25	-0.8865637E-01	-0.8249007E-01	0.1035132E+01	-0.6166299E-02	0.1354699E-02	0.2790680E-02	YES
26	-0.9594938E-01	-0.9188644E-01	0.1039156E+01	-0.4062948E-02	0.1390151E-02	0.2863710E-02	YES
27	-0.5729019E-01	-0.5280464E-01	0.1022419E+01	-0.4485547E-02	0.2071116E-02	0.4264498E-02	YES

RESIDUAL ANALYSIS: # OF POSITIVE VALUES= 14   # OF NEGATIVE VALUES= 13

*******RUN COMPLETE*********

CALIBRATION OF BACKSCATTER GAUGE

TWO VARIABLE LINEAR REGRESSION ANALYSIS
• •

MODEL FORM Y = BO + B1*X
• • • • • • • • • • • • • • • •

INPUT INFORMATION:
NUMBER OF CASES IS 27
DEFAULT "T" (.05,25) STATISTIC IS 2.06
DEFAULT "F" (.05,1,25) STATISTIC IS 4.24

VARIABLE	MEAN	STD DEV	MINIMUM VALUE	MAXIMUM VALUE
X	0.3994563E-01	0.1196046E-02	0.3701340E-01	0.4173142E-01
Y	0.1006026E+02	0.1744882E+00	0.9630489E+01	0.1029180E+02

COEFFICIENT	ESTIMATE	STD ERR B	CONF INT	SIGNIFICANT
BO	0.4256132E+01	0.1046996E+00	0.2152079E+00	YES
B1	0.1453008E+03	0.2614175E+01	0.5385198E+01	YES

(COVARIANCE(BO,B1)=-0.2729848E+00)

ANALYSIS OF VARIANCE

SOURCE	SUM OF SQUARES	DEGREES OF FREEDOM	MEAN SQUARE
REGRESSION(BO)	0.2732641E+04	1	
REGRESSION(B1/BO)	0.7852449E+00	1	0.7852449E+00
RESIDUAL	0.6354453E-02	25	0.2541781E-03
TOTAL (CORR.)	0.7915994E+00	26	
TOTAL (UNCORR.)	0.2733433E+04	27	

COEFFICIENT OF MULTIPLE DETERMINATION(R**2) IS 0.9913

SIGNIFICANCE OF REGRESSION AND PREDICTOR UTILITY
CALC F RATIO= 3087.35   REGRESSION SIGNIFICANT YES   EQUATION CAN BE USED FOR PREDICTION YES

OBSERV. #	Y(OBS)	Y(PRED)	X(OBS)	RESIDUAL	STD ERR	CONF LIMIT	OUTLIER
1	0.1029180E+02	0.1031974E+02	0.4173142E-01	-0.2794447E-01	0.5586398E-02	0.1150798E-01	YES
2	0.1026436E+02	0.1025223E+02	0.4126678E-01	0.1213575E-01	0.4619765E-02	0.9516713E-02	YES
3	0.1021680E+02	0.1021385E+02	0.4100264E-01	0.2952894E-02	0.4129085E-02	0.8505912E-02	NO
4	0.1003133E+02	0.1004309E+02	0.3982744E-01	-0.1176269E-01	0.3083740E-02	0.6352503E-02	YES
5	0.9833685E+01	0.9842167E+01	0.3844462E-01	-0.8484216E-02	0.4981053E-02	0.1026097E-01	NO
6	0.1022528E+02	0.1024140E+02	0.4119224E-01	-0.1611730E-01	0.4475969E-02	0.9220494E-02	YES
7	0.1013600E+02	0.1010623E+02	0.4026198E-01	0.2976998E-01	0.3177726E-02	0.6546113E-02	YES
8	0.9986970E+01	0.9966697E+01	0.3930167E-01	0.2027275E-01	0.3499698E-02	0.7209375E-02	YES
9	0.1013718E+02	0.1012226E+02	0.4037232E-01	0.1491582E-01	0.3264694E-02	0.6725267E-02	YES
10	0.1027251E+02	0.1027468E+02	0.4142130E-01	-0.2168719E-02	0.4929066E-02	0.1015387E-01	NO
11	0.1020507E+02	0.1018874E+02	0.4082983E-01	0.1632966E-01	0.3841469E-02	0.7913425E-02	YES
12	0.1013989E+02	0.1011993E+02	0.4035625E-01	0.1996384E-01	0.3250580E-02	0.6696192E-02	YES
13	0.9923238E+01	0.9909329E+01	0.3890685E-01	0.1390884E-01	0.4097342E-02	0.8440522E-02	NO
14	0.9717968E+01	0.9729858E+01	0.3767167E-01	-0.1189960E-01	0.6689630E-02	0.1378063E-01	NO
15	0.1019065E+02	0.1019072E+02	0.4084347E-01	-0.7042534E-04	0.3863032E-02	0.7957843E-02	YES
16	0.1005221E+02	0.1005908E+02	0.3993748E-01	-0.6871769E-02	0.3068299E-02	0.6320694E-02	YES
17	0.9916616E+01	0.9906802E+01	0.3888945E-01	0.9813880E-02	0.4127615E-02	0.8502884E-02	YES
18	0.1008254E+02	0.1010060E+02	0.4022323E-01	-0.1806114E-01	0.3152882E-02	0.6494935E-02	NO
19	0.1024378E+02	0.1025026E+02	0.4125319E-01	-0.6470100E-02	0.4593272E-02	0.9462139E-02	YES
20	0.1016223E+02	0.1015237E+02	0.4057950E-01	0.9864066E-02	0.3487096E-02	0.7183417E-02	YES
21	0.1008659E+02	0.1006138E+02	0.3955332E-01	0.2520594E-01	0.3068291E-02	0.6320677E-02	NO
22	0.9859798E+01	0.9858916E+01	0.3855989E-01	0.882765E-03	0.4747308E-02	0.9779452E-02	NO
23	0.9630489E+01	0.9634210E+01	0.3701340E-01	-0.3721090E-02	0.8256603E-02	0.1700860E-01	NO
24	0.1014488E+02	0.1015633E+02	0.4060679E-01	-0.1145716E-01	0.3521556E-02	0.7254404E-02	YES
25	0.1000049E+02	0.1001627E+02	0.3964285E-01	-0.1577653E-01	0.3168671E-02	0.6527460E-02	YES
26	0.9841708E+01	0.9850272E+01	0.3850040E-01	-0.8564109E-02	0.4867014E-02	0.1002605E-01	NO
27	0.1003306E+02	0.1005972E+02	0.3994189E-01	-0.2665808E-01	0.3068240E-02	0.6320574E-02	YES

RESIDUAL ANALYSIS: # OF POSITIVE VALUES= 12   # OF NEGATIVE VALUES= 15

••••••••RUN COMPLETE••••••••

CALIBRATION OF IRON GAUGE

TWO VARIABLE LINEAR REGRESSION ANALYSIS

MODEL FORM Y = B0 + B1X

INPUT INFORMATION
NUMBER OF CASES IS 27
DEFAULT "T" (.05,25) STATISTIC IS 2.06
DEFAULT "F" (.05,1,25) STATISTIC IS 4.24

VARIABLE	MEAN	STD DEV	MINIMUM VALUE	MAXIMUM VALUE
X	0.9990426E-04	0.4759909E-04	0.2738495E-04	0.2269182E-03
Y	0.9511148E+01	0.4845197E-01	0.2598000E+01	0.2273900E+02

COEFFICIENT	ESTIMATE	STD ERR B	CONF INT	SIGNIFICANT
B0	-0.5735253E+00	0.2892758E+00	0.5959080E+00	NO
B1	0.1009434E+06	0.2623002E+04	0.5403382E+04	YES

(COVARIANCE(B0,B1)=-0.6873550E+03)

ANALYSIS OF VARIANCE

SOURCE	SUM OF SQUARES	DEGREES OF FREEDOM	MEAN SQUARE
REGRESSION(B0)	0.2442472E+04		
REGRESSION(B1/B0)	0.6002419E+03		0.6002419E+03
RESIDUAL	0.1013229E+02	25	0.4052917E+00
TOTAL (CORR)	0.6103742E+03	26	
TOTAL (UNCORR)	0.3052847E+04	27	

COEFFICIENT OF MULTIPLE DETERMINATION(R**2) IS 0.982?

SIGNIFICANCE OF REGRESSION AND PREDICTOR UTILITY REGRESSION SIGNIFICANT YES, EQUATION CAN BE USED FOR PREDICTION YES
CALC F RATIO= 1479.01

OBSERV. # Y(OBS.) Y(PRED.) X(OBS) RESIDUAL STD ERR CONF. LIMIT OUTLIER

OBSERV. #	Y(OBS.)	Y(PRED.)	X(OBS)	RESIDUAL	STD ERR	CONF. LIMIT	OUTLIER
1	0.2598000E+01	0.2190804E+01	0.2738495E-04	0.4071957E+00	0.2262604E+00	0.4660964E+00	NO
2	0.3973000E+01	0.4318303E+01	0.4846111E-04	-0.3453032E+00	0.1822591E+00	0.3754536E+00	NO
3	0.5889000E+01	0.5329595E+01	0.5847952E-04	0.5594049E+00	0.1637595E+00	0.3734515E+00	YES
4	0.8887000E+01	0.8167324E+01	0.8659160E-04	0.7196761E+00	0.1273976E+00	0.2624290E+00	YES
5	0.1196300E+02	0.1086467E+02	0.1133130E-03	0.1098330E+01	0.1274669E+00	0.2625817E+00	YES
6	0.3809000E+01	0.3387290E+01	0.3923799E-04	0.4217092E+00	0.2008294E+00	0.4137084E+00	YES
7	0.5847000E+01	0.7298449E+01	0.7798406E-04	-0.1451449E+01	0.1353391E+00	0.2787985E+00	YES
8	0.8464000E+01	0.9491424E+01	0.9970886E-04	-0.1027424E+01	0.1225196E+00	0.2523904E+00	YES
9	0.5507000E+01	0.6200814E+01	0.6711029E-04	-0.6938141E+00	0.1496997E+00	0.3080808E+00	NO
10	0.4062000E+01	0.4158428E+01	0.4687330E-04	-0.9642832E-01	0.1853558E+00	0.3818028E+00	YES
11	0.6414000E+01	0.7137784E+01	0.7639442E-04	-0.7237835E+00	0.1371648E+00	0.2825595E+00	YES
12	0.8898000E+01	0.9775560E+01	0.1025237E-03	-0.8775600E+00	0.1227411E+00	0.2527848E+00	YES
13	0.1348200E+02	0.1400074E+02	0.1443806E-03	-0.5187384E+00	0.1691765E+00	0.3485036E+00	NO
14	0.1751800E+02	0.1740457E+02	0.1781008E-03	0.1134288E+00	0.2389158E+00	0.4921665E+00	YES
15	0.6664000E+01	0.5688029E+01	0.6203036E-04	0.9759713E+00	0.1577306E+00	0.3249312E+00	YES
16	0.1048000E+02	0.9628940E+01	0.1010712E-03	0.8510604E+00	0.1225568E+00	0.2524670E+00	NO
17	0.1287600E+02	0.1274818E+02	0.1319721E-03	0.1278163E+00	0.1486435E+00	0.3061407E+00	NO
18	0.8074000E+01	0.7632984E+01	0.8298141E-04	0.4410163E+00	0.1538818E+00	0.3168750E+00	YES
19	0.5519000E+01	0.5301699E+01	0.5820317E-04	0.2173009E+00	0.1642414E+00	0.3383031E+00	YES
20	0.8789000E+01	0.9071152E+01	0.9554541E-04	-0.2821519E+00	0.1230509E+00	0.2534848E+00	NO
21	0.1244900E+02	0.1266744E+02	0.1311722E-03	-0.2184394E+00	0.1474361E+00	0.3037183E+00	NO
22	0.1703900E+02	0.1697039E+02	0.1737996E-03	0.6860870E-01	0.2293031E+00	0.4723643E+00	NO
23	0.2273900E+02	0.2232236E+02	0.2269182E-03	0.4066382E+00	0.3549716E+00	0.7312413E+00	NO
24	0.7212000E+01	0.7456875E+01	0.7955351E-04	-0.2448752E+00	0.1336422E+00	0.2753028E+00	NO
25	0.1201700E+02	0.1186878E+02	0.1236202E-03	0.1482206E+00	0.1369615E+00	0.2821818E+00	NO
26	0.1574900E+02	0.1599480E+02	0.1643480E-03	-0.2457958E+00	0.2080152E+00	0.4291293E+00	NO
27	0.9883000E+01	0.9713615E+01	0.1019100E-03	0.1693852E+00	0.1226315E+00	0.2526208E+00	NO

RESIDUAL ANALYSIS # OF POSITIVE VALUES = 15 # OF NEGATIVE VALUES = 12

········RUN COMPLETE·········

BACK-CALCULATION OF CALIBRATION DATA

CASE NUMBER	OBS	% SOLIDS PRED	RESIDUAL	OBS	...	CONDITION NUMBER
1	7.47	5.97	1.50			30.50
2	13.04	10.52	2.52			30.34
3	16.01	14.95	1.06			30.07
4	16.12	16.06	0.06			29.69
5	16.82	16.64	0.18			29.31
6	7.47	6.92	0.55			30.37
7	11.73	11.10	0.63			30.09
8	12.13	12.76	-0.63			29.75
9	7.57	7.63	-0.06			30.17
10	7.58	6.00	1.58			30.32
11	12.01	11.28	0.73			30.00
12	16.17	15.91	0.26			29.67
13	16.41	16.09	0.32			28.61
14	16.89	17.58	-0.69			29.97
15	7.52	7.13	0.39			29.47
16	11.73	13.56	-1.83			29.17
17	12.01	14.05	-2.04			29.79
18	7.08	8.47	-0.39			30.12
19	7.59	7.79	-0.20			29.68
20	11.95	11.43	0.52			29.20
21	16.28	15.90	0.38			28.65
22	16.18	16.47	-0.29			27.98
23	16.78	17.01	-0.23			29.90
24	7.39	8.84	-1.45			29.27
25	11.66	12.48	-0.82			29.59
26	12.23	12.72	-0.49			28.81
27	7.09	7.57	-0.48			29.55

RESIDUAL ANALYSIS

VARIABLE	MEAN VALUE	RESIDUAL MEAN	RESIDUAL STD DEV	RELATIVE ERROR	RANGE ERROR
% SOLIDS	11.96	0.00	1.04	8.68	10.58
% ASH	16.87	0.06	0.89	5.26	9.35
% IRON	7.16	-0.00	0.81	11.38	13.68